

Kingston University London

**Investigating Azoreductases and NAD(P)H dependent
Quinone Oxidoreductases in *Pseudomonas aeruginosa***

**A thesis submitted in partial fulfilment for the degree of
Doctor of Philosophy**

By

Sinéad HOLLAND

Faculty of Science, Engineering and Computing

August 2017

Declaration

This thesis entitled 'Investigating Azoreductases and NAD(P)H dependent Quinone Oxidoreductases in *Pseudomonas aeruginosa*' is based upon the work conducted in the Faculty of Science, Engineering and Computing at Kingston University London and in collaboration with Dr. Gail Preston's group in the Plant Sciences Department at the University of Oxford. All of the work described here is the candidate's own original work unless otherwise acknowledged in the text or by references. None of the work presented here has been submitted for another degree at this or any other university.

Acknowledgements

The work presented here would not have been possible without the assistance and support of many people. To begin with, I would like to express my sincere gratitude to my director of studies, Dr. Ali Ryan. His enthusiasm and knowledge for the subject along with the endless help and reassurance he has offered have contributed greatly to the completion of this thesis. I would also like to offer a special thank you to Prof. Edith Sim. Her support from beginning to end has been hugely appreciated and her unlimited expertise and drive has added considerably to my PhD experience. I would also like to thank Prof. Mark Fielder and Dr. Gail Preston for the extensive wealth of microbiological knowledge they have offered this study.

I'd like to extend deep gratitude to Rosalind Percival. She is one of the most helpful, accommodating and efficient people that I have ever had the pleasure of working with. Without her, the graduate research school at Kingston University would fall apart.

A special acknowledgement must go to past and present members of the Biotech Lab, Ronni, Elena, Olga and Ruth and in particular Dr. Vincenzo Crescente. This group of people have been so important during my time as a PhD student both emotionally and indeed, scientifically. Their help and friendship have made this experience so much better.

There are many people who have made it so easy to come in to work every day, Nico, Lauren, Loryn, Jon, Tasha and Sharan. Without you all, this thesis would have been submitted much sooner. The many distractions and excuses to procrastinate that you have all offered has made this experience far more fun than it was supposed to be!

I would also like to thank some amazing people who are always there for a welcome break from it all, Lydia, Helena, Guy, Marc, Sam, Nick, Stefanie, Holly and Diarmaid. A special mention goes to Pete, whose help and support in every way has given me such comfort and confidence as I approach the next stage.

Finally, I could not have done any of this without my lovely family. Thank you to my brother Brian and my aunt Kitty just for being yourselves. A massive, massive thank you goes to my wonderful parents, their patience, understanding and constant belief in me along with their incredible and never ending support and encouragement has helped me so much and without which I would not have finished this thesis.

Publications

Characterisation of novel NAD(P)H quinone oxidoreductases from *Pseudomonas aeruginosa* involved in resistance to plant toxins.

Sinead M. Holland & Ali Ryan (Manuscript awaiting reviewers comments)

Investigating nicotinamide binding to azoreductase family members

Sinead M. Holland, Jesus Angulo, Sunny Odedra, Elise Kaplan, Edward Lowe, Chris J. Morris, Ali Ryan (article in preparation)

Identification of novel members of the bacterial azoreductase family in *Pseudomonas aeruginosa*.

Vincenzo Crescente, Sinead M. Holland, Sapna Kashyap, Elena Polycarpou, Edith Sim, Ali Ryan. *Biochemical Journal* Mar 2016, 473 (5) 549-558; DOI: 10.1042/BJ20150856. (Copy attached)

Presentations

Investigating Azoreductases in *Pseudomonas aeruginosa*.

Oral presentation, Interdisciplinary Hub Conference for the Study of Health and Age-related conditions (IhSHA), Kingston University London, June 2016.

Identification and Investigation of Azoreductases in *Pseudomonas aeruginosa*.

Poster presentation, Society for Applied Microbiology Autumn meeting, London, October 2015.

Identification and Investigation of Azoreductases in *Pseudomonas aeruginosa*.

Poster presentation, American Society for Microbiology's 15th International Conference on Pseudomonas, Washington D.C., September 2015.

Bacterial Azoreductases in Metabolism of Xenobiotics.

Oral presentation, British Toxicology Society Annual Congress, Solihull, April 2015.

Bacterial Azoreductases in Metabolism of Xenobiotics.

Poster presentation, British Toxicology Society Annual Congress, Solihull, April 2015.

Identification and Investigation of Azoreductases in *Pseudomonas aeruginosa*.

Poster presentation, Society for Applied Microbiology Autumn meeting, London, October 2014.

List of Acronyms

5-ASA: 5-aminosalicylic acid	NADPH: Nicotinamide adenine dinucleotide phosphate
bp: Base pairs	NQO: NAD(P)H quinone oxidoreductase
CF: Cystic Fibrosis	NTA: Nitrolotriactic acid
CFU: Colony forming units	OD: Optical density
DMSO: Dimethyl sulfoxide	PCR: Polymerase chain reaction
DNA: Deoxyribonucleic Acid	QS: Quorum sensing
DSF: Differential scanning fluorimetry	R _f : Retention factor
DTT: Dithiothreitol	RMSD: Root mean square distance
EDTA: Ethylenediaminetetraacetic acid	RNA: Ribonucleic acid
EPS: Extracellular polymeric substance	RNAP: RNA polymerase
FAD: Flavin dinucleotide	ROS: Reactive oxygen species
FMN: Flavin mononucleotide	RPM: Rotations per minute
ICU: Intensive care unit	RT-PCR: Reverse transcription polymerase chain reaction
IF: Insoluble fraction	SDS-PAGE: Sodium dodecyl sulfate polyacrylamide gel electrophoresis
IMAC: Immobilised metal-ion affinity chromatography	SF: Soluble fraction
IPTG: Isopropyl-β-D-thiogalactopyranoside	TBE: Tris borate EDTA
KO: Knock out	TEMED: Tetramethylethylenediamine
LB: Lysogeny broth	TLC: Thin layer chromatography
MDR: Multi-drug resistant	T _M : Melting temperature
MH: Mueller Hinton	TrM: Transposon mutants
MIC: Minimum inhibitory concentration	WCL: Whole cell lysate
MOPS: 3-(N-morpholino)propanesulfonic acid	WT: Wild type
NADH: Nicotinamide adenine dinucleotide	

Table of Contents

List of Acronyms	iv
Table of Contents	v
List of Figures	xi
List of Tables	xiv
Abstract	xvi
Chapter 1 Introduction	1
1.1 <i>Pseudomonas aeruginosa</i>	1
1.1.1 <i>P. aeruginosa</i> infections	2
1.1.2 Antibiotic resistance in <i>P. aeruginosa</i>	5
1.1.2.1 Intrinsic resistance	5
1.1.2.2 Adaptive resistance.....	7
1.1.2.3 Acquired resistance	8
1.2 Azoreductases	10
1.2.1 Azoreductases in bioremediation and medicine	10
1.2.2 Azoreductases and their associations in physiological functions	11
1.3 Aims.....	17
Chapter 2 Materials and methods	18
2.1 Chemicals and reagents	18
2.2 Bacterial strains and growth conditions.....	18
2.3 Cloning of putative azoreductase genes.....	20
2.3.1 Genomic DNA extraction	20
2.3.2 Agarose gel analysis of DNA samples	20
2.3.3 Plasmid Extraction	21
2.3.4 Putative azoreductase gene amplification for cloning into pET-28b.....	21
2.3.5 Putative azoreductase gene amplification for cloning into pUCP24	23

2.3.6	Double endonuclease restriction digest	24
2.3.7	Antarctic phosphatase digestion	25
2.3.8	DNA purification.....	25
2.3.9	Ligation	26
2.3.10	Preparation of chemically competent <i>E. coli</i>	27
2.3.11	Preparation of chemically competent <i>P. aeruginosa</i> PAO1 wild type and transposon insertion mutants	27
2.3.12	Heat shock transformation.....	27
2.3.13	Selection of successful transformants	28
2.3.14	DNA sequence analysis.....	29
2.4	Gene expression and production of recombinant protein.....	30
2.4.1	Expression of putative azoreductase genes	30
2.4.2	SDS-PAGE analysis of recombinant proteins.....	31
2.5	Purification and quantification of recombinant protein.....	33
2.5.1	Immobilised Metal-ion Affinity Chromatography	33
2.5.2	Dialysis.....	34
2.5.3	Protein quantification and concentration.....	34
2.6	Characterisation of putative azoreductases from <i>P. aeruginosa</i> PAO1	35
2.6.1	Thin Layer Chromatography	35
2.6.2	Differential Scanning Fluorimetry	35
2.6.3	Spectral properties of putative azoreductases and determination of flavin saturation level	36
2.6.4	Absorption spectra of substrates and calculation of molar extinction coefficients	36
2.6.5	Enzymatic activity assays for the putative azoreductases	37
2.7	Crystallisation of PA2580 and x-ray diffraction data collection.....	40
2.7.1	Synthesis of H ₂ NADPH	40
2.7.2	Crystallisation of PA2580 with H ₂ NADPH	40
2.7.3	Optimisation of crystallisation conditions for PA2580	40

2.7.4	X-ray diffraction data collection and analysis	41
2.8	Phenotypic characterisation of <i>P. aeruginosa</i> strains	42
2.8.1	Confirmation of transposon insertion in <i>P. aeruginosa</i> PAO1 gene deletion strains	42
2.8.2	RNA extraction and cDNA synthesis from <i>P. aeruginosa</i> PAO1, the azoreductase-like gene deletion strains and the complemented strains	44
2.8.3	Detection of gene expression in <i>P. aeruginosa</i> PAO1 strains	44
2.8.4	Growth analysis of <i>P. aeruginosa</i> PAO1 and <i>P. aeruginosa</i> TBCF 10839 strains	45
2.8.5	Determination of Minimum Inhibitory Concentration (MIC)	46
2.8.6	Determination of Colony Forming Units (CFU)/mL of <i>P. aeruginosa</i> PAO1 and <i>P. aeruginosa</i> TBCF 10839 strains	46
Chapter 3	Cloning and expression of putative azoreductases PA1224, PA1225 and PA4975	47
3.1	Introduction	47
3.2	Results	54
3.2.1	Cloning of the putative azoreductase genes <i>pa1224</i> and <i>pa1225</i>	54
3.2.1.1	Preparation of genes of interest	54
3.2.1.2	Preparation of the cloning vector	56
3.2.1.3	Obtaining and screening successful clones	57
3.2.2	Expression of putative azoreductases PA1224, PA1225 and PA4975	59
3.2.2.1	Transformation into expression hosts <i>E. coli</i> BL21(DE3) and <i>E. coli</i> BL21 CodonPlus(DE3)-RP	59
3.2.2.2	Overexpression of recombinant proteins	61
3.2.2.2.1	Overexpression of PA1224	61
3.2.2.2.2	Overexpression of PA1225	64
3.2.2.2.3	Overexpression of PA4975	68
3.2.3	Purification and quantification of recombinant proteins	72
3.2.3.1	Purification with Immobilised Metal-ion Affinity Chromatography	72

3.2.3.2	Dialysis and quantification of protein stocks	74
3.2.3.3	Protein molecular weight determination	75
3.3	Discussion	77
Chapter 4	Characterisation of purified recombinant proteins PA1224, PA1225 and PA4975.....	81
4.1	Introduction	81
4.2	Results	85
4.2.1	Characterisation of recombinant putative azoreductases	85
4.2.1.1	Determination of flavin selectivity for putative azoreductase proteins from <i>P. aeruginosa</i> PAO1	85
4.2.1.2	Absorbance spectra of FMN, FAD, PA1224 and PA1225	85
4.2.1.3	Thin Layer Chromatography.....	88
4.2.1.4	Differential Scanning Fluorimetry	90
4.2.2	Enzymatic activity of putative azoreductases from <i>P. aeruginosa</i> PAO1	92
4.2.2.1	Calculation of the molar extinction coefficient for NAD(P)H, ANI and the azo substrates	92
4.2.2.2	Identifying cofactor selectivity of PA1224, PA1225 and PA4975	96
4.2.2.3	Substrate specificity	102
4.2.2.3.1	PA1224.....	103
4.2.2.3.2	PA1225.....	105
4.2.2.3.3	PA4975.....	107
4.3	Discussion	109
Chapter 5	A continued investigation of azoreductases and NAD(P)H quinone oxidoreductases from <i>P. aeruginosa</i> PAO1	112
5.1	Introduction	112
5.2	Results	117
5.2.1	Overexpression and purification of recombinant proteins	117
5.2.2	Dialysis and quantification of PA2580	119

5.2.3	Characterisation of recombinant azoreductases and quinone oxidoreductases ..	120
5.2.3.1	Absorbance spectra of azoreductases and quinone oxidoreductases.....	120
5.2.3.2	Confirming flavin selectivity.....	122
5.2.4	Crystallisation and structural determination of PA2580.....	125
5.2.4.1	Crystallisation of PA2580 with H ₂ NADPH	125
5.2.4.2	Structure determination of PA2580 with bound H ₂ NADPH.....	127
5.3	Discussion.....	130
Chapter 6	Phenotypic analysis of <i>P. aeruginosa</i> wild type and azoreductase-like gene deletion strains.....	137
6.1	Introduction.....	137
6.2	Results.....	143
6.2.1	Generation of complemented strains for the azoreductase-like gene deletion mutants.....	144
6.2.1.1	Preparation of genes of interest	144
6.2.1.2	Preparation of the cloning vector	147
6.2.1.3	Obtaining and screening successful clones	148
6.2.1.4	Transformation into <i>P. aeruginosa</i> PAO1 transposon insertion mutant strains	150
6.2.2	Confirmation of gene expression in the complemented strains	152
6.2.3	Phenotypic analysis of <i>P. aeruginosa</i> PAO1 and TBCF 10839 strains.....	155
6.2.3.1	Growth analysis of <i>P. aeruginosa</i> PAO1 strains along with <i>P. aeruginosa</i> TBCF 10839 strains	155
6.2.3.2	Comparison of CFU/mL of all <i>P. aeruginosa</i> PAO1 strains and all <i>P. aeruginosa</i> TBCF strains	157
6.2.3.3	Minimum Inhibitory Concentration	158
6.3	Discussion.....	161
Chapter 7	Conclusions.....	166
7.1	Cloning of putative <i>P. aeruginosa</i> PAO1 azoreductase genes	166

7.2	Production and purification of suspected <i>P. aeruginosa</i> PAO1 azoreductase enzymes as recombinant proteins	166
7.3	Biochemical and enzymatic analysis of proposed <i>P. aeruginosa</i> PAO1 azoreductase and NQO recombinant proteins	167
7.4	Structural determination and analysis of <i>P. aeruginosa</i> PAO1 azoreductase and NQO, PA2580	168
7.5	Analysis of <i>P. aeruginosa</i> PAO1 antibiotic resistance using azoreductase and NQO single gene transposon mutants and corresponding complemented strains.....	168
APPENDIX I.....		170
APPENDIX II.....		171
APPENDIX III.....		172
APPENDIX IV.....		173
APPENDIX V.....		174
APPENDIX VI.....		175
APPENDIX VII.....		183
References		198

List of Figures

Figure 1.1 Micro-organisms isolated from the lungs of Cystic Fibrosis patients in 2015	4
Figure 1.2 Cellular envelope of gram-negative bacteria	6
Figure 1.3 Phylogenetic tree showing the relationship between known and putative azoreductases from <i>P. aeruginosa</i> PAO1	15
Figure 3.1 Structural comparison of hNQO1 and paAzoR1	49
Figure 3.2 pET-28b vector map	51
Figure 3.3 PCR amplification of <i>pal224</i> and <i>pal225</i> from <i>P. aeruginosa</i> PAO1	55
Figure 3.4 Endonuclease restriction digest of pET-28b	56
Figure 3.5 <i>E. coli</i> JM109 colony screening for successful clones	58
Figure 3.6 <i>E. coli</i> BL21(DE3) and <i>E. coli</i> BL21 CodonPlus(DE3)-RP transformants screening	60
Figure 3.7 Overexpression of PA1224 recombinant protein in <i>E. coli</i> BL21(DE3)	63
Figure 3.8 Optimisation of PA1225 recombinant protein overexpression in <i>E. coli</i> BL21(DE3)	66
Figure 3.9 Overexpression of PA1225 recombinant protein in <i>E. coli</i> BL21(DE3)	67
Figure 3.10 Overexpression of PA4975 recombinant protein in <i>E. coli</i> BL21(DE3)	70
Figure 3.11 Overexpression of PA4975 recombinant protein in <i>E. coli</i> BL21- CodonPlus(DE3)-RP	71
Figure 3.12 Purification of putative <i>P. aeruginosa</i> PAO1 recombinant azoreductase protein using IMAC	73
Figure 3.13 Purified recombinant proteins following ion exchange dialysis preparation for storage	76
Figure 4.1 Proposed reduction mechanism for azo compound balsalazide by paAzoR1	83
Figure 4.2 PA1224 structure modelled on a quinone reductase from <i>Klebsiella pneumoniae</i> with 67% sequence identity superposed against hNQO1	84
Figure 4.3 Absorption spectra for PA1224 and PA1225	87
Figure 4.4 Absorption spectra comparison of recombinant proteins from <i>P. aeruginosa</i> PAO1	87
Figure 4.5 TLC optimisation of free FMN and FAD (a) and TLC profiles of PA1224 and PA1225	89

Figure 4.6 Absorption spectra of NADH (a), NADPH (b), PLU (c), ANI (d), methyl red (e) and amaranth (f)	93
Figure 4.7 Determination of molar extinction coefficient for NADH (a), NADPH (b), ANI (c) and methyl red (d).....	94
Figure 4.8 Rate of ANI reduction by PA1225 with and without NAD(P)H.....	98
Figure 4.9 Nicotinamide and flavin selectivity of <i>P. aeruginosa</i> PAO1 recombinant proteins.....	99
Figure 4.10 Activity assays for PA1224 (a), PA1225 (b) and PA4975 (c) in the presence of varying flavin concentrations.....	101
Figure 4.11 PA1224 substrate specificity profile.....	104
Figure 4.12 PA1225 substrate specificity profile.....	106
Figure 4.13 PA4975 substrate specificity profile.....	108
Figure 5.1 Chemical structures of H ₂ NADPH (a) and cibacron blue (b)	116
Figure 5.2 Overexpression of PA2580 recombinant protein in <i>E. coli</i> BL21(DE3)	118
Figure 5.3 Purification of PA2580 recombinant protein using IMAC	119
Figure 5.4 Absorption spectra for PA2280 (a), PA2580 (b), PA1204 (c) and PA0949 (d)	121
Figure 5.5 Activity assays for PA2280 (a), PA2580 (b), PA1204 (c) and PA0949 (d) in the presence of varying flavin concentrations.....	123
Figure 5.6 Crystals of PA2580	126
Figure 5.7 Crystal structure of the PA2580 homodimer	128
Figure 5.8 Binding of compounds in the active site of PA2580	128
Figure 5.9 Structural comparison of PA2580 and ecMdaB	133
Figure 5.10 Hydrogen bonds are formed between PA2580 and FAD	133
Figure 5.11 Surface comparison of PA2580 against other MdaB structures.....	134
Figure 5.12 Comparison of nicotinamide binding to PA2580 and smMdaB.....	135
Figure 6.1 pUCP24 vector map	145
Figure 6.2 PCR amplification of azoreductases and azoreductase-like genes from <i>P. aeruginosa</i> PAO1 for cloning into pUCP24	146
Figure 6.3 Endonuclease restriction digest of pUCP24.....	147
Figure 6.4 <i>E. coli</i> JM109 transformed with pUCP24 ligated with the azoreductase-like genes.....	149
Figure 6.5 <i>P. aeruginosa</i> PAO1 single gene transposon insertion mutants confirmation in competent cells.....	151
Figure 6.6 <i>P. aeruginosa</i> PAO1 single gene transposon insertion mutants transformed with pUCP24.....	151

Figure 6.7 Total RNA extracted from <i>P. aeruginosa</i> PAO1 strains	153
Figure 6.8 Gene expression of <i>P. aeruginosa</i> PAO1 WT, gene deletion mutants transformed with pUCP24 and the complemented strains.....	154
Figure 6.9 Growth analysis <i>P. aeruginosa</i> PAO1 strains	156
Figure 6.10 Growth analysis <i>P. aeruginosa</i> TBCF 10839 strains.....	156

List of Tables

Table 1.1 New azoreductase-like enzymes identified in <i>P. aeruginosa</i> PAO1	14
Table 1.2 Azoreductases and azoreductase-like genes implicated in bacterial physiological functions	16
Table 2.1 Details of <i>P. aeruginosa</i> and <i>E. coli</i> strains	19
Table 2.2 Media used in this study	19
Table 2.3 Materials used for nucleic acid gel electrophoresis	20
Table 2.4 Plasmids used in this study	21
Table 2.5 Primers used for the cloning process of azoreductase-like genes <i>pa1224</i> and <i>pa1225</i> from <i>P. aeruginosa</i> PAO1	22
Table 2.6 PCR reaction mix for PCR using HotStar HiFi DNA polymerase	22
Table 2.7 Thermocycling conditions for PCR using HotStar HiFi DNA polymerase	22
Table 2.8 Primers used for the cloning process of azoreductase-like genes from <i>P. aeruginosa</i> PAO1 into pUCP24 vector	23
Table 2.9 Restriction digest of vectors and inserts	24
Table 2.10 Antarctic phosphatase digestion components and concentrations	25
Table 2.11 Primers used to screen for successful clones of azoreductase-like genes <i>pa1224</i> , <i>pa1225</i> and <i>pa4975</i>	28
Table 2.12 Primers used for sequencing of positive clones	29
Table 2.13 Materials used for SDS-PAGE	32
Table 2.14 Substrates used for the characterisation of the <i>P. aeruginosa</i> putative azoreductase proteins	38
Table 2.15 Reaction mix used for the enzymatic assays	39
Table 2.16 Gene-specific primers used to confirm the transposon insertion in the azoreductase-like genes	43
Table 2.17 Internal gene-specific primers used to check for gene expression	45
Table 3.1 Gene details of known azoreductases and azoreductase-like genes from <i>P. aeruginosa</i> PAO1	48
Table 3.2 Table listing the total yield of recombinant putative azoreductases produced	74
Table 3.3 Estimated molecular weight of each purified recombinant protein along with the actual molecular weight	76
Table 4.1 Binding of flavin cofactors to purified recombinant proteins	91
Table 4.2 NAD(P)H, ANI and azo compounds λ_{\max} and molar extinction coefficients	95

Table 4.3 Enzymatic reaction component combinations used to test protein activity and NAD(P)H and flavin selectivity	98
Table 5.1 Nucleic acid sequence identity between known and putative <i>P. aeruginosa</i> PAO1 azoreductase/NQO genes.....	113
Table 5.2 Binding of flavin cofactors to azoreductase and NQO enzymes	124
Table 5.3 Successful crystallisation conditions for PA2580.....	126
Table 5.4 Processing and refinement statistics for PA2580 and PA2580-nicotinamide....	129
Table 6.1 Azoreductase and azoreductase-like genes implicated in antimicrobial susceptibility.....	139
Table 6.2 Minimum inhibitory concentration of <i>P. aeruginosa</i> PAO1 wild type and the azoreductase-like gene transposon mutants for a range of antibiotics	142
Table 6.3 Estimated size of amplified putative azoreductase genes compared to actual size of PCR product sizes	146
Table 6.4 CFU/mL for all <i>P. aeruginosa</i> strains	157
Table 6.5 Minimum inhibitory concentration values (in µg/mL) for a range of antimicrobial agents against <i>P. aeruginosa</i> PAO1 strains	159
Table 6.6 Minimum inhibitory concentration values (in µg/mL) for a range of antimicrobial agents against <i>P. aeruginosa</i> TBCF 10839 strains.....	160

Abstract

Pseudomonas aeruginosa is a prevalent nosocomial pathogen predominantly associated with infections in immune compromised individuals and long term colonisation and pathogenesis in the lungs of Cystic Fibrosis patients. With multi-drug resistant strains increasingly common, the discovery of novel targets for antimicrobial chemotherapy is of utmost importance and expansion of data on *P. aeruginosa*'s complex genome could facilitate this. Azoreductases are a group of enzymes mainly noted for their reductive capacity against azo and quinone compounds. Ubiquitous amongst many classes of organism including prokaryotes and eukaryotes, the primary physiological role of azoreductases remains unclear. This study characterises azoreductase-like enzymes from *P. aeruginosa* in terms of biochemical properties, substrate specificity and structural analysis. The effect of these enzymes on bacterial physiology in *P. aeruginosa* is also explored in relation to antibiotic susceptibility.

Three azoreductase-like genes from *P. aeruginosa* (*pa1224*, *pa1225* and *pa4975*) were overexpressed in *E. coli* strains following molecular cloning. Recombinant proteins were biochemically characterised by means of Thin Layer Chromatography, Differential Scanning Fluorimetry and enzymatic assays. All enzymes were noted to be selective for FAD as the flavin cofactor and NADPH as the preferred reductant. All three enzymes were confirmed as NAD(P)H dependent quinone oxidoreductases (NQOs) with PA1224 also catalysing reduction of the azo substrate methyl red, albeit at a rate an order of magnitude lower than that observed for the quinone compounds. The preferred flavin cofactor for four previously characterised azoreductase and NQO enzymes (PA2280, PA2580, PA1204 and PA0949) was also explored and PA2280 and PA0949 were observed to select for FMN while PA2580 and PA1204 were selective for FAD. The crystal structure of PA2580 was solved with the nicotinamide group of NADPH bound and was noted to form a homodimer with the same short flavodoxin-like fold as previously described for other members of this enzyme family. Complemented strains of azoreductase-like gene deletion mutants of *P. aeruginosa* PAO1 were generated via molecular cloning and used to monitor the effects of these enzymes on antibiotic susceptibility. Antimicrobial sensitivity assays were carried out and although the knockout strains displayed increased sensitivity to fluoroquinolones, they did not revert to the wild type phenotype upon reinsertion of the genes of interest.

This study has for the first time characterised three new NQO's from *P. aeruginosa* PAO1 and solved the crystal structure of an azoreductase/NQO with nicotinamide bound. With these findings and a library of complemented strains generated, this original study offers a platform for the continued research into the physiological role of these enzymes.

Chapter 1 Introduction

1.1 *Pseudomonas aeruginosa*

Pseudomonas aeruginosa is a gram-negative rod shaped bacterium. Ubiquitous in a variety of environmental niches, it encompasses a striking ability to adapt to and thrive in both natural and artificial or human-associated ecosystems ranging from plant surfaces and waste water to life support equipment and dilute antiseptics (Todar, 2006, Slekovec *et al.*, 2012). At 6.3 million base pairs, *P. aeruginosa* possesses a large bacterial genome with a high proportion of genes involved in catabolism, efflux and transport of organic compounds (Stover *et al.*, 2000). Consistent with this genetic complexity, it exhibits numerous virulence factors and is versatile in adapting different phenotypes under environmental stress such as mucoidal vs. planktonic growth and aerobic vs. anaerobic respiration and this is attributed to the large percentage of genes devoted to regulatory systems including environmental sensors and transcriptional regulators (Willey *et al.*, 2011, Stover *et al.*, 2000).

Typically an aerobic microorganism, *P. aeruginosa* can survive in anaerobic or oxygen deficient environments such as soil and water or the mucopurulent lung of a Cystic Fibrosis (CF) sufferer (Willey *et al.*, 2011, Worlitzsch *et al.*, 2002). This is facilitated by the bacterium's ability to respire as a facultative anaerobe either by arginine fermentation via the arginine deiminase pathway or by the use of nitrite, nitrate or nitrous oxide as alternative electron acceptors (Vander Wauven *et al.*, 1984, Zannoni, 1989).

P. aeruginosa can exist in a planktonic or mucoidal form. Planktonic cells are free living and exist as single cells suspended in a liquid medium (Spoering and Lewis, 2001). During anaerobic growth or proliferation in a nutrient deficient environment, the mucoidal phenotype is often observed for *P. aeruginosa* (Yoon *et al.*, 2002). Mucoidal growth, or biofilm formation, is bacterial proliferation which forms surface-associated microbial cells that are enclosed in an extracellular polymeric substance (EPS) matrix composed of bacterial-derived biomolecules such as exopolysaccharides, polypeptides and extracellular DNA (Donlan, 2002). The EPS, which forms the majority of the biofilm, offers robustness to the bacterial community both physically and chemically by decreasing penetration of

toxic substances and resisting mechanical forces (Hall-Stoodley and Stoodley, 2009, Lieleg *et al.*, 2011).

Other virulence factors of *P. aeruginosa* include surface appendages such as flagella and pili which facilitate both cell motility and adhesion and are implicated in the establishment of host infection (Kohler *et al.*, 2000, Yeung *et al.*, 2009, Brimer and Montie, 1998). Evolutionally linked to the flagella is the needle-like appendage of the type III secretion system which ‘injects’ bacterial exotoxins into the host cells and it is thought that this mechanism allows *P. aeruginosa* to exploit breaches in the epithelial barrier thus promoting colonisation (Hauser, 2009). In addition, several proteases are secreted by *P. aeruginosa* which can degrade host defence molecules and disrupt epithelial tight junctions (Kipnis *et al.*, 2006). Many of these virulence factors are controlled by quorum sensing (QS), a mechanism by which autoinducer molecules are constitutively expressed by each bacterial cell. The transcriptional regulatory activity of these molecules is concentration dependent: thus when the bacterial population reaches a certain critical mass, a coordinated response occurs (Gellatly and Hancock, 2013).

The versatility of *P. aeruginosa* and its ability to control gene expression in response to environmental stimuli is reflected in the large number of hosts that can be colonised by this pathogen ranging from plants such as *Arabidopsis thaliana* (Thale cress) (Plotnikova *et al.*, 2000) and *Lactuca sativa* (Romaine lettuce) (Starkey and Rahme, 2009) to invertebrates like *Drosophila melanogaster* (fruit fly) (D'Argenio *et al.*, 2001) and *Galleria mellonella* (greater wax moth) (Miyata *et al.*, 2003) and also mammals including humans.

1.1.1 *P. aeruginosa* infections

P. aeruginosa is one of the few microorganism species that can infect both plants and humans. It has been identified as the causative agent for soft rot in numerous plant species including *Panax ginseng* (Ginseng) (Gao *et al.*, 2014), *A. thaliana* (Plotnikova *et al.*, 2000) and *L. sativa* (Starkey and Rahme, 2009) and has also been reported to colonise ornamental plants such as African violet, azaleas, chrysanthemums, hydrangeas and petunias (Cho, 1975). Interestingly, studies have shown that there is a high level of molecular conservation regarding pathogenesis of *P. aeruginosa* across plant, invertebrate and mammalian hosts indicating that the disease causing ability of *P. aeruginosa* is credited to a basic set of virulence genes or that some of these genes may encode regulatory proteins which control different effector molecules which may be specific for plants or animals (Miyata *et al.*, 2003, Rahme *et al.*, 1997).

The incidence of *P. aeruginosa* in the natural human flora can vary and is site-specific. It occurs infrequently in the pharynx and mouth (<5% of the population) but can commonly occupy the lower gastrointestinal tract (approximately 25% of the population) (Morrison Jr and Wenzel, 1984, Todar, 2006). It is an opportunistic pathogen, rarely causing disease in immunocompetent individuals with most cases of community acquired infection occurring as a result of prolonged exposure to contaminated water (Mena and Gerba, 2009). Community acquired infections can often include ulcerative keratitis, otitis externa and skin and soft tissue infections (Driscoll *et al.*, 2007). It is infrequently isolated from patients with community acquired pneumonia (0.9–1.9% incidence) however in such cases it typically results in bacteraemia, thus the mortality rate is relatively high at 30–35% (Fujitani *et al.*, 2011, Tsuji *et al.*, 2014, Hachette *et al.*, 2000).

An important nosocomial pathogen, *P. aeruginosa* is estimated to colonise up to 15% of hospitalised patients (Cuttelod *et al.*, 2011). International investigations have identified it as the most common microorganism to cause infection in intensive care units (ICUs) in Central/South America and Asia. Worldwide, it is the most prevalent gram-negative organism, isolated from approximately 20% of ICU patients with infection in the ICU independently affiliated with prolonged hospitalisation and increased mortality rates (Vincent *et al.*, 2006, Vincent *et al.*, 2009, Dasgupta *et al.*, 2015, Volakli *et al.*, 2010). A major contributing factor in the case of ICU infections is the ability of *P. aeruginosa* to survive on medical devices such as catheters and mechanical ventilators (Driscoll *et al.*, 2007). This bacterium (along with *Staphylococcus aureus*) is the leading cause of ventilator associated pneumonia and is often the most commonly isolated pathogen in infected burn wounds (Fujitani *et al.*, 2011, Ramírez-Estrada *et al.*, 2016, Yildirim *et al.*, 2005, Song *et al.*, 2001). It is also commonly identified as the causal agent in surgical site infections and nosocomial urinary tract infections (Weinstein *et al.*, 2005).

As well as being an important nosocomial pathogen, *P. aeruginosa* is predominantly associated with both acute and chronic infections in individuals with compromised host defences such as cancer patients, HIV sufferers and people with neutropenia (Driscoll *et al.*, 2007, Lyczak *et al.*, 2000). Perhaps most notorious for long term lung colonisation in those suffering from CF, it chronically colonises over 70% of adult CF patients with 25% infected with multi-drug resistant (MDR) strains (Figure 1.1) (CFF, 2015). CF is an autosomal recessive disorder where a mutation in the Cystic Fibrosis transmembrane regulator results in dysregulation of epithelial fluid transport in the lung which subsequently develops a thickened airway surface liquid (Clunes and Boucher, 2007). The

genomic plasticity of *P. aeruginosa* and its capacity to undergo phenotypic alteration enables it to colonise the CF lung long term. As a result, strains from chronic infections are less virulent than those isolated from acute infections with many virulence factors attenuated including loss of flagella and pili and altered metabolic pathways (Sousa and Pereira, 2014). The microorganism's presentation of the mucoidal phenotype within the CF lung forms a protective barrier against the host's immune system as well as antimicrobial treatment making it difficult to eradicate (Ciofu *et al.*, 2012). These phenotypic alterations along with prolonged antibiotic exposure achieved from long term colonisation results in highly drug resistant bacteria. Thus the issue of *P. aeruginosa* infections in immunocompromised hosts is exacerbated by the microorganism's intrinsic, acquired and adaptive resistance to antibiotics.

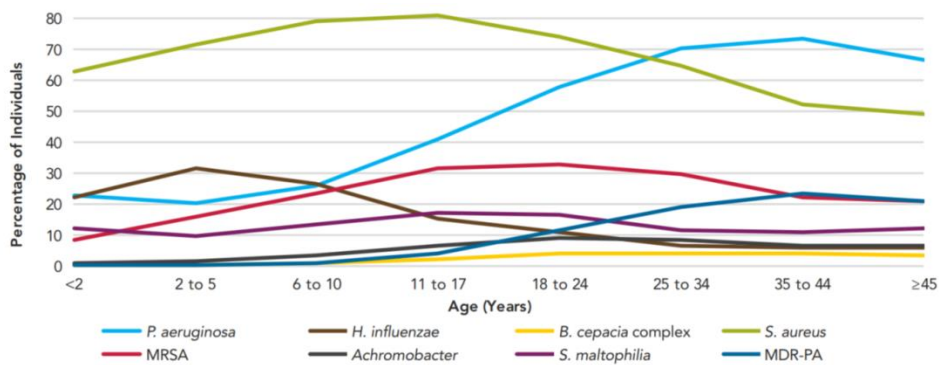


Figure 1.1 Micro-organisms isolated from the lungs of Cystic Fibrosis patients in 2015
 Graph representing the predominant microorganisms isolated from the lungs of CF patients in 2015. Among all species isolated, *S. aureus* and *P. aeruginosa* are the most prevalent with the former present in >80% of individuals aged between 6 and 17 years old and the latter colonising >70% of CF patients aged 25 to 44+. Within the older group approximately 25% are infected with MDR *P. aeruginosa* strains. Figure is taken from the 2015 Annual Data Report by the Cystic Fibrosis Foundation Patient Registry (CFF, 2015).

1.1.2 Antibiotic resistance in *P. aeruginosa*

In recent years the resistance of microorganisms to antimicrobial treatment has become a major challenge to modern medicine. Continued increases in the number of immunocompromised and immune suppressed patients coupled with the ability of bacteria to rapidly mutate in response to environmental stimuli has resulted in the emergence of ‘superbugs’ – strains of bacteria that are resistant to practically all available antimicrobials. Antibiotic resistance occurs when a microorganism develops the capacity to resist chemotherapeutic treatment to which it is normally susceptible. This evolutionary advantage of bacteria is especially true for *P. aeruginosa* which, with its ability to rapidly develop resistance to multiple classes of antibiotics during the course of treating a patient, has been labelled by the Centre for Disease Control as a ‘serious threat’ (CDC, 2013) and listed by the World Health Organisation (along with *Acinetobacter baumannii* and *Enterobacteriaceae*) as the MDR pathogen of most critical importance for the discovery of new antimicrobials (WHO, 2017). Approximately 13% of healthcare associated *P. aeruginosa* infections are multi-drug resistant and the rise in MDR isolates has been estimated to have increased by 10% from the early 1990’s to 2002 (Livermore, 2002, Obritsch *et al.*, 2004). Along with developing resistance via horizontal gene transfer and adaptive mutations, *P. aeruginosa* is naturally resistant to many antimicrobials altogether making it a particularly difficult pathogen to treat once infection has been established.

1.1.2.1 Intrinsic resistance

The intrinsic tolerance of *P. aeruginosa* to many structurally unrelated antibacterial agents is predominantly due to the low permeability of its outer membrane (Figure 1.2). Comprising of a dense lipopolysaccharide matrix, the outer membrane has 12-100 fold lower permeability than other gram-negative bacteria such as *Escherichia coli* (Yoshimura and Nikaido, 1982, Hancock, 1998). The low levels of antibiotic penetration into the cell are thought to be attributed to the small channel size of *P. aeruginosa*’s outer membrane porins OprD and OprB and the limited number of functional large channels of major porin OprF (Yoshihara and Nakae, 1989, Hancock, 1998). On the other hand, these porins can also facilitate uptake of antimicrobials into the cell, for example OprD has been implicated in the diffusion of carbapenems into the bacterial periplasmic space (Lister *et al.*, 2009, Trias and Nikaido, 1990).

The avoidance of antibiotic accumulation in the cell can be aided by another intrinsic mechanism, namely, active export by membrane associated pumps (Lister *et al.*, 2009).

These complexes typically form a channel spanning the entire membrane which allows the transport of toxic molecules from the periplasmic space and cytoplasm into the extracellular environment (Lister *et al.*, 2009). Sequence analysis of *P. aeruginosa* has noted efflux pumps from five different superfamilies present in the genome with the largest number of pumps belonging to the resistance-nodulation-division family (Stover *et al.*, 2000). One such pump, MexAB-OprM, is constitutively expressed in wild type cells and can export β -lactams such as carboxypenicillins, extended spectrum cephalosporins and carbapenems (Poole, 2001).

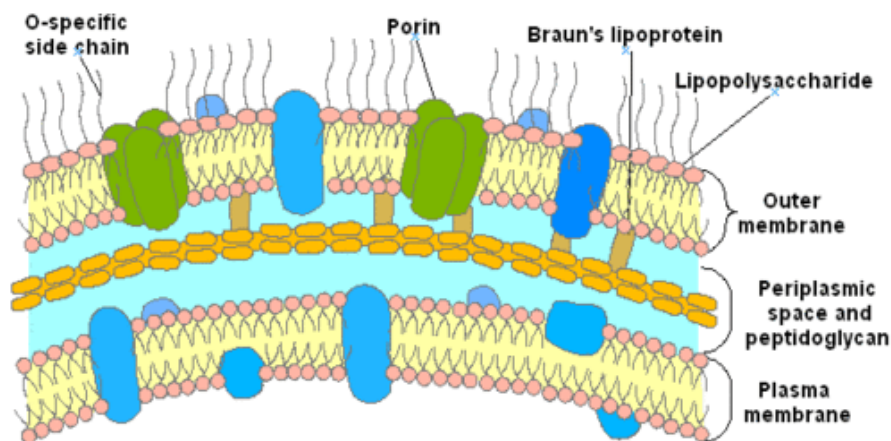


Figure 1.2 Cellular envelope of gram-negative bacteria

The structure of the cell membrane in gram-negative bacteria is illustrated. The cellular envelope is characterised by a cytoplasmic membrane, a periplasmic space and an outer membrane. The outer membrane is mainly comprised of a dense lipopolysaccharide matrix that is highly hydrophobic and has low permeability for exogenous hydrophilic molecules. Figure is from Salmi *et al.* (Salmi *et al.*, 2008).

1.1.2.2 Adaptive resistance

Adaptive resistance is inducible and occurs in *P. aeruginosa* as a response to changing environmental stimuli and stresses such as differing media conditions, altered growth states, a change in pH and of course, antibiotic exposure (Fernandez *et al.*, 2011). These environmental cues modulate gene expression leading to adaptations relating to efflux pumps, outer membrane porins and enzyme production (Lister *et al.*, 2009). Unlike intrinsic resistance, adaptive resistance will be lost upon removal of triggering factors with the organism reverting to wild type susceptibility (Breidenstein *et al.*, 2011). The significance of adaptive resistance in *P. aeruginosa* is consistent with the large repertoire of regulatory genes within its genome (9.4%) (Stover *et al.*, 2000).

As mentioned in the previous section, the low permeability of the outer membrane coupled with efflux pump mediated removal of toxic agents from the cell grants *P. aeruginosa* a high level of intrinsic tolerance to a broad range of antibiotics. To decrease antimicrobial susceptibility in times of environmental strain, the expression of these phenotypes can be altered and result in adaptive resistance.

There is a long since established relationship between outer membrane porin OprD expression and carbapenem sensitivity. OprD has been implicated as the primary portal of entry for carbapenems into the cell with loss of OprD from the outer membrane resulting in an up to 32 fold decreased susceptibility to carbapenems including meropenem, imipenem and doripenem (Trias and Nikaido, 1990). Adaptive resistance relating to OprD involves numerous mechanisms which decrease transcriptional expression of *oprD* and/or mutations that disrupt translational production resulting in a dysfunctional porin. These mechanisms can include *oprD* promoter disruptions and premature termination of *oprD* transcription (Lister *et al.*, 2009).

While loss of OprD assists in developing an effective barrier for drug entry into the cell, active export via membrane associated pumps is also functional in reducing drug accumulation within the cytoplasm. Although constitutively expressed within the cell, *mexAB-oprM* expression is tightly controlled by several regulatory proteins including MexR and NalD (Poole *et al.*, 1996, Sobel *et al.*, 2005). Upregulation of this efflux pump has been shown to occur in times of oxidative stress with oxidised MexR proving inactive in repression of the *mexA* promoter, subsequently reducing the efficiency of antimicrobial agents such as fluoroquinolones, penicillins, cephalosporins and carbapenems (Chen *et al.*, 2008).

Exposure to β -lactam antibiotics results in the induction of a chromosomally encoded β -lactamase, AmpC, which is a major adaptive mechanism in *P. aeruginosa* (Breidenstein *et al.*, 2011). Wild type *P. aeruginosa* constitutively produces low levels of AmpC however when expression is increased, resistance is developed to almost all β -lactams, with the exception of carbapenems (Colom *et al.*, 1995, Sanders and Sanders, 1986). Although the mechanisms by which AmpC is overexpressed are not clear, induction involves the binding of a β -lactam or β -lactamase inhibitor to penicillin binding proteins (Sanders *et al.*, 1997). Like other adaptive mechanisms, once the inducing factor is no longer present, wild type expression is reinstated (Lister *et al.*, 2009).

The molecular mechanisms behind adaptive resistance have only recently begun to be investigated and much remains to be understood. It is evident that the mechanisms are complex involving intricate regulatory responses. Transcriptome analysis upon exposure to antibiotics and toxic compounds could assist in identifying modulating genes and offer new targets to tackle antimicrobial resistance.

1.1.2.3 Acquired resistance

Another attribute of *P. aeruginosa* responsible for reducing its sensitivity to antibiotics is acquired resistance. Acquired resistance manifests via horizontal transfer of genetic elements and chromosomal mutations. Horizontal transfer of antimicrobial resistance genes can be achieved by conjugation, transformation and transduction of DNA elements (including plasmids, transposons, integrons, prophages and resistance cassettes) which can lead to MDR organisms (Breidenstein *et al.*, 2011). This type of acquisition is particularly relevant for aminoglycoside and β -lactam resistance. One such resistance mechanism is a group of enzymes referred to as the aminoglycoside modifying enzymes. Transferred via mobile genetic elements they function by acetylation, phosphorylation or adenylation of the aminoglycoside antibiotics, altering their structure and reducing affinity with their main target, the 30S ribosomal subunit (Vakulenko and Mobashery, 2003). *P. aeruginosa* can also acquire plasmids encoding β -lactamases such as PSE-1 and PSE-4, and of particular concern, extended spectrum β -lactamases including OXA types and IMP and VIM metallo- β -lactamases (Livermore, 1995). A *P. aeruginosa* strain harbouring the latter three is susceptible to only polymyxins and ciprofloxacin (Livermore, 2002).

The second form of acquired resistance is mutational resistance. These spontaneous mutations occur at varying frequencies depending on the bacterial growth conditions. For example, incidence of mutations increases in the presence of DNA damaging agents with

proliferation in the presence of sub-inhibitory levels of ciprofloxacin giving rise to mutational resistance to meropenem (Tanimoto *et al.*, 2008). Similarly, a large increase in mutation frequency for ciprofloxacin resistance (>100 fold) occurs during mucoidal growth compared to that observed in free living cells (Driffield *et al.*, 2008). This is likely due to the downregulation of antioxidant enzymes during growth in a biofilm leading to increased DNA damage.

As with intrinsic and adaptive resistance, outer membrane porins, efflux pumps and AmpC expression are all also implicated in acquired resistance mechanisms. Mutations in the OprD porin or to the regulatory genes *mexT* or *mexS* which control OprD expression can lead to multiple antibiotic resistance (Walsh and Amyes, 2007). Additionally, derepression of the MexAB-OprM pump can occur as a result of mutations in either of the genes encoding *mexR* and *mexZ* which can lead to aminoglycoside, fluoroquinolone and cefepime resistance in *P. aeruginosa* (Stickland *et al.*, 2010, Muller *et al.*, 2011). Finally hyperproduction of β -lactamases results from mutation of an effector of the *ampC* β -lactamase, AmpD, which controls activity of the AmpR regulatory protein (Juan *et al.*, 2006).

From the available literature on mutation-derived acquired resistance, it is evident that such mutations occur in a vast number of unrelated genes and can grant resistance to a variety of antimicrobial agents. To illustrate this point, the aminoglycoside resistome involves 150 different genes relating to energy metabolism, lipopolysaccharide biosynthesis and DNA replication and repair (Dötsch *et al.*, 2009, Alvarez-Ortega *et al.*, 2010). Also, the fluoroquinolone resistome involves efflux regulators, iron transport genes, phage-related genes and NADH dehydrogenase genes (Dötsch *et al.*, 2009, Breidenstein *et al.*, 2008). The vast array of genes and mechanisms involved in acquired resistance to multiple antibiotics highlights the difficulties in finding reliable novel targets for antimicrobial chemotherapy of *P. aeruginosa*.

The genetic versatility of *P. aeruginosa* as discussed here and its outstanding ability to co-regulate multiple resistance mechanisms make it a continuously moving target and a great therapeutic challenge. Despite the increasing pandemic of MDR *P. aeruginosa*, there is a paradoxical decrease in the development of new antibiotics, thus the identification and development of novel targets for antimicrobial chemotherapy is essential. Understanding unexplored parts of the genome may give new leads in the fight against resistance.

1.2 Azoreductases

Azoreductases are a group of enzymes which catalyse the reductive cleavage of the azo bond (-N=N-). The majority of characterised azoreductases are FMN or FAD dependent and require NAD(P)H as an electron donor to carry out the reduction reaction (Nakanishi *et al.*, 2001, Ryan *et al.*, 2010a). The reduction is a double displacement reaction and occurs via an obligate two electron process where a hydride is transferred from NAD(P)H to the flavin and then on to the substrate in question (Ryan *et al.*, 2010a). In addition to azo compounds, the enzymes have been shown to reduce a range of other substrates including quinones and nitroaromatics (Ryan *et al.*, 2010b, Ryan *et al.*, 2014, Liu *et al.*, 2007a, Ryan *et al.*, 2011). The reduction of azo and quinone substrates occurs via a similar mechanism with the exception that azoreduction is a double ping pong bi bi reaction where two NAD(P)H are required to reduce the substrate, while reduction of quinone compounds only requires one NAD(P)H molecule (Ryan *et al.*, 2010a, Ito *et al.*, 2006). For this reason, Ryan and colleagues (2014) proposed that azoreductases and NAD(P)H quinone oxidoreductases (NQOs) are part of the same enzyme superfamily.

1.2.1 Azoreductases in bioremediation and medicine

Azoreductase enzymes are predominantly associated with their ability to detoxify azo dyes and activate azo pro-drugs. Per annum, $1-1.5 \times 10^5$ tons of dyestuff is released into effluent wastewaters from textile and other manufacturing industries and among these, azo dyes are the most common (Rai *et al.*, 2005). This can negatively affect water quality which subsequently disrupts photosynthesis, decreasing dissolved oxygen levels and severely disturbing aquatic ecosystems (Rai *et al.*, 2005, van der Zee and Villaverde, 2005). It also has implications for human health with many of these compounds and their breakdown products (often aromatic amines) toxic and potentially carcinogenic depending on their structure, substitution groups and reactivity (Golka *et al.*, 2004, Schneider *et al.*, 2004, Maran and Slid, 2003). For this reason, much research on azoreductases focuses on their possible use in the bioremediation of these substances as enzymatic treatment can carry out complete mineralisation of dye chemicals and their metabolites while remaining low cost and environmentally friendly (Chen, 2006, Husain, 2006, Mahmood *et al.*, 2016).

Azo pro-drugs such as sulfasalazine and balsalazide are frequently used in the treatment of inflammatory bowel disease. They have been developed by cross linking an inert carrier molecule to the non-steroidal anti-inflammatory, 5-aminosalicylic acid (5-ASA), via an azo bond to prevent rapid adsorption in the gastrointestinal tract (Haagen Nielsen and

Bondesen, 1983, Makins and Cowan, 2001). Upon cleavage of the azo bond by azoreductases synthesised by gut microflora, 5-ASA is released and its anti-inflammatory properties are activated (Peppercorn and Goldman, 1972). Along with anti-inflammatory compounds, azo chemistry has also been used in the development of other drugs such as antibiotics and anticancer therapeutics (Deka *et al.*, 2015, Sharma *et al.*, 2013).

1.2.2 Azoreductases and their associations in physiological functions

Azoreductases are found ubiquitously across many bacterial species including *E. coli*, *Enterococcus faecalis*, *Bacillus subtilis*, *Rhodobacter sphaeroides*, *S. aureus* and pseudomonads as well as in yeasts and humans (Nakanishi *et al.*, 2001, Chen *et al.*, 2004, Sugiura *et al.*, 2006, Liu *et al.*, 2007a, Chen *et al.*, 2005, Wang *et al.*, 2007, Jadhav *et al.*, 2007, Cui *et al.*, 1995). Extensive bioinformatics analysis based on homology of azoreductases from other species has led to the identification of several new azoreductase and NQO enzymes in *P. aeruginosa* including some from previously distinct enzyme families namely, modulator of drug activity B (MdaB), arsenic resistance protein H (ArsH), YieF and tryptophan repressor binding protein A (WrbA) (Wang *et al.*, 2007, Ryan *et al.*, 2014) (Table 1.1, Figure 1.3). Upon characterisation, many of these have been confirmed as NAD(P)H dependent flavoenzymes with the majority of those capable of reduction of azo, nitro and quinone compounds (Wang *et al.*, 2007, Ryan *et al.*, 2014, Ryan *et al.*, 2010a, Ryan *et al.*, 2011, Crescente *et al.*, 2016). The identification of enzymes from this family is difficult due to the large sequence diversity amongst members and this is perhaps why until recently, azoreductases and NQOs were considered two distinct enzyme groups (Ryan *et al.*, 2014).

Although the enzymatic activities of azoreductases from *P. aeruginosa* and other bacterial species have been extensively described, their primary physiological role remains unclear. Along with their uses in medicine and bioremediation and their ability to reduce a range of substrates, azoreductases and NQOs have also been implicated in other seemingly unrelated systems including QS, biofilm formation, host colonisation and antimicrobial resistance (Table 1.2) (Tan *et al.*, 2014, Goudeau *et al.*, 2013, Cattò *et al.*, 2015, Landstorfer *et al.*, 2014, Rakhimova *et al.*, 2008, Wang *et al.*, 2016, Van der Linden *et al.*, 2016).

The *E. coli* NQO, WrbA, which is a homologue of WrbA in *P. aeruginosa* PAO1, has been proven to interact with the anti-biofilm compound, Zosteric Acid, and the *wrbA* gene has been identified as one of the regulation targets for the master regulator of biofilm

formation (CsgD) in *E. coli*, indicating that this enzyme may be involved in the development of biofilms (Cattò *et al.*, 2015, Ogasawara *et al.*, 2011). A role in quorum sensing has been suggested as a result of an azoreductase and NQO from *P. aeruginosa*, MdaB, being significantly upregulated upon treatment with the QS inhibitor, Iberin (Tan *et al.*, 2014).

Azoreductases have been implied to play a fundamental role in plant colonisation with significant overexpression observed during *E. coli* O157 growth on radish sprouts and butterhead lettuce leaves (Landstorfer *et al.*, 2014, Van der Linden *et al.*, 2016). Similarly, AzoR is upregulated >100 fold in *Salmonella enterica serovar typhimurium* during growth on lettuce and cilantro leaves (Goudeau *et al.*, 2013). Evidence for an involvement in mammalian infections has also been observed. Gene deletion mutants of *Yersinia pseudotuberculosis* lacking the NQO encoding gene, *wrbA*, when infecting a mouse caecum display less virulence than the wild type and fail to establish a persistent infection (Avican *et al.*, 2015). In *P. aeruginosa*, azoreductase and NQO knockout strains are less capable of survival and dissemination in a murine infection model with reduced or total lack of survival apparent in the lung, caecum and spleen (Rakhimova *et al.*, 2008, Skurnik *et al.*, 2013).

Perhaps linked to their putative role in host colonisation, these enzymes have also been associated with the response to oxidative stress. Quinones can form semi-quinones when reduced by one electron reductases such as lipoyl dehydrogenase (Gonzalez *et al.*, 2005). These semi-quinones can generate superoxide radicals in the presence of molecular oxygen which can then be converted to hydrogen peroxide which in turn, can yield highly damaging hydroxyl radicals (Valko *et al.*, 2005, Cadenas *et al.*, 1992). Azoreductases and indeed, NQO's, act as two electron reductases which prevent the formation of semi-quinones, instead generating two electron reduced and redox stable quinols which can also scavenge and detoxify reactive oxygen species (ROS) (Soballe and Poole, 2000, Ross and Siegel, 2004). In *Pseudomonas syringae*, a 65% identical homologue of paAzoR2 is significantly upregulated in response to acetosyringae which is a plant phenol that induces oxidative stress against invading pathogens (Postnikova *et al.*, 2015). Liu and colleagues (2009) found that AzoR in *E. coli* protects against thiol-specific stress caused by electrophilic quinones and Landstorfer *et al.* (2015) speculated that this enzyme was involved in detoxification of oxidative stress inducing secondary plant metabolites such as salicylic acid and jasmonic acid. This data implies that these enzymes are important for a detoxification role in nature.

The literature implicates azoreductases and NQOs in a variety of systems crucial for bacterial pathogenesis and resistance to host defence mechanisms as well as antimicrobials (which will be discussed in Chapter 6). As of yet, their primary physiological function remains to be defined. A deeper understanding of their function within the bacterial genome may lead to new pathways in antimicrobial treatments.

Table 1.1 New azoreductase-like enzymes identified in *P. aeruginosa* PAO1

Details of *P. aeruginosa* PAO1 azoreductase-like proteins identified by Ryan and colleagues (2014) based on sequence homology, structural comparisons and enzymatic function. Annotated functions were taken from the Pseudomonas Genome Database (Winsor *et al.*, 2016).

Protein ID	Annotated function	Homologues	Azo/Quinone reduction	Homologues azo/quinone reduction
PA2280	Oxidoreductase	smArsH	Azo- and quinone oxidoreductase (Crescente <i>et al.</i> , 2016)	Azoreductase (Hervás <i>et al.</i> , 2012)
PA2580	Conserved hypothetical protein	ecMdaB and hpMdaB	Azo- and quinone oxidoreductase (Crescente <i>et al.</i> , 2016)	Quinone oxidoreductase (Hayashi <i>et al.</i> , 1996, Wang and Maier, 2004)
PA1204	NAD(P)H quinone oxidoreductase	atNQO	Azo- and quinone oxidoreductase (Crescente <i>et al.</i> , 2016)	Quinone oxidoreductase (Sparla <i>et al.</i> , 1999)
PA0949	Tryptophan repressor binding protein	ecWrbA	Quinone oxidoreductase (Crescente <i>et al.</i> , 2016)	Quinone oxidoreductase (Patridge and Ferry, 2006)
PA4975	NAD(P)H quinone oxidoreductase	hNQO2	Quinone oxidoreductase (Green <i>et al.</i> , 2014)	Azo- and quinone oxidoreductase (Wu <i>et al.</i> , 1997)
PA1224	Probable NAD(P)H dehydrogenase	hNQO1 and hNQO2	-	Azo- and quinone oxidoreductase (Wu <i>et al.</i> , 1997)
PA1225	Probable NAD(P)H dehydrogenase	hNQO1 and hNQO2	-	Azo- and quinone oxidoreductase (Wu <i>et al.</i> , 1997)

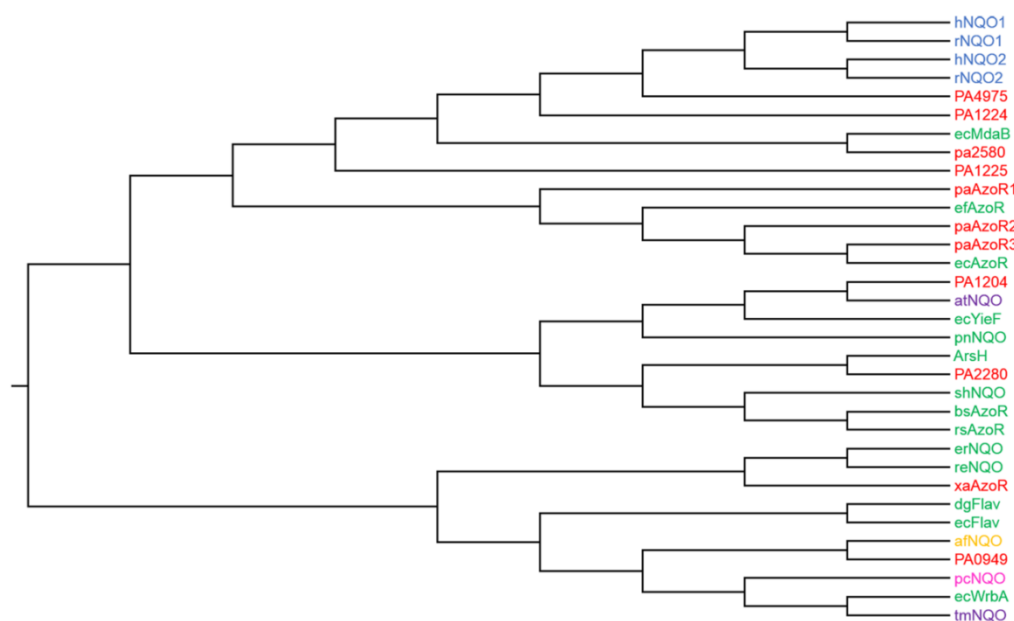


Figure 1.3 Phylogenetic tree showing the relationship between known and putative azoreductases from *P. aeruginosa* PAO1

Phylogenetic tree showing the relationship between enzymes from *P. aeruginosa* (red), other bacterial (green), mammalian (blue), plant (purple), fungal (pink) and archeal (yellow). PA0949, PA1204, PA1224, PA1225, PA2280, PA2580, and PA4975 are proteins from *P. aeruginosa* PAO1. ecAzoR, bsAzoR, efAzoR and rsAzoR are azoreductases from *E. coli*, *B. subtilis*, *E. faecalis* and *R. sphaeroides*. hNQO1 hNQO2, rNQO1 and rNQO2 are human and rat azoreductases. xaAzoR is an azoreductase from *Xenophilus azovorans*. ecMdaB, ecYieF and ecWrbA are NQOs from *E. coli*. afNQO, pnNQO, tmNQO, pcNQO and atNQO are NQOs from *Archaeoglobus fulgidus*, *Paracoccus denitrificans*, *Triticum monococcum*, *Phanerochaete chrysosporium* and *A. thaliana* respectively. ArsH is an azoreductase from *Sinorhizobium meliloti*. dgFlav and ecFlav are flavodoxins from *Desulfovibrio gigas* and *E. coli* respectively. shNQO, reNQO and erNQO are uncharacterised proteins from *Staphylococcus haemolyticus*, *Ralstonia eutropha* and *Erwinia chrysanthemi*. Figure is from Ryan *et al.* (2014).

Table 1.2 Azoreductases and azoreductase-like genes implicated in bacterial physiological functions

Overview of the azoreductase and azoreductase-like genes and their associations in various bacterial phenotypes.

Physiological function	Gene(s)	Bacteria	Observed phenotype
Plant colonisation	<i>ecazoR</i> , <i>seazoR</i>	<i>E. coli</i> , <i>S. enterica</i>	Upregulation during <i>E. coli</i> growth on radish sprouts and butterhead lettuce (Landstorfer <i>et al.</i> , 2014, Van der Linden <i>et al.</i> , 2016), overexpression during <i>S. enterica</i> colonisation of lettuce and coriander (Goudeau <i>et al.</i> , 2013)
Mammalian colonisation	<i>pa0785</i> , <i>pa1962</i> , <i>pa3223</i> , <i>pa2280</i> , <i>pa2580</i> , <i>pa1204</i> , <i>pa4975</i> , <i>ypwrbA</i>	<i>P. aeruginosa</i> , <i>Y. pseudotuberculosis</i>	$\Delta pa0785$ strains fail to survive in murine lung (Rakhimova <i>et al.</i> , 2008), $\Delta pa2280$, $\Delta pa2580$ and $\Delta pa1204$ fail to colonise mouse GI tract or disseminate to spleen, $\Delta pa1962$ colonises GI tract and disseminates at reduced rate compared to the WT, $\Delta pa3223$ and $\Delta pa4975$ fail to spread to spleen from GI tract (Skurnik <i>et al.</i> , 2013), <i>ypwrbA</i> mutants more easily cleared from murine spleen than WT (Avican <i>et al.</i> , 2015)
Virulence	<i>ypwrbA</i>	<i>Y. pseudotuberculosis</i>	<i>wrbA</i> gene deletion mutants cause less severe disease in mouse than WT (Avican <i>et al.</i> , 2015)
Biofilm formation	<i>ecwrbA</i>	<i>E. coli</i>	Target gene for biofilm regulator CsgD (Ogasawara <i>et al.</i> , 2011) interacts with anti-biofilm compound Zosteric acid (Cattò <i>et al.</i> , 2015)
Quorum sensing	<i>pa2580</i>	<i>P. aeruginosa</i>	Significantly upregulated upon treatment with QS inhibitor Iberin (Tan <i>et al.</i> , 2014)
Defence against electrophilic quinones	<i>ecazoR</i>	<i>E. coli</i>	Treatment with catechol, menadione and 2-methylhydroquinone results in significant upregulation of <i>azoR</i> and impaired growth of <i>azoR</i> gene deletion strains compared to WT (Liu <i>et al.</i> , 2009)

1.3 Aims

The prevalence and severity of *P. aeruginosa* infections constitutes a major health concern for immunocompromised individuals, particularly sufferers of CF. With MDR strains continuing to emerge, a comprehensive understanding of the complex *P. aeruginosa* genome would be crucial in developing insights to bacterial pathogenesis and antibiotic resistance.

Numerous studies have demonstrated evidence for the possible role of *P. aeruginosa* azoreductases and NQOs in host infection and antibiotic resistance processes. The identification of new azoreductases and NQOs and a development towards understanding their molecular and physiological roles is therefore a crucial step towards combatting this pathogen.

The aims of this study are:

1. Cloning of putative *P. aeruginosa* PAO1 azoreductase and NQO genes
2. Production and purification of suspected *P. aeruginosa* PAO1 azoreductase and NQO enzymes as recombinant proteins
3. Biochemical and enzymatic analyses of proposed *P. aeruginosa* PAO1 azoreductase and NQO recombinant proteins
4. Structural determination and analysis of *P. aeruginosa* PAO1 azoreductase and NQO, PA2580
5. Analysis of *P. aeruginosa* PAO1 antibiotic resistance using azoreductase and NQO single gene transposon mutants and corresponding complemented strains

Chapter 2 Materials and methods

2.1 Chemicals and reagents

All chemicals and reagents including oligonucleotide primers used in this study were obtained from Sigma-Aldrich unless otherwise stated. DNA and RNA extraction and purification kits were supplied by Qiagen and restriction enzymes were purchased from New England Biolabs (NEB).

2.2 Bacterial strains and growth conditions

P. aeruginosa PAO1 was kindly provided by Dr. Gail Preston, Department of Plant Sciences, University of Oxford. The single gene transposon mutants of *P. aeruginosa* PAO1 were provided by the Manoil laboratory, University of Washington (Jacobs *et al.*, 2003). *E. coli* JM109 and BL21 were supplied by Agilent. *P. aeruginosa* TBCF 10839 strains were kindly provided by Prof. Burkhard Tümmler, Hannover Medical School (Rakhimova *et al.*, 2008). Details of all bacterial strains used are displayed in Table 2.1. Growth medium was prepared in accordance with the manufacturer's instructions and sterilised, by standard sterilisation conditions, for 15 minutes at 121°C. Where necessary, antibiotics were filter sterilised through a 0.22 µm filter and added following the media sterilisation process. Bacterial cultures were routinely grown overnight at 37°C in Lysogeny broth (LB) liquid medium or on LB agar plates with additional supplements added where needed, as shown in Table 2.2. Liquid cultures were grown with gentle shaking at 120 RPM. *P. aeruginosa* PAO1 transposon mutants and *E. coli* JM109 containing the pUCP24 plasmids were cultured in 10 µg/mL gentamicin. For selection of *E. coli* strains transformed with pET-28b 30 µg/mL kanamycin was added.

Table 2.1 Details of *P. aeruginosa* and *E. coli* strains

Bacterial strains used in this study including their mutated genes are listed below. *P. aeruginosa* PAO1 and the transposon insertion mutants were provided by The Manoil lab at the University of Washington (UW), *P. aeruginosa* TBCF 10839 strains were supplied by Prof. Burkhard Tümmler, MH Hannover (MHH), *E. coli* JM109 was sourced from Promega and the *E. coli* BL21 strains were received from Agilent.

Strain	Mutation	Plasmid	Source
<i>P. aeruginosa</i> PAO1	-	-	UW
<i>P. aeruginosa</i> PAO1	<i>pa0785</i>	-	UW
<i>P. aeruginosa</i> PAO1	<i>pa1962</i>	-	UW
<i>P. aeruginosa</i> PAO1	<i>pa3223</i>	-	UW
<i>P. aeruginosa</i> PAO1	<i>pa2280</i>	-	UW
<i>P. aeruginosa</i> PAO1	<i>pa2580</i>	-	UW
<i>P. aeruginosa</i> PAO1	<i>pa1204</i>	-	UW
<i>P. aeruginosa</i> PAO1	<i>pa0949</i>	-	UW
<i>P. aeruginosa</i> PAO1	<i>pa4975</i>	-	UW
<i>P. aeruginosa</i> TBCF10839	-	-	MHH
<i>P. aeruginosa</i> TBCF10839	<i>pa0785</i>	-	MHH
<i>P. aeruginosa</i> TBCF10839	<i>pa0785</i>	pUCP20:: <i>pa0785</i>	MHH
<i>P. aeruginosa</i> TBCF10839	<i>pa0785</i>	pUCP20:: <i>pa0785-0787</i>	MHH
<i>E. coli</i> JM109	-	-	Agilent
<i>E. coli</i> BL21(DE3)	-	-	Agilent
<i>E. coli</i> BL21-CodonPlus(DE3)-RP	-	-	Agilent

Table 2.2 Media used in this study

Table showing the media used in this study including components and concentrations.

Medium	Components	Concentration (g/L)
Lysogeny broth	Trypone	10
	NaCl	10
	Yeast extract	5
Lysogeny broth Agar	Trypone	10
	NaCl	10
	Yeast extract	5
	Bacto agar	15
Mueller Hinton Broth	Beef infusion solids	2
	Casein hydrolysate	17.5
	Starch	1.5

2.3 Cloning of putative azoreductase genes

2.3.1 Genomic DNA extraction

Wild type *P. aeruginosa* PAO1 was grown overnight in 5 mL liquid culture as previously described (section 2.2). Total genomic DNA was extracted using Genra Puregene Yeast/Bact. Kit following the supplier's protocol. Quantitative and qualitative analysis was carried out on the extracted DNA using NanoVue™ Plus spectrophotometers (VWR).

2.3.2 Agarose gel analysis of DNA samples

Except where otherwise stated, DNA samples were analysed on 1% w/v agarose gel (Fisher) in 1 × Tris/Borate/EDTA (TBE) buffer pH 8 (Table 2.3) and Sybr safe (Life Technologies). Gel loading dye (Table 2.3) was added to each DNA sample in a ratio of 1:5. 5 µL DNA plus loading dye samples were added to agarose gel wells and 1 Kb Plus DNA ladder (PCRBIO) was used as a molecular weight marker. Agarose gels were run for 45 minutes to one hour at 90 volts (BIO-RAD Power-Pac 300) in an electrophoresis flow chamber (Flowgen) using 1 × TBE as running buffer. Gels were visualised using Molecular Imager Gel Doc™ XR+ (BIO-RAD) and molecular weights were always determined using the molecular weight analysis tool in ImageLab 5.2.1 (BIO-RAD).

Table 2.3 Materials used for nucleic acid gel electrophoresis

1 × TBE was used as a running buffer and to make the 1% w/v agarose gel. Gel loading dye was added to the DNA sample in a ratio of 1:5.

Buffer	Components	Concentration
1 × TBE	Tris base	89 mM
	Boric acid	89 mM
	EDTA disodium salt	2.6 mM
	HCl	to pH 8
Gel loading dye	Glycerol	30% v/v
	Bromophenol blue	0.25% w/v
	ddH ₂ O	69.75% v/v

2.3.3 Plasmid Extraction

E. coli JM109 strains containing relevant plasmids were grown overnight in 5 mL LB containing appropriate antibiotics (Table 2.4). Plasmids were extracted from the overnight cultures using the QIAprep Spin Miniprep kit in accordance with the instructions provided by the manufacturer. Plasmid preps were quantified using a Nanovue™ Plus spectrophotometer.

Table 2.4 Plasmids used in this study

pET-28b was supplied by Novagen and transformed into *E. coli* strains JM109 and BL21 for cloning and expression respectively. pUCP24, kindly provided by Dr. Gail Preston, Department of Plant Sciences Oxford University, was used to clone the azoreductase-like genes into each corresponding transposon insertion mutant (West *et al.*, 1994).

Plasmid	Selectivity	Source
pET-28b	30 µg/mL Kanamycin	Novagen
pUCP24	10 µg/mL Gentamicin	Dr. Gail Preston (Oxford University)

2.3.4 Putative azoreductase gene amplification for cloning into pET-28b

Gene sequences for putative azoreductase genes *pa1224* and *pa1225* were obtained from the Pseudomonas Genome Database (Winsor *et al.*, 2016). Gene-specific primers were designed for each of these genes (Table 2.5) and analysed for predicted melting temperatures and hairpin formation using Integrated DNA technologies Oligoanalyzer tool (Owczarzy *et al.*, 2008). Primers were designed to amplify the specific gene sequence with the forward and reverse primers incorporating restriction sites NdeI and SacI respectively. Using these primers polymerase chain reaction (PCR) amplification was carried out on *P. aeruginosa* PAO1 genomic DNA using Hotstar HiFi DNA polymerase. The components used for each PCR reaction are listed in Table 2.6. The conditions used for thermal cycling are displayed in Table 2.7. All PCR products were analysed on 1% w/v agarose gel stained with Sybr safe as described in section 2.3.2.

Table 2.5 Primers used for the cloning process of azoreductase-like genes *pa1224* and *pa1225* from *P. aeruginosa* PAO1

Table showing the forward (fwd) and reverse (rev) primers used for the amplification of putative azoreductase genes *pa1224* and *pa1225*. Primers were designed to include restriction sites for NdeI and SacI which are underlined.

Primer	Sequence	Annealing Temp.
<i>pa1224</i> fwd	CCGGAGACCC <u>CATATGA</u> ACGTACTCATCGTCTATGCCC	60°C
<i>pa1224</i> rev	GCCGCTGGAGGCCTGAGCTCCGGGGTCATTCGGCC	
<i>pa1225</i> fwd	CGGAGGAATTCGCATATGCATGCCCTGATCGTCGTCGC	60°C
<i>pa1225</i> rev	CCTGGCCGAATGAGCTCGGGGGTCACGCCTCCAGC	

Table 2.6 PCR reaction mix for PCR using HotStar HiFi DNA polymerase

PCR reaction mix components including their quantities and concentrations are listed below.

Component	Volume (µL)	Concentration
Genomic DNA	1	~100 ng
Forward Primer	5	1 µM
Reverse Primer	5	1 µM
HotStar HiFi DNA polymerase	1	-
HotStar HiFi buffer 5×	10	1×
Q-solution 5×	10	1×
RNase-free H ₂ O	18	-

Table 2.7 Thermocycling conditions for PCR using HotStar HiFi DNA polymerase

Thermocycling conditions and the corresponding duration used with HotStar HiFi DNA polymerase are listed below.

Step	Temperature (°C)	Time	No. of cycles
Denaturation	95	5 minutes	1
Annealing	50-60	30 seconds	35
Extension	72	1 minute	
Denaturation	95	30 seconds	
Annealing	50-60	30 seconds	1
Extension	72	10 minutes	1

2.3.5 Putative azoreductase gene amplification for cloning into pUCP24

Gene sequences for the azoreductase-like genes *pa0785*, *pa1962*, *pa3223*, *pa2280*, *pa2580*, *pa1204*, *pa0949* and *pa4975* were obtained from the Pseudomonas Genome Database (Winsor *et al.*, 2016). Gene-specific primers were designed for each of these genes (Table 2.8) using the methods laid out in section 2.3.4. Primers were designed to amplify the specific gene sequence with the forward and reverse primers incorporating restriction sites BamHI and SalI respectively. PCR amplification was carried out on *P. aeruginosa* PAO1 genomic DNA as described in section 2.3.4. All PCR products were analysed on 1% w/v agarose gel stained with Sybr safe as described in section 2.3.2.

Table 2.8 Primers used for the cloning process of azoreductase-like genes from *P. aeruginosa* PAO1 into pUCP24 vector

Table showing the forward (fwd) and reverse (rev) primers used for the amplification of azoreductase-like genes *pa0785*, *pa1962*, *pa3223*, *pa2280*, *pa2580*, *pa1204*, *pa0949* and *pa4975*. Primers were designed to include restriction sites BamHI and SalI which are underlined.

Primer	Sequence	Annealing temp.
<i>pa0785</i> fwd	CCAAGGGGATCCAGATGAGTAGAATTCTTGC	55°C
<i>pa0785</i> rev	CCAGGCGATGTCGACTCCTCAGGCC	
<i>pa1962</i> fwd	CCACACTGGGATCCCGCACTTTCAGG	50°C
<i>pa1962</i> rev	CCGGCCAGTCGACACGCAGC	
<i>pa3223</i> fwd	GCGCAGTGGATCCAGGTCGAGTCATGTCC	55°C
<i>pa3223</i> rev	GGAAGGGGGTTCGACCCGGGTGCTGC	
<i>pa2280</i> fwd	GGAGGATCCATGTCCGAACAACACTACCC	50°C
<i>pa2280</i> rev	GCGAGTGAGGTCGACGCGGTTTCAGAGCG	
<i>pa2580</i> fwd	GCATCTACGGATCCCATGAAAAACATTCTCCTGC	55°C
<i>pa2580</i> rev	GGCCCGTCGACGAACTCAGCCGGC	
<i>pa1204</i> fwd	CGCACAACGAGGATCCCGGCATGAGCG	55°C
<i>pa1204</i> rev	GGCTCTCCGTCGACGAGGCATTCAACCG	
<i>pa0949</i> fwd	CCTGGGGATCCTCGCTTGAGCAGTCCC	55°C
<i>pa0949</i> rev	GCTGAGCGCCAGGGTTCGACTGCAGCCACGC	
<i>pa4975</i> fwd	CCGGTCACCACGATTCGGATCCACGATGAACG	55°C
<i>pa4975</i> rev	GGCCTGGCGCGCGTTCGACCCGGCTCAGC	

2.3.6 Double endonuclease restriction digest

All restriction digests were carried out using the mixtures laid out in Table 2.9 and incubated at 37°C for 2 hours followed by endonuclease denaturation at 65°C for 15 minutes. The pET-28b plasmid was digested using restriction enzymes NdeI and SacI, the pUCP24 was digested with BamHI and SalI. Digested plasmids were observed on 1% w/v agarose gel stained with Sybr safe.

Table 2.9 Restriction digest of vectors and inserts

Listed below are the reaction mix components and volumes for (double) restriction digests of PCR products and plasmids. Cutsmart buffer was used with restriction enzymes NdeI and SacI. Buffer 3:1 was used with BamHI and SalI.

Solution	Concentration/Volume
DNA	0.1-3 µg
Restriction enzyme I	1 µL/ng DNA
Restriction enzyme II	1 µL/ng DNA
1:10 BSA	4 µL
Buffer	4 µL
RNase/DNase-free H ₂ O	To a final volume of 40 µL

2.3.7 Antarctic phosphatase digestion

Linearised plasmids were treated with Antarctic phosphatase to dephosphorylate the 5' phosphate group and enable ligation with the gene of interest. The reaction was carried out in 0.5 mL microcentrifuge tubes. Samples were prepared as described in Table 2.10 and incubated at 37°C for 2 hours followed by endonuclease denaturation at 65°C for 15 minutes.

Table 2.10 Antarctic phosphatase digestion components and concentrations

Listed below are the reaction mix components and volumes for dephosphorylation of the 5' end of the linearised plasmids.

Solution	Concentration/Volume
DNA	0.1-3 µg
Antarctic phosphatase	1 µL/ng DNA
Antarctic phosphatase buffer 10×	4 µL
RNase/DNase-free H ₂ O	To a final volume of 40 µL

2.3.8 DNA purification

PCR products were purified before and after endonuclease digestion using a MinElute PCR purification kit. Plasmid DNA was purified following both digestion steps using a QIAquick PCR purification kit. In both circumstances, procedures were carried out following the supplier's instructions. Quantity and quality of purified samples were assessed using a Nanovue™ Plus spectrophotometer.

2.3.9 Ligation

The following formula was used to determine the quantities of plasmid and insert to be used in the ligation reaction mixture:

$$\frac{(ng \text{ of vector}) \times (Kb \text{ of insert})}{Kb \text{ size of vector}} \times \text{molar ratio of } \frac{\text{insert}}{\text{vector}} = ng \text{ of insert}$$

* With the molar ratio of insert over vector being 1: 3, 1: 1 and 3: 1

Plasmid concentration was kept constant at 100 ng for each ligation reaction. Reaction volumes of 10 μ L were used and included 1 μ L T4 ligase (Promega) and 1 μ L 10 \times T4 ligase buffer. A negative control where no insert was added to the mix was always included in the procedure to ensure that no plasmid self-ligation was occurring. Ligation reactions were incubated at 22°C for 3 hours.

2.3.10 Preparation of chemically competent *E. coli*

Chemically competent *E. coli* JM109 and *E. coli* BL21(DE3) were prepared in accordance with a procedure kindly offered by Andrew Spiers (Department of Plant Sciences, University of Oxford). LB was inoculated with *E. coli* overnight culture and grown at 37°C 120 RPM to an OD₆₀₀ of 0.6. Cells were harvested by centrifugation at 4,500 × *g* for 5 minutes and resuspended in 1/10 initial volumes of ice-cold 50 mM CaCl₂. Following 30 minutes incubation on ice, cells were harvested again at 4,500 × *g* for 5 minutes. The cell pellet was resuspended in 0.05 volumes of cold 50 mM CaCl₂ and incubated on ice overnight. Glycerol was added to a final concentration v/v of 10% and 200 μL aliquots were flash frozen in liquid nitrogen and stored at -80°C.

2.3.11 Preparation of chemically competent *P. aeruginosa* PAO1 wild type and transposon insertion mutants

Chemically competent *P. aeruginosa* PAO1 were prepared as previously described (Chuanchuen *et al.*, 2002). Briefly, 1 mL of overnight culture was added to a prechilled microcentrifuge tube and centrifuged for 30 seconds at 13,000 × *g*. Cells were resuspended in 1 mL cold 0.1 M MgCl₂. Centrifugation was repeated as before and the cell pellet was resuspended in 1 mL cold transformation salts comprising 75 mM CaCl₂, 6 mM MgCl₂ and 15% v/v glycerol. Following an incubation of ten minutes on ice, centrifugation was repeated again and the cells were resuspended in 200 μL cold transformation salts. Competent cells were flash frozen in liquid nitrogen and stored at -80°C.

2.3.12 Heat shock transformation

Plasmids were transformed into chemically competent cells using a previously described heat shock method (Froger and Hall, 2007). Briefly, 100 μL of competent cells were thawed on ice and added to 10 μL ligation mixture in a 1.5 mL microcentrifuge tube. This mixture was incubated on ice for 5 minutes before being plunged into a water bath at 42°C for 45 seconds. Immediately the tube was returned to the ice and incubated for a further 5 minutes after which 1 mL of LB was added and the mixture was incubated in a static incubator for 1 hour at 37°C. A positive control of competent cells with undigested plasmid was always included in the protocol. When transforming a plasmid extraction instead of a ligation mixture, 2 μL of plasmid solution was used.

2.3.13 Selection of successful transformants

Transformation mixtures were concentrated by centrifugation and spread onto LB agar containing appropriate antibiotics (Table 2.4). Untransformed competent cells were also spread onto antibiotic containing LB agar plates as a negative control. The plates were incubated overnight in a static incubator at 37°C. Colonies were picked and used as a template for PCR analysis. Primers used in this analysis either annealed to the vector on either side of the insertion site (M13 primers for pUCP24 clones, Table 2.12) or were specific for a nucleotide sequence which overlapped plasmid and gene insert (Table 2.11). Colonies with the correct size of inserted DNA were grown in 5 mL LB containing suitable antibiotic for 6 hours before being concentrated in LB containing 10% v/v glycerol and flash frozen in liquid nitrogen for long term storage at -80°C.

Table 2.11 Primers used to screen for successful clones of azoreductase-like genes *pa1224*, *pa1225* and *pa4975*

Table showing the forward (fwd) and reverse (rev) primers used to check for the presence of pET-28b with the inserted gene. The primers were designed specifically to overlap a section which included parts of both the vector sequence and the gene sequence. Primers for CL*pa4975* were designed by Dr. Vincenzo Crescente.

Primer	Sequence	Annealing Temp.
CL <i>pa1224</i> fwd	GCCGCGCGACAGCCATATGAACGTAATAATCG	60°C
CL <i>pa1224</i> rev	GGCCGAATGACCCAGGACCTCCATCGACAAGCTTG CGG	
CL <i>pa1225</i> fwd	GCAGCCGCCATATGCATGCCCTGATCG	60°C
CL <i>pa1225</i> rev	GCTTGTCGGCGGAGCTCGAGGGTCAGGCC	
CL <i>pa4975</i> fwd	CGCGCGGCAGCCATATGAACGTAATGATCGTCC	55°C
CL <i>pa4975</i> rev	CCGCAAGCTTGTCGACGGAGCTCAGCGCGCCAG	

2.3.14 DNA sequence analysis

Plasmid extraction was carried out on successful transformants using the method laid out in section 2.3.3. Plasmid solutions along with appropriate sequencing primers (Table 2.12) were sent to Eurofins MWG Operon for sequencing in the volumes and concentrations recommended by the company. The sequencing results were then compared with the azoreductase-like gene sequence from the *Pseudomonas* Genome Database using the ClustalW multiple alignment feature in Bioedit (Thompson *et al.*, 1994, Hall, 1999).

Table 2.12 Primers used for sequencing of positive clones

Primers used to sequence the azoreductase-like genes cloned. pET-28b seq primers were used to sequence *pa1224* and *pa1225* in the pET-28b vector. M13 primers were used to sequence the azoreductase-like genes in pUCP24.

Primer	Sequence
pET-28b seq fwd	CATCATCACAGCAGCGGCCTGGTGC
pET-28b seq rev	GGCTTTGTTAGCAGCCGGATCTCAGTGG
M13 fwd	GTAAAACGACGGCCAGT
M13 rev	CAGGAAACAGCTATGAC

2.4 Gene expression and production of recombinant protein

For recombinant protein expression, the pET-28b plasmids containing putative azoreductases *pa1224*, *pa1225*, *pa2580* and *pa4975* were extracted from *E. coli* JM109 and transformed into *E. coli* BL21 strains via the heat shock method. Successful transformants were screened using PCR as previously described (section 2.3.13).

2.4.1 Expression of putative azoreductase genes

Overexpression of recombinant protein was carried out following a method adapted from Wang *et al.* (2007). A starter culture of *E. coli* BL21(DE3) containing pET-28b and the gene to be expressed was grown overnight in LB supplemented with 30 µg/mL kanamycin. Fernbach flasks containing LB supplemented with 1 M sorbitol, 2.5 mM betaine and 30 µg/mL kanamycin were inoculated with 1% v/v overnight culture and grown at 37°C 120 RPM until bacteria reached the exponential phase (OD₆₀₀ of 0.4-0.6). As standard, 50 mL cultures in 200 mL flasks were used for expression (small scale), however where appropriate this was scaled up to 500 mL cultures in 2 L flasks (large scale). To induce protein expression, 0.1-0.5 mM isopropyl-β-D-thiogalactopyranoside (IPTG) was added and the cultures were incubated at 16°C 120 RPM for 16 hours. After this expression period, cultures were centrifuged at 4,500 × *g* for 20 minutes at 4°C. The supernatant was discarded and the cells were resuspended in an enzymatic lysis buffer (20 mM Tris HCl, 100 mM NaCl, 1 EDTA-free protease inhibitor tablet (Roche), 0.02 mg/ml DNase and 0.2 mg/ml lysozyme, pH 8). The amount of lysis buffer added was always 2% v/v of the initial culture volume. Samples underwent 4 freeze/thaw cycles using liquid nitrogen and a 37°C static incubator. For large scale protein preparations an extra lysis step was added at this point where samples on ice were sonicated using a MSE Soniprep 150 for 30 cycles - 45 seconds on, 30 seconds off. The cell lysate was then centrifuged at 16,000 × *g* for 20 minutes at 4°C to separate the soluble and insoluble protein fractions (the supernatant and the pellet respectively). Prior to this step, a whole cell lysate sample was taken and set aside for later analysis. The supernatant was collected and stored on ice. To enable a direct comparison to be drawn between fractions the pellet was resuspended in 20 mM Tris HCl 100 mM NaCl pH 8 to the same volume that was used for the lysis buffer. The whole cell lysate, along with samples from the soluble and insoluble fractions were analysed on SDS-PAGE. For every procedure of recombinant protein production carried out, *E. coli* BL21 transformed with empty pET-28b was included in the preparation as a negative control.

2.4.2 SDS-PAGE analysis of recombinant proteins

Except where otherwise stated, all protein samples at each purification stage were analysed by SDS-PAGE. The gels consisted of a 12% w/v acrylamide resolving gel and a 6% w/v acrylamide stacking gel. Gels were run in a MiniProtean Tetra system (BIO-RAD) with a SDS running buffer (National Diagnostics). Protein samples were prepared by adding a loading dye in a ratio of 1:3 (Table 2.13). Sample mixes were then denatured for 5 minutes at 95°C to avoid the protein structure affecting the molecular weight determination. 12 µL of protein sample was always loaded into each well. Except where otherwise stated, ECL Full-range Rainbow Molecular weight marker (Amersham) was used as the molecular weight marker. Electrophoresis was carried out by applying 180 V for 45 to 60 minutes (BIO-RAD Power Pak 300). Gels were stained for 30 minutes in a Coomassie Blue stain solution (Table 2.13) followed by destaining with 10% v/v ethanol, 10% v/v acetic acid for a further 12 hours. Staining and destaining were carried out at room temperature with 90 RPM gentle shaking. Gels were visualised and captured using Molecular Imager Gel DocTM XR+ (BIO-RAD) and molecular weights were determined using the molecular weight analysis tool in ImageLab 5.2.1 (BIO-RAD). Quantification of protein bands was calculated using the volume analysis tool in ImageLab 5.2.1 (BIORAD).

Table 2.13 Materials used for SDS-PAGE

12% SDS-PAGE was used to analyse protein samples. Gel loading dye was added to the protein solution in a 1:3 ratio.

Material	Components	Concentration
Resolving gel	Acrylamide:bis acrylamide (29:1) SDS Ammonium persulphate Tetramethylethylenediamine (TEMED) Tris HCl	12% v/v 0.125% w/v 0.05% w/v 0.002% v/v 390 mM
Stacking gel	Acrylamide:bis acrylamide (29:1) SDS Ammonium persulphate TEMED Tris HCl	6% v/v 0.125% w/v 0.05% w/v 0.002% v/v 116.6 mM
Gel loading dye	Sucrose Bromophenol blue Dithiothreitol (DTT)	40% w/v 0.25% w/v 5 mg/mL
SDS running buffer	Tris Glycine SDS	0.25 M 1.95 M 1% w/v
Staining solution	Coomassie brilliant blue Ethanol Acetic acid H ₂ O	0.0024% w/v 50% v/v 10% v/v 40% v/v
Destaining solution	Ethanol Acetic Acid H ₂ O	10% v/v 10% v/v 80% v/v

2.5 Purification and quantification of recombinant protein

2.5.1 Immobilised Metal-ion Affinity Chromatography

Purification of the recombinant putative azoreductase proteins was carried out using the immobilised metal-ion affinity chromatography (IMAC) method. Ni-NTA agarose mix was purchased from Invitrogen and was used to bind the hexahistidine residues present on each recombinant protein. According to the manufacturer's instructions, 1 mL of resin binds ~10 mg protein therefore 4 mL of Ni-NTA beads suspended as a 50% slurry in 20% v/v ethanol was loaded into a 10 mL IMAC column (BIO-RAD). The beads were left to settle on the porous polymer support at the bottom of the column and the ethanol was slowly removed. The beads were washed twice with 5 mL 20mM Tris HCl 100 mM NaCl pH 8 to remove any residual ethanol. The soluble fraction was then added to the column and mixed with the beads by inverting the tube numerous times. The liquid phase was removed by allowing the beads to settle and applying gentle pressure to the column with the aid of a syringe and halting the process as soon as the solution reached 1 mm above the beads. This fraction was collected as flow through and where a particularly high yield of protein was obtained, it could be reapplied to the column at a later stage. Increasing concentrations of imidazole (0 mM, 10 mM, 25 mM, 50 mM, 100 mM and 250 mM) were prepared in 20 mM Tris HCl 100 mM NaCl pH 8 and used to elute the protein. All elutions were collected and analysed via SDS-PAGE.

2.5.2 Dialysis

The fractions containing recombinant protein were carefully inserted into dialysis tubing - a porous membrane with a molecular weight cut-off point of 12-14 kDa (SPECTRUM®, Spectrum Laboratories Inc.). The dialysis tubing was then sealed and placed into 4 L of dialysis buffer (20 mM Tris HCl 100 mM NaCl pH 8) and stored overnight at 4°C with gentle magnetic stirring. This process was carried out to remove any excess imidazole from the protein solutions.

2.5.3 Protein quantification and concentration

Protein concentration of the purified sample was determined using the Beer -Lambert law, $A = \epsilon CL$, where A is the absorbance, ϵ is the extinction coefficient, C is the protein concentration and L is the light path length in cm. The ϵ value was calculated for each protein by inputting the full amino acid sequence for the protein in question along with the hexahistidine tag residues into the online tool, ExPASy ProtParam (Gasteiger *et al.*, 2005). The absorbance of the purified protein was read at 280 nm using a biophotometer (Eppendorf) and this value along with the ϵ value and the light path length (constant at 1 cm) were used to determine the protein concentration in mg/mL. As standard, all proteins were concentrated to either 1 or 2 mg/mL using a Sartorius ultracentrifugation concentrator with a cut-off of 10 kDa. For long term storage 5% v/v glycerol was added to protein solutions before they were flash frozen in liquid nitrogen and stored at -80°C.

2.6 Characterisation of putative azoreductases from *P. aeruginosa* PAO1

2.6.1 Thin Layer Chromatography

Thin layer chromatography (TLC) was carried out to determine the flavin specificity for PA1224 and PA1225. The method used was adapted from that previously described (Liu *et al.*, 2008). A mobile solvent comprising of N-butanol, acetic acid and H₂O in a 2:1:1 ratio was used with 0.1 mm thick silica gel-coated aluminium plates. The optimum concentration of flavin for TLC was found by testing a range of concentrations comprising of 20 mM, 10 mM, 5 mM, 1 mM and 0.5 mM pure FMN and FAD. Proteins were concentrated to 20 mg/mL using the method described in section 2.5.3. The TLC plate was spotted with 1 µL protein and 1 µL flavin and placed in a sealed beaker containing the mobile solvent. The procedure was stopped when the solvent reached 1 cm from the top of the TLC plate. The retention factor (R_f) of each protein was compared to the R_f of FAD and FMN and was calculated using the formula below:

$$R_f = \frac{\text{distance travelled by the compound}}{\text{distance travelled by the solvent}}$$

2.6.2 Differential Scanning Fluorimetry

Differential scanning fluorimetry (DSF) was carried out using a modified method from that described in Niesen *et al.* (2007). Putative azoreductase proteins were diluted to 64 µg/mL in 20 mM Tris HCl 100 mM NaCl pH 8 containing 5 × Sypro Orange (Invitrogen). Fluorescence was measured using an Mx3005p qRT-PCR instrument (Stratagene) with the temperature increased from 25°C to 95°C at a rate of 1°C/minute. Data analysis was completed in Graphpad Prism (version 7) with fitting to a Boltzman sigmoidal function. DSF was also carried out with 1-20 µM FMN and FAD added to the mix.

2.6.3 Spectral properties of putative azoreductases and determination of flavin saturation level

Samples of purified PA2280, PA2580, PA1204, PA0949, PA1224 and PA1225 were diluted in 20 mM Tris HCl 100 mM NaCl pH 8 to a concentration of 400 µg/mL and added to a synthetic far-UV quartz cuvette (Hellma Worldwide). An absorbance scan was carried out on each protein using an Infinite M200 PRO plate reader (TECAN) and spectra were recorded across the wavelength of 250 nm to 600 nm. Pure stocks of 20 µM FMN and FAD were measured at 450 nm and 445 nm respectively. The molecular ratio of protein to flavin was then determined by comparing the OD₄₅₀ or OD₄₄₅ value of the protein to that of the 20 µM flavin stock.

2.6.4 Absorption spectra of substrates and calculation of molar extinction coefficients

The absorption spectra of NADH, NADPH, the azo compounds and the quinone compounds were generated by adding 100 µL of substrate (500 µM for NAD(P)H in 20 mM Tris HCl 100 mM NaCl, 100 µM for azo/quinone compounds in DMSO) to a 96-well Nunclon flat transparent plate and taking absorbance readings at 5 nm intervals between 300 nm and 700 nm. The maximum wavelengths (λ_{max}) for each compound were used to calculate the molar extinction coefficient (ϵ). This was done by dispensing 100 µL of decreasing concentrations of compound into a 96-well plate (500-0 µM for NAD(P)H, 100-0 µM for azo compounds) and reading absorbance at their λ_{max} . Linear regression analysis was performed on the values using Microsoft Excel to determine the ϵ value for each compound.

2.6.5 Enzymatic activity assays for the putative azoreductases

The activities of the recombinant putative azoreductases were characterised by carrying out enzymatic assays against a range of substrates, predominantly azo and quinone compounds (Table 2.14). A series of assays were completed initially where different combinations of NAD(P)H, FMN and FAD were used and the reduction rates compared to determine the flavin and nicotinamide selectivity. Flavin selectivity was also decided by TLC and DSF analysis (as referred to in sections 2.6.1 and 2.6.2 respectively). This information was then used to carry out assays using a range of azo and quinone substrates where the optimum cofactor (where necessary) was included and the appropriate nicotinamide was used as an electron donor. All enzyme assays were carried out in Nunclon 96-well flat transparent plates in 100 μL volumes. The components of the reaction mixtures are listed in Table 2.15. Varying concentrations of enzyme (in 10 μL volumes) were added to the plate in triplicate (0-20 μg for azo substrates, 0-10 μg for quinones) and the reaction was initiated by the addition of 90 μL master mix comprising of all the other reaction components. Absorbance readings were taken every 10 seconds for 10 minutes using the Infinite M200 PRO plate reader. Absorbance readings were taken at the λ_{max} for each azo compound to monitor azo reduction. For quinone substrates, readings were taken at the λ_{max} for NAD(P)H to observe NAD(P)H oxidation. Given one molecule of NAD(P)H is used to reduce one molecule of quinone, this could be used to determine the rate of quinone reduction. In order to calculate reduction rates, linear regression analysis was performed in Microsoft Excel over the time period for which the reaction was linear (usually within the first 150 seconds). This was then divided by the ϵ value followed by the amount of protein used in the reaction (in mg/mL). This method gave the rate in μM of substrate reduced per second per mg of protein ($\mu\text{M} \cdot \text{s}^{-1} \cdot \text{mg}^{-1}$).

Table 2.14 Substrates used for the characterisation of the *P. aeruginosa* putative azoreductase proteins

Table showing the substrates used for the enzymatic characterisation of the putative azoreductases. A: azo compound; Q: Quinone. Structures of these substrates are listed in APPENDIX I and APPENDIX II.

Name/Abbreviation	Compound	Class
Amaranth	1-(4-sulfo-1-naphthylazo)-2-naphthol-3, 6-disulfonic acid trisodium salt	A
Balsalazide	5-[4-(2-Carboxyethylcarbamoyl)phenylazo]salicylic acid disodium salt	A
Methyl red	2-(4-Dimethylaminophenylazo)benzoic acid	A
Olsalazine	3, 3-azobis(6-hydroxybenzoate)salicylic acid	A
Orange G	1-Phenylazo-2-naphthol-6,8-disulfonic acid disodium salt	A
Orange II	4-[(2-Hydroxy-1-naphthalenyl)azo]benzenesulfonic acid monosodium salt	A
Ponceau BS	Disodium 2-[(2-hydroxy-1-naphthyl)azo]-5-(4-sulfonatophenyl)azo-benzenesulfonate	A
Ponceau S	3-Hydroxy-4-(2-sulfo-4-[4-sulfophenylazo]phenylazo)-2, 7-naphthalenedisulfonic acid sodium salt	A
Sudan I	1-Phenylazo-2-naphthol	A
Sulfasalazine	6-oxo-3-[[4-(2-pyridin-2-ylsulfamoyl)phenyl]hydrazinylidene]cyclohexa-1,4-diene-1-carboxylic acid	A
Tropaeolin	4-([2,4-Dihydroxyphenyl]azo)benzenesulfonic acid	A
ANI	<i>N, N</i> -dimethyloaniline	Q
AQS	Sodium anthraquinone-2 -sulfonic acid	Q
BZQ	1, 4-benzoquinone	Q
DCB	2, 5-dichloro-1, 4-benzoquinone	Q
HNQ	5-hydroxy-1, 4-napthoquinone	Q
IBC	2, 6-dichloroquinone-4-chloroimide	Q
LAW	2-hydroxy-1, 4-napthoquinone	Q
MEN	2-methyl-1, 4-napthoquinone	Q
ONO	1, 2-napthoquinone	Q
PLU	5-hydroxyl-2-methyl-1, 4-napthoquinone	Q
UQO	Coenzyme Q ₁₀	Q

Table 2.15 Reaction mix used for the enzymatic assays

Reaction components and concentrations for characterisation of putative azoreductases, including NAD(P)H and flavin determination and generation of substrate specificity profiles.

Component	Volume (μL)	Concentration
Enzyme	10	0-20 μg
Substrate	5	100 μM
NAD(P)H	5	500 μM
Flavin (where necessary)	5	1 μM
20 mM Tris HCl 100 mM NaCl pH 8	To a final volume of 100 μL	-

2.7 Crystallisation of PA2580 and x-ray diffraction data collection

2.7.1 Synthesis of H₂NADPH

The ultra-pure 1,4,5,6-tetrahydro analogue of NADPH, H₂NADPH, was synthesised by Dr. Onur Atasoylu (University of East Anglia) and purified by Dr. Chris Morris (University of East Anglia). The compound was prepared as previously described (Bhakta, 2007).

2.7.2 Crystallisation of PA2580 with H₂NADPH

To remove NaCl, pure recombinant PA2580 was washed with 20 mM Tris HCl pH 8 using a Sartorius ultracentrifugation concentrator with a cut-off of 10 kDa. The protein was resuspended to a final concentration of 10 mg/mL in 20 mM Tris HCl 500 μM FMN 2 mM H₂NADPH. Crystals were grown at 22°C (room temperature) by the sitting drop vapour diffusion method. Equal volumes (0.2 μL) of protein solution were mixed in sitting drop format with the appropriate precipitation buffer using a Mosquito crystallisation robot (TTP Labtech). The screening conditions trialled were PACT *premier*, JCSG-*plus* and Morpheus (Molecular Dimensions).

2.7.3 Optimisation of crystallisation conditions for PA2580

Larger scale crystal trials were laid down for Morpheus screen conditions B6 (0.09 M Halogens, 0.1 M Sodium HEPES, 0.1 M MOPS, 20% v/v ethylene glycol, 10% w/v polyethylene glycol (PEG) 8000 pH 7.5) and F10 (0.12 M Monosaccharides, 0.1 M Bicine, 0.1 M Tris, 20% v/v ethylene glycol, 10% w/v PEG 8000 pH 8.5) (Gorrec, 2009) by mixing equal volumes (2 μL) of protein solution (containing 2 mM H₂NADPH) with the suitable buffer in MRC maxi plates (Molecular Dimensions). Following crystallisation, some crystals were soaked overnight in 4 μL 10 mM H₂NADPH. All of these were carried out using the sitting drop vapour diffusion method at 23°C.

2.7.4 X-ray diffraction data collection and analysis

Crystals were mounted with a CryoMount mesh set (Molecular Dimensions) and flash frozen in liquid nitrogen. It is important to note that it was not necessary to add cryoprotectant to the crystals prior to freezing as the Morpheus screening conditions B6 and F10 contain 20% ethylene glycol and 10% w/v PEG 8000 which will serve this function (Gorrec, 2009). All x-ray diffraction data was kindly collected by Dr. Edward Lowe (Oxford University). Data for PA2580 was gathered on beamline I03 at Diamond light source using a Pilatus 6M detector. Data from PA2580-H₂NADPH was generated on beamline ID23-2 at the ESRF using a Pilatus 2M detector. Data was processed in xia2 (Winter, 2010) using XDS (Kabsch, 2010) and XSCALE. The 1.29 Å structure of PA2580 was solved using the molecular replacement software PHASER (McCoy *et al.*, 2007). MdaB from *E. coli* (59.4% sequence identity to PA2580) and MdaB from *Yersinia pestis* (51.8% sequence identity to PA2580), PCSB PDB accession codes 2B3D and 3RPE respectively, were used as templates for molecular replacement for the PA2580 model. The atomic model was built and refined with Coot (Emsley *et al.*, 2010) against the electron density map. Further refinement was performed in PHENIX (Adams *et al.*, 2010). FAD model was added with Coot (Emsley *et al.*, 2010) as were water molecules.

2.8 Phenotypic characterisation of *P. aeruginosa* strains

2.8.1 Confirmation of transposon insertion in *P. aeruginosa* PAO1 gene deletion strains

To ensure the presence of the transposon and the subsequent mutation of the azoreductase and azoreductase-like genes, PCR amplification was carried out using the primers listed in Table 2.16. All primers were gene-specific and overlapped part of the coding and non-coding sequence of the gene. Primers were designed by Dr. Vincenzo Crescente (Kingston University) using the same method as laid out in section 2.3.4 with the exceptions of the primers for *pa0785*, *pa1962* and *pa3223* which were designed by Wang and colleagues as described in Wang *et al.* (2007). PCR was carried out using the Hotstar HiFi DNA polymerase kit as described in section 2.3.4 with an annealing temperature of 55°C used for each reaction. The transposon mutants have the ISphoA/hah (5 kb) or ISlacZ/hah (6.7 kb) inserted within the coding region of the mutated gene. The azoreductase-like genes, *pa0785*, *pa1962*, *pa3223*, *pa2280*, *pa2580*, *pa1204*, *pa0949* and *pa4975*, are all less than 800 bp in size. Hotstar HiFi DNA polymerase amplifies DNA at a rate of 1 Kb per minute; therefore an extension time of one minute was used. This would allow any of the azoreductase-like genes in their wild type state to amplify in this time while the transposon containing genes would be too large. PCR products were analysed on 1% w/v agarose gel as described in section 2.3.2.

Table 2.16 Gene-specific primers used to confirm the transposon insertion in the azoreductase-like genes

Primers were designed to overlap the coding and non-coding sequence for each gene. An annealing temperature of 55°C was used for each of these primers. Primers for *pa0785*, *pa1962*, *pa3223* were designed by Dr. Chan Ju Wang (Wang *et al.*, 2007), all other primers listed were designed by Dr. Vincenzo Crescente (Kingston University).

Primer	Sequence
<i>pa0785</i> KO fwd	CATTCGAGTCTAGCCGAATCCAAGGAG
<i>pa0785</i> KO rev	CACCAGCAGATGGAACCAAGGCCATG
<i>pa1962</i> KO fwd	GATGCAAACCACTCGATCGCCAACCACTG
<i>pa1962</i> KO rev	GATGCAAACCACTCGATCGCCAACCACTG
<i>pa3223</i> KO fwd	GATACATATGTCCCGTGTCTTGGTTATCG
<i>pa3223</i> KO rev	CCCGGCCGTACACCCGCAACCAT
<i>pa2280</i> KO fwd	CCGGAGGACATATGTCCGAACAACCTACCCAACCTCG
<i>pa2280</i> KO rev	GGCGGACGGAGCTCAGAGCGAACGCTGGGTTCGACCC
<i>pa2580</i> KO fwd	CCAGCATGTACGGAACCATATGAAAATCATTCTCCTGC
<i>pa2580</i> KO rev	GGCCCGAGCTCGAACTCAGCCGGCGCG
<i>pa1204</i> KO fwd	CGAGGAGCACCATATGAGCGACGACATCAAGGTATTG
<i>pa1204</i> KO rev	CATGTTTCGAGCTCTCCGGTGACGAGGCATTCAAC
<i>pa0949</i> KO fwd	GAGTCCTGGAGATCCTCATATGAGCAGTCCCTACATCCTG
<i>pa0949</i> KO rev	GTGAGCTCTTGCGGGCCATTTCAACTCCCCAGCTTG
<i>pa4975</i> KO fwd	CGGAAACCCATATGAACGTACTGATCGTCCACGC
<i>pa4975</i> KO rev	CACCGAGCTCAGCGCGCCAGCGGCTGG

2.8.2 RNA extraction and cDNA synthesis from *P. aeruginosa* PAO1, the azoreductase-like gene deletion strains and the complemented strains

RNA was extracted from overnight cultures of all the gene deletion mutant strains of *P. aeruginosa* PAO1 and their equivalent complemented strain. Of each culture, 0.5 mL ($\sim 3.5 \times 10^8$ CFU) was treated with RNA protect bacteria reagent (Qiagen) prior to RNA extraction using the RNeasy Mini kit. On column DNase digestion was performed using the RNase-free DNase set (Qiagen). Purified RNA samples were visually analysed via agarose gel electrophoresis and quantified using a Nanovue™ plus spectrophotometer as described in sections 2.3.2 and 2.3.8. cDNA was synthesised from 1 µg of RNA using the QuantiTect kit (Qiagen).

2.8.3 Detection of gene expression in *P. aeruginosa* PAO1 strains

PCR was carried out on the synthesised cDNA using the protocol described in section 2.3.4. Gene-specific primers were designed to amplify within the coding region as per the method in section 2.3.4 and are listed in Table 2.17. Primers specific for the house keeping gene *rpoD* were used as a positive control. PCR products were analysed by agarose gel electrophoresis as described in section 2.3.2.

Table 2.17 Internal gene-specific primers used to check for gene expression

Primers listed below were designed to amplify the sequence between the first and last 100bp of the appropriate gene. cDNA synthesised from extracted RNA was used as the DNA template. *rpoD* primers represented the positive control. An annealing temperature of 55°C was used with these primers.

Primer	Sequence
<i>pa0785</i> exp fwd	GAGTAGAATTCTTGCAGTGCATGCCAG
<i>pa0785</i> exp rev	CCTCGAAGGACCTGCCCGGATTCTCGCC
<i>pa1962</i> exp fwd	CGCCTCCGCTTCCCGCCAACTGAGCG
<i>pa1962</i> exp rev	GCGAACTGCCCCGCGATCTGC
<i>pa3223</i> exp fwd	CCCGTGTCTGGTTATCGAGAGCAGTGCC
<i>pa3223</i> exp rev	GTTGGCAGAGGGACGCAAAGGGA
<i>pa2280</i> exp fwd	CCGAACAACCTACCCAACCTCGATCCC
<i>pa2280</i> exp rev	GCGGTCCACCAGGAAGTCCGTGCGC
<i>pa2580</i> exp fwd	GCGGAAAGCGTTTCGCCCATTCG
<i>pa2580</i> exp rev	CGCGCCCGAACACCCTGTCCAGGTGC
<i>pa1204</i> exp fwd	GCGACGACATCAAGGTATTGGGC
<i>pa1204</i> exp rev	GGCGCACCCATAGCTGCAGGGCC
<i>pa0949</i> exp fwd	CCCTACATCCTGGTGCTGTACTACAGTCGC
<i>pa0949</i> exp rev	CGACACAGGGTCAGTTCGTGCTCATCGAGGC
<i>pa4975</i> exp fwd	CGTCCACGCCCACAACGAACCGC
<i>pa4975</i> exp rev	CGGCTGGAGCAGCGCGTCAACTGC
<i>rpoD</i> exp fwd	GGGCGAAGAAGGAAATGGTC
<i>rpoD</i> exp rev	CAGGTGGCGTAGGTGGAGAA

2.8.4 Growth analysis of *P. aeruginosa* PAO1 and *P. aeruginosa* TBCF 10839 strains

Overnight cultures of all *P. aeruginosa* strains were added in 5 µL volumes to 95 µL Mueller Hinton (MH) broth in Nunclon flat transparent 96-well plates. Each bacterial inoculation was standardised to a final OD₆₀₀ of 0.02. Plates were sealed with sterile thermal adhesive sealing films (Thermo Scientific) and incubated at 37°C in the Infinite M200 PRO plate reader (TECAN) for 18 hours. OD₆₀₀ was measured every 30 minutes with 5 seconds plate shaking before each absorbance reading.

2.8.5 Determination of Minimum Inhibitory Concentration (MIC)

Doubling dilutions of fluoroquinolones (ciprofloxacin, levofloxacin, naladixic acid, sparfloxacin and prulifloxacin), a β -lactam (ceftazidime), an aminoglycoside (amikacin) and a polymyxin (colistin) were prepared in MH broth to cover a 64 fold range of concentrations. Prior to this step the fluoroquinolones were first dissolved in 0.1 M HCl and all other antibiotics dissolved in sterile ddH₂O. Overnight cultures of each *P. aeruginosa* strain were standardised to a final OD₆₀₀ of 0.02 and added in triplicate to each concentration of antibiotic in Nunclon flat transparent 96-well microtitre plates to a final volume of 100 μ L. MH broth containing no antibiotic was added to a sample of each strain as a positive control. Plates were sealed with sterile thermal adhesive sealing films (Thermo Scientific) and incubated in a static incubator at 37°C for 16 hours before OD₆₀₀ of each well was determined using a Tecan Infinite M200PRO plate reader. MIC was assumed to be the lowest concentration at which OD₆₀₀ was <0.1.

2.8.6 Determination of Colony Forming Units (CFU)/mL of *P. aeruginosa* PAO1 and *P. aeruginosa* TBCF 10839 strains

Overnight cultures of *P. aeruginosa* PAO1 along with the transposon insertion mutants and those containing the pUCP24 vector were standardised in LB to an OD₆₀₀ of 0.02. Serial dilutions were prepared in phosphate buffered saline (Oxoid) covering dilution factors of 10⁻¹, 10⁻², 10⁻³, 10⁻⁴, 10⁻⁵, 10⁻⁶ and 10⁻⁷. In triplicate, 5 μ L of each dilution was dropped onto LB agar and incubated overnight at 37°C. Drops containing 20-200 colonies were counted and the mean CFU/mL was determined using the following formula:

$$\text{number of colonies} \times \text{dilution factor} \times \frac{1000}{\text{volume added to LB}} = \text{CFU/mL}$$

Chapter 3 Cloning and expression of putative azoreductases PA1224, PA1225 and PA4975

3.1 Introduction

Azoreductases in *P. aeruginosa* have been gaining interest in recent years following reports that they play a key role in mammalian colonisation (Rakhimova *et al.*, 2008, Skurnik *et al.*, 2013). As of yet, the primary physiological role of azoreductases has not been determined however their function has been closely linked to the reduction of cytotoxic quinones, often secreted by invertebrates and plants as a defence mechanism (Ryan *et al.*, 2014, Cerenius *et al.*, 2008, Mayer, 2006). A BLAST search carried out by Wang *et al.* (2007) identified three azoreductases in *P. aeruginosa* PAO1, PA0785, PA1962 and PA3223. These were subsequently characterised and asserted as NAD(P)H dependent flavoenzymes capable of reducing azo and quinone compounds (Wang *et al.*, 2007, Ryan *et al.*, 2010b). An extensive bioinformatics study by Ryan *et al.* (2014) based on sequence and structural comparisons identified a further seven putative azoreductases in the *P. aeruginosa* PAO1 genome (Table 3.1). Of these, four (PA2280, PA2580, PA1204, PA0949) have successfully been overexpressed in *E. coli* and substrate specificity profiles have been established for each enzyme, confirming each of them as flavin and NAD(P)H dependent quinone reductases and three of them as flavin and NAD(P)H dependent azoreductases (Crescente *et al.*, 2016). The cloning of *pa1224* and *pa1225* will be reported on in this chapter. Expression of these two genes along with the third remaining gene, *pa4975*, followed by purification of the resultant recombinant proteins will also be described.

Table 3.1 Gene details of known azoreductases and azoreductase-like genes from *P. aeruginosa* PAO1

Table showing the name, location in the genome and the size of the azoreductase and azoreductase-like genes from *P. aeruginosa* PAO1.

Gene	Alternative name	Genome location (bp)	Size (bp)
<i>pa0785</i>	<i>azoR1</i>	857998-858636	639
<i>pa1962</i>	<i>azoR2</i>	2145984-2146502	609
<i>pa3223</i>	<i>azoR3</i>	3611254-3611895	642
<i>pa2280</i>	<i>arsH</i>	2508775-2509467	693
<i>pa2580</i>	<i>mdaB</i>	2916158-2916748	591
<i>pa1204</i>	<i>yieF</i>	1303892-1304449	558
<i>pa0949</i>	<i>wrbA</i>	1036579-1037175	597
<i>pa4975</i>	-	5585615-5586319	705
<i>pa1224</i>	-	1327024-1327803	780
<i>pa1225</i>	-	1327813-1328439	627

PA1224 was identified as a suspected azoreductase due to the 54% sequence similarity between PA1224 and the human azoreductase hNQO1, and the 41% sequence identity between PA1224 and hNQO1 and hNQO2 (Ryan *et al.*, 2014). Also, known as a DT-diaphorase, hNQO1 regulates proteasomal degradation, and overexpression in stomach cancer, breast cancer and cervical cancer and has been linked with a poor prognosis (Xu and Jaiswal, 2012, Biasini *et al.*, 2014, Kumar, 2012, Yang *et al.*, 2014). In addition, the structure of hNQO1 has been solved and has the same overall fold as paAzoR1 (Skelly *et al.*, 1999, Ryan *et al.*, 2011) (Figure 3.1). PA1225 and PA4975 were considered as potential azoreductases due to their significant sequence homology to another human azoreductase, hNQO2 (61% and 48% respectively) (Ryan *et al.*, 2014). Like hNQO1, hNQO2 structurally has the same overall fold as paAzoR1 (Foster *et al.*, 1999). The enzyme hNQO2 also plays a role in regulation of proteasomal degradation of proteins and is involved in the tumour necrosis factor signalling pathway (Ahn *et al.*, 2007). Although PA1224 and PA1225 are adjacent on the bacterial chromosome they are encoded on different strands so are therefore unlikely to be co-regulated as an operon. As of yet little is known of the function of either gene in *P. aeruginosa*. PA4975 on the other hand, has been shown to have NQO activity and is likely to play a role in arginine metabolism (Yang and Lu, 2007, Green *et al.*, 2014).

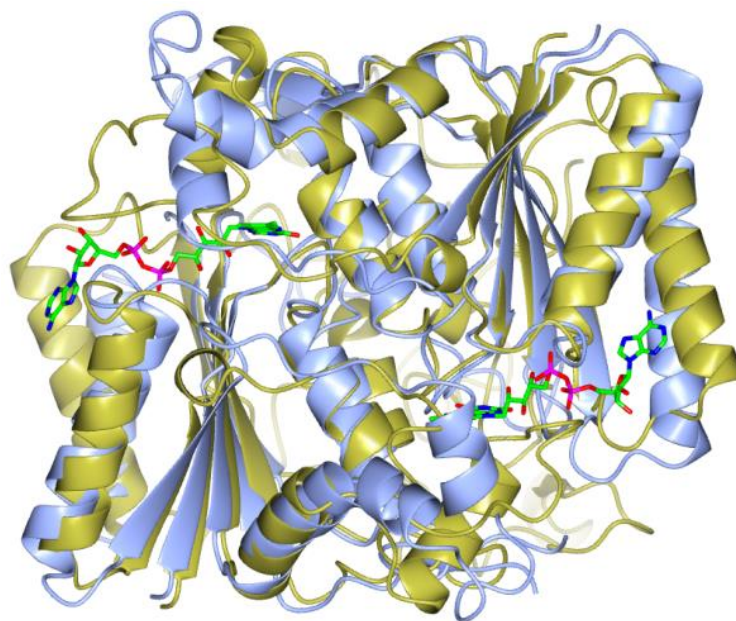


Figure 3.1 Structural comparison of hNQO1 and paAzoR1

paAzoR1 (represented in blue) and hNQO1 (represented in gold) are shown with flavin cofactor bound (green). The structure of paAzoR1 is from PDB 3R6W (Ryan *et al.*, 2011) and the structure of hNQO1 is from PDB 5EAI (Pidugu *et al.*, 2016). The two structures align with an RMSD value of 2.18. The image was generated and manipulated in CCP4MG (McNicholas *et al.*, 2011) and compared using the superpose tool in CCP4MG (Krissinel and Henrick, 2004).

Overexpression and subsequent characterisation of recombinant protein encoded by a gene of interest is one of the most popular means of examining gene function. The first step in this process is molecular cloning. The pET-28b vector (Figure 3.2 a) was previously used to clone azoreductase-like genes from *P. aeruginosa* PAO1 into *E. coli* (Wang *et al.*, 2007, Ryan *et al.*, 2010b, Crescente *et al.*, 2016) and cells containing the plasmid can be selected for by cultivation in kanamycin (Rosano and Ceccarelli, 2014). It carries multiple restriction sites (Figure 3.2 b), appropriate for insertion of a gene sequence, and includes a transcriptional hybrid promoter (T7/lac). The expression system in pET-28b is tightly controlled to eliminate basal expression of the gene of interest by the LacI repressor protein constitutively expressed by *lacI*, present in both the plasmid sequence and the *E. coli* genome (Sorensen and Mortensen, 2005, Rosano and Ceccarelli, 2014). In the absence of lactose, LacI binds to the *lacUV5* promoter of T7 RNA polymerase in the host strain, blocking the binding of *E. coli* RNA polymerase and thus inhibiting production of T7 RNA polymerase (Novagen, 2005). When lactose, or indeed its non-hydrolysable analogue, IPTG, binds to LacI, a conformational change occurs in the protein which renders it unable to bind to the operator sequence (Daber *et al.*, 2007). As a result, the T7 RNA polymerase gene can be transcribed which will in turn induce expression of the target gene in pET-28b.

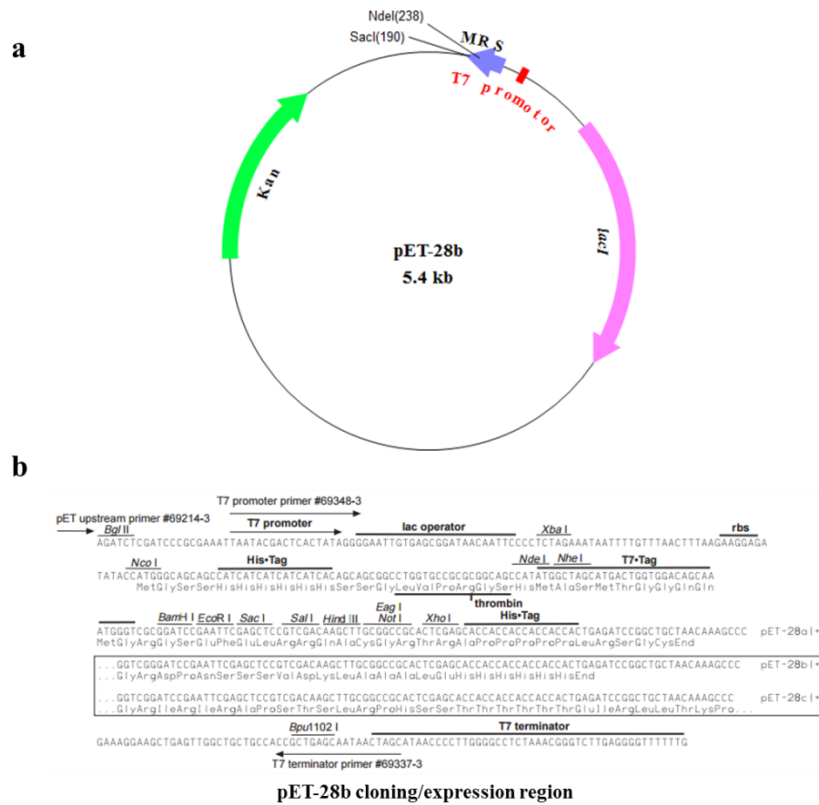


Figure 3.2 pET-28b vector map

pET-28b vector map showing the area of multiple restriction sites (MRS) with NdeI and SacI labelled (a). Multiple cloning site sequence showing the position of each restriction site as well as the His-tag coding region and the thrombin cleavage site (b). This figure was adapted from the Novagen website and the vector map generated using BVTech Plasmid.

In a protein characterisation study where a purified sample is essential, it is helpful to have a means to easily separate the recombinant protein from the host strain cellular milieu. One of the most utilised methods for this is purification via affinity tags which are amino acid sequences with high affinity for a specific biological or chemical ligand (Arnau *et al.*, 2006). The polyhistidine tag (His-tag) is an amino acid sequence that includes at least six consecutive histidine residues and is the most widely used affinity tag with more than 60% of proteins produced for structural studies including a His-tag (Derewenda, 2004). His-tagged proteins are purified using chelated metal ions as affinity ligands where the metal ion is attached to an immobilised chelating agent, with a nitrilotriacetic acid ligand immobilising nickel (Ni-NTA) in a sepharose matrix the most frequently used for purification of His-tagged proteins (Arnau *et al.*, 2006). Thus recombinant protein expression using pET-28b enables purification of the desired protein from the crude extract of the host cells in a single step. This system enables the application of a common protocol for the purification of proteins with a previously unknown biochemical profile, eliminating the need for a customised, protein-specific, and thus time consuming procedure.

Recombinant protein production in a different host strain is often essential as it can be difficult to produce sufficient soluble protein for structural and biochemical characterisation in the natural host. The genome of *E. coli* has been extensively characterised and is well understood so it is often used as the host for molecular cloning and protein overexpression. Also, many strains have been chromosomally engineered to facilitate this process (Baneyx and Mujacic, 2004). *E. coli* JM109 is a suitable strain for the initial transformation of a plasmid ligated with a gene of interest. This is due to the fact it has been genetically modified to be *recA*- and *endA*-. The deletion of *recA* prevents recombination of foreign or extrachromosomal DNA with host DNA, increasing the stability of the cloned plasmid, while the *endA* mutation eliminates the presence of non-specific endonuclease in the cell, improving plasmid quality and yield (Casali, 2003).

As previously mentioned, for recombinant protein expression using the pET system it is essential to transform the cloned vector into a strain that can produce T7 RNA polymerase (RNAP) which will in turn, induce expression of the gene of interest. *E. coli* BL21(DE3) and its derivatives are suitable hosts as they contain a chromosomal copy of the T7 RNAP gene under control of the *lacUV5* promoter (Daegelen *et al.*, 2009, Rosano and Ceccarelli, 2014). An extra advantage of using the *E. coli* BL21 cell lineage is that they are deficient in Lon protease which rapidly degrades proteins foreign to the host (Maurizi *et al.*, 1985). In addition, BL21 cells are also lacking in the OmpT outer membrane protease which has

the function of degrading extracellular proteins (Grodberg and Dunn, 1988). Upon cell lysis during extraction of recombinant protein, the OmpT protease if present, could digest the desired overexpressed protein.

Recombinant protein production in *E. coli* can be limited by a lack of tRNAs in the host strain that would be abundant in the organism from which the protein is derived. This can occur as a result of codon usage bias which is the likelihood that a particular codon will be used to code for a specific amino acid over another codon which codes for the same amino acid. During overexpression of the recombinant protein, a depletion of low abundance tRNA occurs which can lead to translational errors including amino acid substitutions, translational frameshifting and polypeptide truncation (Rosano and Ceccarelli, 2014). When expressing recombinant protein from *P. aeruginosa*, it is important to consider the high GC content (66.6%) of the *P. aeruginosa* genome which can influence codon bias (Stover *et al.*, 2000). A means of remedying the issue of codon bias in recombinant protein expression is co-transforming the host with a plasmid containing a gene encoding the tRNA cognate for the rare codons. *E. coli* BL21-CodonPlus(DE3)-RP, a derivative of *E. coli* BL21, is engineered to contain extra copies of genes that encode tRNAs from organisms with GC-rich genomes (Agilent, 2016).

Previous studies have described the cloning, expression and purification of azoreductases from *P. aeruginosa* PAO1 using methods relating to those listed above (Wang *et al.*, 2007, Ryan *et al.*, 2010b, Crescente *et al.*, 2016). This chapter describes the cloning, expression and purification including molecular weight determination of three putative azoreductases; PA1224, PA1225 and PA4975, from *P. aeruginosa* PAO1.

3.2 Results

3.2.1 Cloning of the putative azoreductase genes *pa1224* and *pa1225*

The protocols used in this section are described in Chapter 2, however the following results are closely linked to the experimental procedures and therefore this results section also describes where specific adaptations were applied to the general methods.

3.2.1.1 Preparation of genes of interest

The DNA sequences of *pa1224* and *pa1225* were obtained from the Pseudomonas Genome Database (Winsor *et al.*, 2016). Gene-specific primers were designed to overlap coding and non-coding regions of the appropriate genes. NdeI and SacI restriction sites were incorporated into the forward and reverse primers respectively. These were chosen to correspond with restriction sites present in pET-28b (Figure 3.2 **b**) and were particularly appropriate due to the NdeI restriction site sequence including the start codon of the three putative azoreductases (CATATG) and the SacI restriction site having a high GC content (GAGCTC). This pairing of restriction sites would also enable the incorporation of a His-tag coding region which encodes hexahistidine residues upstream of the inserted gene sequence (Figure 3.2 **b**). This in turn would include the hexahistidine at the N-terminus of the recombinant protein and thus allow for protein purification using the IMAC method. The primers were used to carry out a PCR reaction using High Fidelity Taq polymerase and extracted *P. aeruginosa* PAO1 genomic DNA as a template. On examination using 1% w/v agarose gel, PCR products estimated at 795 bp and 692 bp for *pa1224* and *pa1225* respectively were to be seen (Figure 3.3). Given the limitations and approximations of the technique these bands were considered to correspond with the expected sizes of 818 bp and 664 bp for *pa1224* and *pa1225* respectively. The PCR products were purified and quantified before a double restriction digest with NdeI and SacI restriction enzymes. Following this, the samples were purified and quantified once more, ready for ligation into the cloning vector.

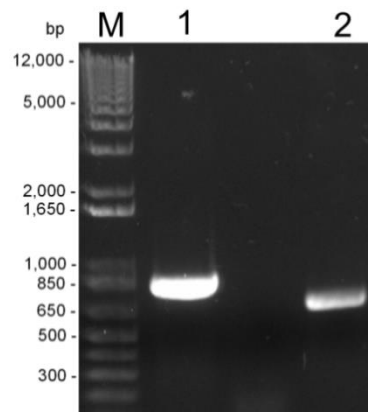


Figure 3.3 PCR amplification of *pa1224* and *pa1225* from *P. aeruginosa* PAO1

1% w/v agarose gel showing the putative azoreductases amplified from total *P. aeruginosa* PAO1 genomic DNA using HiFidelity Taq polymerase. Samples shown are 1 Kb Plus DNA ladder (lane M), *pa1224* (lane 1) and *pa1225* (lane 2). PCR products were of the expected sizes at 795 bp for *pa1224* and 692 bp for *pa1225* – actual sizes are 818 bp and 664 bp respectively.

3.2.1.2 Preparation of the cloning vector

The plasmid pET-28b was extracted from *E. coli* JM109 and quantified. A restriction digest was carried out on the extracted plasmid using the restriction enzymes NdeI and SacI. This double restriction digest was performed to prevent self-ligation of the plasmid. To ensure successful digestion had occurred, a sample of the digested plasmid was run alongside undigested plasmid on 1% w/v agarose gel (Figure 3.4). The undigested plasmid showed typical bands of supercoiled circular plasmid whereas the digested sample appeared as a defined single band representing linearization of the plasmid. Following purification and quantification the digested plasmid was treated with a phosphatase enzyme to remove the phosphate group at the 5' end. It is important to note that this step was omitted in the gene preparation stage as one 5' phosphate group is necessary for the ligation process. The phosphatase-treated plasmid was then purified and quantified.

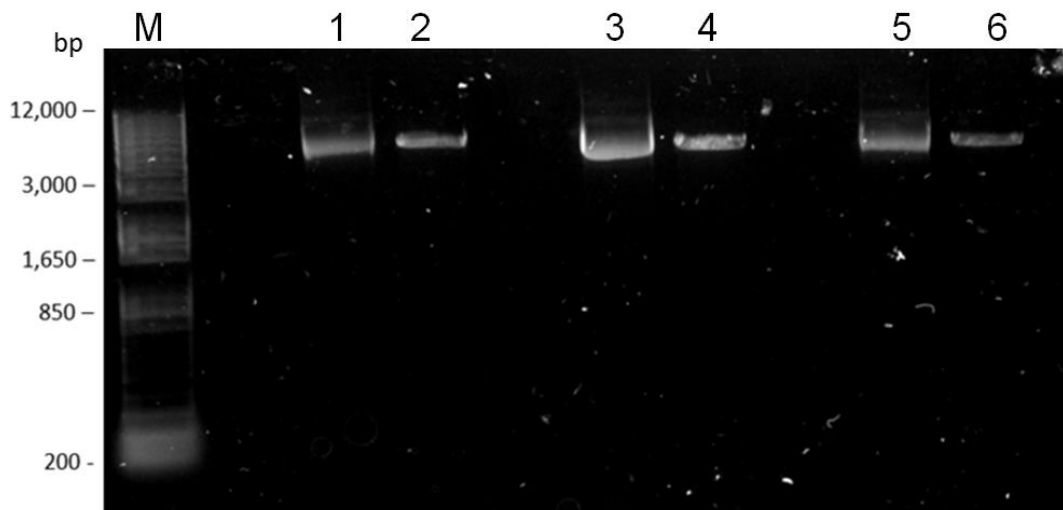


Figure 3.4 Endonuclease restriction digest of pET-28b

1% w/v agarose gel showing the pET-28b plasmid before and after endonuclease digestion with restriction enzymes NdeI and SacI. Digested samples (lanes 2, 4 and 6) display a linearised plasmid while the undigested samples (lanes 1, 3 and 5) show the supercoiled plasmid form. 1 Kb Plus DNA ladder (lane M) was used as standard.

3.2.1.3 Obtaining and screening successful clones

The plasmids and PCR products for *pal224* and *pal225* were ligated together before being transformed via the heat shock method into *E. coli* JM109. The cells were then grown on LB agar containing kanamycin so as to select for cells containing circular pET-28b which confers kanamycin resistance. Colonies were picked and grown in selective LB. Colonies containing empty, undigested pET-28b, which had been used as a positive control for the transformation, were also grown in the same selective medium. Colonies from each potential clone and one containing the empty plasmid were screened via PCR using primers designed to anneal to a section overlapping the vector and gene insert. This would allow for amplification only where both the plasmid and gene of interest were present meaning a PCR product would only be visible on agarose gel where there was a successful clone. PCR products were analysed on 1% w/v agarose gel. Bands of expected size were observed for the potential clones (Figure 3.5) indicating that cloning of the putative azoreductase genes had been successful. PCR-confirmed colonies for each clone were grown in selective LB and the plasmids were extracted and sequenced. The sequencing results were aligned with the appropriate sequences from the Pseudomonas Genome Database (data shown in APPENDIX V). This confirmed that no point mutations had occurred during the cloning process and that successful clones had been obtained.

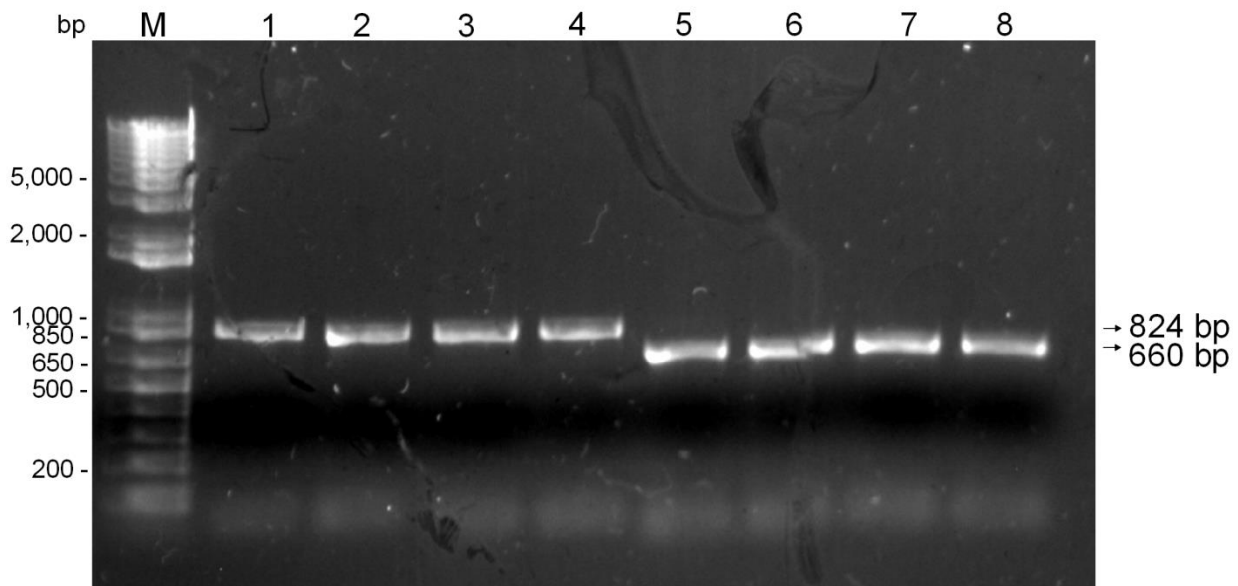


Figure 3.5 *E. coli* JM109 colony screening for successful clones

1% w/v agarose gel showing the PCR products for the genes *pa1224* (lanes 1-4) and *pa1225* (lanes 5-8) in pET-28b transformed into *E. coli* JM109. PCR products were of the expected size indicated by black arrows. 1 Kb plus DNA ladder was used as standard (lane M).

3.2.2 Expression of putative azoreductases PA1224, PA1225 and PA4975

3.2.2.1 Transformation into expression hosts *E. coli* BL21(DE3) and *E. coli* BL21 CodonPlus(DE3)-RP

Following confirmation of successful cloning by PCR and sequencing, plasmid extractions were performed on overnight cultures of positive clones for *pa1224*, *pa1225* and *pa4975*. The *E. coli* JM109 strain containing pET-28b::*pa4975* was generated by Dr. Vincenzo Crescente (Crescente, 2015). The extracted plasmids containing each gene of interest were then transformed into *E. coli* BL21(DE3) and *E. coli* BL21-CodonPlus(DE3)-RP (pET-28b::*pa4975* only). Individual colonies were selected and screened via PCR using primers specific for the gene of interest and the vector (Figure 3.6 **a** and **b**). Each expression host was also transformed with empty pET-28b to be used as a negative control for protein expression.

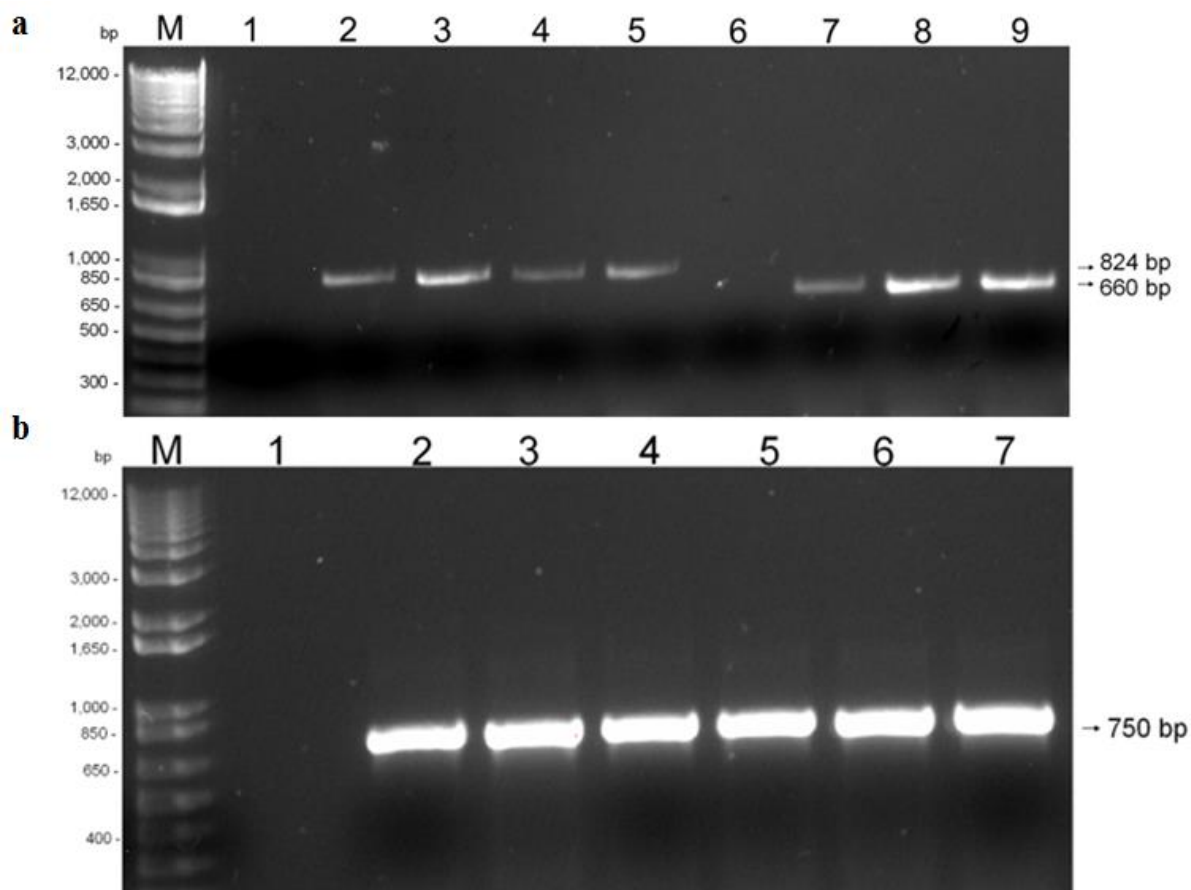


Figure 3.6 *E. coli* BL21(DE3) and *E. coli* BL21 CodonPlus(DE3)-RP transformants screening

1% w/v agarose gels showing the PCR products for the azoreductase-like genes in pET-28b. PCR products displayed represent *pa1224* (lanes 2-5) and *pa1225* (lanes 7-9) in pET-28b transformed into *E. coli* BL21(DE3). Lanes 1 and 6 represent the empty plasmid in *E. coli* BL21(DE3) (a). PCR products from transformants of *E. coli* BL21(DE3) and *E. coli* BL21 CodonPlus(DE3)-RP containing pET-28b::*pa4975* are displayed in lanes 2-4 and 5-7 respectively. The PCR reaction was also performed on *E. coli* BL21 CodonPlus(DE3)-RP containing pET-28b (lane 1) (b). 1 Kb plus DNA ladder was used as standard (lane M).

3.2.2.2 Overexpression of recombinant proteins

The process used to overexpress recombinant protein was adapted from a method published by Wang *et al.* (2007) where azoreductases from *P. aeruginosa* were cloned, expressed and characterised. This method is described in section 2.4.1. In order to optimise the procedure to generate a suitable yield of soluble protein, various parameters were implemented and they will be described briefly for each individual protein.

3.2.2.2.1 Overexpression of PA1224

Small scale (50 mL volume) protein production of PA1224 was initially carried out in LB 1 M sorbitol 2.5 mM betaine 30 µg/mL kanamycin. As the cultures entered the exponential growth phase (OD_{600} 0.4-0.6), expression was induced with the addition of 0.5 mM IPTG. These cultures were then incubated overnight at 16°C 120 RPM. Following bacterial cell lysis and separation of fractions the protein samples were analysed via SDS-PAGE (Figure 3.7 a). The cloned sample showed evidence of protein overproduction characterised by the appearance of a single intense band of appropriate molecular weight (product size estimated at 28.9 kDa using ExPASy ProtParam (Gasteiger E., 2005)) that was not present in the negative control. Comparison of the soluble and insoluble fractions of the clone shows that approximately 46% of the recombinant protein was soluble while 54% was insoluble. In an attempt to increase the yield of soluble protein, the same overexpression process was repeated with 1 mM FMN supplemented into the media. PA1224 is a suspected flavoprotein therefore addition of FMN to the expression media can stabilise the structure due to hydrogen bond formation between the flavin and the protein backbone (Ryan *et al.*, 2010a), limiting the chance of protein aggregation. In addition, the azoreductase active site is often shown as a highly conserved hydrophobic pocket where the flavin cofactor binds (Wang *et al.*, 2007). Binding of the flavin will decrease the exposure of a hydrophobic surface and may increase protein solubility. Comparison of the soluble protein produced with no FMN added against the soluble protein produced with 1 mM FMN in the media did not show any difference in yield with approximately 38% of the protein produced soluble with no FMN incorporated and 36% expressed in the soluble form in the presence of FMN (Figure 3.7 b). For this reason, no FMN was added when the process was scaled up to 500 mL. Results visible on SDS-PAGE indicated that overexpression was successful however a lower yield of protein was generated in the soluble fraction (approximately 24%) while expression appeared majorly in the insoluble counterpart (approximately 76%) (Figure 3.7 c). In order to obtain a desirable quantity of soluble protein, eight 100 mL cultures were induced for expression following the small

scale protein production protocol (section 2.4.1). These individual cultures were combined prior to the first centrifugation step where the cell pellet is formed. The cell pellets were then treated as described for the large scale procedure (section 2.4.1) and equivalent results to those of the small scale production were obtained. By this method, sufficient soluble PA1224 was produced for further analysis.

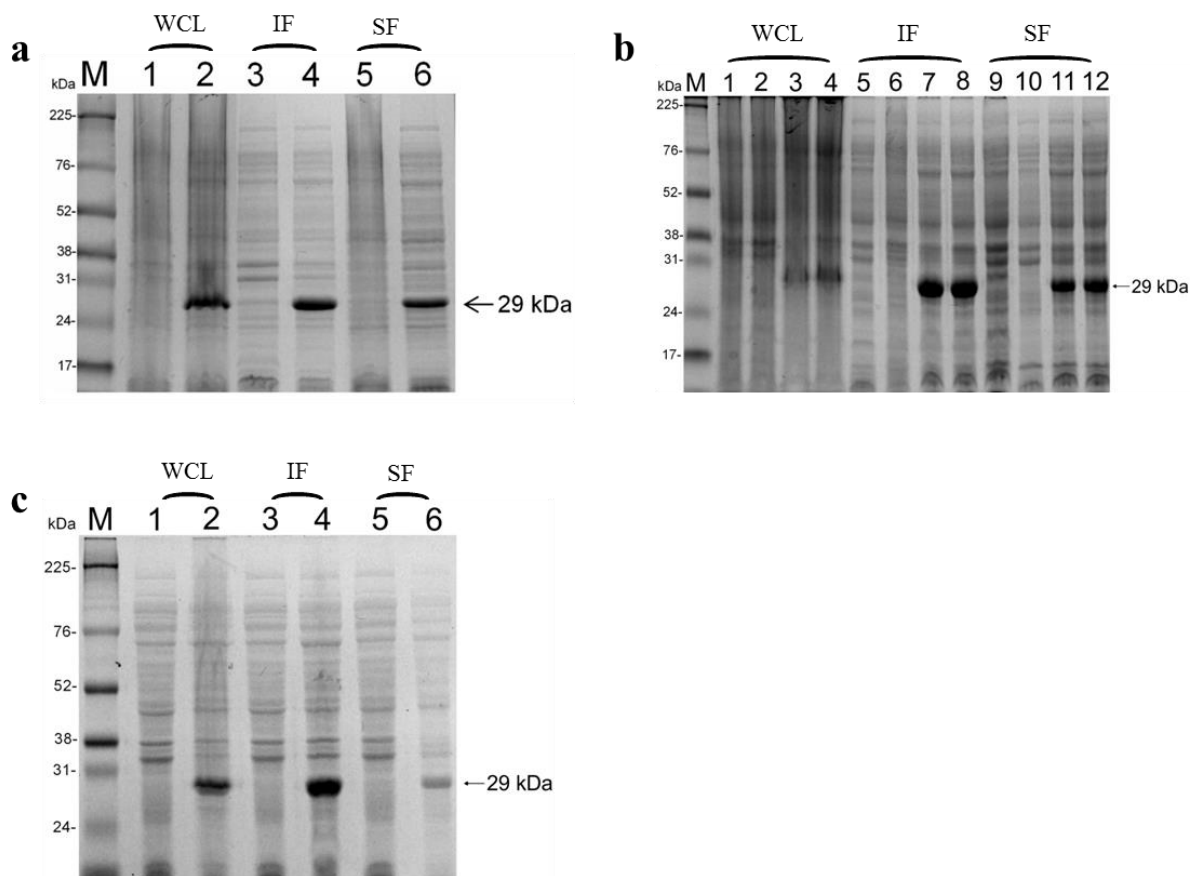


Figure 3.7 Overexpression of PA1224 recombinant protein in *E. coli* BL21(DE3)

Coomassie blue stained SDS-PAGE showing optimisation of PA1224 recombinant protein expression to favour the production of soluble protein. Small scale protein production in 50 mL culture volumes was compared between *E. coli* BL21(DE3) transformed with pET-28b::*pa1224* (lanes 2, 4 and 6) and a negative control of *E. coli* BL21(DE3)-pET-28b (lanes 1, 3 and 5) (a). Protein overexpression was compared in the presence (lanes 2, 4, 6, 8, 10 and 12) and absence (lanes 1, 3, 5, 7, 9 and 11) of FMN in the media. *E. coli* BL21(DE3) containing the empty vector pET-28b was used as a negative control (lanes 1, 2, 5, 6, 9 and 10) (b). Large scale protein production in 500 mL culture volumes depicts overexpression in the *pa1224* clone (lanes 2, 4 and 6) compared to the negative control of *E. coli* BL21(DE3)-pET-28b (lanes 1, 3 and 5) (c). Lanes marked 'M' represent the molecular weight marker.

3.2.2.2.2 Overexpression of PA1225

Small scale (50 mL volume) protein production of PA1225 was carried out in LB with 1 M sorbitol, 2.5 mM betaine and 30 µg/mL kanamycin added. Expression was induced during the exponential growth phase of the cultures (OD_{600} 0.4-0.6) by the addition of 0.5 mM IPTG. These cultures were then incubated overnight at 16°C 120 RPM. Following the separation of fractions the protein samples were analysed via SDS-PAGE. No obvious difference was apparent upon comparison of each fraction; the whole cell lysate, insoluble fraction and soluble fraction, against those from the negative control indicating that protein expression had been unsuccessful with this method (Figure 3.8 a). Considering the OD_{600} measurement of the cloned strain following the overnight expression period was similar to that of the control at 2.77 and 2.67 respectively, it was unlikely that this was due to the protein being toxic to the expression host. The same expression conditions were trialled again however this time using a different isolate of *E. coli* BL21(DE3)-pET-28b::*pa1225* and with 1 mM FMN added to the culture as this has been thought to reduce non-specific protein production and thus increase yield of the desired protein (Rafii *et al.*, 1990). The procedure was also carried out simultaneously in the absence of FMN so as a comparison could be drawn on the effect of flavin using the same bacterial isolate. On examination via SDS-PAGE it was noted that there was small but clear band at the appropriate molecular weight (product size estimated at 24.7 kDa using ExPASy ProtParam (Gasteiger E., 2005)) indicating that this particular isolate was expressing recombinant PA1225 (Figure 3.8 b). The addition of FMN did not appear to have any effect on protein yield or solubility. The presence of 1 M sorbitol and 2.5 mM betaine has been shown to increase the production of soluble protein (Blackwell and Horgan, 1991) however such osmolytes in the media will also put the cells under osmotic stress (Oganessian *et al.*, 2007). It was thus decided to trial expression using just L, the most commonly used media for culturing *E. coli* (Rosano and Ceccarelli, 2014). Initially, three 50 mL cultures were grown to the log phase and overexpression was induced with the addition of 0.1 mM, 0.5 mM and 1 mM IPTG. An expression period of 3 hours at 37°C 120 RPM followed before the cells were lysed and fractions separated. Through SDS-PAGE analysis it was evident that recombinant protein was produced in each sample with the culture induced with 0.1 mM IPTG displaying approximately 75% protein in the soluble fraction when compared to the corresponding insoluble fraction. The 0.5 mM and 1 mM IPTG induced samples had approximately 43% and 51% soluble protein produced respectively (Figure 3.8 c). *E. coli* BL21(DE3)-pET-28b induced with 1 mM IPTG was used as a negative control. Following on from this result, *E. coli* BL21(DE3)-pET-28b::*pa1225* was cultured in 50 mL LB 30 µg/mL kanamycin and

induced at the exponential phase with 0.1 mM IPTG. This time expression was continued for 16 hours at 37°C 120 RPM. Expression was successful with adequate protein yield appearing in the soluble fraction (67%) (Figure 3.9 a). This suggested that scaling up the procedure to 500 mL cultures would be worthwhile in order to obtain a higher volume of soluble protein. SDS-PAGE results of the large scale production showed that overexpression was achieved however less protein was obtained in the soluble fraction (42%) than when expression was carried out on a smaller scale (Figure 3.9 b). The same approach adopted for production of PA1224 (section 3.2.2.2.1) was thus applied where eight 100 mL cultures were used to overexpress soluble PA1225 and a similar percentage of soluble protein was obtained as from the 50 mL culture.

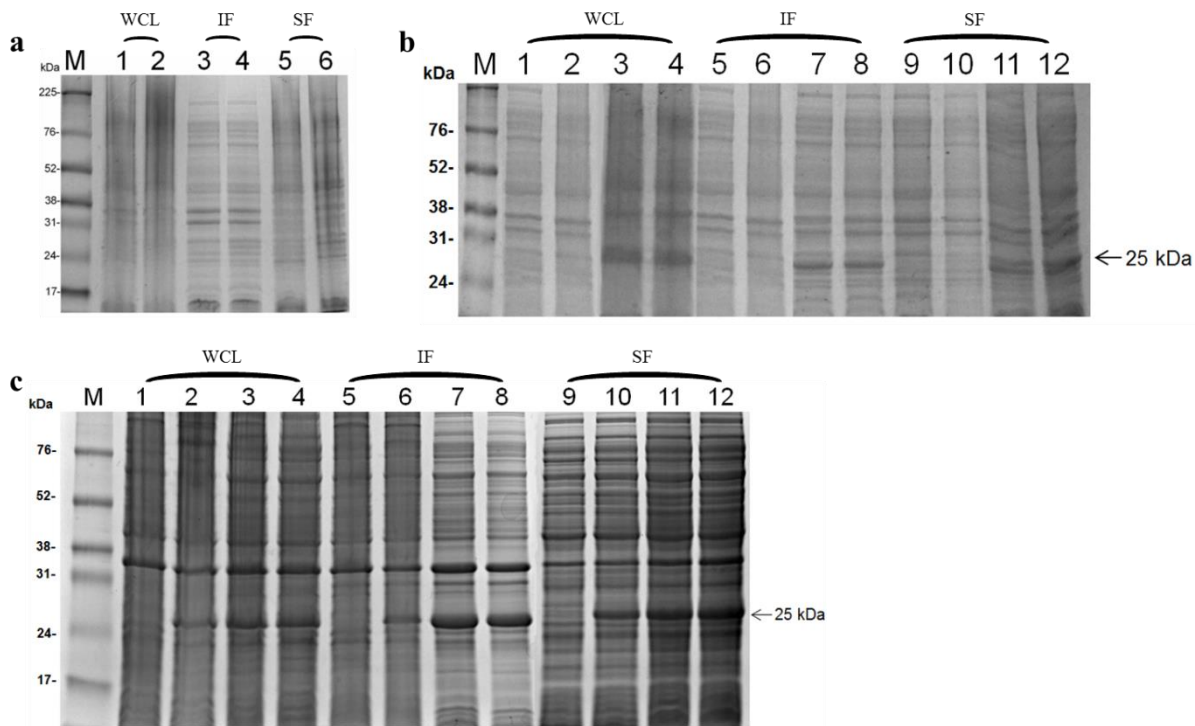


Figure 3.8 Optimisation of PA1225 recombinant protein overexpression in *E. coli* BL21(DE3)

Coomassie blue stained SDS-PAGE showing optimisation of PA1225 recombinant protein expression in 50 mL culture volumes to favour the production of soluble protein. Protein production was compared between *E. coli* BL21(DE3) transformed with pET-28b::pa1225 (lanes 2, 4 and 6) and a negative control of *E. coli* BL21(DE3)-pET-28b (lanes 1, 3 and 5) (a). Protein overexpression was compared in the presence (lanes 2, 4, 6, 8, 10 and 12) and absence (lanes 1, 3, 5, 7, 9 and 11) of FMN in the media. *E. coli* BL21(DE3) containing the empty vector pET-28b was used as a negative control (lanes 1, 2, 5, 6, 9 and 10) (b). Overexpression was trialled using LB as the culturing media. Protein production was initiated by the addition of 0.1 mM (lanes 2, 6 and 10), 0.5 mM (lanes 3, 7 and 11) and 1 mM IPTG (lanes 4, 8 and 12) with an expression period of 3 hours at 37°C to follow. Lanes 1, 5 and 9 represent the *E. coli* BL21(DE3)-pET-28b negative control induced with 1 mM IPTG (c). Lanes marked 'M' represent the molecular weight marker.

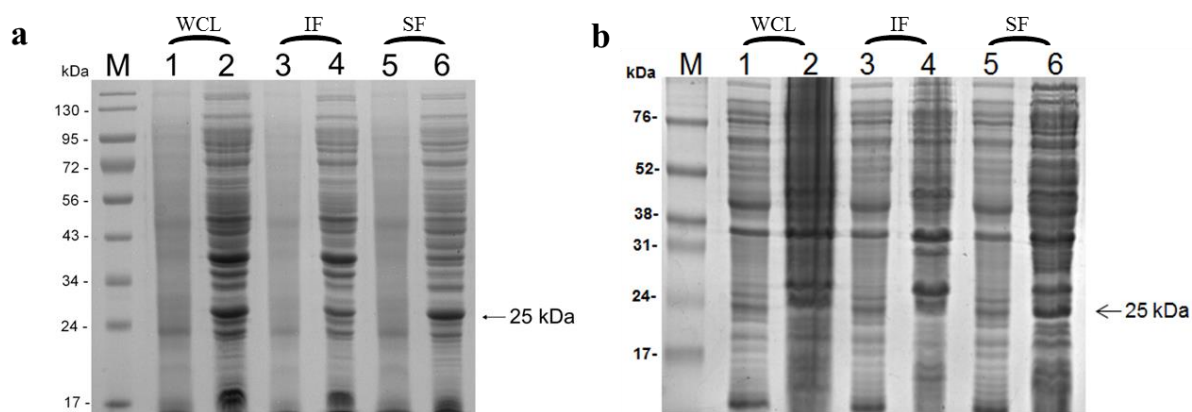


Figure 3.9 Overexpression of PA1225 recombinant protein in *E. coli* BL21(DE3)

Coomassie blue stained SDS-PAGE showing overexpression of PA1225 recombinant protein after 16 hours on a small and large scale. Small scale protein production in 50 mL culture volumes was compared between *E. coli* BL21(DE3) transformed with pET-28b::*pa1225* (lanes 2, 4 and 6) and a negative control of *E. coli* BL21(DE3)-pET-28b (lanes 1, 3 and 5) (a). Large scale production was carried out in 500 mL culture volumes. Lanes 1, 3 and 5 represent the negative control while lanes 2, 4 and 6 depict the *pa1225* clone (b). Lanes marked ‘M’ represent the molecular weight marker (Fisher Pre-stained *Rec* Protein ladder (a)).

3.2.2.2.3 Overexpression of PA4975

Small scale (50 mL volume) protein expression of PA4975 was initially attempted using LB containing 1 M sorbitol 2.5 mM betaine 30 µg/mL kanamycin. When the cultures reached the log phase of growth, indicated by OD₆₀₀ of 0.4-0.6, recombinant protein production was induced by addition of 0.5 mM IPTG. These cultures were then incubated overnight at 16°C 120 RPM. Following the separation of fractions the protein samples were analysed via SDS-PAGE (Figure 3.10 a). Overexpression of PA4975 was successful with a band appearing at the correct molecular weight (28.5 kDa as estimated by ExPASy ProtParam (Gasteiger E., 2005)). Approximately 29% of the protein was soluble compared to the insoluble sample. In order to optimise the method to favour production of soluble protein a range of conditions were trialled. Firstly, expression was induced with 0.1 mM, 0.2 mM, 0.3 mM, 0.4 mM and 0.5 mM IPTG. For this experiment the negative control was uninduced *E. coli* BL21(DE3)-pET-28b::pa4975. When the soluble fractions from each sample were compared on SDS-PAGE (Figure 3.10 b), there was little improvement apparent in the protein yield, however although overall there was little difference to be seen, the sample produced from the induction with 0.4 mM IPTG was arguably the most successful. Overexpression of recombinant protein resulting in a highly concentrated protein sample can sometimes result in aggregation and thus insoluble protein (Rosano and Ceccarelli, 2014), it was therefore decided to test shorter expression periods of 2 hours, 4 hours and 6 hours. Based on the previous result, induction was commenced with the addition of 0.4 mM IPTG. The samples were compared using SDS-PAGE (Figure 3.10 c). Expression was apparent in each sample however there was minimal protein present, even at 6 hours, and the protein remained predominantly in the insoluble fraction. The most soluble protein was produced after 6 hours. In a final attempt to gain soluble protein it was decided to transform pET-28b::pa4975 into a different host strain for expression. *E. coli* BL21-CodonPlus(DE3)-RP was selected it is specially adapted to possess extra tRNAs for rare codons in *E. coli*, in particular those originating from organisms with a high genomic GC content (Kleber-Janke and Becker, 2000). Cells were cultured as before in LB 1 M sorbitol 2.5 mM betaine 30 µg/mL kanamycin and expression was induced with 0.4 mM IPTG. Expression was continued for 16 hours at 16°C. The separated fractions were analysed on SDS-PAGE and overexpression was successful (Figure 3.11 a). The negative control was represented by *E. coli* BL21-CodonPlus(DE3)-RP containing pET-28b and was treated in the same manner as the strain containing the gene of interest. Although most protein remained insoluble (68%), the process was scaled up into two 500 L cultures in a bid to gain and characterise any soluble protein that was produced however low the yield.

When the fractions were viewed on SDS-PAGE it was clear that soluble protein was present although only at a yield of approximately 29% total protein produced (Figure 3.11 **b**).

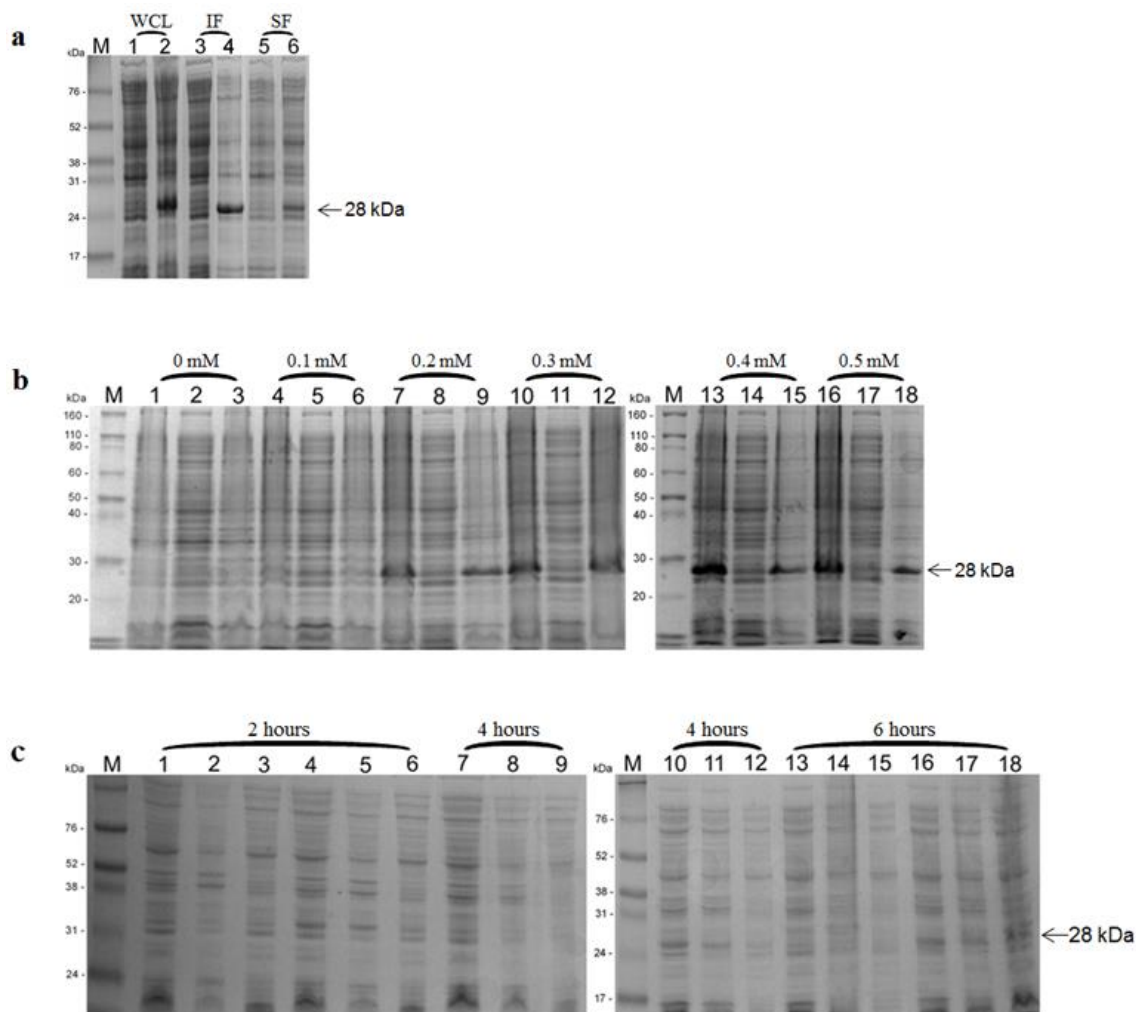


Figure 3.10 Overexpression of PA4975 recombinant protein in *E. coli* BL21(DE3)

Coomassie blue stained SDS-PAGE showing optimisation of PA4975 recombinant protein expression in 50 mL culture volumes to favour the production of soluble protein. Protein production was compared between *E. coli* BL21(DE3) transformed with pET-28b::pa4975 (lanes 2, 4 and 6) and a negative control of *E. coli* BL21(DE3)-pET-28b (lanes 1, 3 and 5) (a). Protein overexpression was trialled using varying concentrations of IPTG for induction. Samples represented include the whole cell lysates (lanes 1, 4, 7, 10, 13 and 16), the soluble fractions (lanes 2, 5, 8, 11, 14 and 17) and the insoluble fractions (lanes 3, 6, 9, 12, 15 and 18) (b). Protein expression was induced with 0.4 mM IPTG and varying induction times at 16°C followed prior to cell lysis and separation of fractions. There is little difference to be seen between the negative control of *E. coli* BL21(DE3)-pET-28b (lanes 1-3, 7-9 and 13-15) and the azoreductase clone (lanes 4-6, 10-12 and 16-18). Samples shown are the whole cell lysates (lanes, 1, 4, 7, 10, 13 and 16), the insoluble fractions (lanes 2, 5, 8, 11, 14 and 17) and the soluble fractions (lanes 3, 6, 9, 12, 15 and 18) (c). Lanes marked 'M' represent the molecular weight marker (ThermoFisher prestained protein ladder (b)).

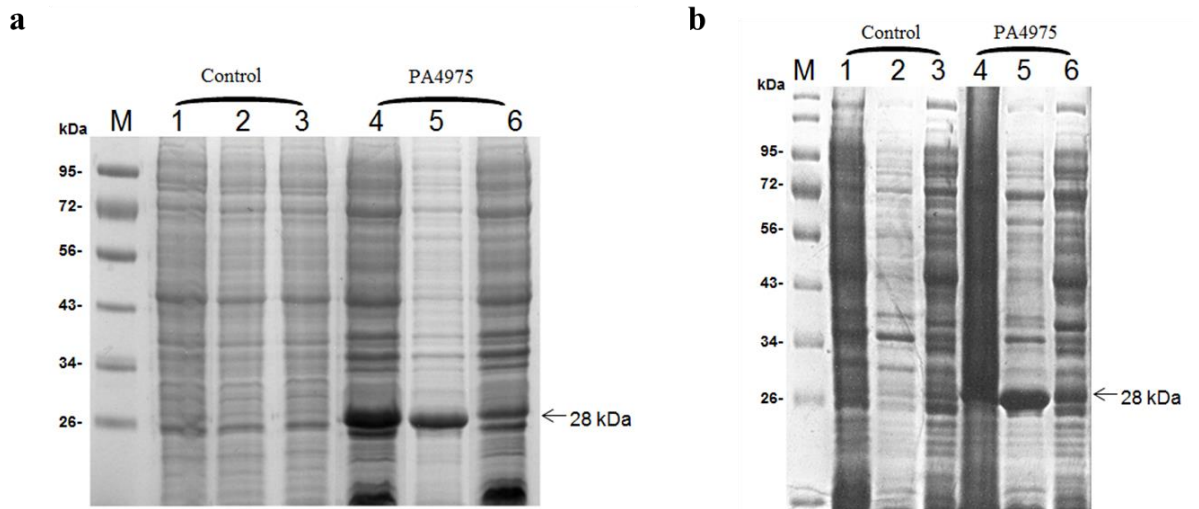


Figure 3.11 Overexpression of PA4975 recombinant protein in *E. coli* BL21-CodonPlus(DE3)-RP

Coomassie blue stained SDS-PAGE showing expression of recombinant PA4975. Small scale protein production in 50 mL culture volumes was compared between *E. coli* BL21-CodonPlus(DE3)-RP transformed with pET-28b::*pa4975* (lanes 4-6) and a negative control of *E. coli* BL21-CodonPlus(DE3)-RP-pET-28b (lanes 1, 3 and 5) (a). The procedure was scaled up to two 500 mL cultures (b). For both gels lanes 1 and 4 depict the whole cell lysates, lanes 2 and 5 represent the insoluble fraction and lanes 3 and 6 show the soluble fraction. Lanes marked ‘M’ represent Fisher Pre-stained *Rec* Protein ladder.

3.2.3 Purification and quantification of recombinant proteins

3.2.3.1 Purification with Immobilised Metal-ion Affinity Chromatography

All protein purification was carried out using the IMAC method. A volume of 4 mL 50% Ni-NTA slurry was loaded into a 10 mL column and the Ni-NTA beads washed twice with 20 mM Tris HCl 100 mM NaCl pH 8. For the purification of PA4975 only 2 mL of 50% Ni-NTA slurry was used due to the apparent low yield of protein as an overload of Ni-NTA can result in non-specific binding. The soluble fraction from each protein produced was applied to the column and mixed with the Ni-NTA before the liquid phase containing any unbound protein was removed by applying gentle pressure using a syringe. This flow through was collected for further analysis to confirm that the protein of interest was not present. The bound protein was eluted using increasing concentrations of imidazole (0-250 mM) which would act as a competitor for the hexahistidine tag. The protein elution depends on the number of histidine residues present; therefore it was likely that the protein would be eluted between the 100 mM and 250 mM imidazole concentrations. The protein of interest, due to the bound flavin, appears bright yellow in colour therefore it was possible to determine whether or not there was bound protein prior to analysis of the elutions on SDS-PAGE as the blue nickel beads would turn green in the presence of this protein. All eluates were analysed via SDS-PAGE along with the flow through and unpurified soluble fraction (Figure 3.12 **a**, **b** and **c**).

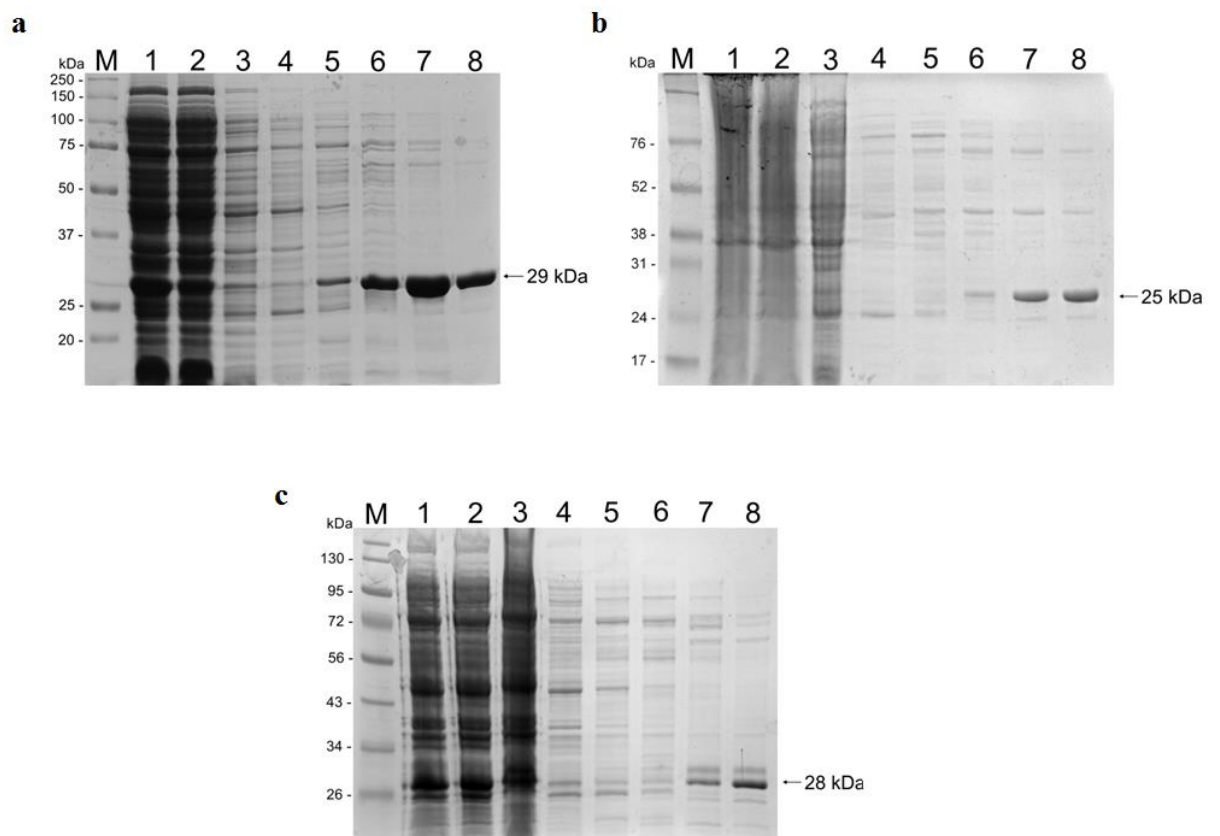


Figure 3.12 Purification of putative *P. aeruginosa* PAO1 recombinant azoreductase protein using IMAC

Coomassie blue stained SDS-PAGE showing the purification of the soluble fractions from expression lysates. Ni-NTA columns were loaded with the soluble fractions and eluted with buffer (20 mM Tris HCl, 100 mM NaCl, pH 8) containing increasing concentrations of imidazole (10, 25, 50, 100 and 250 mM). PA1224 (29 kDa) protein purification (a), PA1225 (25 kDa) protein purification (b), PA4975 (28 kDa) protein purification (c). All gel samples shown are labelled as follows: the molecular weight marker (lane M) (NEB broad range protein ladder (a), Fisher Pre-stained *Rec* Protein ladder (c)), soluble fraction (lane 1), flow through (lane 2), 0 mM imidazole (lane 3), 10 mM imidazole (lane 4), 25 mM imidazole (lane 5), 50 mM imidazole (lane 6), 100 mM imidazole (lane 7) and 250 mM imidazole (lane 8).

3.2.3.2 Dialysis and quantification of protein stocks

Following protein purification each sample was suspended in a buffer containing imidazole (50 mM, 100 mM, 250 mM for PA1224, 100 mM, 250 mM for PA1225 and 250 mM for PA4975). In order to remove excess imidazole, dialysis was performed by suspending molecular porous tubing containing the protein solutions in 4 L of dialysis buffer overnight (section 2.5.2). The molecular weight cut-off of 12-14 kDa of the dialysis tubing minimises protein loss during this process. Considering the difference in protein solution volume (4 mL for PA1224 and PA1225 and 2 mL for PA4975) and dialysis buffer volume (4 L), the imidazole concentration would be diluted roughly 1000 times for PA1224 and PA1225 and 2000 times for PA4975, meaning that the final imidazole concentration would be <1 mM. After removal of imidazole, the concentration of protein in each sample was determined by absorbance measurement at 280 nm and standardised in 20 mM Tris HCl 100 mM NaCl pH 8 5% v/v glycerol to 2 mg/mL for PA1224 and 1 mg/mL for PA1225 and PA4975. The aliquoted samples were stored at -80°C. PA1224 was obtained at 24.2 mg soluble purified protein per L culture. PA1225 expression yielded 16.7 mg purified recombinant protein/L culture in the soluble fraction. Much less soluble protein was gained from PA4975 expression with only 4.2 mg achieved per L culture. The actual amounts of protein obtained are listed in Table 3.2.

Table 3.2 Table listing the total yield of recombinant putative azoreductases produced
The yields of protein achieved following IMAC purification are listed along with the insoluble vs soluble protein percentage. The yields were calculated by determining the concentration of protein using the specific extinction coefficient as calculated by ProtParam available on ExPASy Bioinformatic Resource Portal (Gasteiger *et al.*, 2005). Percentages of insoluble and soluble protein gained were estimated using the volume analysis tool in Image Lab 5.2.1 (BIO-RAD).

Protein	Purified yield (mg)	Insoluble %	Soluble %
PA1224	19.4	62	38
PA1225	13.4	33	67
PA4975	4.2	71	29

3.2.3.3 Protein molecular weight determination

The molecular weight of each protein was determined by comparing their migration against the migration of molecular weight marker bands on SDS-PAGE (Figure 3.13) using the molecular weight analysis tool in ImageLab 5.2.1 (BIO-RAD). The predicted molecular weights for each protein were calculated using ProtParam, available on ExPASy Bioinformatic Resource Portal (Gasteiger *et al.*, 2005) and based on their amino acid sequences with the hexahistidine tag included at the N-terminus. The amino acid sequence was obtained from the *Pseudomonas* Genome Database (Winsor *et al.*, 2016). The calculated molecular weights were similar to those predicted from analysis on SDS-PAGE (Table 3.3).

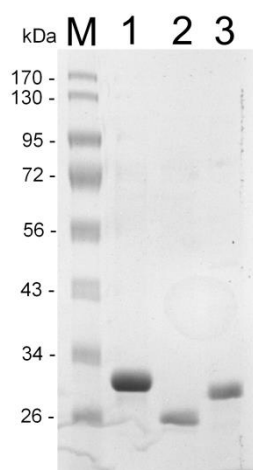


Figure 3.13 Purified recombinant proteins following ion exchange dialysis preparation for storage

Coomassie blue stained SDS-PAGE showing a single band for each putative azoreductase. PA1224 (lane 1) was concentrated to 2 mg/mL and PA1225 (lane 2) and PA4975 (lane 3) were concentrated to 1 mg/mL in 5% v/v glycerol for long term storage at -80°C (lane 1). Lane M represents a Fisher Pre-stained *Rec* Protein ladder.

Table 3.3 Estimated molecular weight of each purified recombinant protein along with the actual molecular weight

The molecular weight of each protein was estimated by comparing the migration of the single protein bands against the migration of bands from a standard molecular weight marker. The molecular weight analysis tool in Image Lab 5.2.1 (BIO-RAD) was used to estimate these molecular weights. The actual molecular weights were calculated using ProtParam available on ExPASy Bioinformatic Resource Portal (Gasteiger *et al.*, 2005) and were based on the amino acid sequences of each protein available from the *Pseudomonas* Genome Database with the His-tag sequence added at the N-terminus.

Protein	Estimated molecular weight (kDa)	Actual molecular weight (kDa)
PA1224	29	29.1
PA1225	26	24.7
PA4975	29	28.5

3.3 Discussion

The objectives listed in section 1.3 have been met as follows:

- i. The azoreductase-like genes *pa1224* and *pa1225* have been amplified by PCR and inserted into the pET-28b vector. The vectors containing the genes of interest were transformed into *E. coli* JM109. Gene sequencing has confirmed successful ligation of these genes into the plasmids with a complete absence of any point mutations.
- ii. The pET-28b vectors containing the azoreductase-like genes *pa1224*, *pa1225* and *pa4975* have been extracted from *E. coli* JM109 and transformed into *E. coli* BL21(DE3). pET-28b::*pa4975* has also been transformed into *E. coli* BL21-CodonPlus(DE3)-RP. This transformation was confirmed by PCR.
- iii. Putative azoreductases, PA1224, PA1225 and PA4975, from *P. aeruginosa* PAO1 were overexpressed in *E. coli* BL21 strains.
- iv. The recombinant proteins produced were purified and molecular weights determined, confirming similarity to the expected molecular weight of each protein.

P. aeruginosa possesses a striking ability to adapt to and thrive in a variety of environments including soil, marine habitats and plant and mammalian tissues. It is thought that this unique capacity of *P. aeruginosa* to activate suitable phenotypes under environmental stress is attributed to its large and complex genome (Stover *et al.*, 2000). The publication of the full genome sequence of *P. aeruginosa* PAO1 by Stover *et al.* (2000) and the subsequent development of the Pseudomonas Genome Database online (Winsor *et al.*, 2011) has enabled full genomic analysis of this organism which can lead to the identification of genes with a putative and potentially critical function. Following the successful identification and characterisation of several new members of the azoreductase family in *P. aeruginosa* PAO1 by Wang *et al.* (2007), Ryan *et al.* (2010b) and Crescente *et al.* (2016), similar methods were adapted in this study to examine suspected azoreductase encoding genes *pa1224*, *pa1225* and *pa4975*.

The process of cloning DNA is a well-established and understood system for examining the molecular and physiological role of specific genes. The particular method used in this study for cloning putative azoreductases from *P. aeruginosa* PAO1 into *E. coli* was directly adapted from that successfully utilised by Crescente *et al.* (2016). Following PCR analysis and gene sequencing, the cloning process was deemed to have worked efficiently with no point mutations occurring within the genes of interest.

In 2007, Wang and colleagues established a protocol for the expression of an azoreductase from *P. aeruginosa* PAO1. Following the successful production of soluble recombinant paAzoR1, the same method was applied by Ryan *et al.* (2010b) to generate stocks of paAzoR2 and paAzoR3 which they would subsequently characterise. The procedure proved effective once more in overexpression of azoreductases from *P. aeruginosa* PAO1 when Crescente and colleagues (2016) employed the pET system in *E. coli* BL21 to produce recombinant PA2280, PA2580, PA1204 and PA0949. It was thus deemed appropriate to initially trial expression of PA1224, PA1225 and PA4975 using this same technique where LB supplemented with 1 M sorbitol 2.5 mM betaine and 30 µg/mL kanamycin would be the expression medium, 0.5 mM IPTG would induce recombinant protein production and expression would be carried out for 16 hours at 16°C 120 RPM.

Upon SDS-PAGE analysis, PA1224 and PA4975 appeared to have been overexpressed using this procedure, although PA4975 was mainly insoluble. The addition of FMN to the media prior to expression did not seem to increase the yield of soluble protein in either PA1224 or PA1225, reasons for which will be discussed in the next chapter.

Given that approximately 40% of PA1224 expressed was in the soluble fraction the process was scaled up ten fold in order to produce sufficient recombinant protein to characterise. It was found to be the case however, that increasing the culture volume to 500 mL reduced the yield of soluble protein. This was potentially due to oxygenation of the cultures which can have a profound influence on growth and can also act as a regulatory signal affecting the metabolic capacities of the cell (Losen *et al.*, 2004, Unden *et al.*, 1995, Islam *et al.*, 2008). To abolish this issue a simple approach was undertaken where expression was induced simultaneously in eight 100 mL culture volumes and the products compiled prior to fractionation. This method achieved a satisfactory yield of soluble recombinant protein.

Gaining protein in the soluble fraction is essential when the objectives of a study include examination of the activity of the protein in question. Methods of solubilising the protein post-purification such as urea or guanidine hydrochloride denaturation are not recommended in this instance as they can reduce or eliminate any enzymatic activity (Dunbar *et al.*, 1997, Hedoux *et al.*, 2010). Non-peptide fusion partners including maltose-binding protein and glutathione *S*-transferase can act as solubility enhancers although the specific mechanism remains unclear (Raran-Kurussi and Waugh, 2012). The attachment of a large fusion tag, however can affect protein functionality so removal is essential prior to

activity assays and the final solubility of the desired product following this can be unpredictable (Esposito and Chatterjee, 2006). Through SDS-PAGE analysis of recombinant PA4975 it was evident that the protein was heavily overexpressed. The *E. coli* microenvironment differs from that of *P. aeruginosa* in terms of pH, osmolarity and folding mechanisms, thus overexpression of a non-native protein can result in protein aggregation and inclusion body formation. For this reason, the method was altered in a bid to slow down expression of PA4975 where lower concentrations of IPTG were used for induction and expression was carried out for substantially shorter time periods. These adaptations however, proved mainly ineffective in increasing the soluble protein yield.

Another reason why insoluble protein is produced may be attributed to codon usage bias where the foreign coding DNA is significantly different to that of the host strain resulting in amino acid misincorporation and/or protein truncation (Rosano and Ceccarelli, 2014). The pattern of codon usage in *P. aeruginosa* differs from that of *E. coli* in that the latter preferentially uses codons which form codon-anticodon interactions with intermediate binding energy while *P. aeruginosa* employs codons with the strongest codon-anticodon interaction – a pattern often observed in microorganisms with a high GC content (West and Iglewski, 1988). For this reason, the pET-28b vector containing *pa4975* was transformed into *E. coli* BL21-CodonPlus(DE3)-RP as this strain produces rare tRNAs often associated with GC-rich genomes (Casali, 2003). This method however, only marginally improved the yield of soluble vs insoluble recombinant protein. On further inspection of the rare tRNA genes present in this *E. coli* strain, namely AGA, AGG (*argU*) and CCC (*proL*), it was found that two of these three (AGA and AGG) are actually rarely, if at all, used in *P. aeruginosa* (West and Iglewski, 1988). This may explain why little improvement was observed with recombinant protein expression in this strain. On the other hand, solving the issue of codon usage bias with a specially designed host strain can often improve overall protein yield but this overexpression can have a deleterious effect on the quantity of soluble protein gained (Rosano and Ceccarelli, 2009). This CodonPlus-RP strain carries an extra plasmid which will carry genes encoding for the rare tRNAs. As the presence of extrachromosomal DNA in the bacterial cytosol is energy draining for the cell (Hayes and Wolf, 1990), it is possible that this may slow down metabolic processes including recombinant protein expression. It could therefore be suggested that although the CodonPlus-RP strain was not suitable to correct codon usage bias in this case, it may have slowed down protein production sufficiently to slightly reduce protein aggregation. The overall soluble protein yield was still very low at 4.2 mg/L however this was decided to be

sufficient as usually minimal protein is needed for enzymatic characterisation. Finally, expression of hNQO2, which is a 43% identical homologue of PA4975, by Wu *et al.* (1997) generated a comparable 3 mg/L protein from expression in *E. coli* so perhaps this low yield, although different to that gained with the other azoreductases from *P. aeruginosa* PAO1, was not so unusual.

The expression of recombinant PA1225 proved more troublesome than anticipated with the typical system for expressing proposed azoreductases from *P. aeruginosa* PAO1 failing to generate any visible protein. To begin with, the same standard process was repeated with all three *E. coli* BL21(DE3) clones. This was to ensure that there was a problem with the expression method rather than a particular isolate as even though precautions such as PCR and agarose gel analysis were implemented to confirm successful transformation of each selected colony, we have found it to be the case that different clones can produce recombinant protein slightly differently (Vethanayagam and Flower, 2005). From this examination, one isolate appeared to express recombinant protein when compared to the negative control although the protein yield was still minimal. To troubleshoot this issue the protocol was altered to provide the *E. coli* strain with its optimum growth conditions for expression. LB was used for bacterial growth and protein expression without the addition of 1 M sorbitol and 2.5 mM betaine as the supplementation of compounds into the media can put the cells under osmotic stress (Oganesyan *et al.*, 2007). Additionally, protein expression following induction with IPTG was carried out at 37°C which is the optimum temperature for growth of *E. coli* (WHO, 2016). Recombinant protein expression under these conditions was successful with a 0.1 mM concentration of IPTG proving most suitable for gaining predominantly soluble protein. Why this clone failed to produce any obvious recombinant protein following the method that was successful for the generation of all the other suspected azoreductases remains unclear however the fact that PA1225 was indeed expressed following a method alteration indicated that this was not due to protein toxicity. Upon scaling up the procedure in order to obtain a higher yield of protein a similar problem was encountered to that experienced with PA1224 expression where little soluble protein was produced. The protocol was thus scaled down once more and 16.4 mg/L soluble protein was achieved following purification.

The next chapter will describe the characterisation of these three recombinant proteins.

Chapter 4 Characterisation of purified recombinant proteins PA1224, PA1225 and PA4975

4.1 Introduction

Azoreductases are a genetically diverse group of flavoenzymes that have been characterised in many bacterial species including *E. coli*, *B. subtilis*, *S. aureus*, *R. sphaeroides* and *P. aeruginosa* (Nakanishi *et al.*, 2001, Sugiura *et al.*, 2006, Chen *et al.*, 2005, Liu *et al.*, 2007a, Wang *et al.*, 2007). Due to their capacity to catalyse reduction of the azo bond (-N=N-) found in azo dyes and azo pro-drugs, much research to date has focused on their use in bioremediation regarding the treatment of effluent waste water from textile and cosmetic industries (Singh *et al.*, 2015). As azo compounds and their breakdown products are often mutagenic and thus harmful in an ecosystem, bioremediation is essential and bacterial degradation via enzyme production has proved a successful method in detoxification (Saratale *et al.*, 2009). It is important to note that many azo compounds are not degraded efficiently; it is therefore advantageous to identify microorganisms that synthesise azoreductases with broad substrate specificity profiles.

Azo compounds, including dyes and pro-drugs, are man-made substances. It is thus unclear the role bacterial azoreductases play in the natural environment. Along with the reduction of azo compounds, azoreductases have also been implicated in mammalian colonisation by *P. aeruginosa* (Rakhimova *et al.*, 2008, Skurnik *et al.*, 2013) and plant infection by *E. coli*, *S. enterica*, *P. syringae* and *E. chrysanthemi* (Landstorfer *et al.*, 2014, Goudeau *et al.*, 2013, Okinaka *et al.*, 2002). The specific function of azoreductases in relation to host survival is not yet known however these enzymes are upregulated in *E. coli*, *P. syringae* and *E. chrysanthemi* during plant colonisation and in response to oxidative stress induced by plant metabolites (Landstorfer *et al.*, 2014, Postnikova *et al.*, 2015, Okinaka *et al.*, 2002).

Water soluble quinones are produced by plants and fungi as a response to bacterial invasion (Mayer, 2006). These quinones are highly redox active molecules which can generate ROS causing severe oxidative stress within the cell (Bolton *et al.*, 2000). NAD(P)H quinone oxidoreductases reduce water soluble quinones to the less reactive quinol via a two electron transfer (Chesis *et al.*, 1984). Until recently, azoreductases and NAD(P)H quinone oxidoreductases were thought to be two distinct classes of enzyme (Nakanishi *et al.*, 2001, Chen *et al.*, 2005), however based on the mechanism of azoreduction (discussed below), Ryan and colleagues (2014) proposed that these two

classes of enzyme are part of an enzyme superfamily. This hypothesis was confirmed by Ryan *et al.* (2014) and Crescente *et al.* (2016) where they described how azoreductases from *P. aeruginosa* PAO1 were capable of reducing both azo and quinone compounds. Keeping in mind the activity of quinones as part of the innate defence mechanism in plants, this may provide an insight into the physiological role of bacterial azoreductases.

The azoreductases catalyse the reaction only in the presence of reducing agents NADH and/or NADPH as these molecules act as electron donors (Singh *et al.*, 2015). These flavin dependent azoreductases have been identified as enzymes which use NADH only (Nakanishi *et al.*, 2001), those that use only NADPH (Chen *et al.*, 2005) and those that can utilise both (Wang *et al.*, 2007). The particular flavin cofactor can also affect activity with some azoreductases showing increased reductive capacity with FMN in the reaction while others favour FAD (Crescente *et al.*, 2016). It is therefore necessary to determine the selectivity of each azoreductase for both NAD(P)H and flavin in order to define the optimal reaction conditions.

Reduction of both azo and quinone substrates occurs via a ping pong bi bi mechanism (Wang *et al.*, 2010). For the reduction of azo substrates, two NAD(P)H molecules are required as $\text{NAD(P)H} + \text{H}^+$ is a two-electron carrier and four electrons are needed to complete the reaction. It could therefore be suggested that the reduction of azo substrates is likely to be a double ping pong bi bi mechanism (Nakanishi *et al.*, 2001, Wang *et al.*, 2007). The bound flavin undergoes two cycles of two-electron reduction (from FMN to FMNH_2 or FAD to FADH_2) with NAD(P)H acting as an electron donor. Before the azo bond can be reduced it must tautomerise to its hydrazone form, creating a quinoneimine structure. This explains the ability of these enzymes to reduce both quinone and azo substrates. Reduction then occurs via a hydride transfer from the flavin to the tautomerised substrate (Ryan *et al.*, 2010a) (Figure 4.1). Since the reducing agent and substrate cannot bind to the enzyme simultaneously this is also known as a double displacement reaction meaning the binding and subsequent reduction of the azo substrate occurs when the NAD(P)^+ leaves the active site (Cleland, 1963, Yang *et al.*, 2005). Reduction of quinones occurs via a similar mechanism however only two electrons are needed to complete this reaction (Ryan *et al.*, 2014).

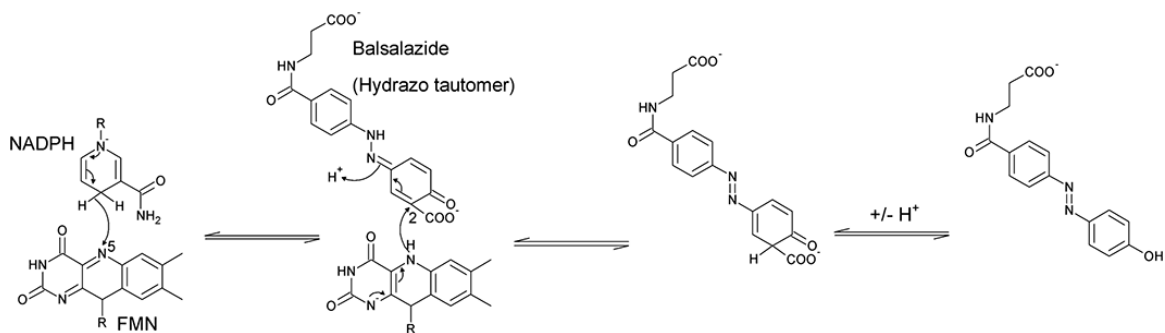


Figure 4.1 Proposed reduction mechanism for azo compound balsalazide by paAzoR1
 Following FMN reduction to FMNH⁻ by NADPH there is a subsequent hydride transfer to balsalazide. For simplicity, only the isoalloxazine ring of FMN and the nicotinamide group of NADPH are shown. Figure is taken from (Ryan, 2017).

As previously mentioned in Chapter 1Chapter 3, multiple enzymes from *P. aeruginosa* PAO1 have been identified as both azoreductases and NAD(P)H quinone oxidoreductases (Table 1.1) (Wang *et al.*, 2007, Ryan *et al.*, 2010a, Crescente *et al.*, 2016). All of these enzymes reduce quinone substrates with greater efficiency than they reduce azo substrates with rates of quinone reduction up to two orders of magnitude higher in all cases (Crescente *et al.*, 2016). Of the seven putative azoreductases identified by Ryan and colleagues (2014), three have yet to be characterised: PA1224, PA1225 and PA4975.

The structure of a quinone reductase from *K. pneumoniae* with 67% sequence identity to PA1224 has been solved (Kumar, 2012). Due to the moderately high sequence identity between this enzyme and PA1224, it is likely that they would have a similar structure and a model of the PA1224 structure based on that of the protein from *K. pneumonia* displays a flavodoxin-like fold similar to that of hNQO1 (Figure 4.2) (Kumar, 2012, Skelly *et al.*, 1999). Given that the overall fold of hNQO1 is similar to that of paAzoR1 (Figure 3.1), it could therefore be suggested that PA1224 may have similar catalytic properties to paAzoR1 and other azoreductases from *P. aeruginosa* PAO1.

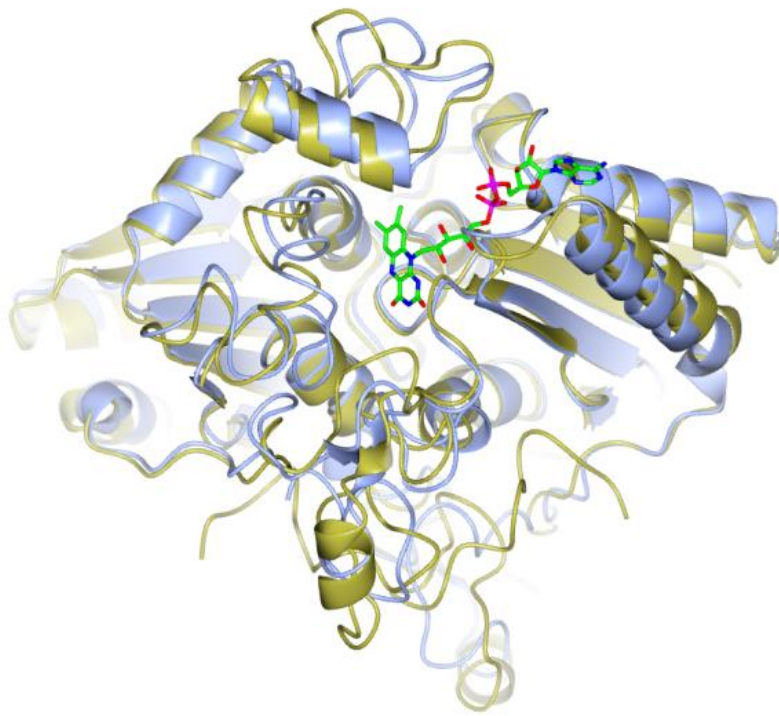


Figure 4.2 PA1224 structure modelled on a quinone reductase from *Klebsiella pneumoniae* with 67% sequence identity superposed against hNQO1

PA1224 (represented in blue) and hNQO1 (represented in gold) shown with the FAD cofactor bound (green). The structure of PA1224 was generated using Swiss-model (Biasini *et al.*, 2014) and based on PDB 4GI5 (Kumar, 2012). The structure of hNQO1 is from PDB 5EAI (Pidugu *et al.*, 2016). The two structures align with an RMSD value of 1.35. The image was generated and manipulated in CCP4MG (McNicholas *et al.*, 2011) and overlaid using the superpose tool in CCP4MG (Krissinel and Henrick, 2004, Goudeau *et al.*, 2013, Postnikova *et al.*, 2015, Okinaka *et al.*, 2002).

As discussed in Chapter 3, hNQO1 displays sequence homology with PA1224 and hNQO2 shows sequence homology with PA1225 and PA4975 (Ryan *et al.*, 2014). Given that hNQO1 and hNQO2 can reduce azo and quinone substrates (Wu *et al.*, 1997), it is possible that these three proteins from *P. aeruginosa* PAO1 may also be able to catalyse such reactions. This chapter describes the biochemical and enzymatic characterisation of PA1224, PA1225 and PA4975 in terms of thermostability, NAD(P)H and flavin selectivity and substrate specificity.

4.2 Results

4.2.1 Characterisation of recombinant putative azoreductases

A number of biochemical assays were carried out on the purified recombinant proteins PA1224, PA1225 and PA4975 in order to determine their flavin and NAD(P)H selectivity for enzymatic reduction and establish their substrate specificity profiles. In addition, the molecular ratio of flavin molecule per protein monomer was calculated. All statistical analysis was performed using GraphPad Prism (version 7).

4.2.1.1 Determination of flavin selectivity for putative azoreductase proteins from *P. aeruginosa* PAO1

To establish the presence of FMN or FAD molecules on recombinant proteins PA1224 and PA1225, absorption spectra and TLC analysis were conducted on each protein and results compared with that of free FMN and FAD molecules. These specific assays were unable to be performed on PA4975 due to the low yield obtained during protein production (section 3.2.3.2).

4.2.1.2 Absorbance spectra of FMN, FAD, PA1224 and PA1225

To ascertain the presence of flavin molecules within the proteins, absorption spectra between 250 and 600 nm were generated for the pure proteins PA1224 and PA1225. Spectra were also obtained using solutions containing 20 μ M free FMN or FAD for comparison with the protein spectral data, due to the overly high absorbance readings obtained for the flavin solutions within the UV spectrum, the readings in this case began at 300 nm. The flavin spectra were typical with two distinct peaks at 360 nm and 450 nm (Figure 4.3 a and b). Both PA1224 and PA1225 displayed spectra similar to the flavin groups (Figure 4.4) with well-defined peaks appearing at 360 and 450 nm with the latter slightly more prominent in both cases. For this reason, the absorbance reading at 450 nm was used to determine the molar ratio of protein molecule to flavin molecule. Upon initial comparison of the absorption spectra of PA1224 against that of PA1225, higher absorbance readings were shown for PA1224 at the two flavin peaks (360 and 450 nm) indicating that this is the protein with the greater flavin content (Figure 4.4).

Ideally, the molar ratio of protein monomer to flavin molecule should be 1:1 however the actual calculated molar ratios were 1.9:1 and 2.4:1 for PA1224 and PA1225 respectively. This indicates a relatively successful incorporation of flavin during recombinant protein expression when compared to other azoreductase-like enzymes from *P. aeruginosa* PAO1

such as PA0949 which has a molar ratio of protein to flavin molecule of 6:1 (Crescente *et al.*, 2016). This data also suggests that PA1224 and PA1225 are indeed flavoproteins and confirms that more flavin is present in PA1224 than in PA1225.

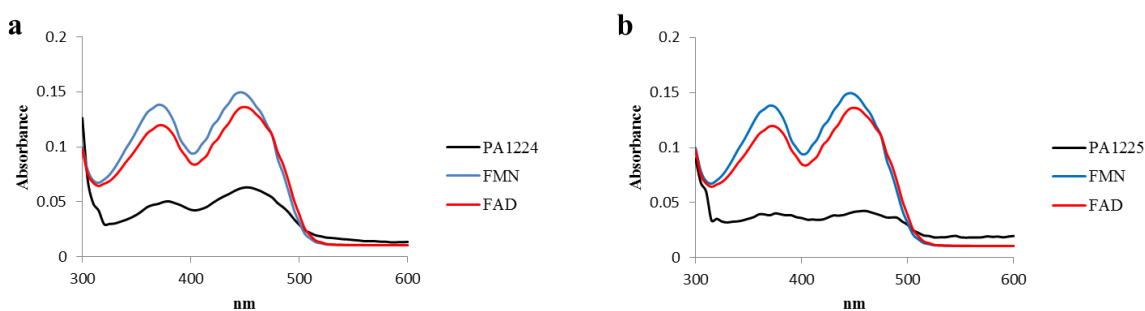


Figure 4.3 Absorption spectra for PA1224 and PA1225

Absorbance spectra of the purified recombinant proteins PA1224 (a) and PA1225 (b) compared with FMN and FAD absorption spectra, showing two absorption shoulders for the free flavin molecules (λ_{max} 360 and 450 nm). 400 $\mu\text{g}/\text{mL}$ protein solutions were prepared in 20 mM Tris HCl 100 mM NaCl pH 8 and placed in UV transparent cuvettes for the spectra determination. 20 μM FMN and FAD solutions were prepared in the same buffer and analysed via the same method as the protein solutions. Absorption spectra were generated in triplicate using Infinite M200 PRO plate reader between 300 and 600 nm.

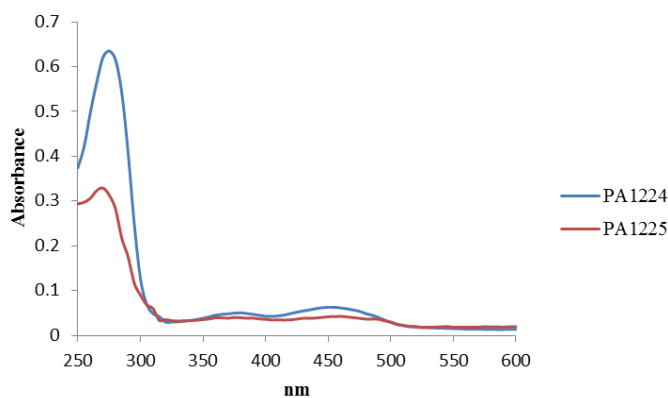


Figure 4.4 Absorption spectra comparison of recombinant proteins from *P. aeruginosa* PAO1

Comparison of absorption spectra of PA1224 (blue) and PA1225 (red) showing the different absorbances at 280, 360 and 450 nm. 400 $\mu\text{g}/\text{mL}$ protein solutions were prepared in 20 mM Tris HCl 100 mM NaCl pH 8 and placed in UV transparent cuvettes for the spectra determination. Absorption spectra were generated in triplicate using Infinite M200 PRO plate reader between 250 and 600 nm.

4.2.1.3 Thin Layer Chromatography

In order to further confirm the presence of flavin within the proteins PA1224 and PA1225 and also to establish whether the flavin in question was FMN or FAD, the proteins were analysed using TLC. Flavin molecules can be separated on TLC plates due to the difference in polarity, thus concentrated protein samples were ran on TLC plates alongside free FMN and FAD for comparison. Prior to this, the experiment was optimised to find the appropriate flavin concentration. Five concentrations ranging from 0.5-20 mM were tested for each flavin and it was decided that 1 mM gave the most suitable result (Figure 4.5 **a**). Purified PA1224 and PA1225 were concentrated to 20 mg/mL and spotted on TLC plates alongside FMN and FAD. The results show a visible spot for both proteins at a similar migrated distance to that of FAD (Figure 4.5 **b**). Consistent with the data from section 4.2.1.2 where PA1224 has a higher ratio of flavin molecule per protein monomer than PA1225, a more intense spot for PA1224 is evident when compared to that of PA1225. Retention factors (R_f) were calculated for both proteins and compared with those obtained for FMN and FAD. Although the FMN samples did not produce a well-defined spot, the R_f was calculated from where the smearing of the sample began as this was comparable to results from previous experiments (Crescente *et al.*, 2016). R_f values of 0.24 and 0.29 were achieved for PA1224 and PA1225 respectively. Although these are not identical to the R_f of 0.27 for FAD, they are much closer to FAD than FMN which was found to have an R_f of 0.44. These results suggest that FAD is the preferred flavin for these proteins and also confirms PA1224 and PA1225 as flavoproteins.

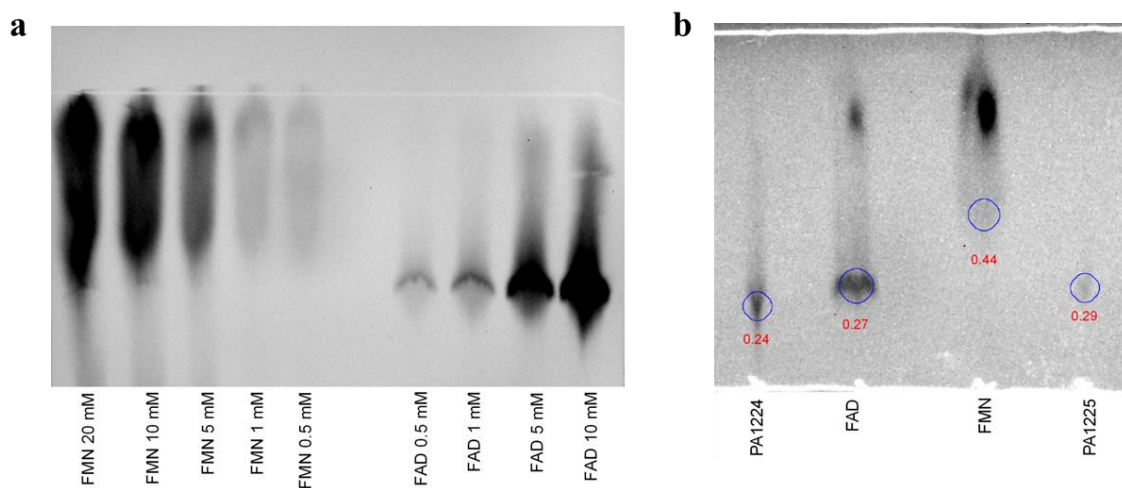


Figure 4.5 TLC optimisation of free FMN and FAD (a) and TLC profiles of PA1224 and PA1225 (b)

TLC analysis of FMN and FAD on silica coated aluminium plates showing the migrations of FMN and FAD. Optimisation was performed using 20, 10, 5, 1 and 0.5 mM of free flavins (a). TLC analysis was performed to compare the migration of PA1224 and PA1225 against that of FMN and FAD. A single spot was found for both proteins similar to that of FAD (R_f : PA1224 0.24, PA1225 0.29, FMN 0.44, FAD 0.27). Solutions used were 20 mg/mL protein and 1 mM flavin (b). All solutions were prepared in 20 mM Tris HCl 100 mM NaCl pH 8, 1 μ L of each solution was spotted on the plates. A mixture of N-butanol, acetic acid and water (2:1:1) was used as solvent.

4.2.1.4 Differential Scanning Fluorimetry

To investigate the thermostability of the recombinant proteins PA1224, PA1225 and PA4975, DSF was carried out. This method was also used to examine any thermal shift occurring upon addition of FMN or FAD to the protein. The procedure was carried out as described in section 2.6.2 where a sample containing protein and a dye (Sypro Orange) is slowly heated. The dye has an affinity for hydrophobic parts of the protein which are exposed upon unfolding. The temperature at which the protein unfolds is ascertained by the increase in fluorescence of the dye as it binds to the unfolded protein (Niesen *et al.*, 2007). All determined melting temperature (T_M) values are listed in Table 4.1. The T_M for PA1224 was 41.1°C. Upon addition of 1 μ M FMN the protein was destabilised while the presence of 1 μ M FAD made no difference. However, a significant increase in thermostability was seen following the introduction of 5 μ M and 10 μ M FAD indicating binding of flavin to the protein. This stabilisation occurs as a result of hydrogen bond formation between the flavin and the protein backbone (Ryan *et al.*, 2010a). No thermal shift was apparent upon the inclusion of 5 μ M or 10 μ M of FMN. A T_M of 57.6°C was established for PA1225. This time a significant thermal shift of >10°C occurred upon inclusion of both FMN and FAD at concentrations of 1 μ M and 5 μ M with a higher increase visible in the samples containing FAD. At 10 μ M flavin, the increase in thermostability remained for the sample with FAD while the solution with FMN had a T_M similar to that of PA1225 without added flavin. These results are consistent with the findings from TLC where both PA1224 and PA1225 are selective for FAD. Regarding PA4975, a significant increase in the T_M of 48.6°C was to be seen upon inclusion of 1 μ M, 5 μ M and 10 μ M FMN while supplementation with 1 μ M and 5 μ M FAD slightly but significantly destabilised the protein. Incorporation of 10 μ M FAD failed to incur any thermal shift. This data indicates FMN binding to PA4975 thus suggesting it to be the preferred flavin for this protein.

Table 4.1 Binding of flavin cofactors to purified recombinant proteins

Changes in protein thermostability were measured in response to addition of either FMN or FAD. Protein was at 64 $\mu\text{g}/\text{mL}$ in 20 mM Tris HCl 100 mM NaCl pH 8. The measurements displayed depict the mean values with \pm standard deviation (n=3). Fitting of the melting curve was performed using Graphpad Prism (version 7) to a Boltzman sigmoidal distribution.

Protein	$T_M/^\circ\text{C}$	+ FMN			+ FAD		
		$T_M + 1 \mu\text{M}$	$T_M + 5 \mu\text{M}$	$T_M + 10 \mu\text{M}$	$T_M + 1 \mu\text{M}$	$T_M + 5 \mu\text{M}$	$T_M + 10 \mu\text{M}$
PA1224	41.1\pm0.1	38.6 \pm 0.4	40.7 \pm 0.6	41.2 \pm 0.4	41.6 \pm 0.0	<u>45.2\pm0.4</u>	<u>46.1\pm0.1</u>
PA1225	57.6\pm0.2	68.0 \pm 0.4	68.0 \pm 0.1	58.1 \pm 0.4	<u>72.1\pm0.5</u>	<u>71.3\pm0.5</u>	<u>71.0\pm0.3</u>
PA4975	48.6\pm0.4	<u>50.5\pm0.2</u>	<u>51.5\pm0.4</u>	<u>51.0\pm0.1</u>	47.0 \pm 0.3	46.8 \pm 0.2	47.9 \pm 0.3

4.2.2 Enzymatic activity of putative azoreductases from *P. aeruginosa* PAO1

To confirm enzymatic activity in the recombinant proteins PA1224, PA1225 and PA4975, a series of assays were conducted initially in the presence of different cofactors and then against a range of azo and quinone substrates. From these enzymatic assays it would also be possible to gain information on the cofactor selectivity regarding FMN and FAD and also verify the preferred nicotinamide reductant. Enzyme activity was calculated by monitoring the reduction of azo compounds. For quinone substrates, NAD(P)H oxidation was recorded. This was due to the fact that many of the quinone reduction reactions would have been difficult to record as the majority of the quinones tested have little absorbance in the visible spectrum however the maximum absorbance (λ_{\max}) of NAD(P)H is 340 nm (Figure 4.6). Each quinone requires a single two electron transfer from one NAD(P)H molecule to complete the reduction while azo compounds require two two electron transfers to complete the process (Ryan *et al.*, 2010a). This means that the rate of quinone reduction is equal to the rate of NAD(P)H oxidation thus NAD(P)H oxidation is a valid method to observe quinone reduction. Each azo substrate tested has a λ_{\max} different from NAD(P)H that lies within the visible spectrum (Table 4.2). Therefore it was possible to directly record the reduction of the azo compounds. In order to obtain the reduction and oxidation data for the substrates it was essential to determine the λ_{\max} for each of the molecules tested.

4.2.2.1 Calculation of the molar extinction coefficient for NAD(P)H, ANI and the azo substrates

Absorbance scans were carried out for all of the azo substrates as well as NADH and NADPH in order to find the λ_{\max} for each compound. This was also carried out for each quinone however as mentioned previously, many failed to have an appropriate λ_{\max} for observing their reduction. Each azo compound as well as NADH and NADPH was found to have a λ_{\max} within the detectable range of 300-700 nm (Figure 4.6, Table 4.2). The maximum wavelengths for each compound were used to determine the molar extinction coefficient (ϵ) needed to calculate the rate of reduction for each substrate. The absorbance of increasing concentrations of each substrate along with NAD(P)H was measured and linear regression analysis was performed on all of the absorbance data (Figure 4.7). From this, the ϵ value was obtained. The λ_{\max} and ϵ value of each substrate is listed in Table 4.2.

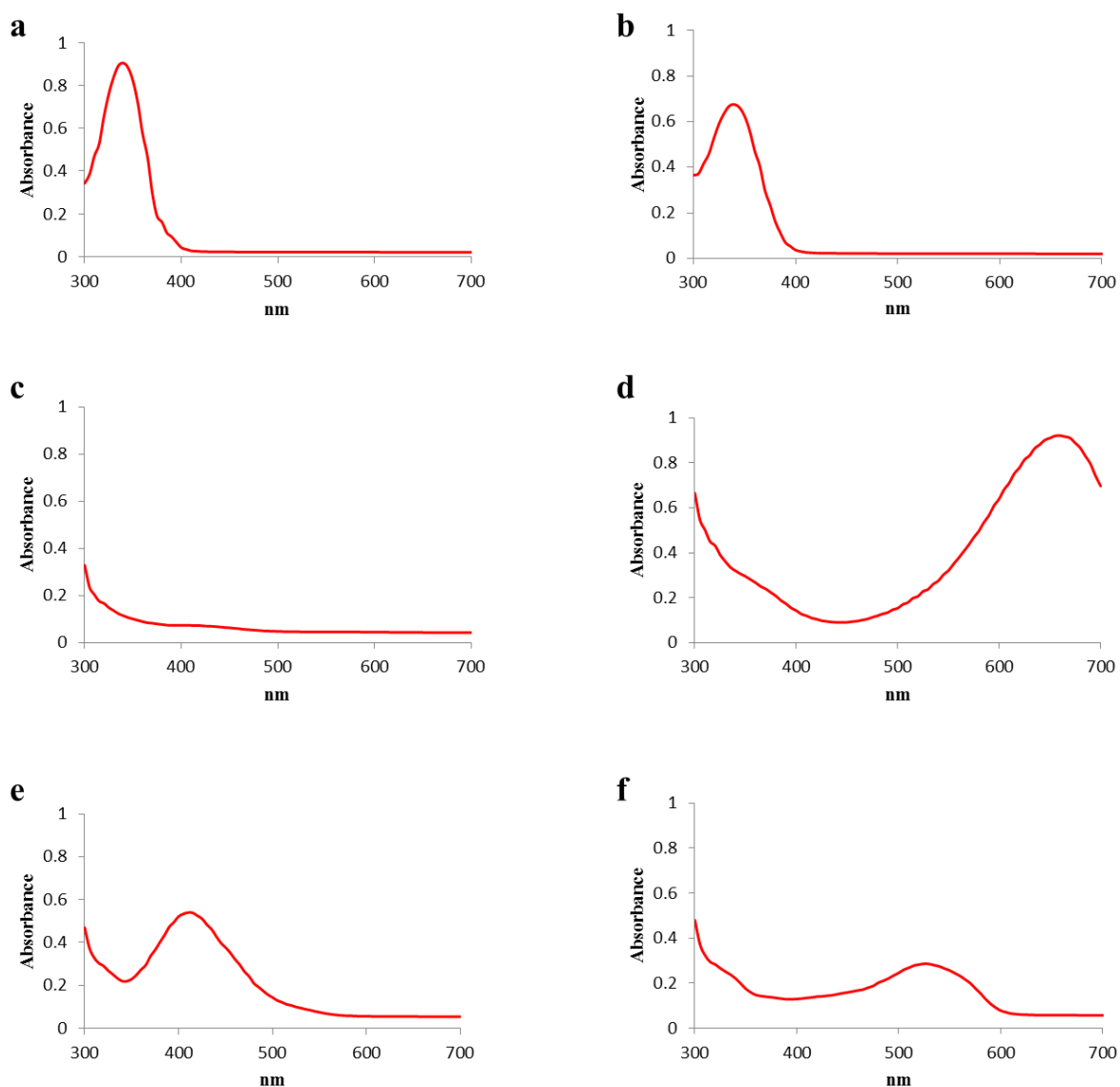


Figure 4.6 Absorption spectra of NADH (a), NADPH (b), PLU (c), ANI (d), methyl red (e) and amaranth (f)

Absorbance spectra for NADH (a) and NADPH (b) showing a λ_{max} for each compound at 340 nm. Of the two quinone substrates listed here PLU (c), like many of the quinone compounds does not show any considerable absorption level within the wavelength range tested while ANI (d) has a λ_{max} of 660 nm. Regarding the azo substrates, methyl red (e) has a λ_{max} of 440 nm and amaranth (f) has a λ_{max} of 540 nm.

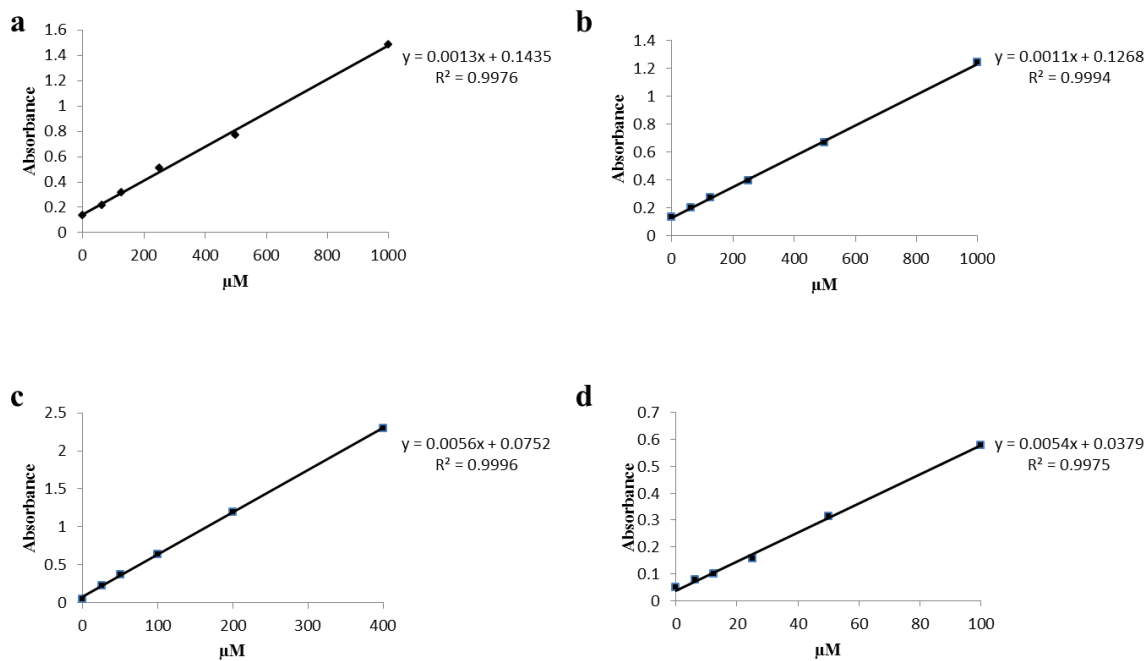


Figure 4.7 Determination of molar extinction coefficient for NADH (a), NADPH (b), ANI (c) and methyl red (d)

Graphs showing molar extinction factor calculation using different concentrations (μM) of NADH (a), NADPH (b), ANI (c) and methyl red (d). Absorbance values were obtained measuring each compound/cofactor using their specific λ_{max} . Linear regression was applied to obtain molar extinction coefficient values.

Table 4.2 NAD(P)H, ANI and azo compounds λ_{\max} and molar extinction coefficients

Maximum absorbance wavelengths obtained for NAD(P)H, ANI and the azo compounds from the absorbance spectra analysis and related molar extinction coefficient values generated for each of them. 100 μM solutions were used and absorption spectra were generated in Nunclon 96-well plates reading within the range of 300 to 700 nm using an Infinite M200 PRO plate reader.

Substrate	Absorbance peak (λ_{\max} , nm)	Molar extinction factor ($\text{M}^{-1} \text{cm}^{-1}$)
NADH	340	$3.3 \cdot 10^3$
NADPH	340	$2.8 \cdot 10^3$
ANI	660	$1.4 \cdot 10^4$
Amaranth	540	$7.5 \cdot 10^3$
Balsalazide	410	$3.3 \cdot 10^3$
Methyl Red	440	$1.4 \cdot 10^4$
Olsalazine	420	$2.3 \cdot 10^4$
Orange G	500	$1.1 \cdot 10^4$
Orange II	480	$2.1 \cdot 10^4$
Ponceau S	540	$2.1 \cdot 10^4$
Ponceau BS	520	$1.8 \cdot 10^5$
Sudan I	475	$1.1 \cdot 10^4$
Sulfasalazine	430	$2.3 \cdot 10^5$
Tropaeolin	410	$9.5 \cdot 10^3$

4.2.2.2 Identifying cofactor selectivity of PA1224, PA1225 and PA4975

To measure the reductive activity of the putative azoreductases and compare the rates when using NADH or NADPH as an electron donor, enzyme assays were carried out using ANI as a substrate. These assays were then repeated in the presence of FMN and FAD separately to observe whether the addition of a flavin cofactor affected the rate of reduction. All reaction components and combinations are listed in Table 4.3. ANI was chosen as the substrate for this part as it has previously been shown as a good substrate for azoreductases from *P. aeruginosa* PAO1 (Crescente *et al.*, 2016) and has a λ_{max} of 660nm, therefore the reduction of this quinone can be measured directly without interference from NAD(P)H oxidation. All reactions were performed in triplicate with the reduction measured every 10 seconds. A decrease in absorbance, representing substrate reduction, was to be seen over time (Figure 4.8). Linear regression analysis was carried out on each data set and the rate was determined in μM of substrate reduced per second per mg of protein. No enzymatic activity was observed in the absence of NAD(P)H confirming PA1224, PA1225 and PA4975 as NAD(P)H dependent enzymes.

The rate of reduction of ANI by PA1224 showed greater efficiency with NADPH as the electron donor ($2328.2 \pm 103.5 \mu\text{M} \cdot \text{s}^{-1} \cdot \text{mg}^{-1}$) as opposed to NADH ($1386.1 \pm 81.4 \mu\text{M} \cdot \text{s}^{-1} \cdot \text{mg}^{-1}$) (Figure 4.9 a). An unpaired t-test was performed on the two data sets which confirmed that they were significantly different ($p < 0.001$), thus PA1224 is selective for NADPH as the electron donor.

Upon addition of $1 \mu\text{M}$ flavin to this reaction, the rates of reduction were slightly lowered with both FMN and FAD at $2191.8 \pm 75.8 \mu\text{M} \cdot \text{s}^{-1} \cdot \text{mg}^{-1}$ with FMN and $2167.3 \pm 168.6 \mu\text{M} \cdot \text{s}^{-1} \cdot \text{mg}^{-1}$ with FAD (Figure 4.9 a). Upon statistical analysis using a one-way ANOVA however, these rates were not found to be statistically different to those obtained with no added flavin.

The putative azoreductase PA1225 reduced ANI at rates of $29.6 \pm 1.4 \mu\text{M} \cdot \text{s}^{-1} \cdot \text{mg}^{-1}$ in the presence of NADPH and $19.71 \pm 1.53 \mu\text{M} \cdot \text{s}^{-1} \cdot \text{mg}^{-1}$ in the presence of NADH (Figure 4.9 b). Statistical analysis was performed on these results (unpaired t-test) which confirmed NADPH as the preferred electron donor with a significantly higher reaction rate than that with NADH.

When FMN was added to the reaction mix the rate of substrate reduction increased to $42.8 \pm 2.1 \mu\text{M} \cdot \text{s}^{-1} \cdot \text{mg}^{-1}$. A similar trend was apparent with the addition of FAD with this assay achieving a rate of $35 \pm 5.4 \mu\text{M} \cdot \text{s}^{-1} \cdot \text{mg}^{-1}$ (Figure 4.9 b). Both of these rates were

statistically different to those obtained in the absence of flavin in the reaction mix (analysis performed using one-way ANOVA). Although the rate of reduction is slightly higher with the addition of 1 μM FMN when compared to that calculated with 1 μM FAD added, an unpaired t-test produced a p value of >0.05 implying that there is no significant preference for FMN over FAD.

PA4975 was found to select for NADPH as the electron donor over NADH with reduction of ANI occurring at a rate of $677.4 \pm 21.5 \mu\text{M} \cdot \text{s}^{-1} \cdot \text{mg}^{-1}$ using NADPH and at a rate of $366.3 \pm 41 \mu\text{M} \cdot \text{s}^{-1} \cdot \text{mg}^{-1}$ with NADH (Figure 4.9 c). Reduction using NADPH as the electron donor was significantly more efficient with an unpaired t-test between the two data sets producing a p value of <0.002 .

The rates of reduction were decreased slightly in this reaction when 1 μM flavin was added. A rate of $642.6 \pm 24.8 \mu\text{M} \cdot \text{s}^{-1} \cdot \text{mg}^{-1}$ was achieved with FMN and $618.8 \pm 38 \mu\text{M} \cdot \text{s}^{-1} \cdot \text{mg}^{-1}$ with FAD (Figure 4.9 c). Statistical analysis was performed on this data using a one-way ANOVA however, and it was found that these rates were not statistically different to those obtained in the absence of added flavin.

Table 4.3 Enzymatic reaction component combinations used to test protein activity and NAD(P)H and flavin selectivity

A number of combinations of reaction components were used in order to establish the protein's activity in the presence and absence of NAD(P)H and FAD or FMN. Samples were prepared using 20 μg of protein, 100 μM of substrate, 500 μM NAD(P)H and 1 μM of either flavin in 20 mM Tris HCl 100 mM NaCl pH 8 buffer.

Enzymatic reaction	Protein	Substrate	NADH	NADPH	FMN	FAD
1	X	X				
2	X	X	X			
3	X	X		X		
4	X	X	X		X	
5	X	X	X			X
6	X	X		X	X	
7	X	X		X		X
8		X	X			
9		X		X		
10		X	X		X	
11		X	X			X
12		X		X	X	
13		X		X		X

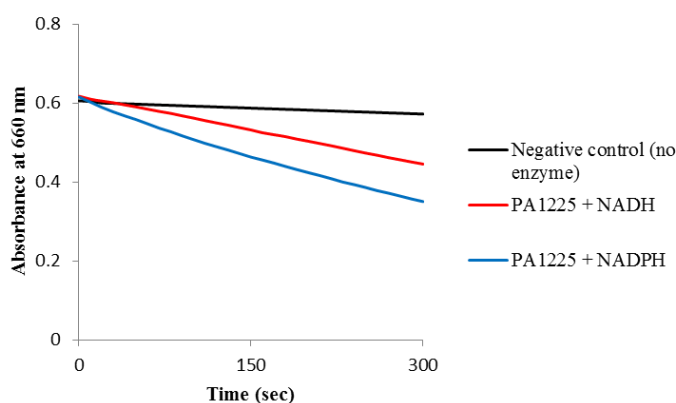


Figure 4.8 Rate of ANI reduction by PA1225 with and without NAD(P)H

Graph showing the ANI absorbance measurements at 660 nm during its reduction catalysed by PA1225 in the presence of NADH (red) and NADPH (blue) compared to the negative control (black) which included no NAD(P)H. The lack of substrate reduction occurring in the negative control confirms that NAD(P)H is essential for the reaction with NADPH proving more efficient as an electron donor.

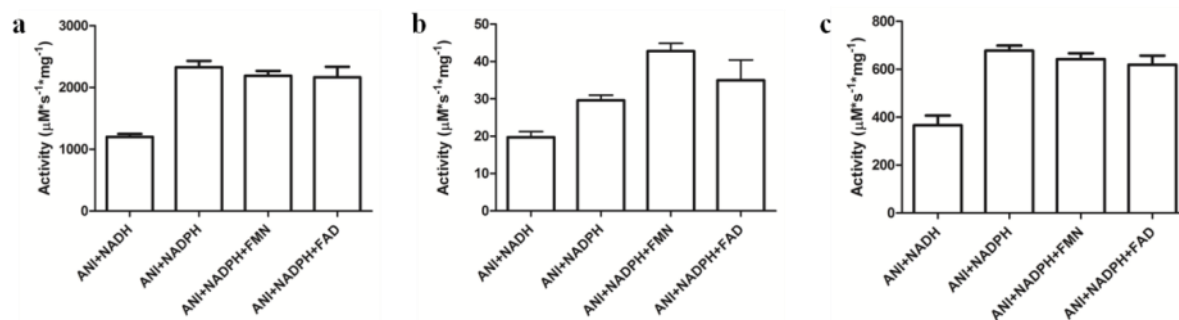


Figure 4.9 Nicotinamide and flavin selectivity of *P. aeruginosa* PAO1 recombinant proteins

Reactions were carried out in 20 mM Tris HCl 100 mM NaCl pH 8 with 100 μM substrate, 500 μM NAD(P)H, 1 μM flavin and 5-0 μg protein. For PA1224 significantly higher reduction ($p=0.0006$) was apparent when using NADPH ($2328.2 \pm 103.5 \mu\text{M}\cdot\text{s}^{-1}\cdot\text{mg}^{-1}$) as an electron donor rather than NADH ($1386.1 \pm 81.4 \mu\text{M}\cdot\text{s}^{-1}\cdot\text{mg}^{-1}$). When 1 μM flavin was added the rates were not significantly different to those that occurred in the absence of added flavin ($2191.8 \pm 75.8 \mu\text{M}\cdot\text{s}^{-1}\cdot\text{mg}^{-1}$ with FMN and $2167.3 \pm 168.6 \mu\text{M}\cdot\text{s}^{-1}\cdot\text{mg}^{-1}$ with FAD) (a). For PA1225 NADPH was confirmed via statistical analysis ($p=0.0012$) as the preferred electron donor ($29.6 \pm 1.4 \mu\text{M}\cdot\text{s}^{-1}\cdot\text{mg}^{-1}$) over NADH ($19.7 \pm 1.5 \mu\text{M}\cdot\text{s}^{-1}\cdot\text{mg}^{-1}$). The reaction rate increased to $42.8 \pm 2.1 \mu\text{M}\cdot\text{s}^{-1}\cdot\text{mg}^{-1}$ in the presence of 1 μM FMN and $35 \pm 5.4 \mu\text{M}\cdot\text{s}^{-1}\cdot\text{mg}^{-1}$ in the presence of FAD. Although these rates were both statistically different to those achieved without flavin they were not statistically different to each other ($p=0.057$) (b). For PA4975 a rate of $677.4 \pm 21.5 \mu\text{M}\cdot\text{s}^{-1}\cdot\text{mg}^{-1}$ was calculated with NADPH as electron donor compared to a rate of $366.3 \pm 41 \mu\text{M}\cdot\text{s}^{-1}\cdot\text{mg}^{-1}$ for NADH. These rates were significantly different ($p=0.0013$). Rates were not statistically different upon addition of FMN ($642.6 \pm 24.8 \mu\text{M}\cdot\text{s}^{-1}\cdot\text{mg}^{-1}$) or FAD ($618.8 \pm 38 \mu\text{M}\cdot\text{s}^{-1}\cdot\text{mg}^{-1}$) (c). Reduction rates were calculated by fitting the change in OD_{660} over 300 seconds. Error bars represent the standard deviation of replicates ($n=3$). All statistical analysis was performed using Graphpad Prism (version 7).

To summarise, all three recombinant proteins PA1224, PA1225 and PA4975, were identified as quinone reductases that can utilise both NADPH and NADH as electron donors, albeit at significantly higher rates using NADPH. The addition of either FMN or FAD to the reaction mix did not significantly change the reduction rate of ANI by either PA1224 or PA4975. Although it significantly improved the rate of reduction with PA1225, the rates calculated for FMN and FAD were not significant to each other. Therefore it was not possible to determine the preferred flavin from these datasets alone.

To further examine the effects of including FMN or FAD in the enzymatic reaction, the process was carried out where each recombinant enzyme concentration was kept constant for each reaction (0.3 μg for PA1224, 2.5 μg for PA1225 and 0.6 μg for PA4975) but the flavin concentration was varied from 0-20 μM . For this experiment ANI was used as the substrate and absorbance was measured at 660 nm to avoid interference from absorbance of the added flavin. The rates obtained for ANI reduction at each flavin concentration were plotted against each other (Figure 4.10). A clear preference for FAD was observed for both PA1224 and PA4975 (Figure 4.10 **a** and **c** respectively) while no obvious difference was seen for PA1225 (Figure 4.10 **b**).

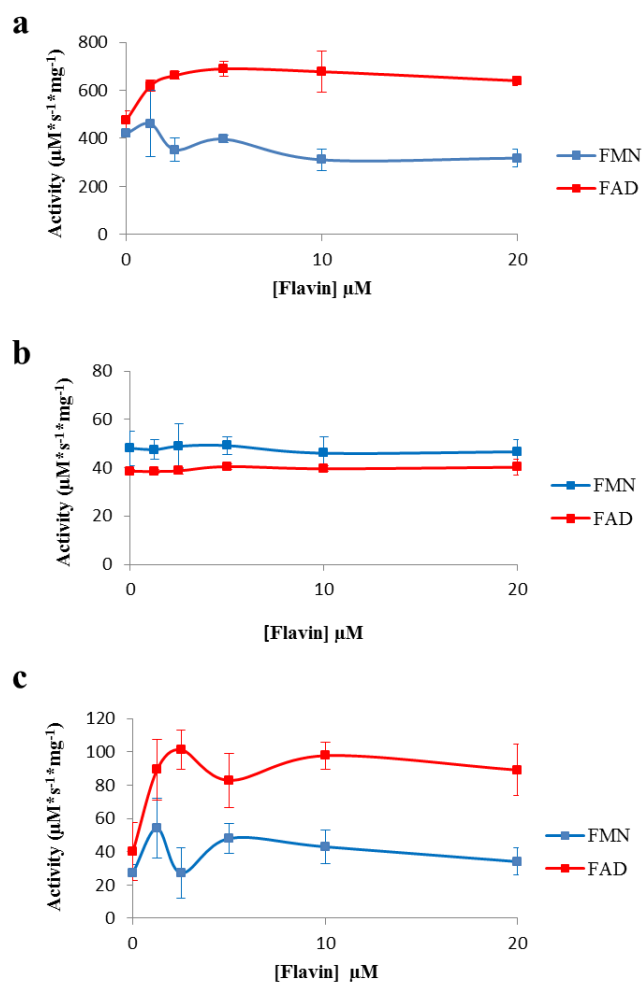


Figure 4.10 Activity assays for PA1224 (a), PA1225 (b) and PA4975 (c) in the presence of varying flavin concentrations

ANI reduction was measured at its specific λ_{\max} of 660 nm to compare the effects of adding FMN (blue) and FAD (red) to the reaction mix. Enzyme concentration was kept constant at 3 $\mu\text{g}/\text{mL}$ for PA1224 (a), 25 $\mu\text{g}/\text{mL}$ for PA1225 (b) and 6 $\mu\text{g}/\text{mL}$ for PA4975 (c). All reactions were carried out in the presence of 500 μM NADPH and 100 μM ANI in 20 mM Tris HCl 100 mM NaCl pH 8 buffer. Measurements were performed in triplicate and error bars represents \pm standard deviation.

4.2.2.3 Substrate specificity

A range of azo and quinone compounds were tested as substrates for each recombinant protein using the method described in section 2.6.5. All compounds tested as substrates are listed in Table 2.14. Following the collection of data, linear regression analysis was performed to determine the rates for reduction of each substrate by each enzyme and substrate specificity profiles were established. It is important to note that ANI achieved higher reduction rates in this section compared to the previous section where nicotinamide and flavin selectivity were determined. This is due to the fact that substrate reduction was measured by monitoring NADPH oxidation at 340 nm. This was deemed a more appropriate measurement for this section so as to standardise the rates obtained against all of the other quinones as the majority tested to do not absorb within the visible spectrum.

4.2.2.3.1 PA1224

Upon analysis of the enzymatic activity of PA1224 in reducing the azo compounds, very low activity was to be seen (Figure 4.11 **a**). This enzyme was only effective at reducing methyl red with a low reaction rate calculated at $2.9 \pm 0.2 \mu\text{M} \cdot \text{s}^{-1} \cdot \text{mg}^{-1}$. Minimal enzymatic activity was observed with some substrates however due to high replicate variability or reduction rates below $1 \mu\text{M} \cdot \text{s}^{-1} \cdot \text{mg}^{-1}$ these could not be considered as examples of proper substrate reduction.

Reduction of quinone compounds with PA1224 was more effective as reduction was apparent with all of the quinones tested with the exception of LAW. Rates of reduction varied across a wide range with the highest rate of reduction calculated at $2859.4 \pm 108.3 \mu\text{M} \cdot \text{s}^{-1} \cdot \text{mg}^{-1}$ with ANI (Figure 4.11 **b**). The next best substrate found for PA1224 was PLU with a rate of $1340 \pm 11.6 \mu\text{M} \cdot \text{s}^{-1} \cdot \text{mg}^{-1}$ determined. This was found to be statistically different (unpaired t-test, p value=0.0017) from that obtained for ANI therefore ANI was deemed the most suitable substrate for PA1224.

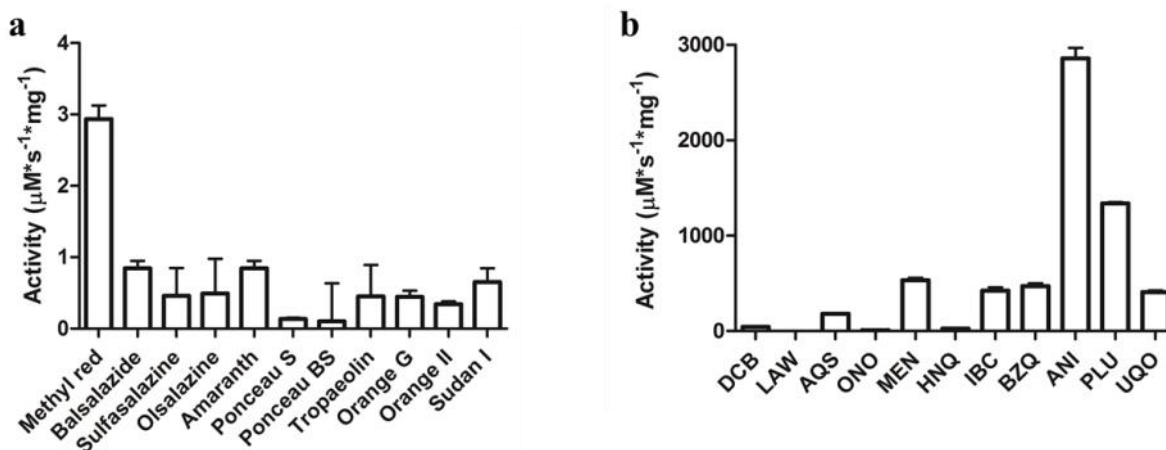


Figure 4.11 PA1224 substrate specificity profile

Reactions were carried out in 20 mM Tris HCl 100 mM NaCl pH 8 with 100 μM substrate, 500 μM NAD(P)H and 20-0 μg protein for azo compounds and 5-0 μg protein for quinones. PA1224 reduction rates of azo compounds: enzyme activity was apparent only with methyl red ($2.9 \pm 0.2 \mu\text{M}\cdot\text{s}^{-1}\cdot\text{mg}^{-1}$). All other rates were below $1 \mu\text{M}\cdot\text{s}^{-1}\cdot\text{mg}^{-1}$ indicating that there are not substrates for this enzyme (a). PA1224 reduction rates with quinones: enzymatic activity obtained with ANI ($2859.4 \pm 108.3 \mu\text{M}\cdot\text{s}^{-1}\cdot\text{mg}^{-1}$), PLU ($1340 \pm 11.6 \mu\text{M}\cdot\text{s}^{-1}\cdot\text{mg}^{-1}$), MEN ($533.9 \pm 24.8 \mu\text{M}\cdot\text{s}^{-1}\cdot\text{mg}^{-1}$), BZQ ($470.6 \pm 30.7 \mu\text{M}\cdot\text{s}^{-1}\cdot\text{mg}^{-1}$), IBC ($424.4 \pm 33.3 \mu\text{M}\cdot\text{s}^{-1}\cdot\text{mg}^{-1}$), UQO ($408.5 \pm 17.9 \mu\text{M}\cdot\text{s}^{-1}\cdot\text{mg}^{-1}$), AQS ($180.3 \pm 8.6 \mu\text{M}\cdot\text{s}^{-1}\cdot\text{mg}^{-1}$), DCB ($43.3 \pm 1.7 \mu\text{M}\cdot\text{s}^{-1}\cdot\text{mg}^{-1}$), HNQ ($25.1 \pm 1 \mu\text{M}\cdot\text{s}^{-1}\cdot\text{mg}^{-1}$), ONO ($9.7 \pm 2 \mu\text{M}\cdot\text{s}^{-1}\cdot\text{mg}^{-1}$), LAW ($0.7 \pm 0.5 \mu\text{M}\cdot\text{s}^{-1}\cdot\text{mg}^{-1}$) (b). Reduction rates were calculated by fitting the change in OD over 300 seconds. Error bars represent the standard deviation of replicates (n=3).

4.2.2.3.2 PA1225

Virtually no azoreductase activity was observed with PA1225. Methyl red was found to be the azo substrate reduced at the highest rate ($0.9 \pm 0.1 \mu\text{M} \cdot \text{s}^{-1} \cdot \text{mg}^{-1}$) however with a substrate reduction rate of less than $1 \mu\text{M} \cdot \text{s}^{-1} \cdot \text{mg}^{-1}$, this was not statistically different to the reduction rate of methyl red with no enzyme present (unpaired t-test, p value=0.053) indicating that PA1225 is not an azoreductase enzyme.

Quinone reductase activity was confirmed with PA1225 with activity exhibited against all substrates tested (Figure 4.12). The highest activity recorded was $296.5 \pm 3.3 \mu\text{M} \cdot \text{s}^{-1} \cdot \text{mg}^{-1}$, where ANI was used as a substrate. Relatively high activity was also apparent against BZQ ($178.4 \pm 10.7 \mu\text{M} \cdot \text{s}^{-1} \cdot \text{mg}^{-1}$), HNQ ($175.8 \pm 8.6 \mu\text{M} \cdot \text{s}^{-1} \cdot \text{mg}^{-1}$) and IBC ($154 \pm 7.9 \mu\text{M} \cdot \text{s}^{-1} \cdot \text{mg}^{-1}$). Statistical analysis (one-way ANOVA, p=0.0001) confirmed ANI as the best substrate tested for PA1225.

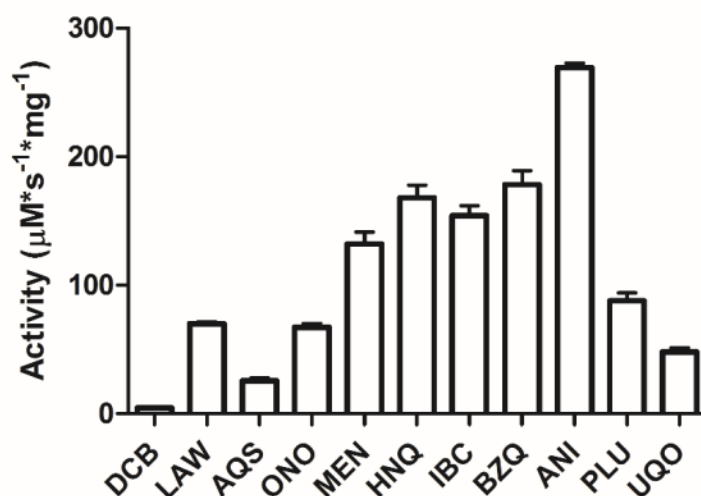


Figure 4.12 PA1225 substrate specificity profile

Reactions were carried out in 20 mM Tris HCl 100 mM NaCl pH 8 with 100 μM substrate, 500 μM NAD(P)H and 5-0 μg protein. PA1225 reduction rates with quinones: enzymatic activity obtained with ANI ($296.5 \pm 3.3 \mu\text{M}\cdot\text{s}^{-1}\cdot\text{mg}^{-1}$), BZQ ($178.4 \pm 10.7 \mu\text{M}\cdot\text{s}^{-1}\cdot\text{mg}^{-1}$), HNQ ($175.8 \pm 8.6 \mu\text{M}\cdot\text{s}^{-1}\cdot\text{mg}^{-1}$), IBC ($154 \pm 7.9 \mu\text{M}\cdot\text{s}^{-1}\cdot\text{mg}^{-1}$), MEN ($132.2 \pm 9.2 \mu\text{M}\cdot\text{s}^{-1}\cdot\text{mg}^{-1}$), PLU ($87.8 \pm 6.2 \mu\text{M}\cdot\text{s}^{-1}\cdot\text{mg}^{-1}$), LAW ($70.2 \pm 1.5 \mu\text{M}\cdot\text{s}^{-1}\cdot\text{mg}^{-1}$), ONO ($67.4 \pm 3.0 \mu\text{M}\cdot\text{s}^{-1}\cdot\text{mg}^{-1}$), UQO ($48.1 \pm 3.2 \mu\text{M}\cdot\text{s}^{-1}\cdot\text{mg}^{-1}$), AQS ($25.5 \pm 2.4 \mu\text{M}\cdot\text{s}^{-1}\cdot\text{mg}^{-1}$), DCB ($4.6 \pm 0.9 \mu\text{M}\cdot\text{s}^{-1}\cdot\text{mg}^{-1}$). Reduction rates were calculated by fitting the change in OD over 300 seconds. Error bars represent the standard deviation of replicates (n=3).

4.2.2.3.3 PA4975

The azo substrate specificity analysis for the protein PA4975 showed a poor reductive capacity against any substrate tested. The highest reduction rates were calculated with the substrates ponceau S ($1 \pm 0.5 \mu\text{M} \cdot \text{s}^{-1} \cdot \text{mg}^{-1}$) and balsalazide ($1 \pm 0.1 \mu\text{M} \cdot \text{s}^{-1} \cdot \text{mg}^{-1}$). Further analysis was carried out using unpaired t-tests however these rates were found not to be significantly different from those calculated from the reactions carried out in the absence of PA4975 (p value=0.4 for ponceau S, p value=0.3 for balsalazide). Thus PA4975 was not considered to reduce azo substrates.

A different situation was evident when quinone compounds were used as substrates. Quinone reductase activity was apparent against all the substrates tested (Figure 4.13). MEN was the substrate reduced at the highest rate ($681 \pm 13.4 \mu\text{M} \cdot \text{s}^{-1} \cdot \text{mg}^{-1}$) with ANI ($677.4 \pm 31.5 \mu\text{M} \cdot \text{s}^{-1} \cdot \text{mg}^{-1}$), ONO ($644.9 \pm 41.5 \mu\text{M} \cdot \text{s}^{-1} \cdot \text{mg}^{-1}$) and PLU ($610.9 \pm 39.2 \mu\text{M} \cdot \text{s}^{-1} \cdot \text{mg}^{-1}$) following closely behind. These rates were not found to be statistically different from one another (one-way ANOVA, p=0.08) meaning that although PA4975 could be confirmed as a quinone reductase, a single best substrate could not be determined.

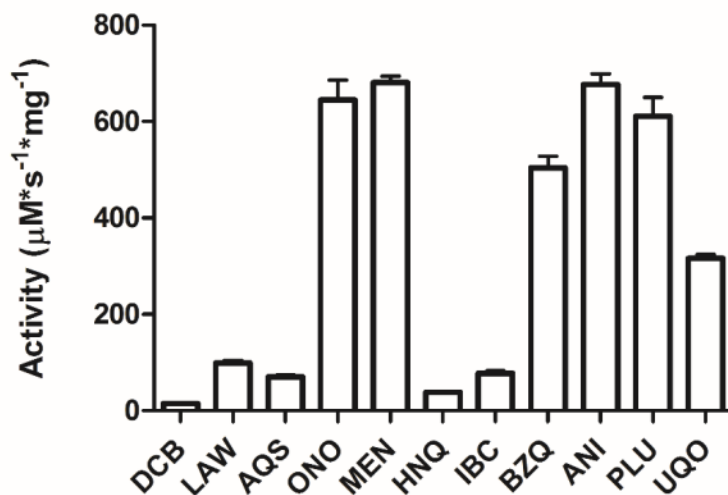


Figure 4.13 PA4975 substrate specificity profile

Reactions were carried out in 20 mM Tris HCl 100 mM NaCl pH 8 with 100 μM substrate, 500 μM NAD(P)H and 5-0 μg protein. Enzymatic activity obtained with MEN ($681 \pm 13.4 \mu\text{M}\cdot\text{s}^{-1}\cdot\text{mg}^{-1}$), ANI ($677.4 \pm 31.5 \mu\text{M}\cdot\text{s}^{-1}\cdot\text{mg}^{-1}$), ONO ($644.9 \pm 41.5 \mu\text{M}\cdot\text{s}^{-1}\cdot\text{mg}^{-1}$), PLU ($610.9 \pm 39.2 \mu\text{M}\cdot\text{s}^{-1}\cdot\text{mg}^{-1}$), BZQ ($504.6 \pm 23.5 \mu\text{M}\cdot\text{s}^{-1}\cdot\text{mg}^{-1}$), UQO ($316.1 \pm 8.4 \mu\text{M}\cdot\text{s}^{-1}\cdot\text{mg}^{-1}$), LAW ($99.3 \pm 4.7 \mu\text{M}\cdot\text{s}^{-1}\cdot\text{mg}^{-1}$), IBC ($77.5 \pm 5.2 \mu\text{M}\cdot\text{s}^{-1}\cdot\text{mg}^{-1}$), AQS ($70.6 \pm 3.7 \mu\text{M}\cdot\text{s}^{-1}\cdot\text{mg}^{-1}$), HNQ ($38.6 \pm 1.6 \mu\text{M}\cdot\text{s}^{-1}\cdot\text{mg}^{-1}$), DCB ($14.8 \pm 0.7 \mu\text{M}\cdot\text{s}^{-1}\cdot\text{mg}^{-1}$). Reduction rates were calculated by fitting the change in OD over 300 seconds. Error bars represent the standard deviation of replicates (n=3).

4.3 Discussion

The objectives listed in section 1.3 have been met as follows:

- i. The prosthetic group, flavin cofactor and enzymatic reaction conditions for the putative azoreductases from *P. aeruginosa* PAO1, PA1224, PA1225 and PA4975, have been established.
- ii. Substrate specificity profiles have been created for the proteins in question with respect to both azo compounds and quinone compounds.

Following the successful biochemical characterisation of PA1224, PA1225 and PA4975, all three were confirmed as flavoproteins with NAD(P)H dependent quinone oxidoreductase activity. Only PA1224 however, was found to catalyse the reduction of azo compounds although as a whole they were not good substrates for this enzyme.

As these three enzymes produced little or no activity against azo substrates, a quinone compound, ANI, was used to determine the nicotinamide and flavin selectivity. The results in this chapter have confirmed all three enzymes to be NAD(P)H dependent enzymes with a significantly faster reaction occurring with NADPH as the hydride donor. Like other NAD(P)H dependent quinone oxidoreductases from *P. aeruginosa* PAO1 (with the exception of PA0949), the three enzymes characterised here can also utilise NADH as an electron donor (Ryan *et al.*, 2014, Crescente *et al.*, 2016). The selectivity of PA1224 for NADPH seen here is consistent with findings that indicate a preference for NADPH over NADH by hNQO1 – the closest homologue of PA1224 (Yang *et al.*, 2005). The structural basis for these enzymes being selective for NADPH over NADH remains unclear but it could be speculated that charged amino acids on the protein surface may affect this preference as research has shown that positively charged residues are frequently involved in the specific recognition of the negatively charged phosphate included in NADPH (Singh *et al.*, 2015). Structural studies would need to be completed on the enzymes concerned in this study however to further examine this idea.

Considering the data obtained from TLC and DSF analysis along with the enzymatic activity, it is clear that FAD is the preferred flavin for PA1224. This is also the case with PA1225 as like PA1224, a spot was observed on the TLC plate which had an R_f value similar to that calculated for FAD. In addition, although the enzyme activity data would suggest otherwise, PA1225 was more effectively stabilised in the presence of FAD over FMN. This is consistent with the FAD selectivity for hNQO1 and hNQO2 (Wu *et al.*,

1997). PA4975 however, poses more of a conundrum where conflicting results were found between DSF analysis and the enzyme assays where DSF indicated a preference for FMN but higher rates of enzymatic activity were achieved using FAD. Bearing in mind the fact that hNQO2, the closest homologue of PA4975 is selective for FAD over FMN it is likely that FAD may also be the preferred flavin in this case (Wu *et al.*, 1997). This could not be confirmed via TLC analysis as the yield of protein gained was too low to carry out this assay.

It is important to note that although the addition of exogenous flavin to the enzymatic reaction mixture can enhance the reduction rate (McDougall *et al.*, 2017), in this case the addition of FMN or FAD did not significantly affect the rate of ANI reduction for PA1224 and PA4975. This is likely due to the fact that flavin was sufficiently incorporated during protein expression. During protein purification (section 3.2.3.1), the protein-containing eluates appeared a yellow colour for all three proteins in this study suggesting the presence of flavin. In addition, in the absorption spectra for PA1224 and PA1225, two distinct peaks were evident at 360 nm and 450 nm indicating the presence of flavin. Calculation of molar ratios of protein molecule per flavin molecule found a ratio of 1.9 molecules of protein per one molecule of flavin for PA1224 and 2.4 molecules of PA1225 per molecule of flavin. The higher number of flavin molecules per protein molecule found with PA1224 over PA1225 may explain why a significant difference was seen in the enzymatic rate of PA1225 upon addition of flavin but not with PA1224. Also, although this molar ratio could not be calculated for PA4975 due to the low protein yield, it is likely that the molar ratio was comparable to PA1224 as introduction of flavin to the enzyme reaction did not increase the reduction rate significantly. The apparent success of flavin incorporation during protein expression perhaps explains why addition of flavin to the expression media did not increase the yield of soluble protein in sections 3.2.2.2.1 and 3.2.2.2.2.

The enzymatic data presented in this chapter indicates a diverse substrate specificity for the three proteins characterised. Of the three, azoreductase activity was apparent only with PA1224. This enzyme however, was not as effective in azoreduction as others previously characterised from *P. aeruginosa* PAO1, namely pAzoR1-3, PA1204, PA2280 and PA2580 (Ryan *et al.*, 2010b, Crescente *et al.*, 2016) with only methyl red reduced out of the eleven azo compounds tested. In addition, the rate of reduction against this substrate was at least one order of magnitude lower than azoreduction rates obtained from the previously characterised azoreductase enzymes (Ryan *et al.*, 2010b, Crescente *et al.*, 2016).

In contrast, all three enzymes characterised in this chapter were effective in the reduction of quinone compounds with rates of reduction comparable to those achieved with other quinone oxidoreductases from *P. aeruginosa* PAO1 (paAzoR1-3, PA1204, PA2280, PA2580 and PA0949) (Ryan *et al.*, 2010b, Crescente *et al.*, 2016). Also, rates of quinone reduction by PA1224 were up to three orders of magnitude higher than that calculated for the only azo substrate, methyl red. This data would suggest that quinone compounds are the primary physiological substrates of the hNQO1 and hNQO2 homologues examined in this chapter. It is interesting to note that the substrates for which each enzyme exhibited the highest levels of reductive activity, ANI for PA1224 and PA4975 and BZQ for PA1225, both contain only a single aromatic ring. This could suggest that the three proteins of concern in this study may possess active sites comparable to those of paAzoR1 and PA2280 as these enzymes have been found to have the higher reduction rates against single aromatic ringed compounds as opposed to the larger naphthoquinones favoured by paAzoR2, paAzoR3, PA2580, PA1204 and PA0949 (Ryan *et al.*, 2010b, Crescente *et al.*, 2016, Ryan *et al.*, 2014). A comparison of the paAzoR1 structure against homology models of paAzoR2 and paAzoR3 confirmed a smaller active site for paAzoR1 than for paAzoR2 or paAzoR3, suggesting that this may influence the size of optimum substrates (Ryan *et al.*, 2010b, Gonçalves *et al.*, 2013, Ito *et al.*, 2008). It is thus likely that the active sites of PA1224, PA1225 and PA4975 are smaller than many of the other quinone reductases characterised from *P. aeruginosa* PAO1.

The findings in this chapter have confirmed three new quinone oxidoreductases and one new azoreductase in the *P. aeruginosa* PAO1 genome. Quinones are harmful to the bacterial cells and used by many plants and invertebrates as a defence mechanism. It is therefore likely that the diversity of quinones produced drives bacteria to encompass a range of NQOs (Mayer, 2006, Ryan *et al.*, 2014). Also, there is an apparent correlation between the size of the host range for bacteria and the number of azoreductases produced. *P. syringae* pv. *tomato* has two azoreductase genes in its genome and infects only two known hosts (Buell *et al.*, 2003, Ryan *et al.*, 2014). With this in consideration, the pathogenic promiscuity of *P. aeruginosa* PAO1, where colonisation of hosts ranging from amoebae to humans is common, may be the reason why new azoreductases are being identified in the *P. aeruginosa* PAO1 genome. The next chapter will continue the biochemical characterisation of four enzymes from *P. aeruginosa* PAO1 including three quinone oxidoreductases/azoreductases and one quinone oxidoreductase. A structural study will also be reported on for one of these proteins.

Chapter 5 A continued investigation of azoreductases and NAD(P)H quinone oxidoreductases from *P. aeruginosa* PAO1

5.1 Introduction

The azoreductase family in *P. aeruginosa* PAO1 has recently been proposed as being significantly larger than previously thought. Although it is difficult to identify new enzymes in this class due to the large sequence diversity amongst members (Table 5.1), a common mechanism for the reduction of azo and quinone compounds, described in Chapter 4, has led to the idea that azoreductases and NQOs are members of a single superfamily (Ryan *et al.*, 2014, Ryan *et al.*, 2010b). A number of formerly unrelated enzyme families including ArsH, MdaB, YieF and WrbA have been implicated as encompassing the capacity for azo and quinone reduction (Ryan *et al.*, 2014).

The gene *pa2280* was initially identified as part of the ArsH operon in *P. aeruginosa* (Cai *et al.*, 1998, Mao *et al.*, 2009) and in *P. putida* is responsible for the detoxification of trivalent methylated and aromatic arsenicals by oxidation to pentavalent species (Chen *et al.*, 2015). It was suggested to encode an azoreductase as it is a homologue of known azoreductases, namely ArsH from both *S. meliloti* (82% similarity) (Ye *et al.*, 2007) and *Synechocystis* sp. PCC 6803 (78% similarity) (Hervás *et al.*, 2012). In addition, ArsH from *S. meliloti* has the same overall core fold as paAzoR1 (Ryan *et al.*, 2014).

Homologues of genes encoding known NQOs include *pa2580*, *pa1204* and *pa0949* (Ryan *et al.*, 2014). Like *pa2280*, homologues of these three genes encode for proteins which possess the same overall fold as paAzoR1 (Ryan *et al.*, 2014, Agarwal *et al.*, 2006, Gorman and Shapiro, 2005). There is significant homology between *pa2580* and enzymes from the MdaB family and NQO activity has been observed in MdaBs from *E. coli* (75% similarity) (Hayashi *et al.*, 1996) and *Helicobacter pylori* (71% similarity) (Wang and Maier, 2004). Similarly, an enzyme from *A. thaliana* shows NQO activity and is the closest homologue of *pa1204* that has been characterised (69% similarity) (Sparla *et al.*, 1999). Finally, *pa0949* forms part of the WrbA family which are known for their strong interaction with tryptophan repressor (Yang *et al.*, 1993) and the *E. coli* homologue of WrbA (56% similarity) has NQO activity (Patridge and Ferry, 2006).

All four proteins listed above have already been cloned and expressed in *E. coli* and the subsequent characterisation has confirmed all but PA0949 as azoreductase enzymes. Quinone reductase activity has been confirmed in all four proteins at a much higher rate than that for azoreduction (Crescente *et al.*, 2016).

Table 5.1 Nucleic acid sequence identity between known and putative *P. aeruginosa* PAO1 azoreductase/NQO genes

Table showing the nucleic acid sequence homology between known (*paazor1*, *paazor2*, *paazor3*, *pa2280*, *pa2580*, *pa1204*, *pa0949*, *pa4975*) and putative (*pa1224*, *pa1225*) azoreductase and/or NQO genes from *P. aeruginosa* PAO1. Values are expressed in percentage of homology. Sequences were taken from the Pseudomonas Genome Database (Winsor *et al.*, 2016) and identity matrix was generated using a ClustalW alignment in Bioedit (Hall, 1999, Thompson *et al.*, 1994).

	<i>paazor1</i>	<i>paazor2</i>	<i>paazor3</i>	<i>pa2280</i>	<i>pa2580</i>	<i>pa1204</i>	<i>pa0949</i>	<i>pa4975</i>	<i>pa1224</i>	<i>pa1225</i>
<i>paazor1</i>	ID	55%	48%	32%	30%	36%	31%	36%	37%	37%
<i>paazor2</i>	55%	ID	50%	33%	29%	33%	31%	35%	33%	37%
<i>paazor3</i>	48%	50%	ID	31%	28%	32%	27%	36%	35%	37%
<i>pa2280</i>	30%	29%	28%	ID	25%	27%	28%	33%	28%	35%
<i>pa2580</i>	32%	33%	31%	25%	ID	33%	28%	32%	32%	32%
<i>pa1204</i>	36%	33%	32%	33%	27%	ID	37%	31%	30%	33%
<i>pa0949</i>	31%	31%	27%	28%	28%	37%	ID	30%	30%	33%
<i>pa4975</i>	36%	35%	36%	32%	33%	31%	30%	ID	56%	37%
<i>pa1224</i>	37%	33%	35%	32%	28%	30%	30%	56%	ID	39%
<i>pa1225</i>	37%	37%	37%	32%	35%	33%	33%	37%	39%	ID

The MdaB family of enzymes has been extensively characterised in a range of bacterial species and linked to many bacterial physiological functions including virulence, host colonisation, survival within macrophages, quorum sensing and antimicrobial susceptibility (Sarva *et al.*, 2016, Wang and Maier, 2004, Kraemer *et al.*, 2009, Skurnik *et al.*, 2013, Asare *et al.*, 2010, Asare and Abu Kwaik, 2010, Ling *et al.*, 2012, Chen *et al.*, 2010, Tan *et al.*, 2014). Colonisation of invertebrate and mammalian hosts with *Francisella* sp. has been demonstrated to be significantly impaired upon deletion of *mdaB* (Kraemer *et al.*, 2009, Asare *et al.*, 2010). *Francisella novicida mdaB* mutants exhibit a loss of survival in both the liver and lung of a murine infection model when compared to the wild type (Kraemer *et al.*, 2009). In addition, *mdaB* gene deletion strains of *Francisella tularensis* show decreased proliferation and loss of virulence in the arthropod vector model *D. melanogaster* and the gene deleted strain also has reduced bacterial survival in U937 derived macrophages (Asare *et al.*, 2010, Asare and Abu Kwaik, 2010). It is likely that this phenotype regarding survival within macrophages is attributed to the quinone reductase function of MdaB which would protect against ROS damage (Sarva *et al.*, 2016). Furthermore, upon comparison of different subspecies of *F. tularensis*, *mdaB* is more highly expressed (≥ 5 fold) in the more virulent strain, Schu S4, as opposed to *holarctica* OR960246 (Sarva *et al.*, 2016).

This apparent role of MdaB in host infection is not exclusive to *Francisella* sp. however. Wang and Maier (2004) noted that *mdaB* deletion mutants of *H. pylori* were significantly less successful in the colonisation of a mouse stomach than the wild type and Skurnik and colleagues (2013) observed that *pa2580 (mdaB)* mutants of *P. aeruginosa* P14 were unviable in the caecum and spleen of a murine model. As well as survival within a host, MdaB in *H. pylori* has been shown to play a key role in oxidative stress management with *mdaB* mutants unable to survive the same extent of air exposure as the wild type, also the gene deleted strains were more sensitive to H₂O₂, organic hydroperoxides and paraquat (Wang and Maier, 2004). A role in quorum sensing in *P. aeruginosa* was implied by Tan *et al.* (2015) where *mdaB* was significantly upregulated upon treatment with the QS inhibitor Iberin. Finally, MdaB has also been linked to antibiotic sensitivity in *P. aeruginosa* and *E. coli* and this will be discussed in the next chapter.

The first azoreductase structure to be solved was that of an enzyme from *E. coli* (Ito *et al.*, 2006). Subsequently, several bacterial azoreductase structures have been solved that all share a characteristic homodimeric short flavodoxin-like fold, with the active sites formed by residues from both monomers and situated at the dimer interface (Wang *et al.*, 2007,

Liu *et al.*, 2007b, Binter *et al.*, 2009, Gonçalves *et al.*, 2013, Yu *et al.*, 2014). The substrate binding pocket is typically lined by hydrophobic aromatic residues, many of which are part of the β -hairpin that forms the active site ‘lid’ and play a role in determining the enzyme’s substrate specificity (Wang *et al.*, 2010). Each active site contains one flavin molecule which is essential for activity. The ‘flavin binding cradle’, conserved in both bacterial and eukaryotic azoreductases, is a structural motif comprising sequence independent hydrogen bonds which anchor the FMN or FAD within the active site (Ryan *et al.*, 2010a). The azoreductase family has large sequence diversity amongst members resulting in few conserved residues between the proteins which indicates a possibility that those that are conserved may provide structural stability (Ryan *et al.*, 2014, Ryan *et al.*, 2010a).

Many structures of azoreductases in complex with substrates such as quinones, azo and nitroaromatic compounds have been solved including paAzoR1 with methyl red, balsalazide, Coenzyme Q₁, anthraquinone-2-sulfonate and nitrofurazone (Wang *et al.*, 2007, Ryan *et al.*, 2014, Ryan *et al.*, 2011, Ryan *et al.*, 2010a), ppAzoR (from *P. putida*) with anthraquinone-2-sulfonate and reactive black 5 (Gonçalves *et al.*, 2013) and AzrA and AzrC (from *Bacillus* sp.) with acid red 88 and orange I (Yu *et al.*, 2014). All substrates bind between the aromatic residues of the β -hairpin and the isoalloxazine rings of the flavin, with which they form π - π stacking interactions.

As of yet, no azoreductase structure has been solved in complex with a nicotinamide cofactor. Yu and colleagues (2014) solved the structure of the NAD(P)H competitive inhibitor cibacron blue in complex with azoreductases from *Bacillus* sp. however due to structural differences between it and NAD(P)H this does not provide details of the nicotinamide binding (Figure 5.1). The structure of MdaB from *Streptococcus mutans* in complex with NADPH has been solved and is the only structural evidence available in the literature of nicotinamide binding in this family (Wang *et al.*, 2014). While this may be useful, it is important to note that the residues lining the active sites of MdaB enzymes from *P. aeruginosa*, *E. coli* and *Y. pestis* are completely conserved with an overall sequence identity of ~60%. In contrast, smMdaB shares little sequence similarity with any member of this family (21% similarity with paMdaB (Edgar, 2004)). In addition, no azoreductase activity has so far been observed with smMdaB so this cannot yet be confirmed as an appropriate nicotinamide binding model for an azoreductase enzyme.

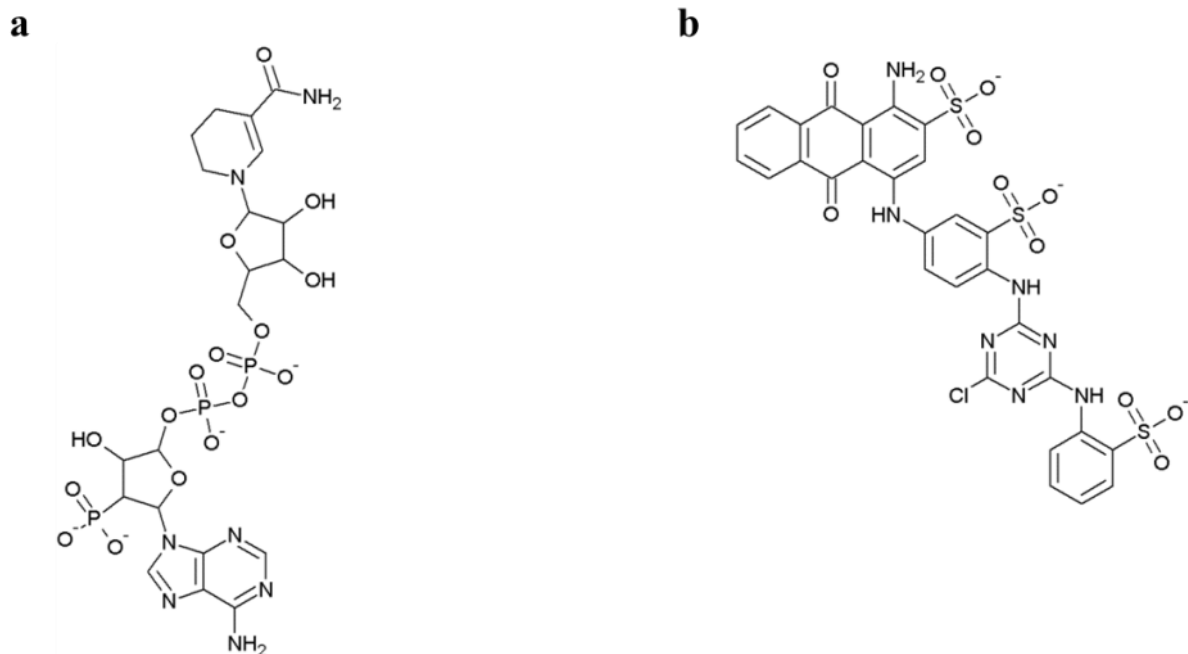


Figure 5.1 Chemical structures of H₂NADPH (a) and cibacron blue (b)

The chemical structures of H₂NADPH (a) and cibacron blue (b) are displayed. Both images were generated in ChemSketch (ChemSketch, 2015).

X-ray crystallography is a powerful tool for examining biological function and is based on x-ray diffraction datasets obtained from crystals (in this case, protein crystals) grown in a supersaturated solution that exhibits conditions that do not significantly perturb the molecules natural state (McPherson and Gavira, 2014, Wlodawer *et al.*, 2008). To improve understanding of the binding of the nicotinamide cofactor to azoreductase-like enzymes in *P. aeruginosa*, this technique has been employed and is described in this chapter to examine the structure of PA2580/paMdaB in complex with a non-reactive form of NADPH. In addition, the four proteins, PA2280, PA2580, PA1204 and PA0949, identified as putative azoreductases by Ryan *et al.* (2014) and previously characterised by Crescente (2015) are investigated here in order to confirm the flavin selectivity for each enzyme and examine their properties in relation to thermostability.

5.2 Results

The continuation of the characterisation of the newly identified azoreductase and NQO proteins from *P. aeruginosa* PAO1, as started by Crescente (2015), is covered in this chapter. In order to confirm their flavin selectivity a range of biochemical assays were performed. The molecular ratio of flavin molecule per protein monomer was calculated for each protein and a structural study of PA2580 was carried out.

5.2.1 Overexpression and purification of recombinant proteins

All recombinant proteins used in this section were generated by Dr. Vincenzo Crescente as described in Crescente (2015) with the exception of PA2580. The cloned strain, *E. coli* BL21-pET-28b::*pa2580* used for the production of PA2580, was also kindly supplied by Dr. Vincenzo Crescente. Recombinant PA2580 was overexpressed in two 500 mL culture volumes using the method described in section 2.4.1. Following cell lysis and separation, the soluble and insoluble fractions along with the whole cell lysate were observed using SDS-PAGE (Figure 5.2). For each fraction, distinct bands were seen at approximately 24 kDa (actual size estimated at 24.1 kDa using ProtParam (Gasteiger E., 2005)) which did not appear in the negative control indicating that overexpression had been successful. It was clear that soluble protein had been produced with approximately 80% of recombinant protein appearing in the soluble fraction. This was then purified via the IMAC method as described in section 2.5.1. Samples of the eluates containing purified protein along with the flow through and un-purified soluble fraction were examined on SDS-PAGE (Figure 5.3).

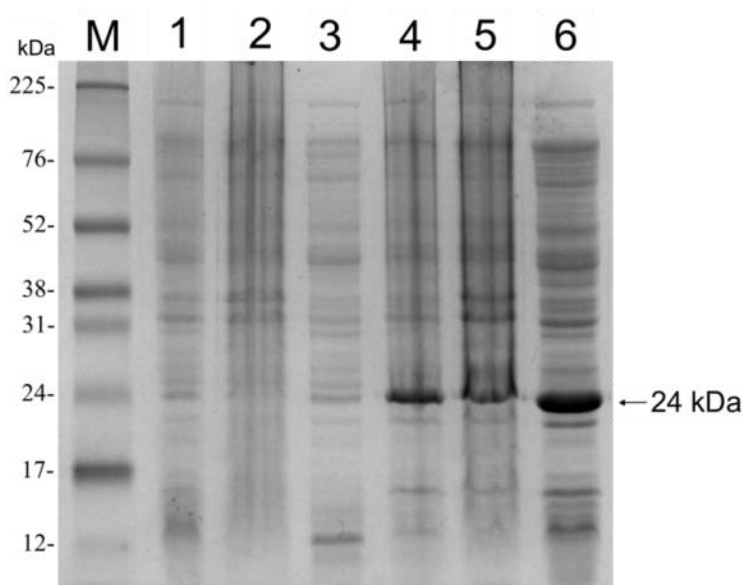


Figure 5.2 Overexpression of PA2580 recombinant protein in *E. coli* BL21(DE3)

Coomassie blue stained SDS-PAGE showing overexpression of PA2580 recombinant protein. Large scale protein production in 500 mL culture volumes was compared between *E. coli* BL21(DE3) transformed with pET-28b::*pa2580* induced with 0.5 mM IPTG (lanes 4-6) and a negative control of *E. coli* BL21(DE3)-pET-28b (lanes 1-3). Overproduction at approximately 24 kDa was evident only in the induced azoreductase clone. Lanes depict the whole cell lysate (1, 4), insoluble fraction (2, 5) and soluble fraction (3, 6). Lane M represents the molecular weight marker.

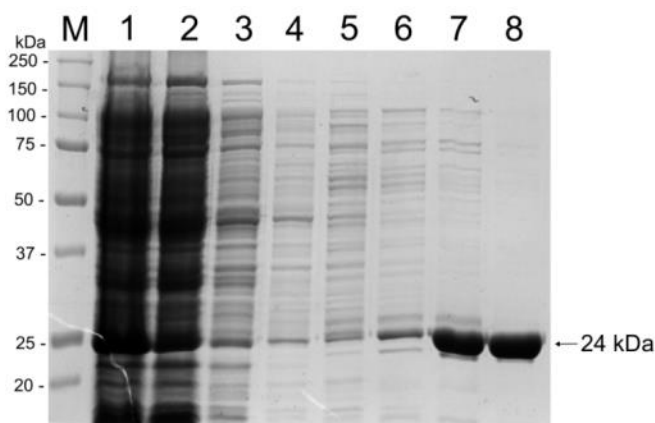


Figure 5.3 Purification of PA2580 recombinant protein using IMAC

Coomassie blue stained SDS-PAGE showing the purification of the soluble fraction from the expression lysate. An Ni-NTA column was loaded with the soluble fractions from 500 mL cultures and eluted with buffer (20 mM Tris HCl, 100 mM NaCl, pH 8) containing increasing concentrations of imidazole (10, 25, 50, 100 and 250 mM). Lanes depict the molecular weight marker (M), soluble fraction (1), flow through (2), 0 mM imidazole (3), 10 mM imidazole (4), 25 mM imidazole (5), 50 mM imidazole (6), 100 mM imidazole (7) and 250 mM imidazole (8). Lane M represents the molecular weight marker (NEB broad range protein ladder).

5.2.2 Dialysis and quantification of PA2580

Following protein purification, PA2580 was eluted in 20 mM Tris HCl 100 mM NaCl pH 8 containing 100 mM and 250 mM imidazole. To reduce the amount of imidazole to <1 mM, the samples which had been eluted from the IMAC column in 4 mL volumes with 100 mM and 250 mM imidazole were added separately to porous tubing with a molecular weight cut-off of 12-14 kDa. This tubing was then suspended in 4 L buffer (20 mM Tris HCl 100 mM NaCl pH 8). Following overnight dialysis, the protein samples were quantified and concentrated to 2 mg/mL in 20 mM Tris HCl 100 mM NaCl pH 8 5% v/v glycerol before being flash frozen in liquid nitrogen and stored at -80°C. This method resulted in a yield of 33.3 mg of pure soluble protein from 1 L culture.

5.2.3 Characterisation of recombinant azoreductases and quinone oxidoreductases

5.2.3.1 Absorbance spectra of azoreductases and quinone oxidoreductases

The proteins in this section have already been confirmed as flavoproteins (Crescente, 2015). Although it is never certain that flavin is incorporated during expression in *E. coli* it was assumed that flavin would indeed be present in PA2280, PA2580 and PA1204 as the TLC results (for PA2580 and PA1204 only) and enzymatic activity data from Crescente (2015) indicates that flavin is bound. However to quantify the ratio of protein monomers to flavin molecules, absorbance readings were taken between 300 and 600 nm. The absorbance spectra for FMN and FAD obtained in section 4.2.1.2 were used as a means of comparison. The spectra obtained for PA2280, PA2580 and PA1204 displayed the characteristic flavin absorption peaks (Figure 5.4). No flavin absorption peaks were apparent for PA0949. To determine the ratio of protein monomer to flavin molecule the absorbance measurements at 280 and 450 nm were examined. The molar ratios for each protein to flavin were as follows, 4.3:1 for PA2280, 2.5:1 for PA2580, 3.4:1 for PA1204 and 6.2:1 for PA0949.

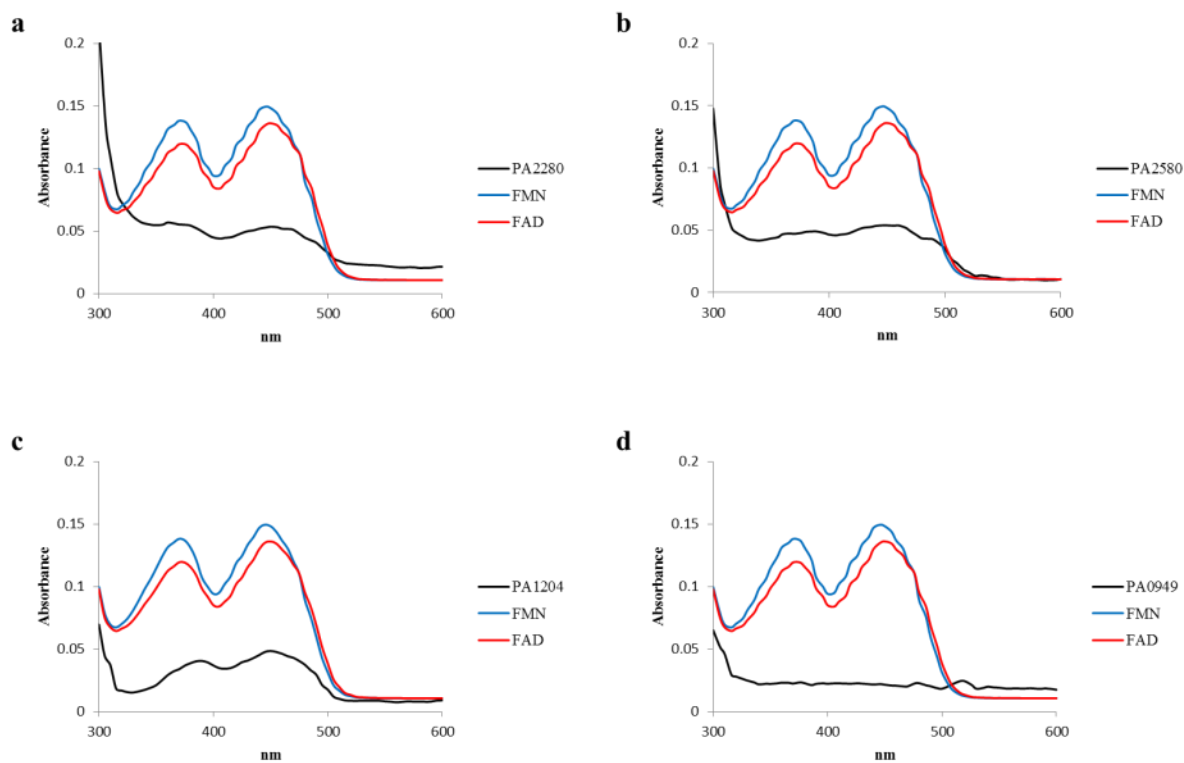


Figure 5.4 Absorption spectra for PA2280 (a), PA2580 (b), PA1204 (c) and PA0949 (d) Absorbance spectra of the purified recombinant proteins PA2280 (a), PA2580 (b), PA1204 (c) and PA0949 (d) compared with FMN and FAD absorption spectra, showing two absorption shoulders for the free flavin molecules (λ_{max} 360 and 450 nm). 400 $\mu\text{g/mL}$ protein solutions were prepared in 20 mM Tris HCl 100 mM NaCl pH 8 and placed in UV transparent cuvettes for the spectra determination. 20 μM FMN and FAD solutions were prepared in the same buffer and analysed via the same method as the protein solutions. Absorption spectra were generated in three replicates ($n=3$) using Infinite M200 PRO plate reader between 300 and 600 nm.

5.2.3.2 Confirming flavin selectivity

The characterisation of PA2280, PA2580, PA1204 and PA0949 carried out in Crescente (2015) followed a similar process to that described in section 4.2.2.2 where a series of activity assays were performed and the rates compared to establish the preferred electron donor and flavin cofactor. For all four proteins, NADPH was confirmed as the preferred electron donor over NADH with significantly higher activity rates achieved with the former. Regarding flavin selectivity, Crescente (2015) observed that PA2280 and PA0949 reduced their substrate more efficiently in the presence of FMN over FAD while PA2580 and PA1204 achieved higher reduction rates with FAD as the cofactor. The flavin selectivity was confirmed for PA2580 and PA1204 only via TLC analysis where a spot was observed for both proteins with an R_f similar to that of FAD. As mentioned in the previous section, no spot was observed for either PA2280 or PA0949 thus the flavin selectivity in this case could not be confirmed (Crescente, 2015).

To further investigate the flavin selectivity of these proteins, the reduction of ANI by each enzyme was monitored in the presence of increasing concentrations of each flavin. ANI was selected as the substrate in this case as it is a universal substrate for these enzymes (Crescente *et al.*, 2016) and the λ_{max} of 660 nm would not be interfered with by the presence of either flavin. Consistent with the findings of Crescente (2015), FMN appears to be the preferred flavin for PA2280 and PA0949. For PA2280, a much steeper increase in reduction rates was apparent with FMN over FAD (Figure 5.5 a) while PA0949 showed no reductive capacity in the presence of FAD at any concentration but as FMN concentration increased so did the rate of activity (Figure 5.5 d). A preference for FMN over FAD was also evident with PA1204 (Figure 5.5 c). Regarding PA2580, it was not possible to determine flavin selectivity via this method as both sets of reduction rates were similar (Figure 5.5 b).

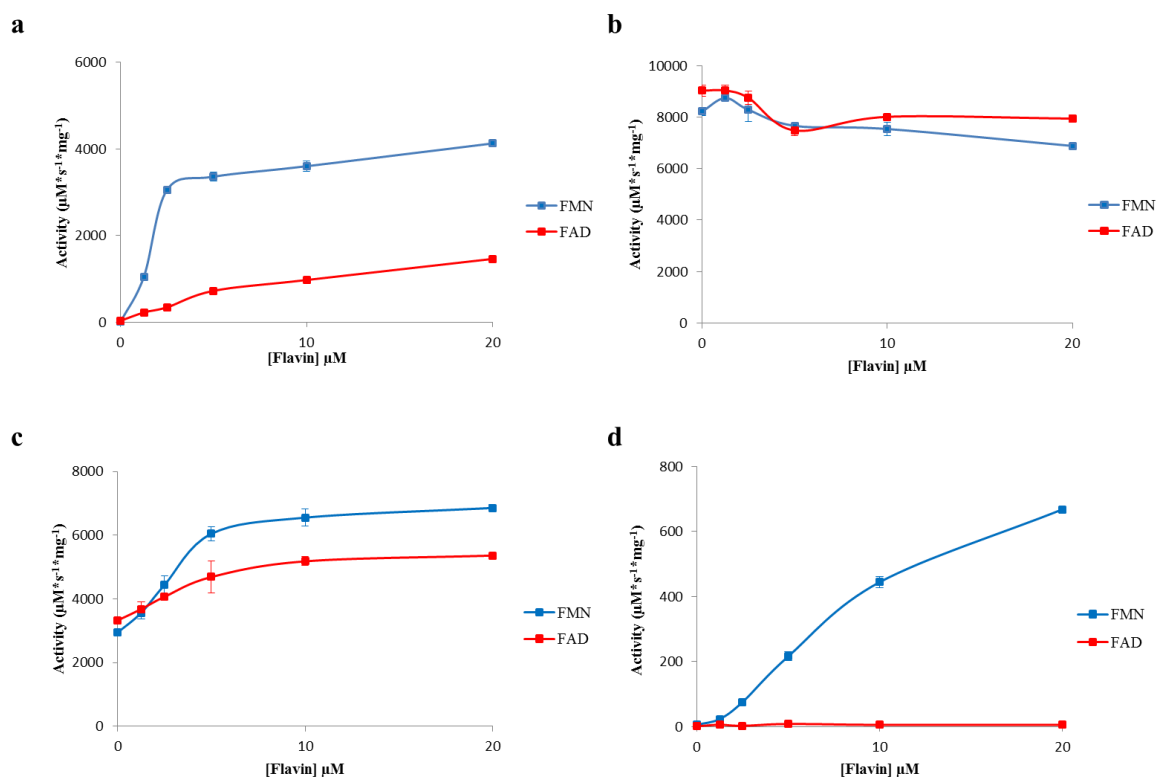


Figure 5.5 Activity assays for PA2280 (a), PA2580 (b), PA1204 (c) and PA0949 (d) in the presence of varying flavin concentrations

ANI reduction was measured at its specific λ_{max} of 660 nm to compare the effects of adding FMN (blue) and FAD (red) to the reaction mix. Enzyme concentration was kept constant at 0.2 $\mu\text{g}/\text{mL}$ for PA2280 (a), 5 $\mu\text{g}/\text{mL}$ for PA2580 (b), 1 $\mu\text{g}/\text{mL}$ for PA1204 (c) and 10 $\mu\text{g}/\text{mL}$ for PA0949 (d). All reactions were carried out in the presence of 500 μM NADPH and 100 μM ANI in 20 mM Tris HCl 100 mM NaCl pH 8 buffer. Measurements were performed in triplicate and error bars represents \pm standard deviation.

To provide further evidence of the flavin selectivity of these proteins, the effects on protein stability upon addition of FMN and/or FAD were monitored using DSF. The T_M of each protein was calculated in the presence and absence of flavin. An increase in T_M upon addition of flavin would indicate the binding of flavin to the protein. For PA2280, a small but significant thermal shift was observed in the presence of 1 μ M FMN while no change was evident with 1 μ M FAD. Upon addition of 1 μ M of either flavin to PA2580 a significant thermal shift was noted, however the shift was much greater at 16°C with FAD as opposed to 5°C with FMN. Regarding PA1204 and PA0949, no significant difference was apparent upon addition of either 1 or 5 μ M flavin however when the FMN concentration was increased to 20 μ M, PA1204 was destabilised. In contrast, addition of 20 μ M FAD significantly increased the T_M of this protein by 6°C. The addition of 20 μ M or either flavin stabilised PA0949 with a much larger increase in thermostability evident with FMN compared to FAD (12°C and 2°C respectively). All DSF results are listed in Table 5.2.

Table 5.2 Binding of flavin cofactors to azoreductase and NQO enzymes

Changes in protein thermostability were measured in response to addition of either FMN or FAD. *20 μ M or †1 μ M flavin was added to the mixture. Thermostability was measured for 64 μ g/mL enzyme in 20 mM Tris HCl pH 8 and 100 mM NaCl. All measurements were performed in triplicate. Fitting of the melting curve was performed using Graphpad Prism (version 7) to a Boltzman sigmoidal distribution.

Azoreductase	$T_M/^\circ\text{C}$	$T_M + \text{FMN}/^\circ\text{C}$	$T_M + \text{FAD}/^\circ\text{C}$
PA2280 [†]	47.3 \pm 0.1	49.1 \pm 0.7	47.4 \pm 0.2
PA2580 [†]	47.1 \pm 0.1	52.6 \pm 0.2	63.5 \pm 0.1
PA1204 [*]	71.1 \pm 0.6	49.2 \pm 2.0	77.3 \pm 0.5
PA0949 [*]	55.7 \pm 0.3	64.4 \pm 0.8	57.7 \pm 0.3

5.2.4 Crystallisation and structural determination of PA2580

5.2.4.1 Crystallisation of PA2580 with H₂NADPH

The purified protein PA2580 was concentrated via an ultracentrifugation concentrator to 10 mg/mL and washed in 20 mM Tris HCl 500 μ M FAD 2 mM H₂NADPH. Initial small scale crystal trials (0.2 μ L protein solution) were set down using a Mosquito crystallisation robot (TTP Labtech). Screens were performed in sitting drop 96-well plates and the buffer conditions trialled were PACT *premier* HT-96, JCSG-*plus* and Morpheus (Molecular Dimensions). The conditions which grew crystals are listed in Table 5.3. Typical protein crystals of approximately 93 μ m across were obtained within 3 to 4 days (Figure 5.6).

Although crystals were obtained in some PACT *premier* conditions, the scaling up procedure (2 μ L of protein solution) was only performed for the successful Morpheus screens, B6 (0.09 M Halogens, 0.1 M Sodium HEPES, 0.1 M MOPS, 20% v/v ethylene glycol, 10% w/v polyethylene glycol (PEG) 8000 pH 7.5) and F10 (0.12 M Monosaccharides, 0.1 M Bicine, 0.1 M Tris, 20% v/v ethylene glycol, 10% w/v PEG 8000 pH 8.5). This was due to the fact that these particular Morpheus screens contain 20% ethylene glycol and 10% w/v PEG 8000 thus an extra soaking stage in cryoprotectant prior to freezing could be omitted (Gorrec, 2009). Crystals from both sets of conditions were picked and soaked overnight in 4 μ L 10 mM H₂NADPH prepared in the appropriate Morpheus buffer prior to snap freezing in liquid nitrogen.

Table 5.3 Successful crystallisation conditions for PA2580

Conditions					
Screen	Well	Additives	Buffer	pH	Precipitant
PACT <i>premier</i> HT-96	F6	0.2 M sodium formate	0.1 M Bis Tris propane	6.5	20% w/v PEG 3350
	G6				
	G2	0.2 M Sodium bromide		7.5	
	G3	0.2 M Sodium iodide			
	F7	0.2 M Sodium acetate trihydrate		6.5	
Morpheus	B6	0.09 M Sodium fluoride; 0.09 M Sodium bromide; 0.9 M Sodium iodide;	0.1 M HEPES 0.1 M MOPS	7.5	20% v/v Ethylene glycol 10% w/v PEG 8000
	F10	0.12 M D-Glucose; 0.12 M D-Mannose; 0.12 M D-Galactose; 0.12 M L-Fructose; 0.12 M D-Xylose; 0.12 M N-Acetyl-D-Glucosamine	0.1 M Bicine Tris	8.5	

**Figure 5.6 Crystals of PA2580**

Crystals of PA2580 in mother liquor 0.1 M HEPES 0.1 M MOPS pH 7.5 and 20% v/v ethylene glycol 10% w/v PEG 8000. These crystals were grown by the sitting drop vapour diffusion method in 48-well Maxi plates. These crystals were imaged using Xli Cap.

5.2.4.2 Structure determination of PA2580 with bound H₂NADPH

The frozen mounted crystals were transported to the Diamond light source by Dr. Edward Lowe (Oxford University). The gathering of data and subsequent molecular replacement is described in section 2.7.4. The structure of PA2580 obtained from crystals grown in 2 mM H₂NADPH was solved at 1.29 Å with good stereochemistry and R_{free} and R_{work} values of 15.7% and 13.9% respectively. Two PA2580 monomers each with the same flavodoxin fold found in other MdaB structures were evident in the asymmetric unit of the crystal. There was strong density in both active sites obtained after molecular replacement for the expected bound FAD which allowed unambiguous building of the complete FAD molecule (Figure 5.7). Subsequent rounds of refinement which included the addition of water molecules revealed density in the active site pocket consistent with the binding of MOPS (one of the buffer components in the crystallisation solution) (Figure 5.8 a).

The crystals which had been soaked overnight in H₂NADPH were used as an attempt to overcome the binding of MOPS in the active site. A second dataset was collected using the same method as used above and the structure solved at 1.35 Å. The structure of PA2580 solved above was stripped of its ligands and used to phase the new structure via molecular replacement. In this case, refinement resulted in a density consistent with the nicotinamide group of H₂NADPH and this was subsequently refined in place (Figure 5.8 b). All processing and refinement statistics are available in Table 5.4.

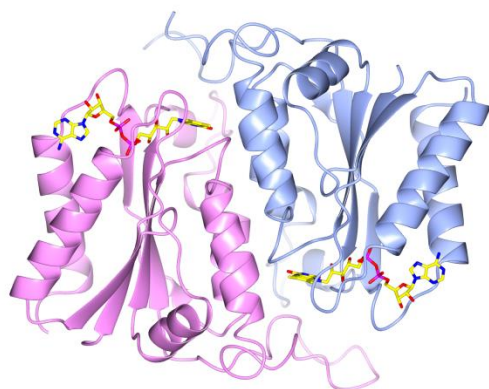


Figure 5.7 Crystal structure of the PA2580 homodimer

Each monomer (represented in pink and blue) is shown with the FAD cofactor bound (yellow). This image was generated and manipulated in CCP4MG (McNicholas *et al.*, 2011).

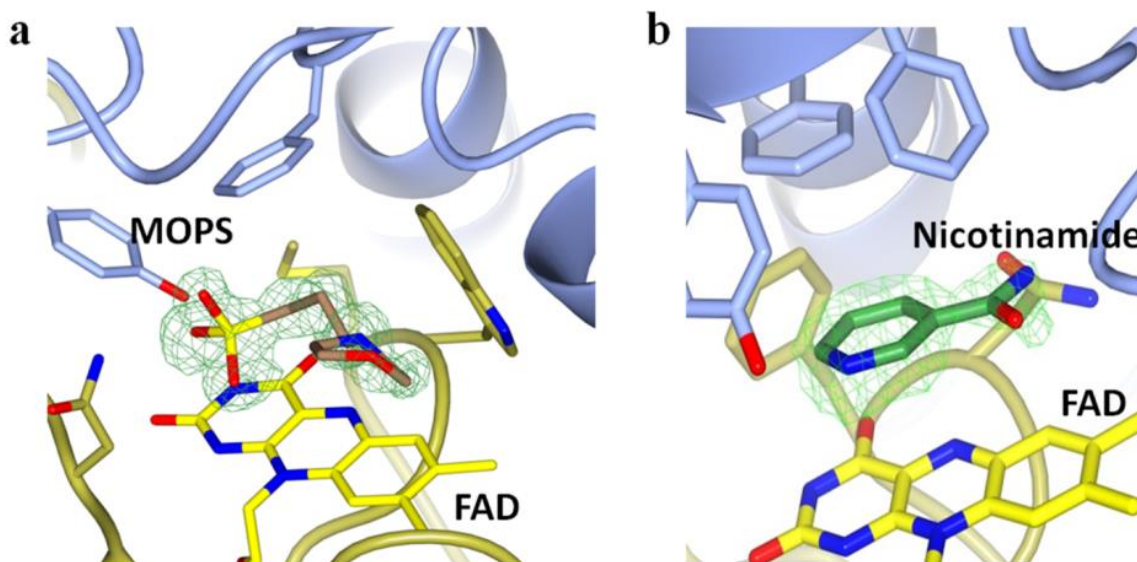


Figure 5.8 Binding of compounds in the active site of PA2580

Electron density consistent with MOPS is displayed bound to the FAD cofactor of PA2580 (a). Following overnight soaking of preformed crystals in 10 mM H₂NADPH, electron density consistent with the nicotinamide group of H₂NADPH was present bound to the FAD cofactor of PA2580 (b). These images were generated using CCP4MG (McNicholas *et al.*, 2011).

Table 5.4 Processing and refinement statistics for PA2580 and PA2580-nicotinamide

Structure	PA2580	PA2580-nicotinamide
Space Group	P2 ₁ 2 ₁ 2 ₁	P2 ₁ 2 ₁ 2 ₁
α, β, γ (°)	90, 90, 90	90, 90, 90
a, b, c (Å)	61.47, 64.01, 99.59	61.58, 63.84, 99.57
Processing Statistics		
Resolution Range (Å)	53.85-1.29	49.78-1.35
Unique reflections	96132 (5516)	85976 (7704)
R_{merge}	0.067 (0.612)	0.078 (0.880)
$\langle I/\sigma(I) \rangle$	13.5 (2.3)	13.0 (1.7)
Completeness %	96.6 (75.9)	99.1 (92.1)
Multiplicity ^a	5.4 (2.3)	6.3 (4.4)
Refinement Statistics		
R_{work} %	15.7	15.7
R_{free} % ^c	13.9	13.2
RMSD bond angle (°)	1.09	1.03
RMSD bond length (Å)	0.008	0.008

5.3 Discussion

The aims of this chapter as laid out in section 1.3 have been completed as follows:

- i. Characterisation of the enzymes PA2280, PA2580, PA1204 and PA0949 from *P. aeruginosa* PAO1 (including flavin cofactor selectivity and thermostability analysis) has been completed.
- ii. The crystal structure of PA2580 in complex with the non-reactive H₂NADPH has been solved at a resolution of 1.3 Å.

In agreement with the biochemical and enzymatic analysis carried out by Crescente (2015), the four proteins PA2280, PA2580, PA1204 and PA0949 have different cofactor and substrate preferences. They have also been noted here to encompass different thermostability profiles.

All proteins were expected to be flavin dependent enzymes and this was confirmed by Crescente (2015). However, the level of flavin incorporation during recombinant protein expression in *E. coli* was unclear. A low flavin to protein ratio could also occur as a result of dissociation of flavin from the enzyme during overnight dialysis as the flavin is not covalently bound to the enzyme (Ryan *et al.*, 2010a). How much flavin will dissociate is dependent on the affinity of the protein for the flavin. Upon collection of UV-visible spectra for each protein it was evident that flavin was present in a different molar ratio for each enzyme. The data obtained here was consistent with that the TLC results gathered by Crescente (2015) where a spot was visible for PA1204 and PA2580 (flavin to protein ratios of 3.4:1 and 2.5:1 respectively) but not for PA2280 or PA0949 (flavin to protein ratios of 4.3:1 and 6.2:1 respectively) thus confirming that there is less incorporation or increased loss of flavin in the latter two proteins. Also, neither PA2280 nor PA0949 displayed reductive activity against ANI without the addition of flavin to the reaction mix. It is therefore not surprising that these were the two enzymes with the lowest flavin to protein ratio.

Regarding flavin selectivity, PA2280 has shown a clear preference for FMN over FAD in both DSF analysis and the activity assays which included increasing concentrations of FMN and FAD. This data is consistent with the findings of Crescente (2015) where reduction of methyl red was significantly higher with FMN included the reaction mix. Also, ArsH from *S. meliloti* has been confirmed via TLC analysis to select for FMN (Ye *et al.*, 2007). Although the activity assays completed here for PA2580 failed to show any

obvious preference for either flavin, previous work has shown that methyl red is reduced at a higher rate upon inclusion of FAD (Crescente, 2015). In addition, TLC analysis completed by Crescente (2015) yielded an obvious FAD spot for this protein. The DSF data compiled here has also confirmed FAD as the cofactor with a higher thermal shift apparent with FAD as opposed to FMN indicating selective binding of FAD to the protein. This result is consistent with data from a study on MdaB from *E. coli* (75% sequence similarity) that showed that the enzyme was selective for FAD when reducing quinones (Hayashi *et al.*, 1996). PA1204 presents a more confusing result however with the DSF data showing selectivity for FAD while the activity assays including increasing flavin concentrations imply a clear preference for FMN. The FMN selectivity is supported by Agarwal *et al.* (2006) where the crystal structure of PA1204 was solved with FMN bound. It is important to note however that no experimental evidence was suggested in this study for introduction of FMN over FAD. Considering the findings in Crescente (2015), it is likely that FAD is the preferred cofactor as a weak TLC spot was observed for FAD and MEN was reduced at a significantly higher rate with FAD over FMN. Finally, PA0949 appears to select for FMN over FAD. No reduction of ANI occurs upon addition of 5-20 μM FAD in the reaction mix while when FMN is included the reaction rate increases steadily with FMN concentration. A similar result was obtained by Crescente (2015) where reduction of MEN only occurred in the presence of FMN. The DSF results gathered here also indicate FMN as the more suitable cofactor with a larger increase in thermostability evident when FMN was included compared to FAD. This is consistent with literature that has demonstrated FMN being selectively incorporated into WrbA from *E. coli* by means of activity assays and structural analysis (Kishko *et al.*, 2013).

The unusually high thermostability of PA1204 coupled with its ability to reduce azo compounds, as demonstrated by Crescente (2015), is likely to be of particular use in bioremediation as high thermostability implies a longer lifetime and higher tolerance to extreme pH values, high salt concentration, elevated pressure and the presence of organic co-solvents (Brissos *et al.*, 2014). In addition, previous research has shown the capacity of YieF from *E. coli* in reducing heavy metal ions such as Cr^{6+} and U^{6+} to the less water soluble Cr^{3+} and U^{3+} (Ackerley *et al.*, 2004). In aquatic environments these heavy metals can be absorbed by living organisms and enter into the food chain which can result in the accumulation of large concentrations within the human body and serious health disorders thus decreasing water solubility of these ions is essential (Babel and Kurniawan, 2004).

With this in mind, it is possible that engineered members of the YieF family could prove highly beneficial in bioremediation of both heavy metals and azo dyes.

Structural analysis of PA2580 was carried out by means of x-ray crystallography. This protein was selected for structural studies as a high yield of pure protein was easily and reproducibly obtained from recombinant expression. This protein has previously been demonstrated to preferentially utilise NADPH over NADH during reduction reactions thus it was decided to co-crystallise the protein with the chemically reduced non-oxidisable form of NADPH, H₂NADPH. The structure was solved and displayed two PA2580 monomers which form a homodimer with one molecule of FAD bound to each monomer. The active site, similar to other solved azoreductases sits at the interface between the two monomers.

The overall fold of PA2580 was found to be the same short flavodoxin-like fold as previously described for other enzymes of the MdaB family from *E. coli* and *Y. pestis* (Adams and Jia, 2006, Minasov *et al.*, 2011) (Figure 5.9 a). Similar to other azoreductase enzymes from *P. aeruginosa* such as paAzoR1, the active site is lined with predominantly hydrophobic and aromatic amino acids which assist in the binding of substrates, the majority of which are hydrophobic (Ryan *et al.*, 2010a). Interestingly, these residues in the substrate binding pocket are highly conserved between MdaB from *E. coli* and PA2580 indicating that these two enzymes would have similar substrate specificity profiles and possibly interchangeable primary functions (Adams and Jia, 2006) (Figure 5.9 b). PISA analysis (Krissinel and Henrick, 2007) identified that PA2580 is likely to exist as a homodimer in solution, as is MdaB from *E. coli* (Adams and Jia, 2006). The Gibbs free energy of dissociation (ΔG^{diss}) for dimeric association of PA2580 is calculated as 24.5 kcal mol⁻¹ suggesting that the homodimer is likely to be stable in solution.

As expected, FAD is accommodated into the active site of each monomer. Like other known azoreductases including paAzoR1-3 from *P. aeruginosa*, the amino acid sequence in the flavin binding cradle of PA2580 bears no similarity to other known azoreductases (Ryan *et al.*, 2010a). Similar to other azoreductases, the binding occurs via hydrogen bonds formed between the flavin and the peptide backbone which are sequence independent (Figure 5.10). As the enzymatic reaction occurs via the bound flavin, this explains why such high sequence diversity is possible amongst the azoreductase-like enzymes (Ryan *et al.*, 2014).

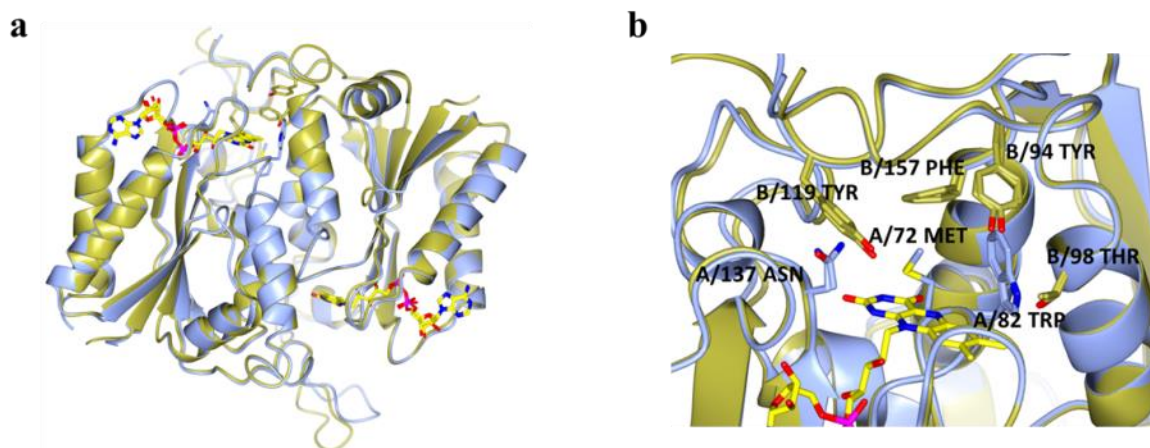


Figure 5.9 Structural comparison of PA2580 and ecMdaB

Crystal structure of PA2580 (represented in blue) and ecMdaB (represented in gold) shown with FAD cofactor bound (yellow). The structure of ecMdaB is from PDB 2B3D (Adams and Jia, 2006). The two structures align with an RMSD value of 0.6. The image was generated and manipulated in CCP4MG (McNicholas *et al.*, 2011) and compared using the superpose secondary structure matching tool in CCP4MG (Krissinel and Henrick, 2004). The overall structure of both proteins overlaid is displayed (a). The amino acids labelled in the substrate binding pocket are conserved across the two proteins (b).

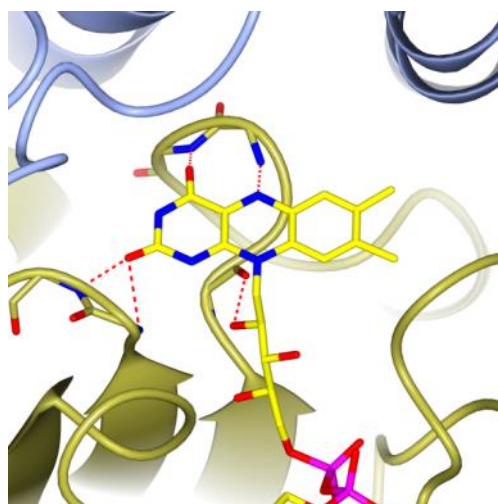


Figure 5.10 Hydrogen bonds are formed between PA2580 and FAD

The FAD (represented in yellow) is anchored in place via hydrogen bonds (depicted in red) formed with the sequence independent peptide backbone. The image was generated and manipulated in CCP4MG (McNicholas *et al.*, 2011).

As mentioned in section 5.1, the structure of smMdaB in complex with NADPH, solved by Wang and colleagues (2014), is unlikely to be representative of paMdaB/PA2580 due to the low level of conservation of residues in the active site compared to other MdaB members. This was confirmed upon comparison of the smMdaB structure to that of PA2580. After 3D structural alignment using secondary structure matching of C_{α} atoms (Krissinel and Henrick, 2004), a high RMSD value of 1.8 was obtained for PA2580 superposed against smMdaB (compared to a value of 0.6 for PA2580 and ecMdaB). A visual representation of the surfaces smMdaB and PA2580 (Figure 5.11 a) and of ecMdaB and PA2580 (Figure 5.11 b) further proves the difference in structure of smMdaB and the protein of interest in this study. Thus the structure of NADPH bound to smMdaB is not a useful tool in examining nicotinamide binding to the azoreductase-like enzymes in *P. aeruginosa*.

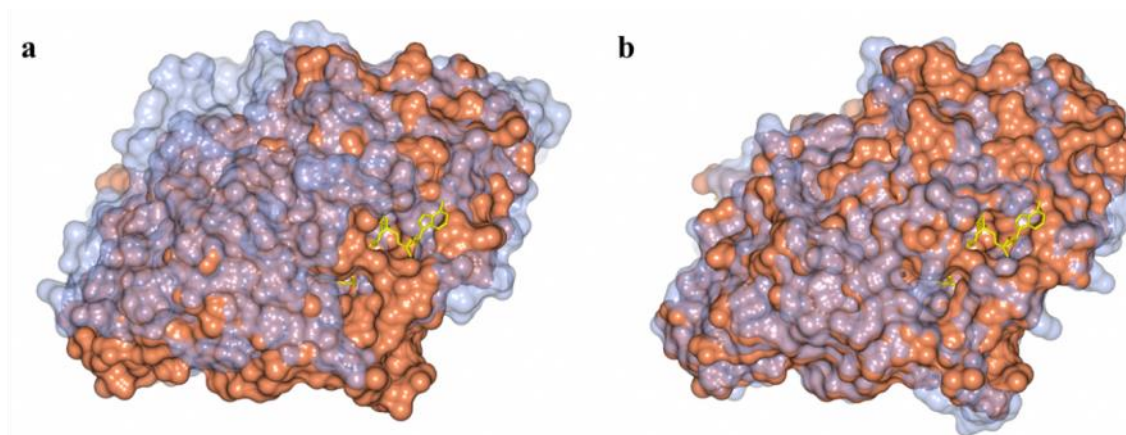


Figure 5.11 Surface comparison of PA2580 against other MdaB structures

Surface comparison of PA2580 (represented in orange) and smMdaB (represented in blue). A high RMSD value of 1.8 was obtained indicating that these are not closely related molecules. The structure of smMdaB is from PDB 3LCM (Wang *et al.*, 2014) (a). Surface comparison of PA2580 (represented in orange) and ecMdaB (represented in blue). Superposing the two structures yielded an RMSD value of 0.6. The structure of ecMdaB is from PDB 2B3D (Adams and Jia, 2006) (b). Both models display bound FAD (shown in yellow). The images were generated and manipulated in CCP4MG (McNicholas *et al.*, 2011) and compared using the superpose tool in CCP4MG (Krissinel and Henrick, 2007).

Due to the occupation of the protein's active site with MOPS, the decision was made to gather diffraction data from crystals soaked overnight in concentrated H₂NADPH, a non-reactive analogue of NADPH. Refinement from this second dataset resulted in unbiased difference density consistent with the nicotinamide group of H₂NADPH. Following subsequent refinement with this in place it was clear to see that the nicotinamide binds coplanar with the ring system of FAD, with the C4 atom of the nicotinamide from which the hydride is transferred, approximately 3.8 Å from the N5 acceptor of FAD (Figure 5.12 a). The amide group of the nicotinamide makes hydrogen bonds with the side chains of both Tyr108 and Asn126. Although the 3.6 Å distance from C4 → N5 is similar to that observed in the structure of nicotinamide in complex with smMdaB (Figure 5.12 b), the binding orientation of nicotinamide within the active site is rotated approximately 75° between the two structures which is likely due to the amide group interacting with hydrogen bonding groups (Arg55 and Tyr106) in a radically different part of the active site (Figure 5.12 c). As previously mentioned, the residues lining the active sites of MdaB enzymes from *P. aeruginosa*, *E. coli* and *Y. pestis* are completely conserved, it is therefore likely that the nicotinamide binding to PA2580 observed in this study is likely to be representative of the other MdaB family members.

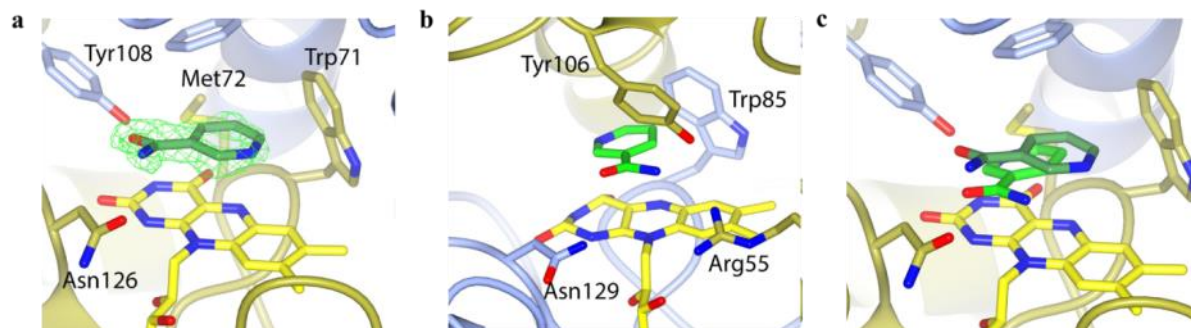


Figure 5.12 Comparison of nicotinamide binding to PA2580 and smMdaB

Nicotinamide is displayed bound within PA2580. Unbiased positive density consistent with the nicotinamide group of H₂NADPH is shown as green mesh (a). The nicotinamide group is depicted bound to smMdaB in a different orientation to that observed for PA2580 (b). The overlaid structures of nicotinamide binding to PA2580 and smMdaB are displayed. RMSD from secondary structure matching gave a value of 1.8 (c). The structure of smMdaB is from PDB 3LCM (Wang *et al.*, 2014). The images were generated and manipulated in CCP4MG (McNicholas *et al.*, 2011) and compared using the superpose tool in CCP4MG (Krissinel and Henrick, 2007).

The structure of PA2580 bound to nicotinamide solved here highlights the importance of hydrogen bonding in the determination of binding orientation of the cofactor. It also serves to highlight the limitations of using cibacron blue to predict NAD(P)H interactions (as carried out by Yu and colleagues (2014)) as this compound lacks equivalent hydrogen bonding groups. The continuation of the work initiated by Crescente (2015) presented here confirms the azoreductase-like proteins in *P. aeruginosa* as flavin dependent enzymes with differing cofactor selectivity. The primary physiological role of these enzymes in *P. aeruginosa* still remains unclear. The physiological role of the azoreductases and azoreductases-like enzymes in *P. aeruginosa* will be examined in the next chapter.

Chapter 6 Phenotypic analysis of *P. aeruginosa* wild type and azoreductase-like gene deletion strains

6.1 Introduction

P. aeruginosa is a prevalent microbe in the natural environment which can colonise and invade many hosts, including humans, to cause serious and potentially life threatening infections (Mena and Gerba, 2009). Predominantly an opportunistic pathogen, it is the most prevalent gram-negative bacteria to cause infection in intensive care units worldwide and in the ICU it is independently affiliated with increased mortality rates, an issue exacerbated by its intrinsic and acquired resistance to many antimicrobial agents (Rosenthal *et al.*, 2012, Nathwani *et al.*, 2014). The intrinsic resistance of *P. aeruginosa* to many antibiotics has been attributed mainly to the nature of its hydrophilic lipopolysaccharide outer membrane which forms a barrier against numerous toxic agents (Nikaido and Vaara, 1985). It is, however, the astounding capacity of *P. aeruginosa* to demonstrate many enzymatic and mutational mechanisms of bacterial resistance that has led to the emergence of MDR strains unsusceptible to aminoglycosides, cephalosporins, fluoroquinolones and carbapenems (Pechère and Köhler, 1999, CDC, 2013). Thus, the identification of genes in the *P. aeruginosa* genome that may influence this resistance is essential and could subsequently lead to the development of novel targets for antimicrobial chemotherapy.

Although azoreductases are predominantly associated with their ability to cleave the azo bond found in azo dyes and azo pro-drugs it is unlikely that the breakdown of these synthetic substances is the primary physiological role of this class of enzyme (Wang *et al.*, 2007). As previously mentioned in Chapter 4, many azoreductases including those produced by *P. aeruginosa*, are capable of reducing quinone compounds, with much higher rates achieved in this case than for the reduction of azo substrates which indicates that this may be their principal function (Ryan *et al.*, 2010b, Ryan *et al.*, 2014, Crescente *et al.*, 2016). In addition to this, recent publications have suggested that they may also be involved in antimicrobial sensitivity (Table 6.1).

Resistance in *P. aeruginosa* is complex and can be attributed to many mechanisms including lipopolysaccharide modification of the outer membrane, alteration of outer membrane porins, target protein mutations, expression of modifying enzymes such as β -

lactamases and multi-drug efflux pumps (Moskowitz *et al.*, 2004, Redgrave *et al.*, 2014, Aldred *et al.*, 2014). The potential role that azoreductases may play in any of these systems remains unclear however there is evidence to suggest that they are somehow involved. For instance, paAzoR3 (*pa3223*) mutants of *P. aeruginosa* PAO1 are up to two fold more susceptible to carbapenems, specifically meropenem, than the wild type (Wang *et al.*, 2016). It has also been found that sub inhibitory levels of tetracycline, chloramphenicol and spectinomycin induce upregulation of *pa2580* in *P. aeruginosa* PAO1 and that mutants lacking this gene are more sensitive to treatment with carbenicillin, chloramphenicol, ciprofloxacin and hydrogen peroxide, also, these traits are reversed in the complemented strain (Chen *et al.*, 2010). In contrast, expression of another azoreductase homologue, *pa0949*, is downregulated up to three fold upon exposure of *P. aeruginosa* PAO1 to tobramycin and ciprofloxacin but upregulated (1.5 fold) in the presence of tetracycline (Linares *et al.*, 2006). Downregulation of this gene has also been reported in *E. coli* following gentamicin treatment (Al-Majdoub *et al.*, 2013). Finally in *P. aeruginosa* PAO1, *pa1224* harbours a mutation of alanine (position 251 on the protein surface) to valine when resistance to the polymyxin colistin occurs however the significance of this remains unclear as this modification is conserved when the resistance is lost (Lee *et al.*, 2016).

This apparent involvement of azoreductases and their homologues in the response to antibiotics is not specific to *P. aeruginosa* PAO1 and is also observed in other microorganisms. For example, plasmid derived overexpression of azoreductases *azoR* and *mdaB* in *E. coli* leads to increased MICs for aminoglycosides streptomycin and kanamycin compared to the wild type strain. Confusingly, the same result is unexpectedly seen upon deletion of *azoR* therefore it is decidedly unclear what effect the azoreductases actually have regarding aminoglycoside susceptibility in *E. coli* (Ling *et al.*, 2012). Nonetheless, this data indicates some involvement of the azoreductases in antibiotic sensitivity. In addition, quinolone resistant *S. typhimurium* display 1-3 fold upregulation of the azoreductase homologues *mdaB* and *wrbA* in comparison to non-resistant strains, again suggesting that these enzymes play a role in antibiotic sensitivity (Correia *et al.*, 2016).

Table 6.1 Azoreductase and azoreductase-like genes implicated in antimicrobial susceptibility

Overview of the azoreductase and azoreductase-like genes and their associations in antibiotic sensitivity in different bacterial strains.

Gene	Bacterium	Phenotype
<i>paAzoR3</i>	<i>P. aeruginosa</i> PAO1	Transposon insertion mutants more susceptible to meropenem (Wang <i>et al.</i> , 2016)
<i>pa2580</i>		Upregulated in response to tetracycline, chloramphenicol and spectinomycin, transposon insertion mutants more susceptible to carbenicillin, chloramphenicol and ciprofloxacin (Chen <i>et al.</i> , 2010)
<i>pa0949</i>		Upregulated in response to tetracycline, downregulated in response to tobramycin and ciprofloxacin (Linares <i>et al.</i> , 2006)
<i>pa1224</i>		Mutation observed in colistin resistant strains (Lee <i>et al.</i> , 2016)
<i>azoR</i>	<i>E. coli</i>	Overexpression and gene deletion results in higher tolerance to streptomycin and kanamycin (Ling <i>et al.</i> , 2012)
<i>mdaB</i>		Overexpression results in greater tolerance to streptomycin and kanamycin (Ling <i>et al.</i> , 2012)
<i>wrbA</i>		Downregulated in response to treatment with gentamicin (Al-Majdoub <i>et al.</i> , 2013)
<i>mdaB</i> <i>wrbA</i>	<i>S. typhimurium</i>	Upregulated in quinolone-resistant strains when compared to the wild type (Correia <i>et al.</i> , 2016)

The three major classes of antibiotics; β -lactams, aminoglycosides and fluoroquinolones, have all been reported to generate ROS, specifically hydroxyl radicals, in bacteria which contribute to the killing efficiency of these chemotherapeutic agents. These antimicrobials use internal iron to promote Fenton-mediated hydroxyl radical formation which is mediated by the tricarboxylic acid cycle and depletion of NADH (Dwyer *et al.*, 2007, Kohanski *et al.*, 2007). It has been suggested that although different antibiotic classes have specific targets upon which they exert their mechanism of action (for example β -lactams target penicillin binding proteins, fluoroquinolones target DNA gyrase), antimicrobial treatment also sets off a complex series of metabolic changes within the cell, downstream of their direct point of interaction which results in the production of ROS and the subsequent breakage of double stranded DNA and protein mistranslation (Belenky *et al.*, 2015). Treatment of bacterial cells with natural antioxidants such as glutathione and ascorbic acid increases cell survival following exposure to the major classes of antibiotics, supporting this hypothesis that ROS are generated by antimicrobials and are involved in their bactericidal action (Dwyer *et al.*, 2014). As discussed in section 1.2.2, azoreductases and quinone reductases can act as defence mechanisms during oxidative stress, with this in mind it is possible that this may be the mechanism by which these enzymes influence the susceptibility of bacteria to antimicrobial treatment.

With a pool of literature, touched upon above, linking azoreductases and azoreductase homologues to antibiotic susceptibility across bacterial strains, a library of azoreductase-like gene deletion mutants were obtained from the Manoil laboratory, University of Washington (Jacobs *et al.*, 2003). A series of phenotypic experiments including antibiotic sensitivity assays were carried out by Dr. Vincenzo Crecente (Crescente, 2015). It was observed that the strains lacking the azoreductase-like genes had altered susceptibility to numerous antibiotics including fluoroquinolones and aminoglycosides by up to ten fold (Table 6.2), reinforcing the suggestion that azoreductases in *P. aeruginosa* play a role in antimicrobial sensitivity. In order to confirm this finding however, it is essential to complement each transposon mutant with the relevant knocked out gene and witness reversion, if, any, to the wild type phenotype.

So far, the primary focus of this thesis has been describing the characterisation of the gene products of azoreductase-like genes in *P. aeruginosa* PAO1. This chapter will report on the phenotypic effects of these genes in relation to antibiotic susceptibility, while also examining if the findings are consistent in another *P. aeruginosa* strain, specifically the clinical strain *P. aeruginosa* TBCF 10839. The aim of this chapter is to generate a library

of complemented strains of the azoreductase-like gene deletion mutants and subsequently investigate the effects that the azoreductase-like genes may have on sensitivity to different classes of antibiotics.

6.2 Results

It has previously been shown that single gene transposon mutants of *P. aeruginosa* PAO1 are more susceptible to certain antibiotics, specifically fluoroquinolones and colistin (Crescente, 2015). To prove this effect however, it was essential to reintroduce the gene of interest into either the chromosomal or extra chromosomal DNA of the mutated strain. Following this, antibiotic sensitivity assays were carried out to observe whether the microorganism would revert to the phenotype of the wild type strain, thus confirming whether or not it was the gene of interest responsible for the change in sensitivity.

The results listed below include the generation of the *P. aeruginosa* PAO1 transposon insertion mutant strains complemented with the relevant gene, RNA extraction followed by cDNA synthesis and PCR to confirm expression of the gene of interest followed by MIC assays to observe the effects of this gene on antimicrobial sensitivity. MIC assays were also carried out for *P. aeruginosa* TBCF 10839, *P. aeruginosa* TBCF 10839 $\Delta pa0785$, *P. aeruginosa* TBCF 10839 $\Delta pa0785$ -pUCP20::*pa0785* and *P. aeruginosa* TBCF 10839 $\Delta pa0785$ -pUCP20::*pa0785-0787* so as to compare the effects of an azoreductase gene deletion on a clinical strain.

6.2.1 Generation of complemented strains for the azoreductase-like gene deletion mutants

6.2.1.1 Preparation of genes of interest

The DNA sequences of *pa0785*, *pa1962*, *pa3223*, *pa2280*, *pa2580*, *pa1204*, *pa0949* and *pa4975* were obtained from The Pseudomonas Genome Database (Winsor *et al.*, 2016). The genes of interest were prepared for cloning into pUCP24 in the same manner described for the cloning of *pa1224* and *pa1225* in section 3.2.1.1. Gene specific primers were designed to incorporate BamHI and SalI restriction sites into the forward and reverse primers respectively and were chosen to correspond with restriction sites present in pUCP24 (Figure 6.1). Following PCR, products estimated at the correct size for each gene cloned were to be seen on 1% w/v agarose gel (Figure 6.2, Table 6.3). PCR product sizes were estimated using the molecular weight analysis tool in Image Lab 5.2.1 (BIO-RAD). The PCR products were purified and quantified before a double restriction digest with BamHI and SalI restriction enzymes. Following this, the samples were purified and quantified once more, ready for ligation into the cloning vector.

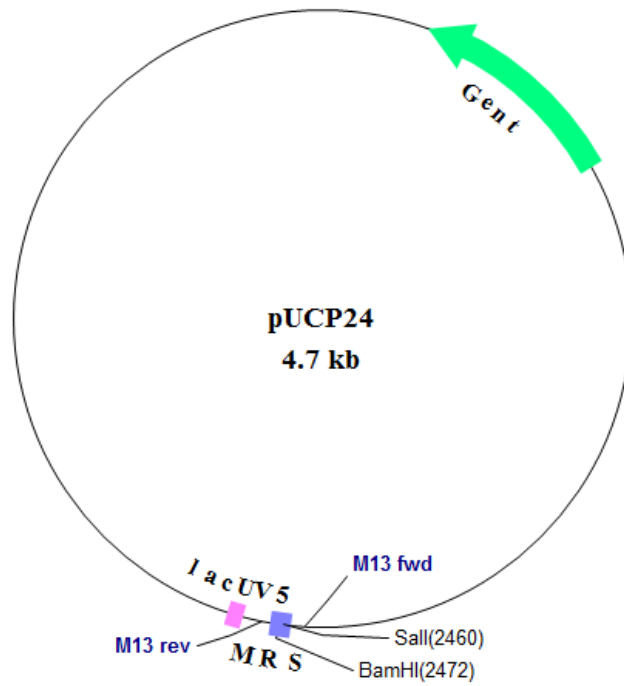


Figure 6.1 pUCP24 vector map

pUCP24 vector map showing the area of multiple restriction sites (MRS) with BamHI and SalI labelled along with the annealing sites of M13 forward and reverse primers. This figure was adapted from the Addgene website and the vector map generated using BVTech Plasmid.

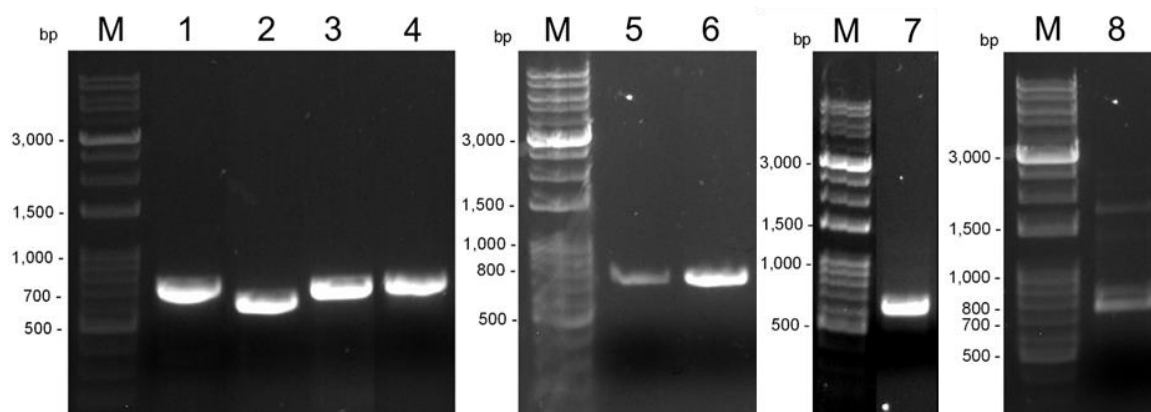


Figure 6.2 PCR amplification of azoreductases and azoreductase-like genes from *P. aeruginosa* PAO1 for cloning into pUCP24

1% w/v agarose gel showing the azoreductases and azoreductase-like genes amplified from total *P. aeruginosa* PAO1 genomic DNA using HiFidelity Taq polymerase. Samples shown are 1 Kb Plus DNA ladder (lanes M), *pa3223* (lane 1), *pa1204* (lane 2), *pa0949* (lane 3), *pa0785* (lane 4), *pa1962* (lane 5), *pa2280* (lane 6) *pa2580* (lane 7) and *pa4975* (lane 8).

Table 6.3 Estimated size of amplified putative azoreductase genes compared to actual size of PCR product sizes

These estimations are based on the migration of the band compared to the migration of bands of known sizes and they correspond to the actual expected gene sizes as predicted using the Pseudomonas Genome Database. All estimations were calculated using the molecular weight analysis tool in Image Lab 5.2.1

PCR product	Estimated size of PCR product (bp)	Actual size of amplified DNA (bp)	Percentage error
<i>pa3223</i>	705	695	1.4%
<i>pa1204</i>	611	599	2%
<i>pa0949</i>	709	676	4.9%
<i>pa0785</i>	703	671	4.8%
<i>pa1962</i>	761	722	5.4%
<i>pa2280</i>	755	722	4.6%
<i>pa2580</i>	608	622	2.3%
<i>pa4975</i>	771	753	2.4%

6.2.1.2 Preparation of the cloning vector

Plasmid pUCP24 was extracted from *E. coli* JM109 and quantified. The vector was then prepared for ligation with the genes of interest in the same manner as described for pET-28b in section 3.2.1.2 with the exception being the use of restriction enzymes BamHI and Sall for the double restriction digest. As before, a sample of the digested plasmid was ran alongside undigested plasmid on 1% w/v agarose gel (Figure 6.1). A typical band of supercoiled circular plasmid was evident for the undigested plasmid while a defined single band appeared for the digested sample.

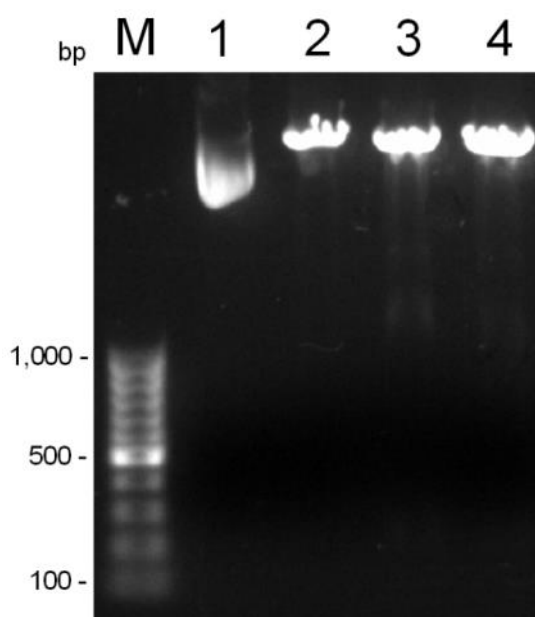


Figure 6.3 Endonuclease restriction digest of pUCP24

1% w/v agarose gel showing the pUCP24 plasmid before and after endonuclease digestion with restriction enzymes BamHI and Sall. Digested samples (lanes 2, 3 and 4) display a linearised plasmid while the undigested sample (lane 1) shows the supercoiled plasmid form. Thermo Scientific 100 bp Plus DNA ladder (lane M) was used as standard.

6.2.1.3 Obtaining and screening successful clones

The plasmids and PCR products for each gene of interest were ligated and transformed into *E. coli* JM109 in the same manner as described for the cloning of the azoreductase-like genes into pET-28b (section 3.2.1.3). This same procedure was also used to select for and screen for positive clones with the exception being that pUCP24 confers gentamicin resistance, thus in this case LB agar was supplemented with gentamicin rather than kanamycin. PCR was carried out on each positive clone using M13 primers which are designed to anneal to pUCP24 in sections upstream and downstream of the inserted gene sequence. PCR products were analysed on 1% w/v agarose gel. Bands of expected sizes ranging between approximately 600 and 750 bp were observed for the potential clones representing insertion of gene of interest (Figure 6.4). Should ligation have been unsuccessful, the M13 primers would have amplified a sequence comprising of only 114 bp. PCR product sizes were estimated using the molecular weight analysis tool in Image Lab 5.2.1 (BIO-RAD). Following the sequencing of potential clones and alignment of results with the appropriate sequences from the Pseudomonas Genome Database it was clear that no point mutations had occurred during the cloning process and successful clones had been obtained (data shown in APPENDIX VII).

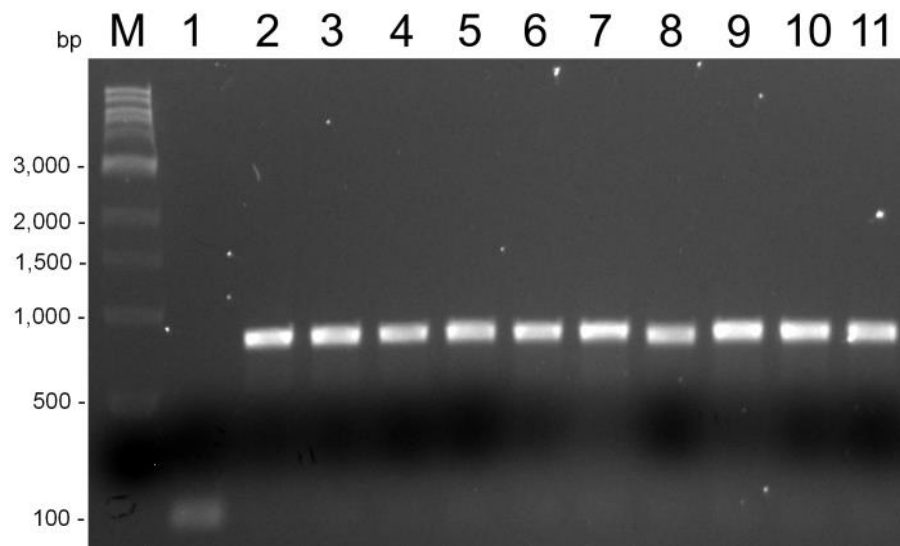


Figure 6.4 *E. coli* JM109 transformed with pUCP24 ligated with the azoreductase-like genes

1% w/v agarose gels showing the PCR products from transformant colonies amplified using M13 primers. PCR products displayed represent the negative control pUCP24 (lane 1), pUCP24::*pa0785* (lanes 2-4), pUCP24::*pa3223* (lanes 5-7) and pUCP24::*pa0949* (lanes 8-11). 1 Kb plus DNA ladder was used as standard (lane M).

6.2.1.4 Transformation into *P. aeruginosa* PAO1 transposon insertion mutant strains

Following confirmation of successful cloning by PCR and sequencing, plasmid extractions were performed on overnight cultures of positive clones for each strain. Following the preparation of chemically competent cells for each *P. aeruginosa* PAO1 gene deletion mutant, PCR was carried out on each strain using the appropriate primers for each gene deletion (Table 2.16) to confirm the presence of the transposon insertion. The same reactions were also carried out on the wild type strain to confirm amplification of the genes of interest and thus compare the wild type vs. the knockout. Upon analysis on 1% w/v agarose gel it was clear that the transposon insertion was present in each competent gene deletion mutant (Figure 6.5). Following this confirmation, heat shock transformations were carried out to insert pUCP24 containing each azoreductase-like sequence into the appropriate mutant strain. Empty pUCP24 was also transformed into each mutant strain so as to create a negative control to be used later in the MIC assays. PCR was carried out on each transformant using the M13 primers. This would enable screening for strains containing both the cloned plasmids and the empty plasmids. Upon observation on 1% w/v agarose gel, bands of appropriate sizes were to be seen for each transformant confirming successful generation of complemented strains for each azoreductase-like gene deletion mutant (Figure 6.6 **a** and **b**, APPENDIX III). PCR product sizes were estimated using the molecular weight analysis tool in Image Lab 5.2.1 (BIO-RAD).

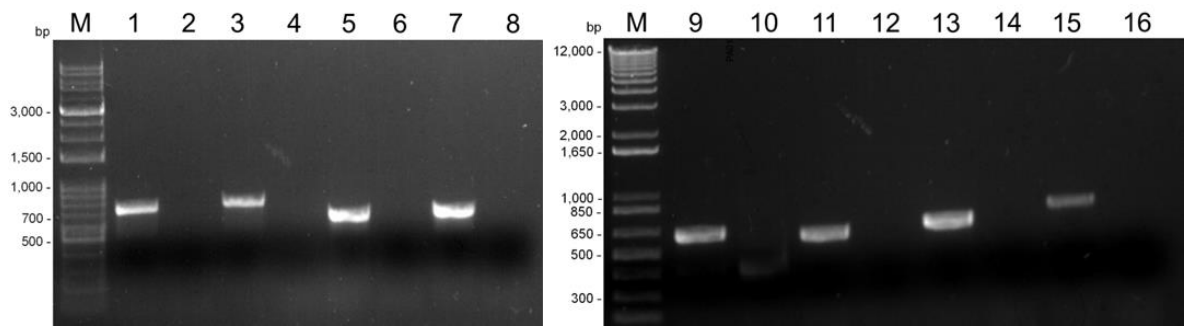


Figure 6.5 *P. aeruginosa* PAO1 single gene transposon insertion mutants confirmation in competent cells

1% w/v agarose gels showing the azoreductase-like genes amplified from colonies of chemically competent *P. aeruginosa* PAO1 WT and the single gene transposon mutants (TrM). Amplification of the azoreductase-like genes is only apparent in the reactions performed on the WT strain. Lanes displayed represent 1 Kb Plus DNA ladder (lanes M), *pa0785* WT (lane 1), *pa0785* TrM (lane 2), *pa1962* WT (lane 3), *pa1962* TrM (lane 4), *pa3223* WT (lane 5), *pa3223* TrM (lane 6), *pa2280* WT (lane 7), *pa2280* TrM (lane 8), *pa2580* WT (lane 9), *pa2580* TrM (lane 10), *pa1204* WT (lane 11), *pa1204* TrM (lane 12), *pa0949* WT (lane 13), *pa0949* TrM (lane 14), *pa4975* WT (lane 15) and *pa4975* TrM (lane 16).

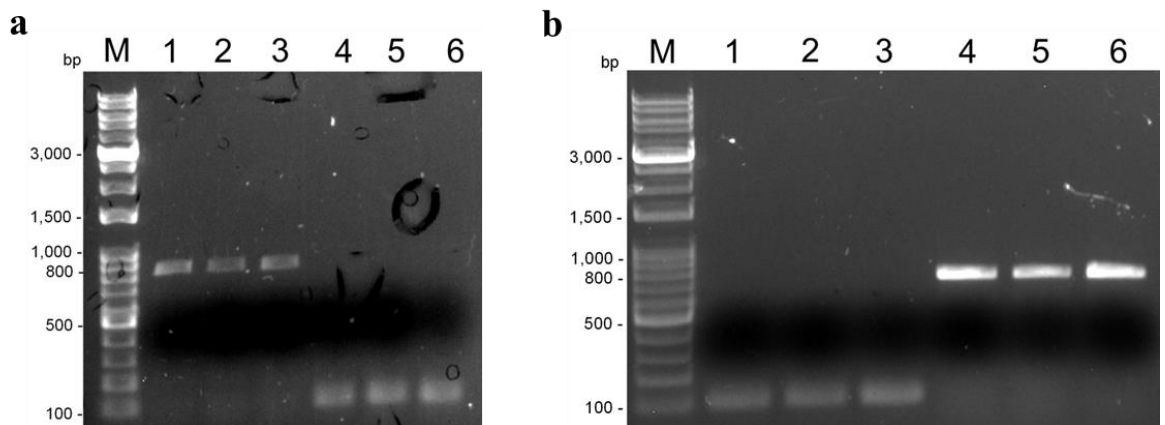


Figure 6.6 *P. aeruginosa* PAO1 single gene transposon insertion mutants transformed with pUCP24

1% w/v agarose gels showing the PCR products for pUCP24 amplified using M13 primers. PCR products are displayed representing pUCP24::*pa2280* (lanes 1-3) and pUCP24 (lanes 4-6) transformed into *P. aeruginosa* PAO1 $\Delta 2280$. PCR products were estimated at 804 bp for pUCP24::*pa2280* (869 bp actual size) and 142 bp for pUCP24 (114 bp actual size) (a). PCR products are displayed representing pUCP24 (lanes 1-3) and pUCP24::*pa2580* (lanes 4-6) transformed into *P. aeruginosa* PAO1 $\Delta 2580$. PCR products were estimated at 802 bp for pUCP24::*pa2580* (736 bp actual size) and 120 bp for pUCP24 (114 bp actual size) (b). 1 Kb plus DNA ladder was used as standard for each gel (lane M).

6.2.2 Confirmation of gene expression in the complemented strains

To confirm the expression of the gene of interest in each complemented strain, and also the lack of gene expression in the controls containing the empty vector, RNA extraction was performed on cultures in the exponential phase of each gene deletion mutant containing empty pUCP24 and its corresponding complemented strain. On column DNase digestion was carried out and was essential so as to remove any residual genomic DNA which would interfere with the results of the RT-PCR. RNA extraction was deemed successful by examination on 1% w/v agarose gel when a characteristic double band was to be seen (Figure 6.7, APPENDIX IV). Following cDNA synthesis, PCR was carried out on each sample using the appropriate primers designed to amplify within the coding region of the gene in question. Upon observation on 1% w/v agarose gel it was apparent that the relevant genes were being expressed in the complemented strains but not in the negative controls (Figure 6.8). The single band representing the positive control, housekeeping gene *rpoD* (APPENDIX V), confirmed that RNA extraction and cDNA synthesis had been successful thus the data here verifies that the complemented strains generated in this chapter were a reliable means to examine the phenotypic effects of the gene in question in relation to antibiotic susceptibility.

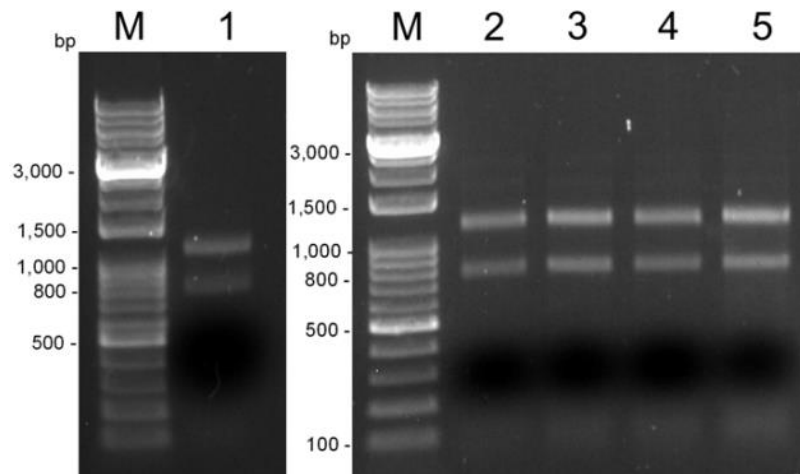


Figure 6.7 Total RNA extracted from *P. aeruginosa* PAO1 strains

1% w/v agarose gels showing the RNA extracted from *P. aeruginosa* PAO1 WT, knockout strains containing empty pUCP24 (KO) and complemented strains (Comp). Extraction was performed on liquid cultures in the exponential phase using the RNeasy Mini Kit (Qiagen). Bands displayed depict RNA from PAO1 WT (lane 1), *pa1962* KO (lane 2), *pa1962* Comp (lane 3), *pa2580* KO (lane 4) and *pa2580* Comp (lane 6). 1 Kb plus DNA ladder was used as standard for each gel (lanes M).

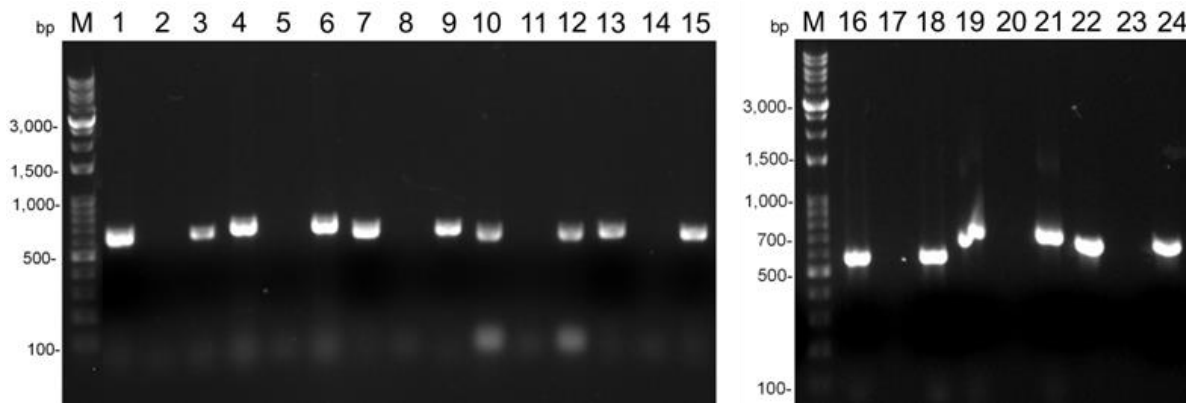


Figure 6.8 Gene expression of *P. aeruginosa* PAO1 WT, gene deletion mutants transformed with pUCP24 and the complemented strains

1% w/v agarose gels showing PCR products where cDNA synthesised from extracted total RNA was used as a template. PCR was performed on cDNA from *P. aeruginosa* PAO1 WT, each knockout strain containing empty pUCP24 (KO) and each complemented strain using primers specific for the coding region of each azoreductase-like gene (Comp). Products displayed are 1 Kb Plus DNA ladder (lanes M), *pa1962* WT (lane 1), *pa1962* KO (lane 2), *pa1962* Comp (lane 3), *pa3223* WT (lane 4), *pa3223* KO (lane 5), *pa3223* Comp (lane 6), *pa2580* WT (lane 7), *pa2580* KO (lane 8), *pa2580* Comp (lane 9), *pa1204* WT (lane 10), *pa1204* KO (lane 11), *pa1204* Comp (lane 12), *pa0949* WT (lane 13), *pa0949* KO (lane 14), *pa0949* Comp (lane 15), *pa0785* WT (lane 16), *pa0785* KO (lane 17), *pa0785* Comp (lane 18), *pa2280* WT (lane 19), *pa2280* KO (lane 20), *pa2280* Comp (lane 21), *pa4975* WT (lane 22), *pa4975* KO (lane 23) and *pa4975* Comp (lane 24).

6.2.3 Phenotypic analysis of *P. aeruginosa* PAO1 and TBCF 10839 strains

For convenience, '*P. aeruginosa* PAO1 strains' refers to wild type *P. aeruginosa* PAO1, each azoreductase-like gene transposon mutant obtained from the Manoil laboratory transformed with the pUCP24 vector and each transposon mutant complemented with the pUCP24 vector containing the knocked out gene. '*P. aeruginosa* TBCF 10839 strains' refers to wild type *P. aeruginosa* TBCF 10839, *P. aeruginosa* TBCF 10839 $\Delta pa0785$, *P. aeruginosa* TBCF 10839 $\Delta pa0785$ -pUCP20::*pa0785* and *P. aeruginosa* TBCF 10839 $\Delta pa0785$ -pUCP20::*pa0785-0787*.

6.2.3.1 Growth analysis of *P. aeruginosa* PAO1 strains along with *P. aeruginosa* TBCF 10839 strains

Analysis of planktonic growth was performed on all *P. aeruginosa* PAO1 strains (Figure 6.9). The results show that no significant growth difference compared to the wild type was apparent after a period of 20 hours ($p > 0.05$). After seven hours of growth, all strains, with the exception of the wild type and the transposon insertion mutant transformed with pUCP24::*paI204*, had entered the stationary phase with the other two entering the stationary phase at the eight hour time point. There was no significant difference in cell density amongst strains after seven or eight hours of growth ($p > 0.05$). This data indicates that the transposon insertion along with the inclusion of the pUCP24 vector does not affect the growth of *P. aeruginosa* PAO1.

For all *P. aeruginosa* TBCF 10839 strains the cultures reached the stationary phase after 6 hours (Figure 6.10). There was no significant difference between the wild type and the genetically modified strains ($p > 0.05$) indicating that the genetic adaptations do not alter bacterial growth rate.

All of the statistical analysis presented here was carried out using a one-way ANOVA.

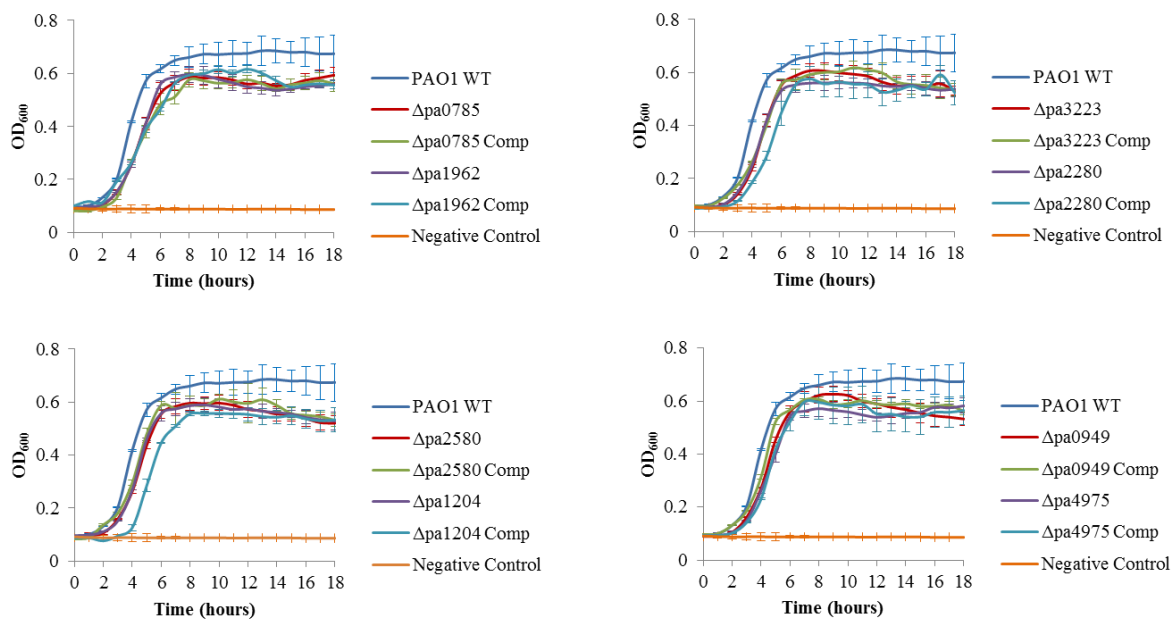


Figure 6.9 Growth analysis *P. aeruginosa* PAO1 strains

Graph showing the growth curves of all *P. aeruginosa* PAO1 strains at 37°C in MH broth (supplemented with 10 µg/mL gentamicin for all samples with the exception of the WT). Strains tested include the wild type (WT), the transposon insertion mutants containing pUCP24 ($\Delta paAzoR$) and the complemented strains ($\Delta paAzoR$ Comp). There was no significant difference observed in the growth rates between strains. All strains were grown in triplicate in 96-well plates for 18 hours in an Infinite M200 PRO plate reader. Uninoculated broth was used as a negative control. Error bars represent standard deviation (n=3).

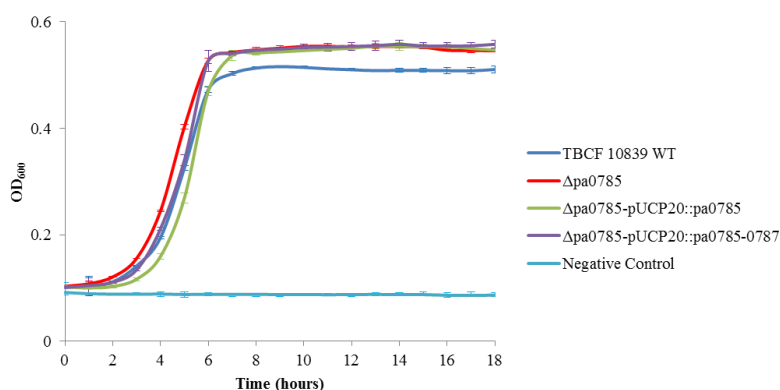


Figure 6.10 Growth analysis *P. aeruginosa* TBCF 10839 strains

Graph showing the growth curves of all *P. aeruginosa* TBCF 10839 strains at 37°C in MH broth. There was no significant difference observed in the growth rates between strains. All strains were grown in triplicate in 96-well plates for 18 hours in an Infinite M200 PRO plate reader. Uninoculated broth was used as a negative control. Error bars represent standard deviation (n=3).

6.2.3.2 Comparison of CFU/mL of all *P. aeruginosa* PAO1 strains and all *P. aeruginosa* TBCF strains

The value for CFU/mL for *P. aeruginosa* PAO1 was calculated and compared against the values found for all of the knockout strains containing pUCP24 and their corresponding complemented strains. The same process was executed for all *P. aeruginosa* TBCF 10839 strains. All values are listed in Table 6.4. These results indicate that cell size is not greatly affected by the genetic modifications across strains and obtaining readings at OD₆₀₀ is an accurate way to compare cell density.

Table 6.4 CFU/mL for all *P. aeruginosa* strains

Overnight liquid cultures of all *P. aeruginosa* strains were standardised to OD₆₀₀ 0.02 and serial dilutions ranging from 10⁻¹ to 10⁻⁷ were prepared for each sample. 5 µL of each dilution was dropped onto LB agar. Drops containing 20-200 colonies were counted and used to determine CFU/mL for each strain. The results listed here indicate that cell size is not greatly affected by the genetic modifications. All experiments were performed in triplicate.

Strain	Modification	CFU/ mL
<i>P. aeruginosa</i> PAO1	Wild Type	6.4±0.7 × 10 ⁷
	Δ <i>pa0785</i> -pUCP24	5.3±0.2 × 10 ⁷
	Δ <i>pa0785</i> -pUCP24:: <i>pa0785</i>	6.1±0.4 × 10 ⁷
	Δ <i>pa1962</i> -pUCP24	6.6±0.5 × 10 ⁷
	Δ <i>pa1962</i> -pUCP24:: <i>pa1962</i>	7.5±0.2 × 10 ⁷
	Δ <i>pa3223</i> -pUCP24	7.2±0.3 × 10 ⁷
	Δ <i>pa3223</i> -pUCP24:: <i>pa3223</i>	5.6±0.3 × 10 ⁷
	Δ <i>pa2280</i> -pUCP24	6.5±0.3 × 10 ⁷
	Δ <i>pa2280</i> -pUCP24:: <i>pa2280</i>	7.3±0.7 × 10 ⁷
	Δ <i>pa2580</i> -pUCP24	6.1±0.4 × 10 ⁷
	Δ <i>pa2580</i> -pUCP24:: <i>pa2580</i>	7.5±0.3 × 10 ⁷
	Δ <i>pa1204</i> -pUCP24	6.2±0.6 × 10 ⁷
	Δ <i>pa1204</i> -pUCP24:: <i>pa1204</i>	6.4±0.2 × 10 ⁷
	Δ <i>pa0949</i> -pUCP24	6.2±0.2 × 10 ⁷
	Δ <i>pa0949</i> -pUCP24:: <i>pa0949</i>	7.3±0.3 × 10 ⁷
	Δ <i>pa4975</i> -pUCP24	6.5±0.5 × 10 ⁷
Δ <i>pa4975</i> -pUCP24:: <i>pa4975</i>	6.9±0.3 × 10 ⁷	
<i>P. aeruginosa</i> TBCF 10839	Wild Type	7.1±0.8 × 10 ⁷
	Δ <i>pa0785</i>	7.4±0.6 × 10 ⁷
	Δ <i>pa0785</i> -pUCP20:: <i>pa0785</i>	7.3±0.8 × 10 ⁷
	Δ <i>pa0785</i> -pUCP20:: <i>pa0785-0787</i>	6.5±0.2 × 10 ⁷

6.2.3.3 Minimum Inhibitory Concentration

The antibiotic sensitivity was tested for all *P. aeruginosa* PAO1 strains and all *P. aeruginosa* TBCF 10839 strains by determining the MIC for each strain against a range of antibiotics. The antibiotics trialled in this section were selected based on previous data (Crescente, 2015) where it was noted that the MIC of azoreductase-like gene deletion mutants tended to differ from that of the wild type, thus indicating that these genes may be involved in antibiotic susceptibility. To confirm this idea, it was necessary to examine whether the addition of the knocked out gene back into the bacteria would result in reversion to the wild type phenotype.

The results gathered show that in most cases different MIC values were obtained for the wild type strains compared to their genetically modified counterparts and are listed in Table 6.5 and 6.6. In the presence of the fluoroquinolones (ciprofloxacin, levofloxacin, sparfloxacin and prulifloxacin) and naladixic acid, the wild type for both *P. aeruginosa* PAO1 and *P. aeruginosa* TBCF 10839 were more resistant to the antibiotics than any of the genetically manipulated strains. It is important to note however, that the complemented strains exhibited an MIC value comparable to that of the relevant knock outs rather than the wild type. For the *P. aeruginosa* TBCF 10839 strains, the MIC result for ceftiazidime and amikacin were constant at 8 µg/mL and 2 µg/mL respectively. For *P. aeruginosa* PAO1 strains, the MIC of amikacin was either the same as that for the wild type or two fold higher with the exception of *P. aeruginosa* PAO1 $\Delta pa0785$ -pUCP24::*pa0785* where the MIC was half that of the wild type. With ceftiazidime, a similar trend was seen where all strains containing the pUCP24 plasmid had a lower sensitivity to the antibiotic than the wild type. Upon culturing of the *P. aeruginosa* PAO1 strains in colistin, the majority had the same MIC as the wild type. Of those that did not, the MIC was lower but no pattern regarding whether the strains included the azoreductase gene or not was apparent. Regarding growth inhibition of the *P. aeruginosa* TBCF 10839 strains with colistin, the paAzoR1 knockout had a MIC four fold lower than that of the wild type while the strain complemented with the paAzoR1 gene did indeed mirror that of the wild type. The strain complemented with the full operon, *pa0785-0787*, had a two fold higher MIC than the paAzoR1 knock out however it still remained lower than that of the wild type.

Table 6.5 Minimum inhibitory concentration values (in µg/mL) for a range of antimicrobial agents against *P. aeruginosa* PAO1 strains

Table showing the MIC values for all antibiotics tested against *P. aeruginosa* PAO1 wild type (WT), the transposon insertion mutants containing pUCP24 ($\Delta paAzoR$) and the complemented strains ($\Delta paAzoR$ Comp). Although differences in sensitivity were seen when the azoreductase-like gene deletion mutants were compared to the wild type, reversion to the wild type phenotype was not apparent upon complementation with the gene of interest. MICs were determined using the microdilution method in 96-well plates. Each experiment was carried out in triplicate.

Antibiotic Class	Antibiotic	WT	$\Delta pa0785$	$\Delta pa0785$ Comp	$\Delta pa1962$	$\Delta pa1962$ Comp	$\Delta pa3223$	$\Delta pa3223$ Comp	$\Delta pa2280$	$\Delta pa2280$ Comp
Fluoroquinolones	Ciprofloxacin	1	0.125	0.0625	0.125	0.125	0.125	0.25	0.125	0.125
	Levofloxacin	8	1	0.5	1	1	1	1	1	1
	Naladixic Acid	1000	125	125	250	250	500	250	250	250
	Sparfloxacin	8	2	1	2	2	2	2	2	2
	Prulifloxacin	4	0.125	0.125	0.125	0.125	0.125	0.125	0.125	0.125
β-lactams	Ceftiazidime	2	4	4	4	4	8	8	4	4
Aminoglycosides	Amikacin	2	4	1	4	4	4	4	2	2
Polymyxins	Colistin	4	4	2	4	4	2	4	4	2

Antibiotic Class	Antibiotic	WT	$\Delta pa2580$	$\Delta pa2580$ Comp	$\Delta pa1204$	$\Delta pa1204$ Comp	$\Delta pa0949$	$\Delta pa0949$ Comp	$\Delta pa4975$	$\Delta pa4975$ Comp
Fluoroquinolones	Ciprofloxacin	1	0.125	0.125	0.25	0.125	0.125	0.125	0.25	0.125
	Levofloxacin	8	1	0.5	1	0.5	1	1	1	1
	Naladixic Acid	1000	125	500	250	250	125	125	125	125
	Sparfloxacin	8	2	2	4	2	2	2	2	2
	Prulifloxacin	4	0.125	0.125	0.125	0.125	0.125	0.125	0.125	0.25
β-lactams	Ceftiazidime	2	4	4	8	8	4	4	4	4
Aminoglycosides	Amikacin	2	4	4	4	4	2	2	4	4
Polymyxins	Colistin	4	4	4	2	4	4	2	4	4

Table 6.6 Minimum inhibitory concentration values (in $\mu\text{g/mL}$) for a range of antimicrobial agents against *P. aeruginosa* TBCF 10839 strains

Table showing the MIC values for all antibiotics tested against *P. aeruginosa* TBCF 10839 wild type (WT), the azoreductase knockout ($\Delta 0785$) and the strains complemented with the gene of interest ($\Delta pa0785$ -pUCP20::*pa0785*) and the operon containing the gene of interest ($\Delta pa0785$ -pUCP20::*pa0785-0787*). Although differences in sensitivity were seen when the *pa0785* mutants were compared to the wild type, reversion to the wild type phenotype was not apparent upon complementation with the gene of interest or with the full operon encoding the gene of interest. MICs were determined using the microdilution method in 96-well plates. Each experiment was carried out in triplicate.

Antibiotic Class	Antibiotic	WT	$\Delta pa0785$	$\Delta pa0785$ - pUCP20:: <i>pa0785</i>	$\Delta pa0785$ - pUCP20:: <i>pa0785-0787</i>
Fluoroquinolones	Ciprofloxacin	1	0.5	0.25	0.5
	Levofloxacin	4	2	1	2
	Naladixic Acid	500	250	250	500
	Sparfloxacin	4	4	2	4
	Prulifloxacin	8	1	2	2
β-lactams	Ceftiazidime	8	8	8	8
Aminoglycosides	Amikacin	2	2	2	2
Polymyxins	Colistin	32	8	32	16

6.3 Discussion

The aims of this chapter as laid out in section 1.3 have been met as follows:

- i. Complemented strains of *P. aeruginosa* PAO1 azoreductase-like gene deletion mutants were generated and the gene insertion confirmed via PCR and DNA sequencing.
- ii. The relevant genes were successfully expressed in all of the complemented strains. This was confirmed by RT-PCR. The same method was also used to observe non-expression of the knocked out gene in the appropriate strains.
- iii. Any relevant difference in cell size amongst all strains in question including the *P. aeruginosa* PAO1 strains and *P. aeruginosa* TBCF 10839 strains was ruled out by determining CFU/mL. This ensured that the OD₆₀₀ reading was a suitable method of standardising bacterial concentration.
- iv. Growth rate analysis of all *P. aeruginosa* PAO1 strains and all *P. aeruginosa* TBCF 10839 strains confirmed that there was no significant effect on growth of the genetically modified strains meaning that MIC assays could be carried out without having to alter incubation times for particular strains.
- v. MICs for all *P. aeruginosa* PAO1 and *P. aeruginosa* TBCF 10839 strains were determined for a range of antibiotics so antibiotic susceptibility between the wild type and the knock out and complemented strains could be compared. While differences in susceptibility were noted between the azoreductase-like gene deletion mutants and the wild type strains, they did not revert to the wild type phenotype upon reintroduction of the gene of interest.

P. aeruginosa, specifically MDR strains, have been labelled a 'serious threat' by the Centre for Disease Control with approximately 13% of severe healthcare-associated infections unsusceptible to several classes of antibiotics (CDC, 2013). Recent trends have shown an increase in strains resistant to aminoglycosides, β -lactams and fluoroquinolones as the cause of nosocomial pneumonia (Zilberberg and Shorr, 2013, Sievert *et al.*, 2013). With the current therapeutics increasingly less effective, there is an urgent need for novel targets for antimicrobial chemotherapy.

To further expand the study of the physiological role of azoreductases and azoreductase-like genes in *P. aeruginosa* PAO1, a library of knockout strains complemented with the

appropriate gene was successfully generated using molecular cloning. The gene of interest was inserted under control of the *lacUV5* promoter. As neither *P. aeruginosa* nor the cloning vector possess a *lacI* repressor, the gene of interest was constitutively expressed without any need for induction (Winsor *et al.*, 2016, Olsen *et al.*, 1982, Bagdasarian, 1983). This was confirmed with RT-PCR, a method by which total RNA is extracted from bacterial cultures in the log phase and used as a template for cDNA synthesis upon which PCR is performed using gene-specific primers. Total RNA is a reliable means for monitoring protein expression as it is produced when genes are transcribed from DNA as complementary base pairs which are then transferred to a ribosome for translation to a protein (Clancy, 2008). This procedure proved that the complemented strains were expressing the genes of interest while the knockout strains transformed with the empty vector were not.

The MIC results showed that the transformants containing empty pUCP24 retained the same phenotype of altered sensitivity to the antibiotics tested as the gene deletion mutants lacking the plasmid, indicating that the vector alone was not affecting susceptibility to antibiotics. The absence of any significant changes in growth rates or values for CFU/mL assured that any changes in growth or cell size were not limiting factors in the MIC assays. Upon addition of the plasmids for complementation, the phenotype remained the same as that for the corresponding knockout with no reversion to the wild type apparent whatsoever. Unfortunately this result means that it cannot be said with confidence that it is any of the genes in question specifically that are causing this altered susceptibility.

Unlike the laboratory strain *P. aeruginosa* PAO1, *P. aeruginosa* TBCF 10839 is a clinical isolate which has caused numerous nosocomial outbreaks (Klockgether *et al.*, 2013). Originally detected in a CF lung at a point of critical illness (Tümmler *et al.*, 1991), it is phenotypically different from *P. aeruginosa* PAO1 in relation to quorum sensing, virulence effector protein production and biofilm formation (Rakhimova *et al.*, 2008, Cullen *et al.*, 2015). It is interesting to note is that this current study has shown that this clinical strain has greatly reduced sensitivity to colistin when compared to PAO1 (8 fold increase in MIC). As polymyxins are reserved as a treatment of last resort for MDR gram-negative bacteria, this result further highlights the need for the development of new antibiotics (Lee *et al.*, 2016). The *P. aeruginosa* TBCF 10839 paAzoR1 knockout strain used in this study was generated by insertion of a pTnMOD-OGM mini-Tn5 plasmid and the complemented strains were constructed by addition of an episomal pUCP20 vector cloned with the gene(s) of interest (Rakhimova *et al.*, 2008). Although this gene deletion

and subsequent complementation along with the gene expression were not confirmed in this pilot study, these strains were included here so as to monitor whether the phenotype regarding antibiotic susceptibility was consistent across two different *P. aeruginosa* strains. In addition, it was a means to observe whether the effects of azoreductase gene deletion stayed the same when a different method of knocking out the gene(s) of interest was implemented. Interestingly, like the *P. aeruginosa* PAO1 strains, the antimicrobial sensitivity was altered upon deletion of the azoreductase genes and the phenotype for the most part remained unchanged upon complementation with the knocked out gene. This similarity amongst strains is indicative that although we do not see reversion to the wild type upon complementation, it is important not to rule out these genes as participants in the determination of antimicrobial susceptibility.

The results obtained in this chapter where almost identical antibiotic susceptibility patterns for the gene deletion and complemented strains (in both *P. aeruginosa* PAO1 and *P. aeruginosa* TBCF 10839) are seen correlate to the findings of Ling *et al.* (2012) where overexpression and deletion of *azoR* in *E. coli* exhibited the same result of decreased sensitivity to aminoglycosides. This effect was not exclusive to *azoR* and was also noted in other unrelated genes including *hyfA* (probable electron transfer protein), *lpdA* (a lipoamide dehydrogenase), *paaD* (putative phenylacetate-CoA oxygenase subunit) and *yeyG* (hypothetical protein) (Andrews *et al.*, 1997, Stephens *et al.*, 1983, Karp *et al.*, 2014). Overexpression of a wild type gene product can sometimes cause a mutant phenotype (Prelich, 2012). Evidences of such an effect have been documented in the yeast *Saccharomyces cerevisiae* where overexpression of regulatory proteins mirrors the phenotype of the strain when the gene encoding for the protein in question is knocked out. For example, overexpression of MIF1, implicated in mitotic chromosome transmission, results in increased frequency of chromosome loss, a consequence also apparent in the *MIF1* mutant strain (Meeks-Wagner *et al.*, 1986). Another regulatory protein in the same species encoded by *SPT5*, when overexpressed or indeed under expressed, exhibits the same altered transcription of several genes as the *SPT5* deletion mutant (Swanson *et al.*, 1991). These genes all function as part of multiprotein complexes insinuating that this phenomenon may be due to disrupting protein stoichiometry which subsequently interferes with the overall function. It could thus be tempting to suggest that the observed phenotypic effects of gene deletion and subsequent complementation in this current study may be attributed to a precise level of gene expression which is crucial to gene function whereby any deviation from this may have a detrimental effect on the overall role. It is important to

note however, that the aforementioned evidence is derived from eukaryotic cells and thus cannot be directly applied to bacteria so without extensive further research into this idea, it must remain simply as speculation.

In order to control the expression levels of the complemented genes so that they replicate those of the wild type a different method of complementation could be applied. As previously stated, all complemented genes were expressed under control of the *lacUV5* promoter (Olsen *et al.*, 1982). As this is a promoter derived from the *lac* promoter native to *E. coli* and is often used in expression systems in molecular biology it is highly likely that the genes of interest are not being expressed at identical rates as they would be under the control of their native promoter (Rosano and Ceccarelli, 2014). Also, as pUCP24 is a high copy number plasmid with 500-700 copies per cell, overexpression of the gene(s) of interest is most probable (Minton, 1984). A means of troubleshooting this would be to reinsert the gene of interest back into the chromosome. This could be achieved by using a mini-Tn7 system whereby the appropriate gene sequence would be cloned into a mini-Tn7 vector. When transformed along with a helper plasmid encoding the Tn7 site-specific transposition pathway the gene of interest would be successfully integrated back into the chromosomal genome and expression levels should simulate those of the wild type (Choi and Schweizer, 2006). It is important to note however that this system would not circumvent the issue of the lost native promoter. Ideally the gene of interest would be cloned into the mini-Tn7 vector along with its native promoter however identification of each specific promoter sequence would require an extensive bioinformatics study beyond the scope of this investigation. Following utilisation of the mini-Tn7 system, quantitative real time-PCR could be performed on the wild type and the complemented strain. Assuming expression levels were interchangeable, MIC results obtained from this method could give definitive answers as to whether or not these genes play a role in antibiotic sensitivity.

The process applied by the Manoil laboratory to knock out the azoreductase-like genes involves adding a tetracycline resistance (*tet*) cassette so as to select for the transposon insertion mutants (Jacobs *et al.*, 2003). As the resistance conferred here involves efflux pump activity (Allard and Bertrand, 1992, de Lorenzo *et al.*, 1990), there is a possibility that this may affect the MIC data gathered for these strains, although debatable given that the *P. aeruginosa* TBCF 10839 paAzoR1 knockout was created using a different method and no resistance cassette is left in the mutant strain (Rakhimova *et al.*, 2008), yet the same result was still apparent. The pCRE vector, a derivative of pUT which carries the *cre* gene

from pRH133, can excise the sequences situated between the *loxP* sites in the transposon (which includes *tet*) via cre-mediated recombination (Jacobs *et al.*, 2003, Manoil, 2000). Thus, transformation of these strains with the pCRE vector prior to complementation would remove this resistance cassette and eliminate any possible likelihood that this resistance determinant is altering the MIC results.

The data presented in this chapter presents more questions as opposed to answers. From these pilot results alone a conclusive result cannot be derived concerning whether or not the azoreductases and azoreductase-like genes play a key role in antibiotic sensitivity in *P. aeruginosa*. However based on previous literature and the fact that the phenotype observed here is conserved across two strains it would be beneficial to conduct a further extensive study involving the approaches listed above in order to further investigate this potential involvement.

Chapter 7 Conclusions

The aims of the work presented in this thesis were developed to improve understanding of azoreductases and NQOs in *P. aeruginosa* PAO1. Investigating the role of these genes and their products was in turn, directed towards gaining insight as to whether these genes may serve as suitable novel targets for antimicrobial chemotherapy. In the following sections, each aim as stated in section 1.3 will be addressed.

7.1 Cloning of putative *P. aeruginosa* PAO1 azoreductase genes

The cloning of two putative azoreductase genes is described in Chapter 3. Ryan *et al.* (2014) proposed that azoreductases and NQOs in *P. aeruginosa* form a superfamily which is more extensive than previously thought with that particular study suggesting there are at least ten in the *P. aeruginosa* PAO1 genome (*pa0785*, *pa1962*, *pa3223*, *pa2280*, *pa2580*, *pa1204*, *pa0949*, *pa4975*, *pa1224*, *pa1225*). Eight of these have previously been cloned by Wang *et al.* (2007), Ryan *et al.* (2010b) and Crescente (2015). The cloning of the final two, *pa1224* and *pa1225* is discussed in Chapter 3. Briefly, these genes were cloned into pET-28b and the constructs transformed into *E. coli* JM109 and BL21 strains. Positive clones were screened via PCR of individual colonies and confirmed by sequencing. The cloned genes were shown to correspond precisely with the published gene sequences as listed on the Pseudomonas Genome Database (Winsor *et al.*, 2011).

7.2 Production and purification of suspected *P. aeruginosa* PAO1 azoreductase enzymes as recombinant proteins

The expression and purification of PA1224, PA1225 and PA4975 is described in Chapter 3. Production and purification of the other seven azoreductases and NQOs from *P. aeruginosa* PAO1 has previously been completed by Wang *et al.* (2007), Ryan *et al.* (2010b) and Crescente *et al.* (2016). Overexpression of *pa1224*, *pa1225* and *pa4975* was achieved by inducing the *lacUV5* promoter with IPTG.

Following expression, proteins were extracted and purified using Ni-NTA (IMAC). The expression method required adaption for each protein implying that, unlike other azoreductase-like enzymes in *P. aeruginosa*, they are not all expressed by *E. coli* in the same way. Adding to this, a relatively large range in the amount of soluble protein gained was apparent (4–25 mg/L of culture compared to 30–40 mg/L for the other azoreductases).

7.3 Biochemical and enzymatic analysis of proposed *P. aeruginosa* PAO1 azoreductase and NQO recombinant proteins

In chapter 4, biochemical and enzymatic characterisation of PA1224, PA1225 and PA4975 is described. The presence of flavin molecules, selectivity for NAD(P)H and flavin and substrate specificity profiles are determined.

Analysis of the presence of flavin molecules shows that they can be detected via absorption spectra and TLC for PA1224 and PA1225 (FAD in both cases). The purification of PA4975 did not yield adequate soluble protein for these procedures to be completed however it is assumed FAD was incorporated during expression as addition to the enzymatic assays did not significantly affect reduction of ANI. DSF analysis suggested FAD as the cofactor for all three however PA4975 showed higher enzymatic reduction rates with FMN. Due to DSF and evidence in the literature it is likely that FAD is the preferred cofactor.

All enzymes were biochemically active and NADPH was indicated as the preferred reductant for all three enzymes.

Substrate specificity was assessed using a range of azo and quinone compounds. The data obtained showed that all three were capable of catalysing reduction of quinones with the rates comparable to other NQOs from *P. aeruginosa* PAO1. PA1224 was the only enzyme with which azo reduction was observed. The rates of quinone reduction calculated for PA1224 were an order of magnitude higher than those gathered for PA1225 and PA4975 which corresponds with previous azoreductase enzymatic data where evidence of azo reduction is only seen in those with higher rates of quinone reduction (Wang *et al.*, 2007, Crescente, 2015). In this study, the characterisation of PA4975 as initiated by Green *et al.* (2014) has been expanded upon and PA1224 and PA1225 have been characterised for the first time and confirmed as NAD(P)H dependent quinone reductases.

Chapter 5 describes the continued characterisation of PA2280, PA2580, PA1204 and PA0949 as initiated by Crescente (2015) and published in Crescente *et al.* (2016). The TLC analysis completed by Crescente (2015) confirmed FAD as the flavin for which PA2580 and PA1204 are selective and this was reiterated here using DSF analysis. Through enzymatic assays and DSF, FMN was identified as the preferred flavin for PA2280 and PA0949, consistent with the preliminary enzymatic data gathered by Crescente (2015).

The work presented in chapters 3, 4 and 5 paves the way for investigating the effects of inhibitors on this family of enzymes in *P. aeruginosa*. Inhibitors such as β -sultams (Kolb *et al.*, 2014), resveratrol and quercetin have been identified and could be used to further examine these enzymes both biochemically and phenotypically in a bid to gain increased understanding of their biological function.

7.4 Structural determination and analysis of *P. aeruginosa* PAO1 azoreductase and NQO, PA2580

Chapter 5 describes how the crystal structure of PA2580 was solved at 1.3 Å and confirmed as two monomers which form a homodimer with one molecule of FAD bound to each monomer. The active site sits between the two monomers and is similar to other solved azoreductases with the same short flavodoxin-like fold as previously described for other enzymes of the MdaB family. It was found that the nicotinamide binds co-planar with the ring system of FAD in a position which would allow electron transfer to the N5 atom of FAD. This is the first time this structure has been solved and the first time an azoreductase protein structure has been solved with nicotinamide bound thus presenting an opportunity for further expansion on the binding properties of NAD(P)H to azoreductases.

7.5 Analysis of *P. aeruginosa* PAO1 antibiotic resistance using azoreductase and NQO single gene transposon mutants and corresponding complemented strains

Chapter 6 describes the generation of complemented strains of *P. aeruginosa* PAO1 using molecular cloning. The individual knockout strains were confirmed via PCR and the gene insertions of the complemented strains were confirmed via sequencing. All sequences corresponded exactly with those published on the Pseudomonas Genome Database (Winsor *et al.*, 2011). Transcription of inserted genes was observed using RT-PCR and this approach was also implemented to ensure that none of the gene deletion strains were expressing the gene of interest. Although the initial knockout results looked promising with isolates showing increased sensitivity to fluoroquinolones, the complemented strains failed to revert to the wild type. Interesting results were observed by Crescente (2015) where the azoreductase gene deletion mutants appeared to have an involvement in biofilm formation and motility. Now that complemented strains have been generated and

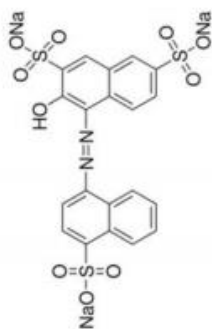
gene transcription has been confirmed, this is currently being further examined by Greg Cooper at Kingston University.

The aims of this thesis have been met as discussed above. The findings presented here add to the current body of knowledge surrounding the extensive and complex genome of *P. aeruginosa* and generates a platform for continued exploration of the physiological role of these enzymes.

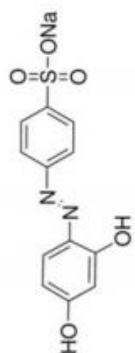
APPENDIX I

Azo compound structures

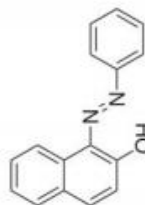
Amaranth



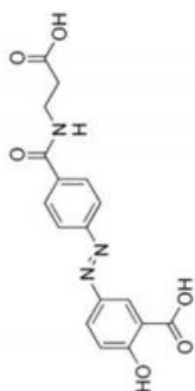
Tropaeolin



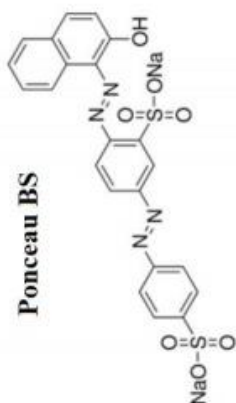
Sudan I



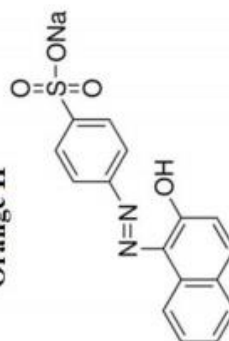
Balsalazide



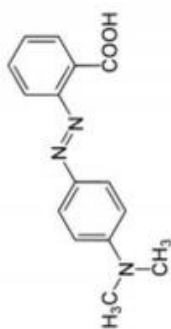
Ponceau BS



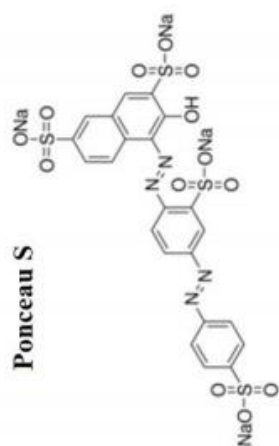
Orange II



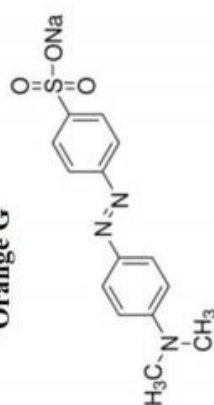
Methyl red



Ponceau S

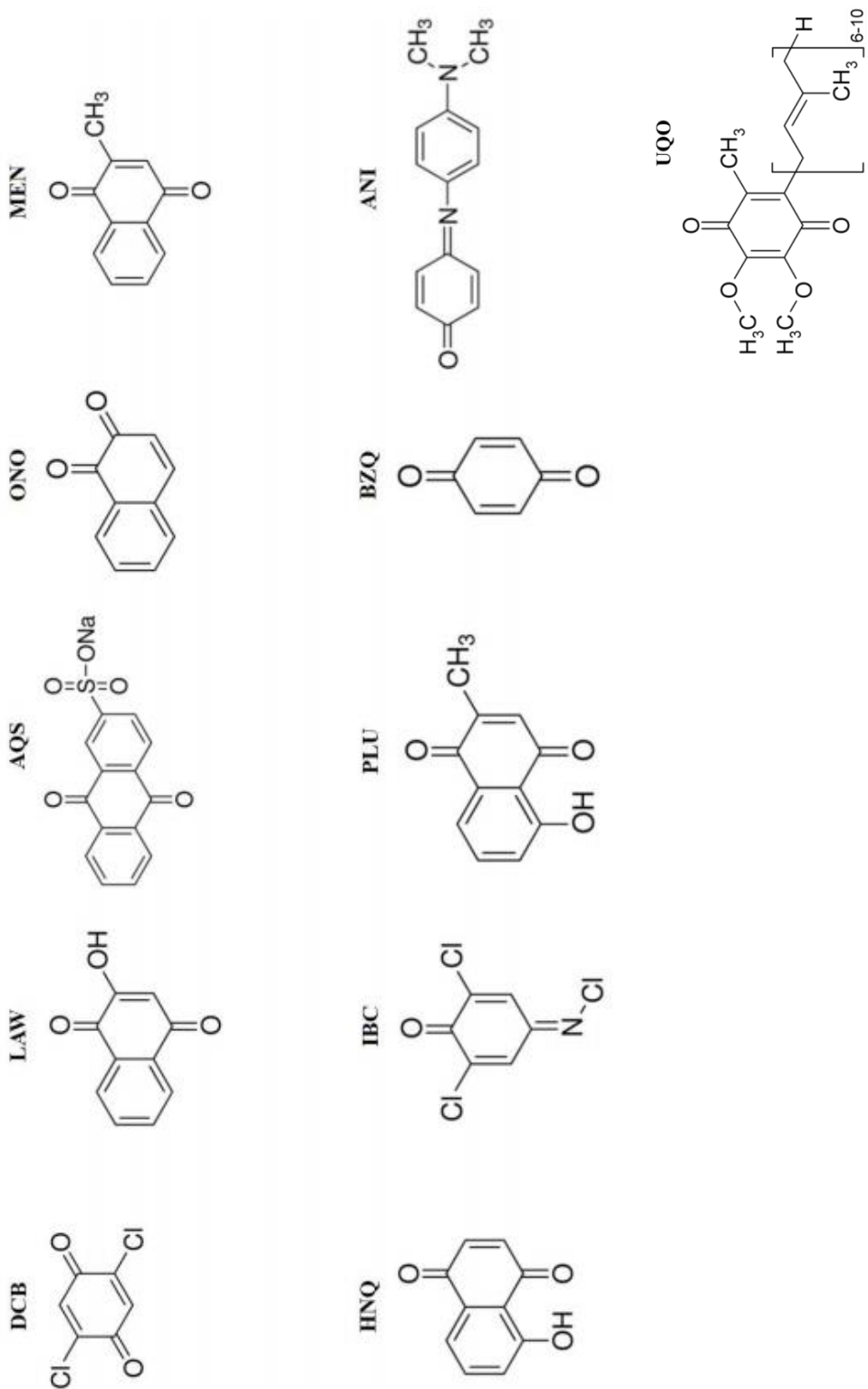


Orange G

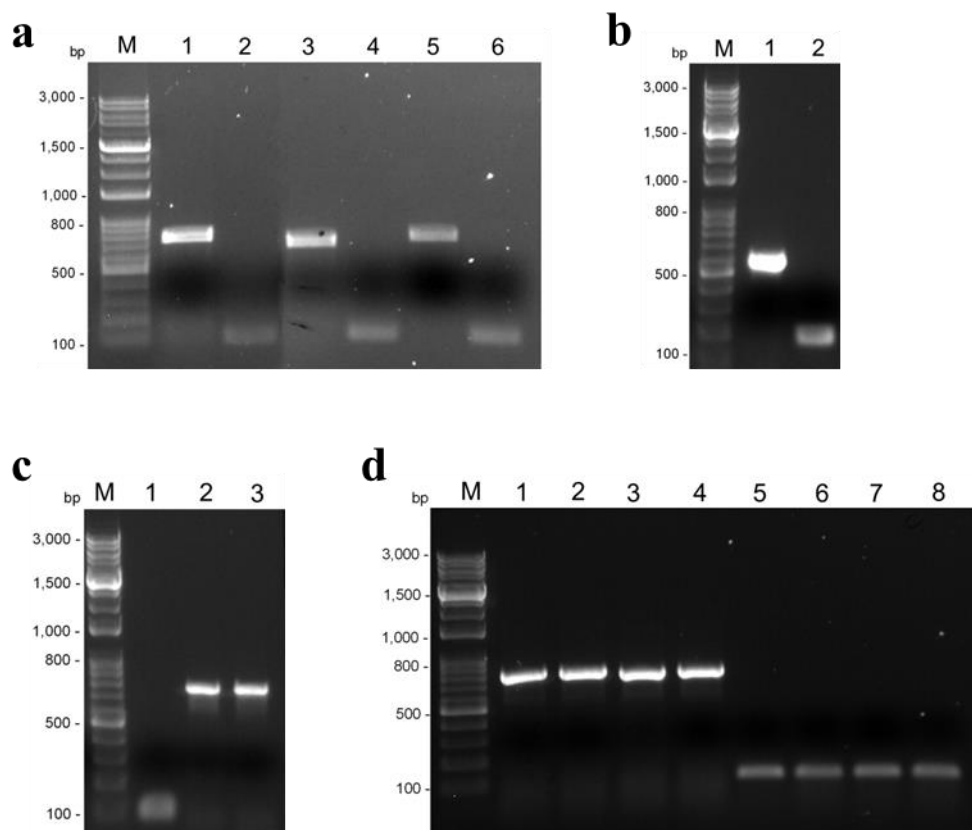


APPENDIX II

Quinone compound structures



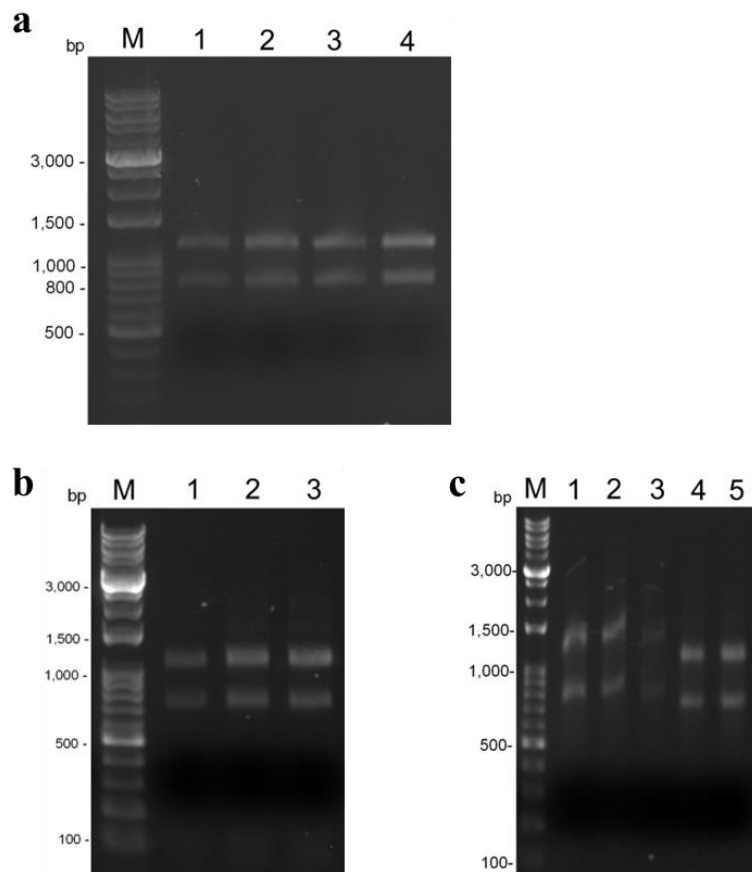
APPENDIX III



***P. aeruginosa* PAO1 single gene transposon insertion mutants transformed with pUCP24**

1% w/v agarose gels showing the PCR products for pUCP24 amplified using M13 primers. PCR products are displayed representing PAO1 $\Delta pa0785$ -pUCP24::*pa0785* (lane 1), PAO1 $\Delta pa0785$ -pUCP24 (lane 2), PAO1 $\Delta pa1204$ -pUCP24::*pa1204* (lane 3), PAO1 $\Delta pa1204$ -pUCP24 (lane 4), PAO1 $\Delta pa0949$ -pUCP24::*pa0949* (lane 5), PAO1 $\Delta pa0949$ -pUCP24 (lane 6) (**a**), PAO1 $\Delta pa3223$ -pUCP24::*pa3223* (lane 1), PAO1 $\Delta pa3223$ -pUCP24 (lane 2) (**b**), PAO1 $\Delta pa4975$ -pUCP24 (lane 1), PAO1 $\Delta pa4975$ -pUCP24::*pa4975* (lanes 2 and 3) (**c**), PAO1 $\Delta pa1962$ -pUCP24::*pa1962* (lanes 1-4), PAO1 $\Delta pa1962$ -pUCP24 (lanes 5-8) (**d**). 1 Kb plus DNA ladder was used as standard for each gel (lanes M).

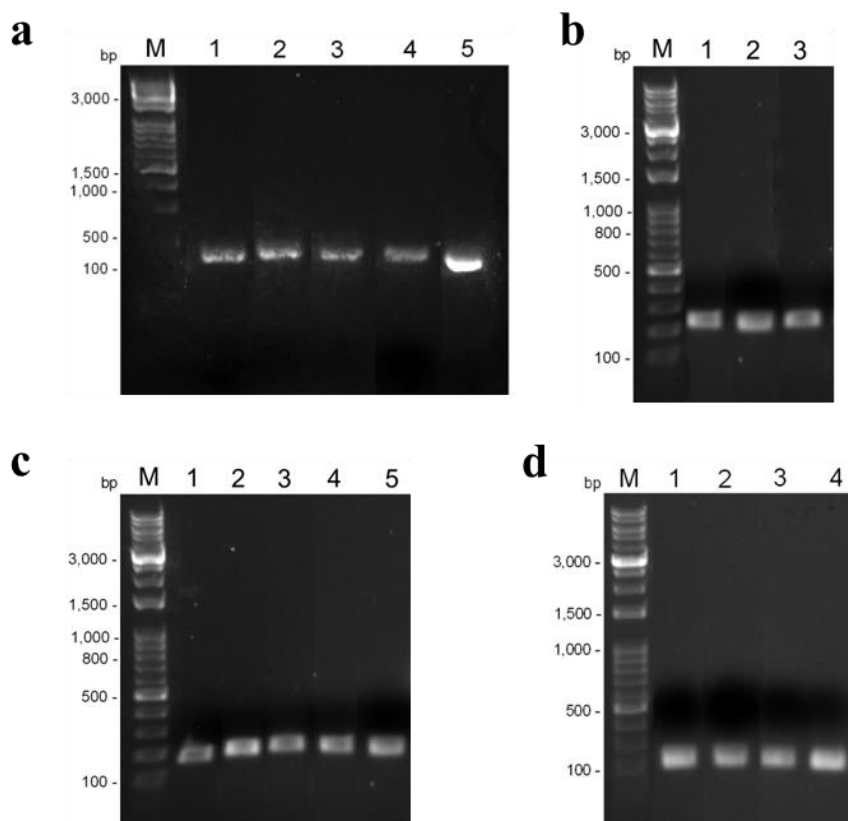
APPENDIX IV



Total RNA extracted from *P. aeruginosa* PAO1 strains.

1% w/v agarose gels showing the total RNA extracted from *P. aeruginosa* PAO1 knockout strains containing empty pUCP24 (KO) and complemented strains (Comp). Extraction was performed on liquid cultures in the exponential phase using the RNeasy Mini Kit (Qiagen). Bands displayed depict RNA from PAO1 *pa0785* KO (lane 1), *pa0785* Comp (lane 2), *pa3223* KO (lane 3), *pa3223* Comp (lane 4) (a), *pa1204* Comp (lane 1) *pa0949* KO (lane 2), *pa0949* Comp (lane 3) (b), *pa1204* KO (lane 1), *pa2280* KO (lane 2), *pa2280* Comp (lane 3), *pa4975* KO (lane 4), *pa4975* Comp (lane 5) (c). 1 Kb plus DNA ladder was used as standard for each gel (lanes M).

APPENDIX V



Positive control for RNA extraction and cDNA synthesis

1% w/v agarose gels showing PCR products where cDNA synthesised from extracted total RNA was used as a template. PCR was performed on cDNA from *P. aeruginosa* PAO1 WT, each knockout strain containing empty pUCP24 (KO) and each complemented strain using primers specific for the house keeping gene, *rpoD*. PCR products displayed are from PAO1 WT (lane 1), *pa1962* KO (lane 2), *pa1962* Comp (lane 3), *pa2580* KO (lane 4), *pa2580* Comp (lane 5) (**a**), *pa1204* Comp (lane 1) *pa0949* KO (lane 2), *pa0949* Comp (lane 3) (**b**), *pa1204* KO (lane 1), *pa2280* KO (lane 2), *pa2280* Comp (lane 3), *pa4975* KO (lane 4), *pa4975* Comp (lane 5) (**c**), *pa0785* KO (lane 1), *pa0785* Comp (lane 2), *pa3223* KO (lane 3), *pa3223* Comp (lane 4) (**d**). 1 Kb plus DNA ladder was used as standard for each gel (lanes M).

APPENDIX VI

Alignment of *pa1224* sequence in pET-28b in *E. coli* JM109 (FWD and REV) against *pa1224* sequence from *P. aeruginosa* PAO1 in the Pseudomonas Genome Database

	5	15	25	35	45
<i>pa1224</i>	-----				
FWD	-----				
REV	AATTGTGAGC	GGATAACAAT	TCCCCTCTAG	AAATAATTTT	GTTTAACTTT

	55	65	75	85	95
<i>pa1224</i>	-----				
FWD	-----				
REV	AAGAAGGAGA	TATACCATGG	GCAGCAGCCA	TCATCATCAT	CATCACAGCA

	105	115	125	135	145
<i>pa1224</i>	-----				
FWD	-----				
REV	GCGGCCTGGT	GCCGCGCGGC	AGCCATATGA	ACGTACTCAT	CGTCTATGCC

	155	165	175	185	195
<i>pa1224</i>	-----				
FWD	-----				
REV	CATCCCGAGC	CGCGCTCCCT	CAACGGTGCG	CTCAAGGACT	TCGCGGTTCG

	205	215	225	235	245
<i>pa1224</i>	-----				
FWD	-----				
REV	CCGCCTCGAG	GCGGCCGGCC	ATGCGGTGCA	GGTTTCGGAC	CTCTACGCGA

	255	265	275	285	295
<i>pa1224</i>	-----				
FWD	-----				
REV	TGGGCTGGAA	GGCCGTGCTC	GATGCCGCGC	ACAGCCTCGA	GCGCGAGGCC

	305	315	325	335	345
<i>pa1224</i>	-----				
FWD	-----				
REV	AGCGAACGCT	TCGATCCTTC	CGCAACTTCC	CTGCGCGCCT	TCGAGAACGG

	355	365	375	385	395
<i>pa1224</i>	-----				
FWD	-----				
REV	TTGGCAGAGC	GTCGACATCG	CCGGTGAGCA	GGACAAGCTG	CGCTGGGCCG

	405	415	425	435	445
<i>pa1224</i>	-----				
FWD	-----				
REV	ATACGCTGAT	CCTGCAATTC	CCGCTCTGGT	GGTTCAGCAT	GCCGGCGATC

	455	465	475	485	495
<i>pa1224</i>	CTCAAGGGTT	GGATCGATCG	CGTCTATGCC	TGCGGCTTCG	CCTACGGGGT
FWD	CTCAAGGGTT	GGATCGATCG	CGTCTATGCC	TGCGGCTTCG	CCTACGGGGT
REV	CTCAAGGGTT	GGATCGATCG	CGTCTATGCC	TGCGGCTTCG	CCTACGGGGT

	505	515	525	535	545
<i>pa1224</i>	CGGCGAACAT	TCCGACAGCC	ACTGGGGCGA	CCGCTACGGC	GAGGGCCGGA
FWD	CGGCGAACAT	TCCGACAGCC	ACTGGGGCGA	CCGCTACGGC	GAGGGCCGGA
REV	CGGCGAACAT	TCCGACAGCC	ACTGGGGCGA	CCGCTACGGC	GAGGGCCGGA

	555	565	575	585	595
<i>pa1224</i>	TGCAGGGCAA	GCGGGCGATG	CTGGTAGTCA	CCGCCGGCGG	CTGGGAGTCG
FWD	TGCAGGGCAA	GCGGGCGATG	CTGGTAGTCA	CCGCCGGCGG	CTGGGAGTCG
REV	TGCAGGGCAA	GCGGGCGATG	CTGGTAGTCA	CCGCCGGCGG	CTGGGAGTCG

	605	615	625	635	645
<i>pa1224</i>	CACTACGCCG	CGCGCGGTAT	CAACGGACCG	ATGGACGACC	TGCTGTTCCC
FWD	CACTACGCCG	CGCGCGGTAT	CAACGGACCG	ATGGACGACC	TGCTGTTCCC
REV	CACTACGCCG	CGCGCGGTAT	CAACGGACCG	ATGGACGACC	TGCTGTTCCC

	655	665	675	685	695
<i>pa1224</i>	CATCCACCAC	GGCATCCTGC	ATTACCCCGG	CTTCGAGGTA	TTGCCGCCGT
FWD	CATCCACCAC	GGCATCCTGC	ATTACCCCGG	CTTCGAGGTA	TTGCCGCCGT
REV	CATCCACCAC	GGCATCCTGC	ATTACCCCGG	CTTCGAGGTA	TTGCCGCCGT

	705	715	725	735	745
<i>pa1224</i>	TCGTTCGTCTA	TCGCAGCGGC	CGGATCGACG	CGGAGCGTTT	CGCCGCGCTG
FWD	TCGTTCGTCTA	TCGCAGCGGC	CGGATCGACG	CGGAGCGTTT	CGCCGCGCTG
REV	TCGTTCGTCTA	TCGCAGCGGC	CGGATCGACG	CGGAGCGTTT	CGCCGCGCTG

	755	765	775	785	795
<i>pa1224</i>	AGCGAGCAGT	TGGGCCGGCG	CCTCGATGAC	CTGCAGCGCG	CTGCGCCGAT
FWD	AGCGAGCAGT	TGGGCCGGCG	CCTCGATGAC	CTGCAGCGCG	CTGCGCCGAT
REV	AGCGAGCAGT	TGGGCCGGCG	CCTCGATGAC	CTGCAGCGCG	CTGCGCCGAT

	805	815	825	835	845
<i>pa1224</i>	CCC GTTCCGC	CGGCAGAACG	GCGGCGACTA	CCTGATCCCG	GCGCTGACCC
FWD	CCC GTTCCGC	CGGCAGAACG	GCGGCGACTA	CCTGATCCCG	GCGCTGACCC
REV	CCC GTTCCGC	CGGCAGAACG	GCGGCGACTA	CCTGATCCCG	GCGCTGACCC

	855	865	875	885	895
<i>pa1224</i>	TGCGCGACGA	ACTTGCCCCG	CAGCGGGCCG	GTTTCGCCAT	GCACCTGGCC
FWD	TGCGCGACGA	ACTTGCCCCG	CAGCGGGCCG	GTTTCGCCAT	GCACCTGGCC
REV	TGCGCGACGA	ACTTGCCCCG	CAGCGGGCCG	GTTTCGCCAT	GCACCTGGCC

	905	915	925	935	945
<i>pa1224</i>	GAATGA----	-----	-----	-----	-----
FWD	GAATGACCCC	GGAGCTCCGT	CGACAAGCTT	GCGGCCGCAC	TCGAGCACCA
REV	GAATGACCCC	GGAGCTCCGT	CGACAAGCTT	GCGGCCGCAC	TCGAGCACCA

```

          .....|.....| .....|.....| .....|.....| .....|.....| .....|.....|
          955      965      975      985      995
pa1224
-----
FWD      CCACCACCAC CACTGAGATC CGGCTGCTAA CAAAGCCCGA AAGGAAGCTG
REV      -----
          .....|.....| .....|.....| .....|.....| .....|.....| .....|.....|
          1005     1015     1025     1035     1045
pa1224
-----
FWD      AGTTGGCTGC TGCCACCGCT GAGCAATAAC TAGCATAACC CCTTGGGGCC
REV      -----
          .....|.....| .....|.....| .....|
          1055     1065     1075     1085
pa1224
-----
FWD      TCTAAACGGG TCTTGAGGGG TTTTGTGCTGA AGGAG
REV      -----

```

Alignment of *pa1225* sequence in pET-28b in *E. coli* JM109 (FWD and REV) against *pa1225* sequence from *P. aeruginosa* PAO1 in the Pseudomonas Genome Database

```

          .....|.....| .....|.....| .....|.....| .....|.....| .....|.....|
          5      15      25      35      45
pa1225
-----
FWD      -----
REV      CTGCCACCAT ACCCACGCCG AAACAAGCGC TCATGAGCCC GAAGTGGCGA
          .....|.....| .....|.....| .....|.....| .....|.....| .....|.....|
          55     65     75     85     95
pa1225
-----
FWD      -----
REV      GCCCGATCTT CCCCATCGGT GATGTCGGCG ATATAGGCGC CAGCAACCCG
          .....|.....| .....|.....| .....|.....| .....|.....| .....|.....|
          105     115     125     135     145
pa1225
-----
FWD      -----
REV      CACCTGTGGC GCCGGTGATG CCGGGCCACG ATGCGTCCGG CGTAGAGGAT
          .....|.....| .....|.....| .....|.....| .....|.....| .....|.....|
          155     165     175     185     195
pa1225
-----
FWD      -----
REV      CGAGATCTCG ATCCC GCGAA ATTAATACGA CTCACTATAG GGAATTGTG
          .....|.....| .....|.....| .....|.....| .....|.....| .....|.....|
          205     215     225     235     245
pa1225
-----
FWD      -----
REV      AGCGGATAAC AATTC CCTC TAGAAATAAT TTTGTTTAAC TTAAGAAGG

```


	255	265	275	285	295
<i>pa1225</i>	-----	-----	-----	-----	-----
FWD	-----	-----	-----	-----	-----
REV	AGATATACCA	TGGGCAGCAG	CCATCATCAT	CATCATCACA	GCAGCGGCCT

	305	315	325	335	345
<i>pa1225</i>	-----	-----A	TGCATGCCCT	GATCGTCGTC	GCTCATCATC
FWD	-----	-----	-----	-----	--TCATCATC
REV	GGTGCCGCGC	GGCAGCCATA	TGCATGCCCT	GATCGTCGTC	GCTCATCATC

	355	365	375	385	395
<i>pa1225</i>	ATCCCCGCTC	TCTCACCCAC	GCCCTCGCCG	CGCGCATCGC	CGAAGGCGTG
FWD	ATCCCCGCTC	TCTCACCCAC	GCCCTCGCCG	CGCGCATCGC	CGAAGGCGTG
REV	ATCCCCGCTC	TCTCACCCAC	GCCCTCGCCG	CGCGCATCGC	CGAAGGCGTG

	405	415	425	435	445
<i>pa1225</i>	GTCCGCGCCG	GTCATTCCGC	GGAAACCGCC	GACCTGGCGG	CGGAAGGCTT
FWD	GTCCGCGCCG	GTCATTCCGC	GGAAACCGCC	GACCTGGCGG	CGGAAGGCTT
REV	GTCCGCGCCG	GTCATTCCGC	GGAAACCGCC	GACCTGGCGG	CGGAAGGCTT

	455	465	475	485	495
<i>pa1225</i>	CGAGCCGCGC	TTCGGCCTGG	CCGACCACGC	CGTGCATCGC	GGCCAGGCGT
FWD	CGAGCCGCGC	TTCGGCCTGG	CCGACCACGC	CGTGCATCGC	GGCCAGGCGT
REV	CGAGCCGCGC	TTCGGCCTGG	CCGACCACGC	CGTGCATCGC	GGCCAGGCGT

	505	515	525	535	545
<i>pa1225</i>	CGCCTCCCGC	CGACGTCCTC	GCCGAGCAGG	CGCGCATCGA	TCGCGCCGAT
FWD	CGCCTCCCGC	CGACGTCCTC	GCCGAGCAGG	CGCGCATCGA	TCGCGCCGAT
REV	CGCCTCCCGC	CGACGTCCTC	GCCGAGCAGG	CGCGCATCGA	TCGCGCCGAT

	555	565	575	585	595
<i>pa1225</i>	ACCCTGGTGC	TGGTCTACCC	GATCTACTGG	TGGTCGATGC	CGGCCCTGCT
FWD	ACCCTGGTGC	TGGTCTACCC	GATCTACTGG	TGGTCGATGC	CGGCCCTGCT
REV	ACCCTGGTGC	TGGTCTACCC	GATCTACTGG	TGGTCGATGC	CGGCCCTGCT

	605	615	625	635	645
<i>pa1225</i>	CAAGGGCTGG	ATCGATCGCG	TGTTCTCCAA	TGGCTGGGCC	TTCGACTACA
FWD	CAAGGGCTGG	ATCGATCGCG	TGTTCTCCAA	TGGCTGGGCC	TTCGACTACA
REV	CAAGGGCTGG	ATCGATCGCG	TGTTCTCCAA	TGGCTGGGCC	TTCGACTACA

	655	665	675	685	695
<i>pa1225</i>	GCATCGGCGG	CGACCTGCGG	AAAAAGCTGC	AGCGCCTGCG	CGTGGTGCTG
FWD	GCATCGGCGG	CGACCTGCGG	AAAAAGCTGC	AGCGCCTGCG	CGTGGTGCTG
REV	GCATCGGCGG	CGACCTGCGG	AAAAAGCTGC	AGCGCCTGCG	CGTGGTGCTG

	705	715	725	735	745
<i>pa1225</i>	GTCGGTGTCG	GCGGCGCCGA	TGCCGGCACC	TTCGAGCGGC	ACGGCTACGC
FWD	GTCGGTGTCG	GCGGCGCCGA	TGCCGGCACC	TTCGAGCGGC	ACGGCTACGC
REV	GTCGGTGTCG	GCGGCGCCGA	TGCCGGCACC	TTCGAGCGGC	ACGGCTACGC

	755	765	775	785	795
<i>pa1225</i>	CGGGGCGATG	CGCACCCAGA	TCGACCATGG	CATCTTCGAT	TACTGCGGCG
FWD	CGGGGCGATG	CGCACCCAGA	TCGACCATGG	CATCTTCGAT	TACTGCGGCG
REV	CGGGGCGATG	CGCACCCAGA	TCGACCATGG	CATCTTCGAT	TACTGCGGCG

	805	815	825	835	845
<i>pa1225</i>	CACGGGTGGT	CCGTTCCGAA	CTGTTGCTGG	AGTCGGAGAG	CGCCGATCCG
FWD	CACGGGTGGT	CCGTTCCGAA	CTGTTGCTGG	AGTCGGAGAG	CGCCGATCCG
REV	CACGGGTGGT	CCGTTCCGAA	CTGTTGCTGG	AGTCGGAGAG	CGCCGATCCG

	855	865	875	885	895
<i>pa1225</i>	ATCCGGCATC	TGGACCAGGC	CCTGCACATC	GGCAGCCAGC	TCTTCGCCGC
FWD	ATCCGGCATC	TGGACCAGGC	CCTGCACATC	GGCAGCCAGC	TCTTCGCCGC
REV	ATCCGGCATC	TGGACCAGGC	CCTGCACATC	GGCAGCCAGC	TCTTCGCCGC

	905	915	925	935	945
<i>pa1225</i>	ACGCGGCGCG	CAGGGGGCCG	CCCAGGCGCA	GCCGCTGGAG	GCCTGA----
FWD	ACGCGGCGCG	CAGGGGGCCG	CCCAGGCGCA	GCCGCTGGAG	GCGTGACCCC
REV	ACGCGGCGCG	CAGGGGGCCG	CCCAGGCGCA	GCCGCTGGAG	GCGTGACCCC

	955	965	975	985	995
<i>pa1225</i>	-----	-----	-----	-----	-----
FWD	CGAGCTCCGT	CGACAAGCTT	GCGGCCGCAC	TCGAGCACCA	CCACCACCAC
REV	CGAGCTCCGT	CGACAAGCTT	GCGGCCGCAC	TCGAGCAC--	-----

	1005	1015	1025	1035	1045
<i>pa1225</i>	-----	-----	-----	-----	-----
FWD	CACTGAGATC	CGGCTGCTAA	CAAAGCCCGA	AAGGAAGCTG	AGTTGGCTGC
REV	-----	-----	-----	-----	-----

	1055	1065	1075	1085	1095
<i>pa1225</i>	-----	-----	-----	-----	-----
FWD	TGCCACCGCT	GAGCAATAAC	TAGCATAACC	CCTTGGGGCC	TCTAAACGGG
REV	-----	-----	-----	-----	-----

	1105	1115	1125	1135	1145
<i>pa1225</i>	-----	-----	-----	-----	-----
FWD	TCTTGAGGGG	TTTTTTGCTG	AAAGGAGGAA	CTATATCCGG	ATTGGCGAAT
REV	-----	-----	-----	-----	-----

	1155	1165	1175	1185	1195
<i>pa1225</i>	-----	-----	-----	-----	-----
FWD	GGGACGCGCC	CTGTAGCGGC	GCATTAAGCG	CGGCGGGTGT	GGTGGTTACG
REV	-----	-----	-----	-----	-----

	1205	1215	1225	1235	1245
<i>pa1225</i>	-----	-----	-----	-----	-----
FWD	CGCAGCGTGA	CCGCTACACT	TGCCAGCGCC	CTAGCGCCCG	CTCCTTTCGC
REV	-----	-----	-----	-----	-----

```

      .....|.....| .....|.....| .....|.....| .....|.....| .....|.....|
      1255      1265      1275      1285      1295
pa1225
-----
FWD  TTTCTTCCCT TCCTTTCTCG CCACGTTCGC CGGCTTTCCC CGTCAAGCTC
REV  -----

```

```

      .....|.....| .....|.....| .....|.
      1305      1315      1325      1335
pa1225
-----
FWD  TAATCGGGGG CTCCCTTTAG GGTCCGATT TAGTGC
REV  -----

```

Alignment of *pa4975* sequence in pET-28b in *E. coli* JM109 (FWD and REV) against *pa4975* sequence from *P. aeruginosa* PAO1 in the Pseudomonas Genome Database

```

      .....|.....| .....|.....| .....|.....|
      5      15      25      35      45
pa4975
-----
FWD  TGCGCCGGAC GCGCGCATGT TCGTGATGGT CGACATCCGT CCCACCGGAC
REV  -----

```

```

      .....|.....| .....|.....| .....|.....|
      55      65      75      85      95
pa4975
-----
FWD  TTTCCGCCCA GGCCTTCGCC GACCGCCTGC TGGACCGCCA TGGCGTATCG
REV  -----

```

```

      .....|.....| .....|.....| .....|.....|
      105     115     125     135     145
pa4975
-----
FWD  GTGCTCGCCG GCGAAGCCTT CGGCCCGAGC GCCGCCGGTC ACATCCGCCT
REV  -----ATCCCGC GAAATTAATA CGACTACTA

```

```

      .....|.....| .....|.....| .....|.....|
      155     165     175     185     195
pa4975
-----
FWD  CGGCCTGGTG TTGGGCGCCG AACCGCTGCG CGAAGCCTGT CGGCGCATTG
REV  TAGGGGAATT GTGAGCGGAT AACAATTCCC CTCTAGAAAT AATTTTGTT-

```

```

      .....|.....| .....|.....| .....|.....|
      205     215     225     235     245
pa4975
-----
FWD  CGGCTGTGCG CCGCCGAGTT GCT-CGGCCA GGCCTGAACC CCTCGGCCGC
REV  TAACTTTAAG AAGGAGATAT ACCATGGGCA GCAGCCATCA TCATCATCAT

```

```

      .....|.....| .....|.....| .....|.....|
      255     265     275     285     295
pa4975
-----
FWD  GAGCGATGCG GCCGGTCACC ACGATTCGGA AACCACGATG AACGTACTION
REV  CACAGCAGCG GCCTGGTGCC GCG---CGGC AGCCAT-ATG AACGTACTION

```

```

      .....|.....| .....|.....| .....|.....|
      305     315     325     335     345
pa4975
-----
FWD  TCGTCCACGC CCACAACGAA CCGCAATCCT TCACCCGCGC GCTCTGTGAC
REV  TCGTCCACGC CCACAACGAA CCGCAATCCT TCACCCGCGC GCTCTGTGAC

```


	355	365	375	385	395
<i>pa4975</i>	CAGGCATGCG	AGACCCTGGC	AGGCCAGGGC	CACGCGGTGC	AGGTCTCGGA
FWD	CAGGCATGCG	AGACCCTGGC	AGGCCAGGGC	CACGCGGTGC	AGGTCTCGGA
REV	CAGGCATGCG	AGACCCTGGC	AGGCCAGGGC	CACGCGGTGC	AGGTCTCGGA

	405	415	425	435	445
<i>pa4975</i>	TCTCTACGCG	ATGAACTGGA	ATCCGGTGGC	CAGTGCCGCC	GACTTCGCCG
FWD	TCTCTACGCG	ATGAACTGGA	ATCCGGTGGC	CAGTGCCGCC	GACTTCGCCG
REV	TCTCTACGCG	ATGAACTGGA	ATCCGGTGGC	CAGTGCCGCC	GACTTCGCCG

	455	465	475	485	495
<i>pa4975</i>	AGCGCGCCGA	TCCCGACTAC	CTGGTGTACG	CCCTGGAGCA	GCGCGAGAGC
FWD	AGCGCGCCGA	TCCCGACTAC	CTGGTGTACG	CCCTGGAGCA	GCGCGAGAGC
REV	AGCGCGCCGA	TCCCGACTAC	CTGGTGTACG	CCCTGGAGCA	GCGCGAGAGC

	505	515	525	535	545
<i>pa4975</i>	GTCAAGCGCC	AGAGCCTGGC	CGCCGACATC	CAGGCCGAGC	TGGACAAGCT
FWD	GTCAAGCGCC	AGAGCCTGGC	CGCCGACATC	CAGGCCGAGC	TGGACAAGCT
REV	GTCAAGCGCC	AGAGCCTGGC	CGCCGACATC	CAGGCCGAGC	TGGACAAGCT

	555	565	575	585	595
<i>pa4975</i>	GCTGTGGGCC	GACCTGCTGA	TCCTCAACTT	TCCGATCTAC	TGGTTCTCGG
FWD	GCTGTGGGCC	GACCTGCTGA	TCCTCAACTT	TCCGATCTAC	TGGTTCTCGG
REV	GCTGTGGGCC	GACCTGCTGA	TCCTCAACTT	TCCGATCTAC	TGGTTCTCGG

	605	615	625	635	645
<i>pa4975</i>	TGCCGGCGAT	CCTCAAGGGG	TGGTTCGACC	GGGTACTGGT	GTCCGGGGTC
FWD	TGCCGGCGAT	CCTCAAGGGG	TGGTTCGACC	GGGTACTGGT	GTCCGGGGTC
REV	TGCCGGCGAT	CCTCAAGGGG	TGGTTCGACC	GGGTACTGGT	GTCCGGGGTC

	655	665	675	685	695
<i>pa4975</i>	TGCTATGGCG	GCAAGCGCTT	CTACGACCAG	GGTGGCCTGG	CCGGCAAGAA
FWD	TGCTATGGCG	GCAAGCGCTT	CTACGACCAG	GGTGGCCTGG	CCGGCAAGAA
REV	TGCTATGGCG	GCAAGCGCTT	CTACGACCAG	GGTGGCCTGG	CCGGCAAGAA

	705	715	725	735	745
<i>pa4975</i>	GGCGCTGGTC	AGCCTGACCC	TGGGCGGGCG	CCAGCACATG	TTCGGCGAGG
FWD	GGCGCTGGTC	AGCCTGACCC	TGGGCGGGCG	CCAGCACATG	TTCGGCGAGG
REV	GGCGCTGGTC	AGCCTGACCC	TGGGCGGGCG	CCAGCACATG	TTCGGCGAGG

	755	765	775	785	795
<i>pa4975</i>	GTGCCATCCA	CGGACCGCTG	GAGGACATGC	TGCGGCCGAT	CCTGCGCGGC
FWD	GTGCCATCCA	CGGACCGCTG	GAGGACATGC	TGCGGCCGAT	CCTGCGCGGC
REV	GTGCCATCCA	CGGACCGCTG	GAGGACATGC	TGCGGCCGAT	CCTGCGCGGC

	805	815	825	835	845
<i>pa4975</i>	ACCCTGGCCT	ATGTCGGCAT	GCAGGTGCTG	GAGCCCTTCG	TCGCCTGGCA
FWD	ACCCTGGCCT	ATGTCGGCAT	GCAGGTGCTG	GAGCCCTTCG	TCGCC-----
REV	ACCCTGGCCT	ATGTCGGCAT	GCAGGTGCTG	GAGCCCTTCG	TCGCCTGGCA

```

      .....|.....| .....|.....| .....|.....| .....|.....| .....|.....|
      855      865      875      885      895
pa4975  CGTGCCATAC ATCAGCGAGG AAGCGCGCGG CAACTTCCTG CGCGCCTACC
FWD     -----
REV     CGTGCCATAC ATCAGCGAGG AAGCGCGCGG CAACTTCCTG CGCGCCTACC

      .....|.....| .....|.....| .....|.....| .....|.....| .....|.....|
      905      915      925      935      945
pa4975  GGGCGCGGCT GGAAAATCTC GAGCAGGATG TACCCCTGCG GTTCCCGCGG
FWD     -----
REV     GGGCGCGGCT GGAAAATCTC GAGCAGGATG TACCCCTGCG GTTCCCGCGG

      .....|.....| .....|.....| .....|.....| .....|.....| .....|.....|
      955      965      975      985      995
pa4975  CTGGAGCAGT TCGACGCGCT GCTCCAGCCG CTGGCGCGCT GA-----
FWD     -----
REV     CTGGAGCAGT TCGACGCGCT GCTCCAGCCG CTGGCGCGCT GAGCTCCGTC

      .....|.....| ..
      1005
pa4975  ----- --
FWD     ----- --
REV     GACAAGCTTG CG

```

APPENDIX VII

Alignment of *pa0785* sequence in pUCP24 in *P. aeruginosa* PAO1 $\Delta pa0785$ (FWD) against *pa0785* sequence from *P. aeruginosa* PAO1 in the Pseudomonas Genome Database

	5	15	25	35	45
<i>pa0785</i>	-----				
FWD	AGTCAGTGAG	CGAGGAAGCG	GAAGAGCGCC	CAATACGCAA	ACCGCCTCTC

	55	65	75	85	95
<i>pa0785</i>	-----				
FWD	CCCGCGCGTT	GGCCGATTCA	TTAATGCAGC	TGGCACGACA	GGTTTCCCGA

	105	115	125	135	145
<i>pa0785</i>	-----				
FWD	CTGGAAAGCG	GGCAGTGAGC	GCAACGCAAT	TAATGTGAGT	TAGCTCACTC

	155	165	175	185	195
<i>pa0785</i>	-----				
FWD	ATTAGGCACC	CCAGGCTTTA	CACTTTATGC	TTCCGGCTCG	TATGTTGTGT

	205	215	225	235	245
<i>pa0785</i>	-----				
FWD	GGAATTGTGA	GCGGATAACA	ATTTACACACA	GGAAACAGCT	ATGACATGAT

	255	265	275	285	295
<i>pa0785</i>	-----				
FWD	TACGAATTCG	AGCTCGGTAC	CCGGGGATCC	AGATGAGTAG	AATTCTTGCA

	305	315	325	335	345
<i>pa0785</i>	-----				
FWD	GTGCATGCCA	GTCCGCGAGG	CGAGCGCTCG	CAGTCCCGGC	GTCTCGCCGA

	355	365	375	385	395
<i>pa0785</i>	-----				
FWD	GGTTTTCCTG	GCGGCCTATC	GCGAAGCCCA	TCCGCAGGCC	CGCGTGCTC

	405	415	425	435	445
<i>pa0785</i>	-----				
FWD	GCCGCGAAGT	CGGCCGGGTA	CCGCTTCCGG	CGGTCACCGA	GGCCTTCGTC

	455	465	475	485	495
<i>pa0785</i>	-----				
FWD	GCCGCGCCT	TCCATCCCCA	GCCGGAACAG	CGTTCGCTGG	CGATGCAGGC

```

      .....|.....| .....|.....| .....|.....| .....|.....| .....|.....|
      505      515      525      535      545
pa0785    CGACCTGGCG CTGAGCGACC AACTGGTCGG CGAACTGTTC GACAGCGACC
FWD       CGACCTGGCG CTGAGCGACC AACTGGTCGG CGAACTGTTC GACAGCGACC

      .....|.....| .....|.....| .....|.....| .....|.....|
      555      565      575      585      595
pa0785    TGCTGGTGAT CTCCACGCCG ATGTACAAC T CAGCGTGCC CAGCGGCCTG
FWD       TGCTGGTGAT CTCCACGCCG ATGTACAAC T CAGCGTGCC CAGCGGCCTG

      .....|.....| .....|.....| .....|.....| .....|.....|
      605      615      625      635      645
pa0785    AAGGCCTGGA TCGACCAGAT CGTGCGCCTC GGGGTGACCT TCGATTTTCG
FWD       AAGGCCTGGA TCGACCAGAT CGTGCGCCTC GGGGTGACCT TCGATTTTCG

      .....|.....| .....|.....| .....|.....| .....|.....|
      655      665      675      685      695
pa0785    CCTCGACAAT GGCCTCGCCC AGTACCGGCC GCTGCTGCGT GGCAAGCGTG
FWD       CCTCGACAAT GGCCTCGCCC AGTACCGGCC GCTGCTGCGT GGCAAGCGTG

      .....|.....| .....|.....| .....|.....| .....|.....|
      705      715      725      735      745
pa0785    CGCTGATCGT CACCAGTCGC GGTGGCCATG GCTTCGGCCC GGGCGGCGAG
FWD       CGCTGATCGT CACCAGTCGC GGTGGCCATG GCTTCGGCCC GGGCGGCGAG

      .....|.....| .....|.....| .....|.....| .....|.....|
      755      765      775      785      795
pa0785    AACCAGGCGA TGAACCACGC CGATCCCTGG TTGCGCACCG CGCTGGGTTT
FWD       AACCAGGCGA TGAACCATGC CGATCCCTGG TTGCGCACCG CGCTGGGTTT

      .....|.....| .....|.....| .....|.....| .....|.....|
      805      815      825      835      845
pa0785    CATCGGCATC GACGAGGTCA CGGTGGTCGC GGCGGAAGGC GAGGAATCCG
FWD       CATCGGCATC GACGAGGTCA CGGTGGTCGC GGCGGAAGGC GAGGAATCCG

      .....|.....| .....|.....| .....|.....| .....|.....|
      855      865      875      885      895
pa0785    GCGGCAGGTC CTTGAGGAC TCCTGCGACG AGGCGGAACA GCGCCTGCTG
FWD       GCGGCAGGTC CTTGAGGAC TCCTGCGACG AGGCGGAACA GCGCCTGCTG

      .....|.....| .....|.....| .....|.....| .....|.....|
      905      915      925      935      945
pa0785    GCGCTGGCGC GGTCGGCCTG A----- -----
FWD       GCGCTGGCGC GGTCGGCCTG AGGAGTCGAC CTGCAGGCAT GCAAGCTGGC

      ..
pa0785    --
FWD       AC

```

Alignment of *pa1962* sequence in pUCP24 in *P. aeruginosa* PAO1 Δ *pa1962* (FWD) against *pa1962* sequence from *P. aeruginosa* PAO1 in the Pseudomonas Genome Database

```

      .....|.....| .....|.....| .....|.....| .....|.....|
      5      15      25      35      45
pa1962    -----
FWD       GTCAGTGAGC GAGGAAGCGG AAGAGCGCCC AATACGCAA CCGCCTCTCC

```


	55	65	75	85	95
<i>pa1962</i>	-----	-----	-----	-----	-----
FWD	CCGCGCGTTG	GCCGATTCAT	TAATGCAGCT	GGCACGACAG	GTTTCCCGAC

	105	115	125	135	145
<i>pa1962</i>	-----	-----	-----	-----	-----
FWD	TGGAAAGCGG	GCAGTGAGCG	CAACGCAATT	AATGTGAGTT	AGCTCACTCA

	155	165	175	185	195
<i>pa1962</i>	-----	-----	-----	-----	-----
FWD	TTAGGCACCC	CAGGCTTTAC	ACTTTATGCT	TCCGGCTCGT	ATGTTGTGTG

	205	215	225	235	245
<i>pa1962</i>	-----	-----	-----	-----	-----
FWD	GAATTGTGAG	CGGATAACAA	TTTCACACAG	GAAACAGCTA	TGACATGATT

	255	265	275	285	295
<i>pa1962</i>	-----	-----	-----	-----	-----A
FWD	ACGAATTCGA	GCTCGGTACC	CGGGGATCCC	GCACTTTCAG	GAGCGAGACA

	305	315	325	335	345
<i>pa1962</i>	-----	-----	-----	-----	-----
FWD	TGAAACTTTT	GCATATCGAT	TCCAGCATCC	TCGGCGACGC	CTCCGCTTCC

	355	365	375	385	395
<i>pa1962</i>	-----	-----	-----	-----	-----
FWD	CGCCAACTGA	GCGCCGAGCT	GGTCCAGGCC	TGGCGGCAGA	ACGAAGACGG

	405	415	425	435	445
<i>pa1962</i>	-----	-----	-----	-----	-----
FWD	GCTTGACGTC	ACCTACCGCG	ACCTGGCCGC	CGACGCGGTG	GCGCATTTCT

	455	465	475	485	495
<i>pa1962</i>	-----	-----	-----	-----	-----
FWD	CCGCCCTGAC	CCTGGCCGCC	GGCAGCACCC	CGGCGGAGCT	GCGCGATGCC

	505	515	525	535	545
<i>pa1962</i>	-----	-----	-----	-----	-----
FWD	GCGCTGAAGC	ATGAAGTCGC	GGTGGGTGAA	GAAGTGCTGG	AAGAGTTCCT

	555	565	575	585	595
<i>pa1962</i>	-----	-----	-----	-----	-----
FWD	CGCCGCCGAC	GTCGTGGTAA	TCGGCGCGCC	GATGTACAAC	TTCACCATCT

	605	615	625	635	645
<i>pa1962</i>	-----	-----	-----	-----	-----
FWD	CCAGCCAGCT	CAAGGCCTGG	ATCGATCGCA	TCGCGGTTCG	CGGCAAGACC

```

      .....|.....| .....|.....| .....|.....| .....|.....| .....|.....|
      655      665      675      685      695
pa1962  TTCCGCTACA CCGAGAACGG CCCGGTTGGC CTGGCCGGCG ACAAGAAAGT
FWD     TTCCGCTACA CCGAGAACGG CCCGGTTGGC CTGGCCGGCG ACAAGAAAGT

      .....|.....| .....|.....| .....|.....| .....|.....| .....|.....|
      705      715      725      735      745
pa1962  GGTGATCGTC TCCACCGCCG GTGGCGTGCA TGCCGGCCAG CCGACCGGCG
FWD     GGTGATCGTC TCCACCGCCG GTGGCGTGCA TGCCGGCCAG CCGACCGGCG

      .....|.....| .....|.....| .....|.....| .....|.....| .....|.....|
      755      765      775      785      795
pa1962  CGGCCACGA  AGGCTACCTG CGCACCGTGC TGGGTTTCTT CGGCATCACC
FWD     CGGCCACGA  AGGCTACCTG CGCACCGTGC TGGGTTTCTT CGGCATCACC

      .....|.....| .....|.....| .....|.....| .....|.....| .....|.....|
      805      815      825      835      845
pa1962  GATATCGAAG TGGTTCGCGC CGAAGGCCCTG GCCTATGGCG AGGAGCCCCG
FWD     GATATCGAAG TGGTTCGCGC CGAAGGCCCTG GCCTATGGCG AGGAGCCCCG

      .....|.....| .....|.....| .....|.....| .....|.....| .....|.....|
      855      865      875      885      895
pa1962  CACCCAGGCC ATCGCCGCCG CCCGCCGGCA GATCGCCGGG CAGTTCGCCG
FWD     CACCCAGGCC ATCGCCGCCG CCCGCCGGCA GATCGCCGGG CAGTTCGCCG

      .....|.....| .....|.....| .....|.....| .....|.....| .....|.....|
      905      915      925      935      945
pa1962  CGGCCTG--- -----
FWD     CGGCCTGATC CCCGCGTCAT CGGAAAACCC CGCTTCGGCG GGTTTTTTCGC

      .....|.....| .....|.....| .....|.....| .....|.....|
      955      965      975      985
pa1962  -----
FWD     GTTGTGCGCA GCGGCGCGCT GCGTGTGAC  CTGCAGGCAG

```

Alignment of *pa3223* sequence in pUCP24 in *P. aeruginosa* PAO1 *Apa3223* (FWD) against *pa3223* sequence from *P. aeruginosa* PAO1 in the Pseudomonas Genome Database

```

      .....|.....| .....|.....| .....|.....| .....|.....| .....|.....|
      5      15      25      35      45
pa3223  -----
FWD     TCCCCGCGCG TTGGCCGATT CATTAATGCA GCTGGCACGA CAGGTTTCCC

      .....|.....| .....|.....| .....|.....| .....|.....| .....|.....|
      55      65      75      85      95
pa3223  -----
FWD     GACTGGAAAG CGGGCAGTGA GCGCAACGCA ATTAATGTGA GTTAGCTCAC

      .....|.....| .....|.....| .....|.....| .....|.....| .....|.....|
      105     115     125     135     145
pa3223  -----
FWD     TCATTAGGCA CCCCAGGCTT TACACTTTAT GCTTCCGGCT CGTATGTTGT

```


	155	165	175	185	195
<i>pa3223</i>	-----	-----	-----	-----	-----
FWD	GTGGAATTGT	GAGCGGATAA	CAATTTACACA	CAGGAAACAG	CTATGACATG

	205	215	225	235	245
<i>pa3223</i>	-----	-----	-----	-----	-----
FWD	ATTACGAATT	CGAGCTCGGT	ACCCGGGGAT	CCAGGTCGAG	TCATGTCCCG

	255	265	275	285	295
<i>pa3223</i>	-----	-----	-----	-----	-----
FWD	TGTCCTGGTT	ATCGAGAGCA	GTGCCCGCCA	ACGGGGCTCG	GTTTCCCGCC

	305	315	325	335	345
<i>pa3223</i>	-----	-----	-----	-----	-----
FWD	TGCTGACGGC	GGAATTCATC	TCCCCTGGA	AAATCGCGCA	TCCCGCTGAT

	355	365	375	385	395
<i>pa3223</i>	-----	-----	-----	-----	-----
FWD	CGCTTCCAGG	TTCGCGACCT	GGCGCGGAG	CCGCTGCCGC	ACCTCGATGA

	405	415	425	435	445
<i>pa3223</i>	-----	-----	-----	-----	-----
FWD	ATTATTGCTG	GGAGCCTGGA	CCACCCCTG	TGATGGCCAT	AGCGCTGCGG

	455	465	475	485	495
<i>pa3223</i>	-----	-----	-----	-----	-----
FWD	AAAGGCGCGC	CCTCGAGCGT	TCCAATCGCC	TGACCGAGGA	GTTGCGGATG

	505	515	525	535	545
<i>pa3223</i>	-----	-----	-----	-----	-----
FWD	GCGGACGTGC	TGGTGCTGGC	GGCACCGATG	TACAACCTCG	CCATTCCCAG

	555	565	575	585	595
<i>pa3223</i>	-----	-----	-----	-----	-----
FWD	CAGCCTGAAG	AGCTGGTTTCG	ACCATGTGCT	GCGCGCCGGC	CTGACCTTCC

	605	615	625	635	645
<i>pa3223</i>	-----	-----	-----	-----	-----
FWD	GTTACGCCGA	GCAGGGGCCG	GAAGGCCTGC	TACAGGGCAA	GCGCGCCTTC

	655	665	675	685	695
<i>pa3223</i>	-----	-----	-----	-----	-----
FWD	GTTCTCACCG	CCCgcgGCGG	GATCTACGCC	GGCGGTGGTC	TCGATCACCA

	705	715	725	735	745
<i>pa3223</i>	-----	-----	-----	-----	-----
FWD	GGAACCTAT	CTGCGCCAGG	TGCTGGGCTT	CGTCGGCATC	CACGACGTCA

	755	765	775	785	795
<i>pa3223</i>	CCTTCATCCA	CGCGGAGGGC	ATGAACATGG	GCCCCGAATT	CCGTGAGAAA
FWD	CCTTCATCCA	CGCGGAGGGC	ATGAACATGG	GCCCCGAATT	CCGTGAGAAA

	805	815	825	835	845
<i>pa3223</i>	GGCCTGGCGC	GAGCCCCTGA	GCGGATGCGG	CAGGCGCTGG	AAACCGACAC
FWD	GGCCTGGCGC	GAGCCCCTGA	GCGGATGCGG	CAGGCGCTGG	AAACCGACAC

	855	865	875	885	895
<i>pa3223</i>	CTCCCTTTGC	GTCCCTCTGC	CAACGCTCCG	GTGA-----	-----
FWD	CTCCCTTTGC	GTCCCTCTGC	CAACGCTCCG	GTGATTGGAC	GCAGCACCCG
		
	905	915	925		
<i>pa3223</i>	-----	-----	-----		
FWD	GTCGACCTGC	AGGCATGCAA	GCTGCAC		

Alignment of *pa2280* sequence in pUCP24 in *P. aeruginosa* PAO1 Δ *pa2280* (FWD) against *pa2280* sequence from *P. aeruginosa* PAO1 in the Pseudomonas Genome Database

	5	15	25	35	45
<i>pa2280</i>	-----	-----	-----	-----	-----
FWD	CCGCCTCTCC	CCGCGCGTTG	GCCGATTCAT	TAATGCAGCT	GGCACGACAG

	55	65	75	85	95
<i>pa2280</i>	-----	-----	-----	-----	-----
FWD	GTTTCCCGAC	TGAAAGCGG	GCAGTGAGCG	CAACGCAATT	AATGTGAGTT

	105	115	125	135	145
<i>pa2280</i>	-----	-----	-----	-----	-----
FWD	AGCTCACTCA	TTAGGCACCC	CAGGCTTTAC	ACTTTATGCT	TCCGGCTCGT

	155	165	175	185	195
<i>pa2280</i>	-----	-----	-----	-----	-----
FWD	ATGTTGTGTG	GAATTGTGAG	CGGATAACAA	TTTACACACAG	GAAACAGCTA

	205	215	225	235	245
<i>pa2280</i>	-----	-----	-----	-----A	-----
FWD	TGACATGATT	ACGAATTCGA	GCTCGGTACC	CGGGGATCCA	TGTCCGAACA

	255	265	275	285	295
<i>pa2280</i>	-----	-----	-----	-----	-----
FWD	ACTACCCAAC	CTCGATCCCG	CGCTGCTCGG	CGACCCGCCC	CCCGTCTCCG
	ACTACCCAAC	CTCGATCCCG	CGCTGCTCGG	CGACCCGCCC	CCCGTCTCCG

	305	315	325	335	345
<i>pa2280</i>	GGCACAGGCC	GCGCATCCTC	CTGCTCTACG	GCTCGACCCG	CGAGCGCTCC
FWD	GGCACAGGCC	GCGCATCCTC	CTGCTCTACG	GCTCGACCCG	CGAGCGCTCC

	355	365	375	385	395
<i>pa2280</i>	TTCAGCCGCC	TGCTGGTGCT	GGAGGCCGCA	CGCCTGCTCG	AACGCTTCGG
FWD	TTCAGCCGCC	TGCTGGTGCT	GGAGGCCGCA	CGCCTGCTCG	AACGCTTCGG

	405	415	425	435	445
<i>pa2280</i>	TGCCGAAACG	CGGATTTTCG	ACCCTTCCGG	GCTGCCATTG	CCCGATGATG
FWD	TGCCGAAACG	CGGATTTTCG	ACCCTTCCGG	GCTGCCATTG	CCCGATGATG

	455	465	475	485	495
<i>pa2280</i>	CACCGGTGGA	GCATCCCAAG	GTCCGCGAGT	TGCGCGACCT	GGTGCAGTGG
FWD	CACCGGTGGA	GCATCCCAAG	GTCCGCGAGT	TGCGCGACCT	GGTGCAGTGG

	505	515	525	535	545
<i>pa2280</i>	TCGGAAGGCC	AGGTCTGGTG	CTCGCCCGAG	CGCCACGGTG	CGCTGTCCGC
FWD	TCGGAAGGCC	AGGTCTGGTG	CTCGCCCGAG	CGCCACGGTG	CGCTGTCCGC

	555	565	575	585	595
<i>pa2280</i>	GGTATTCAAG	GCGCAGATCG	ACTGGATTCC	CCTGGCACTC	GGGGCGGTGC
FWD	GGTATTCAAG	GCGCAGATCG	ACTGGATTCC	CCTGGCACTC	GGGGCGGTGC

	605	615	625	635	645
<i>pa2280</i>	GCCCGACCCA	GGGCAAGACC	CTGGCGCTGA	TGCAGGTCTG	CGGCGGCTCG
FWD	GCCCGACCCA	GGGCAAGACC	CTGGCGCTGA	TGCAGGTCTG	CGGCGGCTCG

	655	665	675	685	695
<i>pa2280</i>	CAGTCGTTCA	ACGTGGTCAA	CCAGTTGCGC	GTGCTGGGTC	GCTGGATGCG
FWD	CAGTCGTTCA	ACGTGGTCAA	CCAGTTGCGC	GTGCTGGGTC	GCTGGATGCG

	705	715	725	735	745
<i>pa2280</i>	CATGTTCAAC	ATCCCCAACC	AGTCCTCGGT	TCCCAAGGCC	TACCTGGAGT
FWD	CATGTTCAAC	ATCCCCAACC	AGTCCTCGGT	TCCCAAGGCC	TACCTGGAGT

	755	765	775	785	795
<i>pa2280</i>	TCGACGAAGC	GGGCCGGATG	AAGCCATCGC	CCTACTACGA	CCGGGTGGTC
FWD	TCGACGAAGC	GGGCCGGATG	AAGCCATCGC	CCTACTACGA	CCGGGTGGTC

	805	815	825	835	845
<i>pa2280</i>	GACGTGATGG	AGGAGTTGTT	CAAGTTCACC	CTGCTCCTGC	GCGAGCGCAC
FWD	GACGTGATGG	AGGAGTTGTT	CAAGTTCACC	CTGCTCCTGC	GCGAGCGCAC

	855	865	875	885	895
<i>pa2280</i>	GGACTTCCTG	GTGGACCGCT	ATTTCGGAGCG	CAAGGAAAGC	GCCGAGCAGC
FWD	GGACTTCCTG	GTGGACCGCT	ATTTCGGAGCG	CAAGGAAAGC	GCCGAGCAGC

```

          .....|.....| .....|.....| .....|.....| .....|.....| .....|.....|
          905          915          925          935          945
pa2280   TTTCCGCGCG GGTCGACCAG CGTTCGCTCT GA----- -----
FWD      TTTCCGCGCG GGTCGACCAG CGTTCGCTCT GAACCGCGTC GACCTGCAGG

          .....|.....| .
          955
pa2280   ----- -
FWD      CATGCAAGCT G

```

Alignment of *pa2580* sequence in pUCP24 in *P. aeruginosa* PAO1 Δ *pa2580* (FWD) against *pa2580* sequence from *P. aeruginosa* PAO1 in the Pseudomonas Genome Database

```

          .....|.....| .....|.....| .....|.....| .....|.....|
          5          15          25          35          45
pa2580   -----
FWD      ACATGTTCTT TCCTGCGTTA TCCCCTGATT CTGTGGATAA CCGTATTACC

          .....|.....| .....|.....| .....|.....| .....|.....|
          55          65          75          85          95
pa2580   -----
FWD      GCCTTTGAGT GAGCTGATAC CGCTCGCCGC AGCCGAACGA CCGAGCGCAG

          .....|.....| .....|.....| .....|.....| .....|.....|
          105         115         125         135         145
pa2580   -----
FWD      CGAGTCAGTG AGCGAGGAAG CGGAAGAGCG CCCAATACGC AAACCGCCTC

          .....|.....| .....|.....| .....|.....| .....|.....|
          155         165         175         185         195
pa2580   -----
FWD      TCCCCGCGCG TTGGCCGATT CATTAATGCA GCTGGCACGA CAGGTTTCCC

          .....|.....| .....|.....| .....|.....| .....|.....|
          205         215         225         235         245
pa2580   -----
FWD      GACTGGAAAAG CGGGCAGTGA GCGCAACGCA ATTAATGTGA GTTAGCTCAC

          .....|.....| .....|.....| .....|.....| .....|.....|
          255         265         275         285         295
pa2580   -----
FWD      TCATTAGGCA CCCAGGCTT TACACTTTAT GCTTCCGGCT CGTATGTTGT

          .....|.....| .....|.....| .....|.....| .....|.....|
          305         315         325         335         345
pa2580   -----
FWD      GTGGAATTGT GAGCGGATAA CAATTTACA CAGGAAACAG CTATGACATG

          .....|.....| .....|.....| .....|.....| .....|.....|
          355         365         375         385         395
pa2580   -----
FWD      ATTACGAATT CGAGCTCGGT ACCCGGGGAT ----ATGAAA AACATTCTCC

          .....|.....| .....|.....| .....|.....| .....|.....|
          405         415         425         435         445
pa2580   -----
FWD      TGCTCAACGG CGGAAAGCGT TTCGCCATT CCGACGGTCG CCTCAACCAG

```


	455	465	475	485	495
<i>pa2580</i>	ACCCTGCACG	AAACCGCCCT	GGCCCATCTG	GACCGCCGTG	GCTTCGACCT
FWD	ACCCTGCACG	AAACCGCCCT	GGCCCATCTG	GACCGCCGTG	GCTTCGACCT

	505	515	525	535	545
<i>pa2580</i>	GCGCCAGACC	TTCATCGACG	GTGGCTATGA	TATCCCAGACG	GAGGTGGACA
FWD	GCGCCAGACC	TTCATCGACG	GTGGCTATGA	TATCCCAGACG	GAGGTGGACA

	555	565	575	585	595
<i>pa2580</i>	AGTTCCTCTG	GGCCGACGTG	GTGATCTACC	AGATGCCCGG	CTGGTGGATG
FWD	AGTTCCTCTG	GGCCGACGTG	GTGATCTACC	AGATGCCCGG	CTGGTGGATG

	605	615	625	635	645
<i>pa2580</i>	GGCGCCCCGT	GGACAGTGAA	GCGCTACATC	GACGAAGTCT	TCACGGCCCG
FWD	GGCGCCCCGT	GGACAGTGAA	GCGCTACATC	GACGAAGTCT	TCACGGCCCG

	655	665	675	685	695
<i>pa2580</i>	ACACGGCAGC	CTCTATGCCA	ACGACGGTCG	TACCCGCTCC	GACAGCACGC
FWD	ACACGGCAGC	CTCTATGCCA	ACGACGGTCG	TACCCGCTCC	GACAGCACGC

	705	715	725	735	745
<i>pa2580</i>	AGAAATATGG	CAGCGGCGGT	CTGGTGCAGG	GCAAGCGCTA	CATGATCTCG
FWD	AGAAATATGG	CAGCGGCGGT	CTGGTGCAGG	GCAAGCGCTA	CATGATCTCG

	755	765	775	785	795
<i>pa2580</i>	GCGACCTGGA	ATGCACCACG	GCAGGCGTTC	GACGATCCGA	GCGACTTCTT
FWD	GCGACCTGGA	ATGCACCACG	GCAGGCGTTC	GACGATCCGA	GCGACTTCTT

	805	815	825	835	845
<i>pa2580</i>	CGAAGGAAAA	GGCGTGGATG	CGGTGTATTT	CCCCTTCCAC	AAGGCCAACC
FWD	CGAAGGAAAA	GGCGTGGATG	CGGTGTATTT	CCCCTTCCAC	AAGGCCAACC

	855	865	875	885	895
<i>pa2580</i>	AGTTCCTCGG	CATGTCCGGC	CTGCCGACGT	TCCTCGCGGT	GGATGTGATG
FWD	AGTTCCTCGG	CATGTCCGGC	CTGCCGACGT	TCCTCGCGGT	GGATGTGATG

	905	915	925	935	945
<i>pa2580</i>	AAGCGCCCGG	ACGTCCCAGC	TACCGTCGCT	GCCTACCAGG	CGCACCTGGA
FWD	AAGCGCCCGG	ACGTCCCAGC	TACCGTCGCT	GCCTACCAGG	CGCACCTGGA

	955	965	975	985	995
<i>pa2580</i>	CAGGGTGTTT	GGGCGCGCCG	GCTGA-----	-----	-----
FWD	CAGGGTGTTT	GGGCGCGCCG	GCTGAGTTTC	TCGACCTGCA	GGCATGCAAG
	..				
<i>pa2580</i>	--				
FWD	CT				

Alignment of *pa1204* sequence in pUCP24 in *P. aeruginosa* PAO1 $\Delta pa1204$ (FWD) against *pa1204* sequence from *P. aeruginosa* PAO1 in the Pseudomonas Genome Database

```

      .....|.....| .....|.....| .....|.....| .....|.....| .....|.....|
      5      15      25      35      45
pa1204
FWD    -----
CATGTTCTTT CCTGCGTTAT CCCCTGATTC TGTGGATAAC CGTATTACCG

      .....|.....| .....|.....| .....|.....| .....|.....|
      55     65     75     85     95
pa1204
FWD    -----
CCTTTGAGTG AGCTGATAACC GCTCGCCGCA GCCGAACGAC CGAGCGCAGC

      .....|.....| .....|.....| .....|.....| .....|.....|
      105    115    125    135    145
pa1204
FWD    -----
GAGTCAGTGA GCGAGGAAGC GGAAGAGCGC CCAATACGCA AACCGCCTCT

      .....|.....| .....|.....| .....|.....| .....|.....|
      155    165    175    185    195
pa1204
FWD    -----
CCCCGCGCGT TGGCCGATTC ATTAATGCAG CTGGCACGAC AGGTTTCCCG

      .....|.....| .....|.....| .....|.....| .....|.....|
      205    215    225    235    245
pa1204
FWD    -----
ACTGGAAAGC GGGCAGTGAG CGCAACGCAA TTAATGTGAG TTAGCTCACT

      .....|.....| .....|.....| .....|.....| .....|.....|
      255    265    275    285    295
pa1204
FWD    -----
CATTAGGCAC CCCAGGCTTT ACACTTTATG CTTCCGGCTC GTATGTTGTG

      .....|.....| .....|.....| .....|.....| .....|.....|
      305    315    325    335    345
pa1204
FWD    -----
TGGAATTGTG AGCGGATAAC AATTTACAC AGGAAACAGC TATGACATGA

      .....|.....| .....|.....| .....|.....| .....|.....|
      355    365    375    385    395
pa1204
FWD    -----
TTACGAATTC GAGCTCGGTA CCCGGGGATC CCGGCATGAG CGACGACATC

      .....|.....| .....|.....| .....|.....| .....|.....|
      405    415    425    435    445
pa1204
FWD    -----
AAGGTATTGG GCATTTCCGG CAGCCTGCGC AGCGGCTCCT ACAACAGCGC
AAGGTATTGG GCATTTCCGG CAGCCTGCGC AGCGGCTCCT ACAACAGCGC

      .....|.....| .....|.....| .....|.....| .....|.....|
      455    465    475    485    495
pa1204
FWD    -----
GGCGCTGCAG GAGGCGATTG GCCTGGTCCC GCCGGGCATG AGCATCGAGC
GGCGCTGCAG GAGGCGATTG GCCTGGTCCC GCCGGGCATG AGCATCGAGC

      .....|.....| .....|.....| .....|.....| .....|.....|
      505    515    525    535    545
pa1204
FWD    -----
TGGCGGACAT CTCCGGCATC CCGCTGTACA ACGAGGACGT CTACGCCCTC
TGGCGGACAT CTCCGGCATC CCGCTGTACA ACGAGGACGT CTACGCCCTC

```


	555	565	575	585	595
<i>pa1204</i>	GGCTTCCCGC	CCGCGGTGGA	ACGCTTCCGC	GAGCAGATTC	GCGCGGCGGA
FWD	GGCTTCCCGC	CCGCGGTGGA	ACGCTTCCGC	GAGCAGATTC	GCGCGGCGGA

	605	615	625	635	645
<i>pa1204</i>	CGCGCTGCTG	TTCGCCACCC	CGGAATACAA	CTATTTCGATG	GCCGGGGTGC
FWD	CGCGCTGCTG	TTCGCCACCC	CGGAATACAA	CTATTTCGATG	GCCGGGGTGC

	655	665	675	685	695
<i>pa1204</i>	TGAAGAATGC	CATCGACTGG	GCCTCGCGGC	CGCCGGAGCA	GCCGTTCTCC
FWD	TGAAGAATGC	CATCGACTGG	GCCTCGCGGC	CGCCGGAGCA	GCCGTTCTCC

	705	715	725	735	745
<i>pa1204</i>	GGCAAGCCGG	CGGCGATCCT	CGGCGCCAGC	GCCGGGCGTT	TCGGCACC GC
FWD	GGCAAGCCGG	CGGCGATCCT	CGGCGCCAGC	GCCGGGCGTT	TCGGCACC GC

	755	765	775	785	795
<i>pa1204</i>	GCGGGCGCAG	TATCACTTGC	GCCAGACGCT	GGTGTTCCTC	GACGTTTCATC
FWD	GCGGGCGCAG	TATCACTTGC	GCCAGACGCT	GGTGTTCCTC	GACGTTTCATC

	805	815	825	835	845
<i>pa1204</i>	CGCTGAACAA	GCCGGAAGTG	ATGATCTCCA	GCGCGCAGAA	CGCCTTCGAT
FWD	CGCTGAACAA	GCCGGAAGTG	ATGATCTCCA	GCGCGCAGAA	CGCCTTCGAT

	855	865	875	885	895
<i>pa1204</i>	GCCCAGGGCC	GGCTGCTCGA	CGACAAGGCG	CGCGAGCTGA	TCCAGCAGCA
FWD	GCCCAGGGCC	GGCTGCTCGA	CGACAAGGCG	CGCGAGCTGA	TCCAGCAGCA

	905	915	925	935	945
<i>pa1204</i>	GTTGCAGGCC	CTGCAGCTAT	GGGTGCGCCG	CCTGCGCGGT	TGA-----
FWD	GTTGCAGGCC	CTGCAGCTAT	GGGTGCGCCG	CCTGCGCGGT	TGAATGCCTC
		
	955	965	975		
<i>pa1204</i>	-----	-----	-----		
FWD	GTCGACCTGC	AGGCATGCAA	GCTGC		

Alignment of *pa0949* sequence in pUCP24 in *P. aeruginosa* PAO1 Δ *pa0949* (FWD) against *pa0949* sequence from *P. aeruginosa* PAO1 in the Pseudomonas Genome Database

	5	15	25	35	45
<i>pa0949</i>	-----	-----	-----	-----	-----
fwd	ACCGCTTGCC	GCAGCCGAAC	GACCGAGCGC	AGCGAGTCAG	TGAGCGAGGA

	55	65	75	85	95
<i>pa0949</i>	-----	-----	-----	-----	-----
fwd	AGCGGAAGAG	CGCCCAATAC	GCAAACCGCC	TCTCCCCGCG	CGTTGGCCGA

	105	115	125	135	145
<i>pa0949</i>	-----	-----	-----	-----	-----
fwd	TTCATTAATG	CAGCTGGCAC	GACAGGTTTC	CCGACTGGAA	AGCGGGCAGT

	155	165	175	185	195
<i>pa0949</i>	-----	-----	-----	-----	-----
fwd	GAGCGCAACG	CAATTAATGT	GAGTTAGCTC	ACTCATTAGG	CACCCCAGGC

	205	215	225	235	245
<i>pa0949</i>	-----	-----	-----	-----	-----
fwd	TTTACACTTT	ATGCTTCCGG	CTCGTATGTT	GTGTGGAATT	GTGAGCGGAT

	255	265	275	285	295
<i>pa0949</i>	-----	-----	-----	-----	-----
fwd	AACAATTTCA	CACAGGAAAC	AGCTATGACA	TGATTACGAA	TTCGAGCTCG

	305	315	325	335	345
<i>pa0949</i>	-----	-----TT	GAGCAGTCCC	TACATCCTGG	TGCTGTACTA
fwd	GTACCCGGGG	ATCCTCGCTT	GAGCAGTCCC	TACATCCTGG	TGCTGTACTA

	355	365	375	385	395
<i>pa0949</i>	-----	-----	-----	-----	-----
fwd	CAGTCGCCAT	GGCGCTACCG	CGGAAATGGC	CCGGCAGATC	GCCCGTGGCG

	405	415	425	435	445
<i>pa0949</i>	-----	-----	-----	-----	-----
fwd	TCGAACAGGG	CGGCTTCGAG	GCGCGTGTAC	GCACGGTTCC	CGCGGTATCC

	455	465	475	485	495
<i>pa0949</i>	-----	-----	-----	-----	-----
fwd	ACCGAATGCG	AAGCGGTCGC	CCCCGACATC	CCCGCGGAGG	GGGCGCTGTA

	505	515	525	535	545
<i>pa0949</i>	-----	-----	-----	-----	-----
fwd	CGCAACCCTG	GAGGACCTGA	AGAACTGCGC	GGGCCTGGCC	CTCGGCAGCC

	555	565	575	585	595
<i>pa0949</i>	-----	-----	-----	-----	-----
fwd	CGACCCGCTT	CGGCAACATG	GCTTCCCCGC	TGAAATACTT	CCTCGACGGT

	605	615	625	635	645
<i>pa0949</i>	-----	-----	-----	-----	-----
fwd	ACCAGCAGCC	TGTGGCTGAC	CGGCAGCCTG	GTCGGCAAGC	CGGCAGCGGT

	655	665	675	685	695
<i>pa0949</i>	-----	-----	-----	-----	-----
fwd	CTTCACCTCC	ACCGCCAGCC	TGCACGGCGG	CCAGGAGACC	ACTCAGTTAT

	705	715	725	735	745
<i>pa0949</i>	CGATGCTGTT	GCCATTGCTG	CACCACGGCA	TGCTGGTCCT	GGGCATTCCC
fwd	CGATGCTGTT	GCCATTGCTG	CACCACGGCA	TGCTGGTCCT	GGGCATTCCC

	755	765	775	785	795
<i>pa0949</i>	TACAGCGAAC	CCGCCCTGCT	GGAAACCCGC	GGCGGCGGCA	CGCCTTACGG
fwd	TACAGCGAAC	CCGCCCTGCT	GGAAACCCGC	GGCGGCGGCA	CGCCTTACGG

	805	815	825	835	845
<i>pa0949</i>	CGCCAGCCAC	TTCGCCGGCG	CCGATGGCAA	GCGCAGCCTC	GATGAGCACG
fwd	CGCCAGCCAC	TTCGCCGGCG	CCGATGGCAA	GCGCAGCCTC	GATGAGCACG

	855	865	875	885	895
<i>pa0949</i>	AACTGACCCT	GTGTCGCGCG	CTGGGCAAAC	GCCTGGCGGA	AACCGCCGGC
fwd	AACTGACCCT	GTGTCGCGCG	CTGGGCAAAC	GCCTGGCGGA	AACCGCCGGC

	905	915	925	935	945
<i>pa0949</i>	AAGCTGGGGA	GTTGA-----	-----	-----	-----
fwd	AAGCTGGGGA	GTTGAAATGG	CCCGCAAGAA	CAAACCGCCT	GCAGGCATGC

	955	965	975	985	
<i>pa0949</i>	-----	-----	-----	-----	
fwd	AAGCTGGCAC	G-----	-----	-----	

Alignment of *pa4975* sequence in pUCP24 in *P. aeruginosa* PAO1 Δ *pa4975* (FWD) against *pa4975* sequence from *P. aeruginosa* PAO1 in the Pseudomonas Genome Database

	5	15	25	35	45
<i>pa4975</i>	-----	-----	-----	-----	-----
FWD	TTGACCGAGG	AAGCGGAAGA	GCGCCCAATA	CGCAAACCGC	CTCTCCCCGC

	55	65	75	85	95
<i>pa4975</i>	-----	-----	-----	-----	-----
FWD	GCGTTGGCCG	ATTCATTAAT	GCAGCTGGCA	CGACAGGTTT	CCCGACTGGA

	105	115	125	135	145
<i>pa4975</i>	-----	-----	-----	-----	-----
FWD	AAGCGGGCAG	TGAGCGCAAC	GCAATTAATG	TGAGTTAGCT	CACTCATTAG

	155	165	175	185	195
<i>pa4975</i>	-----	-----	-----	-----	-----
FWD	GCACCCCAGG	CTTTACACTT	TATGCTTCCG	GCTCGTATGT	TGTGTGGAAT

	205	215	225	235	245
<i>pa4975</i>	-----	-----	-----	-----	-----
FWD	TGTGAGCGGA	TAACAATTTT	ACACAGGAAA	CAGCTATGAC	ATGATTACGA

	255	265	275	285	295
<i>pa4975</i>	-----	-----	-----A	TGAACGTACT	GATCGTCCAC
FWD	ATTCGAGCTC	GGTACCCGGG	GATCCCACGA	TGAACGTACT	GATCGTCCAC

	305	315	325	335	345
<i>pa4975</i>	GCCCACAACG	AACCGCAATC	CTTCACCCGC	GCGCTCTGTG	ACCAGGCATG
FWD	GCCCACAACG	AACCGCAATC	CTTCACCCGC	GCGCTCTGTG	ACCAGGCATG

	355	365	375	385	395
<i>pa4975</i>	CGAGACCCTG	GCAGGCCAGG	GCCACGCGGT	GCAGGTCTCG	GATCTCTACG
FWD	CGAGACCCTG	GCAGGCCAGG	GCCACGCGGT	GCAGGTCTCG	GATCTCTACG

	405	415	425	435	445
<i>pa4975</i>	CGATGAACTG	GAATCCGGTG	GCCAGTGCCG	CCGACTTCGC	CGAGCGCGCC
FWD	CGATGAACTG	GAATCCGGTG	GCCAGTGCCG	CCGACTTCGC	CGAGCGCGCC

	455	465	475	485	495
<i>pa4975</i>	GATCCCGACT	ACCTGGTGTA	CGCCCTGGAG	CAGCGCGAGA	GCGTCAAGCG
FWD	GATCCCGACT	ACCTGGTGTA	CGCCCTGGAG	CAGCGCGAGA	GCGTCAAGCG

	505	515	525	535	545
<i>pa4975</i>	CCAGAGCCTG	GCCGCCGACA	TCCAGGCCGA	GCTGGACAAG	CTGCTGTGGG
FWD	CCAGAGCCTG	GCCGCCGACA	TCCAGGCCGA	GCTGGACAAG	CTGCTGTGGG

	555	565	575	585	595
<i>pa4975</i>	CCGACCTGCT	GATCCTCAAC	TTTCCGATCT	ACTGGTTCTC	GGTGCCGGCG
FWD	CCGACCTGCT	GATCCTCAAC	TTTCCGATCT	ACTGGTTCTC	GGTGCCGGCG

	605	615	625	635	645
<i>pa4975</i>	ATCCTCAAGG	GGTGGTTCGA	CCGGGTACTG	GTGTCCGGGG	TCTGCTATGG
FWD	ATCCTCAAGG	GGTGGTTCGA	CCGGGTACTG	GTGTCCGGGG	TCTGCTATGG

	655	665	675	685	695
<i>pa4975</i>	CGGCAAGCGC	TTCTACGACC	AGGGTGGCCT	GGCCGGCAAG	AAGGCGCTGG
FWD	CGGCAAGCGC	TTCTACGACC	AGGGTGGCCT	GGCCGGCAAG	AAGGCGCTGG

	705	715	725	735	745
<i>pa4975</i>	TCAGCCTGAC	CCTGGGCGGG	CGCCAGCACA	TGTTCCGGCGA	GGGTGCCATC
FWD	TCAGCCTGAC	CCTGGGCGGG	CGCCAGCACA	TGTTCCGGCGA	GGGTGCCATC

	755	765	775	785	795
<i>pa4975</i>	CACGGACCGC	TGGAGGACAT	GCTGCGGCCG	ATCCTGCGCG	GCACCCTGGC
FWD	CACGGACCGC	TGGAGGACAT	GCTGCGGCCG	ATCCTGCGCG	GCACCCTGGC

	805	815	825	835	845
<i>pa4975</i>	CTATGTCCGC	ATGCAGGTGC	TGGAGCCCTT	CGTCGCCTGG	CACGTGCCAT
FWD	CTATGTCCGC	ATGCAGGTGC	TGGAGCCCTT	CGTCGCCTGG	CACGTGCCAT

```

      .....|.....| .....|.....| .....|.....| .....|.....| .....|.....|
      855      865      875      885      895
pa4975 ACATCAGCGA GGAAGCGCGC GGCAACTTCC TGC GCGCCTA CCGGGCGCGG
FWD      ACATCAGCGA GGAAGCGCGC GGCAACTTCC TGC GCGCCTA CCGGGCGCGG

      .....|.....| .....|.....| .....|.....| .....|.....| .....|.....|
      905      915      925      935      945
pa4975 CTGGAAAATC TCGAGCAGGA TGTACCCCTG CGGTTCCCGC GGCTGGAGCA
FWD      CTGGAAAATC TCGAGCAGGA TGTACCCCTG CGGTTCCCGC GGCTGGAGCA

      .....|.....| .....|.....| .....|.....| .....|.....| .....|.....|
      955      965      975      985      995
pa4975 GTTCGACGCG CTGCTCCAGC CGCTGGCGCG CTGA----- -----
FWD      GTTCGACGCG CTGCTCCAGC CGCTGGCGCG CTGAGCCGGT CGACCTGCAG

      .....|.....| .....|.
      1005      1015
pa4975 -----
FWD      GCATGCAAGC TGGCAC

```

References

- ACKERLEY, D. F., *et al.* 2004. Chromate-reducing properties of soluble flavoproteins from *Pseudomonas putida* and *Escherichia coli*. *Appl Environ Microbiol*, 70, 873-82.
- ADAMS, M. A. & JIA, Z. 2006. Modulator of drug activity B from *Escherichia coli*: crystal structure of a prokaryotic homologue of DT-diaphorase. *J Mol Biol*, 359, 455-65.
- ADAMS, P. D., *et al.* 2010. PHENIX: a comprehensive Python-based system for macromolecular structure solution. *Acta Crystallogr D*, 66, 213-21.
- AGARWAL, R., BONANNO, J. B., BURLEY, S. K. & SWAMINATHAN, S. 2006. Structure determination of an FMN reductase from *Pseudomonas aeruginosa* PA01 using sulfur anomalous signal. *Acta Crystallogr D*, 62, 383-91.
- AGILENT 2016. BL21-CodonPlus Competent Cells Instruction Manual.
- AHN, K. S., *et al.* 2007. Deficiency of NRH:quinone oxidoreductase 2 differentially regulates TNF signaling in keratinocytes: up-regulation of apoptosis correlates with down-regulation of cell survival kinases. *Cancer Res*, 67, 10004-11.
- AL-MAJDOUB, Z. M., OWOSENI, A., GASKELL, S. J. & BARBER, J. 2013. Effects of gentamicin on the proteomes of aerobic and oxygen-limited *Escherichia coli*. *J Med Chem*, 56, 2904-10.
- ALDRED, K. J., KERNS, R. J. & OSHEROFF, N. 2014. Mechanism of Quinolone Action and Resistance. *Biochemistry*, 53, 1565-1574.
- ALLARD, J. D. & BERTRAND, K. P. 1992. Membrane topology of the pBR322 tetracycline resistance protein. TetA-PhoA gene fusions and implications for the mechanism of TetA membrane insertion. *J Biol Chem*, 267, 17809-19.
- ALVAREZ-ORTEGA, C., WIEGAND, I., OLIVARES, J., HANCOCK, R. E. W. & MARTÍNEZ, J. L. 2010. Genetic Determinants Involved in the Susceptibility of *Pseudomonas aeruginosa* to β -Lactam Antibiotics. *Antimicrobial Agents and Chemotherapy*, 54, 4159-4167.
- ANDREWS, S. C., *et al.* 1997. A 12-cistron *Escherichia coli* operon (hyf) encoding a putative proton-translocating formate hydrogenlyase system. *Microbiology*, 143, 3633-3647.
- ARNAU, J., LAURITZEN, C., PETERSEN, G. E. & PEDERSEN, J. 2006. Current strategies for the use of affinity tags and tag removal for the purification of recombinant proteins. *Protein Expr Purif*, 48, 1-13.
- ASARE, R. & ABU KWAİK, Y. 2010. Molecular complexity orchestrates modulation of phagosome biogenesis and escape to the cytosol of macrophages by *Francisella tularensis*. *Environmental microbiology*, 12, 2559-86.
- ASARE, R., AKIMANA, C., JONES, S. & KWAİK, Y. A. 2010. Molecular bases of proliferation of *Francisella tularensis* in Arthropod vectors. *Environmental microbiology*, 12, 2587-2612.

- AVICAN, K., *et al.* 2015. Reprogramming of *Yersinia* from virulent to persistent mode revealed by complex in vivo RNA-seq analysis. *PLoS Pathog*, 11, e1004600.
- BABEL, S. & KURNIAWAN, T. A. 2004. Cr(VI) removal from synthetic wastewater using coconut shell charcoal and commercial activated carbon modified with oxidizing agents and/or chitosan. *Chemosphere*, 54, 951-967.
- BAGDASARIAN, M., AMANN, E., LURZ, R., RUCKERT, B., BAGDASARIAN, M. 1983. Activity of the hybrid *trp-lac (tat)* promoter of *Escherichia coli* in *Pseudomonas putida*. Construction of broad-host-range, controlled-expression vectors *Gene*, 26, 10.
- BANEYX, F. & MUJACIC, M. 2004. Recombinant protein folding and misfolding in *Escherichia coli*. *Nat Biotech*, 22, 1399-1408.
- BELENKY, P., *et al.* 2015. Bactericidal antibiotics induce toxic metabolic perturbations that lead to cellular damage. *Cell reports*, 13, 968-980.
- BHAKTA, T., WHITEHEAD, S. J., SNAITH, J. S., DAFFORN, T. R., WILKIE, J., RAJESH, S., WHITE, S. A., JACKSON, J. B. 2007. Structures of the dI2dIII1 complex of proton-translocating transhydrogenase with bound, inactive analogues of NADH and NADPH reveal active site geometries. *Biochemistry*, 46, 15.
- BIASINI, M., *et al.* 2014. SWISS-MODEL: modelling protein tertiary and quaternary structure using evolutionary information. *Nucleic Acids Research*, 42, W252-W258.
- BINTER, A., *et al.* 2009. A single intersubunit salt bridge affects oligomerization and catalytic activity in a bacterial quinone reductase. *FEBS J*, 276, 5263-74.
- BLACKWELL, J. R. & HORGAN, R. 1991. A novel strategy for production of a highly expressed recombinant protein in an active form. *FEBS Letters*, 295, 10-12.
- BOLTON, J. L., TRUSH, M. A., PENNING, T. M., DRYHURST, G. & MONKS, T. J. 2000. Role of quinones in toxicology. *Chem Res Toxicol*, 13, 135-60.
- BREIDENSTEIN, E. B. M., DE LA FUENTE-NÚÑEZ, C. & HANCOCK, R. E. W. 2011. *Pseudomonas aeruginosa*: all roads lead to resistance. *Trends in Microbiology*, 19, 419-426.
- BREIDENSTEIN, E. B. M., KHAIRA, B. K., WIEGAND, I., OVERHAGE, J. & HANCOCK, R. E. W. 2008. Complex Ciprofloxacin Resistome Revealed by Screening a *Pseudomonas aeruginosa* Mutant Library for Altered Susceptibility. *Antimicrobial Agents and Chemotherapy*, 52, 4486-4491.
- BRIMER, C. D. & MONTIE, T. C. 1998. Cloning and comparison of *fliC* genes and identification of glycosylation in the flagellin of *Pseudomonas aeruginosa* a-type strains. *J Bacteriol*, 180, 3209-17.
- BRISSOS, V., GONÇALVES, N., MELO, E. P. & MARTINS, L. O. 2014. Improving Kinetic or Thermodynamic Stability of an Azoreductase by Directed Evolution. *PLOS ONE*, 9, e87209.

- BUELL, C. R., *et al.* 2003. The complete genome sequence of the Arabidopsis and tomato pathogen *Pseudomonas syringae* pv. tomato DC3000. *Proc Natl Acad Sci U S A*, 100, 10181-6.
- CADENAS, E., HOCHSTEIN, P. & ERNSTER, L. 1992. Pro- and antioxidant functions of quinones and quinone reductases in mammalian cells. *Adv Enzymol Relat Areas Mol Biol*, 65, 97-146.
- CAI, J., SALMON, K. & DUBOW, M. S. 1998. A chromosomal ars operon homologue of *Pseudomonas aeruginosa* confers increased resistance to arsenic and antimony in *Escherichia coli*. *Microbiology*, 144 (Pt 10), 2705-13.
- CASALI, N. 2003. Escherichia coli host strains. *Methods Mol. Biol.*, 235, 27.
- CATTÒ, C., *et al.* 2015. Unravelling the Structural and Molecular Basis Responsible for the Anti-Biofilm Activity of Zosteric Acid. *PLoS ONE*, 10, e0131519.
- CDC 2013. Antibiotic resistance threats in the United States, 2013. US department of health, centers for disease control.
- CERENIUS, L., LEE, B. L. & SODERHALL, K. 2008. The proPO-system: pros and cons for its role in invertebrate immunity. *Trends Immunol*, 29, 263-71.
- CFF 2015. Cystic Fibrosis Foundation Patient Registry Annual Data report. *Cystic Fibrosis Foundation*.
- CHEMSKETCH 2015. ChemSketch Version 15.01. *Advanced Chemistry Development*
- CHEN, H. 2006. Recent advances in azo dye degrading enzyme research. *Curr Protein Pept Sci*, 7, 101-11.
- CHEN, H., HOPPER, S. L. & CERNIGLIA, C. E. 2005. Biochemical and molecular characterization of an azoreductase from *Staphylococcus aureus*, a tetrameric NADPH-dependent flavoprotein. *Microbiology*, 151, 1433-41.
- CHEN, H., *et al.* 2008. The *Pseudomonas aeruginosa* multidrug efflux regulator MexR uses an oxidation-sensing mechanism. *Proceedings of the National Academy of Sciences of the United States of America*, 105, 13586-13591.
- CHEN, H., WANG, R. F. & CERNIGLIA, C. E. 2004. Molecular cloning, overexpression, purification, and characterization of an aerobic FMN-dependent azoreductase from *Enterococcus faecalis*. *Protein Expr. Purif.*, 34, 302-10.
- CHEN, J., BHATTACHARJEE, H. & ROSEN, B. P. 2015. ArsH is an organoarsenical oxidase that confers resistance to trivalent forms of the herbicide MSMA and the poultry growth promoter roxarsone. *Molecular microbiology*, 96, 1042-1052.
- CHEN, L., YANG, L., ZHAO, X., SHEN, L. & DUAN, K. 2010. Identification of *Pseudomonas aeruginosa* genes associated with antibiotic susceptibility. *Science China Life Sciences*, 53, 1247-1251.

- CHESIS, P. L., LEVIN, D. E., SMITH, M. T., ERNSTER, L. & AMES, B. N. 1984. Mutagenicity of quinones: pathways of metabolic activation and detoxification. *Proc Natl Acad Sci U S A*, 81, 1696-700.
- CHO, J. J., SCHROTH, M. N., KOMINOS, S. D., GREEN S. K. 1975. Ornamental plants as carriers of *Pseudomonas aeruginosa*. *Phytopathology*. *Phytopathology*, 65, 6.
- CHOI, K.-H. & SCHWEIZER, H. P. 2006. mini-Tn7 insertion in bacteria with single attTn7 sites: example *Pseudomonas aeruginosa*. *Nat. Protocols*, 1, 153-161.
- CHUANCHUEN, R., NARASAKI, C. T. & SCHWEIZER, H. P. 2002. Benchtop and microcentrifuge preparation of *Pseudomonas aeruginosa* competent cells. *Biotechniques*, 33, 760, 762-3.
- CIOFU, O., MANDSBERG, L. F., WANG, H. & HØIBY, N. 2012. Phenotypes selected during chronic lung infection in cystic fibrosis patients: implications for the treatment of *Pseudomonas aeruginosa* biofilm infections. *FEMS Immunology & Medical Microbiology*, 65, 215-225.
- CLANCY, S. B., W. 2008. Translation: DNA to mRNA to Protein. *Nature Education*, 1(1).
- CLELAND, W. W. 1963. The kinetics of enzyme-catalyzed reactions with two or more substrates or products. *Biochimica et Biophysica Acta (BBA) - Specialized Section on Enzymological Subjects*, 67, 104-137.
- CLUNES, M. T. & BOUCHER, R. C. 2007. Cystic Fibrosis: The Mechanisms of Pathogenesis of an Inherited Lung Disorder. *Drug discovery today. Disease mechanisms*, 4, 63-72.
- COLOM, K., FDZ-ARANGUIZ, A., SUINAGA, E. & CISTERNA, R. 1995. Emergence of resistance to beta-lactam agents in *Pseudomonas aeruginosa* with group I beta-lactamases in Spain. *Eur J Clin Microbiol Infect Dis*, 14, 964-71.
- CORREIA, S., *et al.* 2016. Impacts of experimentally induced and clinically acquired quinolone resistance on the membrane and intracellular subproteomes of *Salmonella Typhimurium* DT104B. *J Proteomics*, 145, 46-59.
- CRESCENTE, V. 2015. *Azoreductases: genes and proteins in P. aeruginosa*. PhD, Kingston University.
- CRESCENTE, V., *et al.* 2016. Identification of novel members of the bacterial azoreductase family in *Pseudomonas aeruginosa*. *Biochemical Journal*, 473, 549.
- CUI, K., LU, A. Y. & YANG, C. S. 1995. Subunit functional studies of NAD(P)H:quinone oxidoreductase with a heterodimer approach. *Proc Natl Acad Sci U S A*, 92, 1043-7.
- CULLEN, L., *et al.* 2015. Phenotypic characterization of an international *Pseudomonas aeruginosa* reference panel: strains of cystic fibrosis (CF) origin show less in vivo virulence than non-CF strains. *Microbiology*, 161, 1961-77.
- CUTTELOD, M., *et al.* 2011. Molecular epidemiology of *Pseudomonas aeruginosa* in intensive care units over a 10-year period (1998–2007). *Clinical Microbiology and Infection*, 17, 57-62.

- D'ARGENIO, D. A., GALLAGHER, L. A., BERG, C. A. & MANOIL, C. 2001. *Drosophila* as a model host for *Pseudomonas aeruginosa* infection. *J Bacteriol*, 183, 1466-71.
- DABER, R., STAYROOK, S., ROSENBERG, A. & LEWIS, M. 2007. Structural Analysis of Lac Repressor Bound to Allosteric Effectors. *Journal of molecular biology*, 370, 609-619.
- DAEGELEN, P., STUDIER, F. W., LENSKI, R. E., CURE, S. & KIM, J. F. 2009. Tracing Ancestors and Relatives of *Escherichia coli* B, and the Derivation of B Strains REL606 and BL21(DE3). *Journal of Molecular Biology*, 394, 634-643.
- DASGUPTA, S., DAS, S., CHAWAN, N. S. & HAZRA, A. 2015. Nosocomial infections in the intensive care unit: Incidence, risk factors, outcome and associated pathogens in a public tertiary teaching hospital of Eastern India. *Indian Journal of Critical Care Medicine : Peer-reviewed, Official Publication of Indian Society of Critical Care Medicine*, 19, 14-20.
- DE LORENZO, V., HERRERO, M., JAKUBZIK, U. & TIMMIS, K. N. 1990. Mini-Tn5 transposon derivatives for insertion mutagenesis, promoter probing, and chromosomal insertion of cloned DNA in gram-negative eubacteria. *J Bacteriol*, 172, 6568-72.
- DEKA, S. R., YADAV, S., MAHATO, M. & SHARMA, A. K. 2015. Azobenzene-aminoglycoside: Self-assembled smart amphiphilic nanostructures for drug delivery. *Colloids and Surfaces B: Biointerfaces*, 135, 150-157.
- DEREWENDA, Z. S. 2004. The use of recombinant methods and molecular engineering in protein crystallization. *Macromolecular Crystallization*, 34, 10.
- DONLAN, R. M. 2002. Biofilms: Microbial Life on Surfaces. *Emerging Infectious Diseases*, 8, 881-890.
- DÖTSCH, A., *et al.* 2009. Genomewide Identification of Genetic Determinants of Antimicrobial Drug Resistance in *Pseudomonas aeruginosa*. *Antimicrobial Agents and Chemotherapy*, 53, 2522-2531.
- DRIFFIELD, K., MILLER, K., BOSTOCK, J. M., O'NEILL, A. J. & CHOPRA, I. 2008. Increased mutability of *Pseudomonas aeruginosa* in biofilms. *Journal of Antimicrobial Chemotherapy*, 61, 1053-1056.
- DRISCOLL, J. A., BRODY, S. L. & KOLLEF, M. H. 2007. The Epidemiology, Pathogenesis and Treatment of *Pseudomonas aeruginosa* Infections. *Drugs*, 67, 351-368.
- DUNBAR, J., YENNAWAR, H. P., BANERJEE, S., LUO, J. B. & FARBER, G. K. 1997. The effect of denaturants on protein structure. *Protein Science*, 6, 1727-1733.
- DWYER, D. J., *et al.* 2014. Antibiotics induce redox-related physiological alterations as part of their lethality. *Proceedings of the National Academy of Sciences of the United States of America*, 111, E2100-E2109.
- DWYER, D. J., KOHANSKI, M. A., HAYETE, B. & COLLINS, J. J. 2007. Gyrase inhibitors induce an oxidative damage cellular death pathway in *Escherichia coli*. *Molecular Systems Biology*, 3, 91-91.

- EDGAR, R. C. 2004. MUSCLE: multiple sequence alignment with high accuracy and high throughput. *Nucleic Acids Res*, 32, 1792-7.
- EMSLEY, P., LOHKAMP, B., SCOTT, W. G. & COWTAN, K. 2010. Features and development of Coot. *Acta Crystallogr D*, 66, 486-501.
- ESPOSITO, D. & CHATTERJEE, D. K. 2006. Enhancement of soluble protein expression through the use of fusion tags. *Current Opinion in Biotechnology*, 17, 353-358.
- FERNANDEZ, L., BREIDENSTEIN, E. B. & HANCOCK, R. E. 2011. Creeping baselines and adaptive resistance to antibiotics. *Drug Resist Updat*, 14, 1-21.
- FOSTER, C. E., BIANCHET, M. A., TALALAY, P., ZHAO, Q. & AMZEL, L. M. 1999. Crystal Structure of Human Quinone Reductase Type 2, a Metalloflavoprotein. *Biochemistry*, 38, 9881-9886.
- FROGER, A. & HALL, J. E. 2007. Transformation of Plasmid DNA into E. coli Using the Heat Shock Method. *Journal of Visualized Experiments : JoVE*, 253.
- FUJITANI, S., SUN, H.-Y., YU, V. L. & WEINGARTEN, J. A. 2011. Pneumonia Due to *Pseudomonas aeruginosa*: Part I: Epidemiology, Clinical Diagnosis, and Source. *Chest*, 139, 909-919.
- GAO, J., WANG, Y., WANG, C. W. & LU, B. H. 2014. First Report of Bacterial Root Rot of Ginseng Caused by *Pseudomonas aeruginosa* in China. *Plant Disease*, 98, 1577-1577.
- GASTEIGER, E., *et al.* 2005. Protein Identification and Analysis Tools on the ExpASY Server. In: WALKER, J. M. (ed.) *The Proteomics Protocols Handbook*. Totowa: Humana Press.
- GASTEIGER E., H. C., GATTIKER A., DUVAUD S., WILKINS M.R., APPEL R.D., BAIROCH A. 2005. Protein Identification and Analysis Tools on the ExpASY Server. *The Proteomics Protocols Handbook*, 47.
- GELLATLY, S. L. & HANCOCK, R. E. 2013. *Pseudomonas aeruginosa*: new insights into pathogenesis and host defenses. *Pathog Dis*, 67, 159-73.
- GOLKA, K., KOPPS, S. & MYSLAK, Z. W. 2004. Carcinogenicity of azo colorants: influence of solubility and bioavailability. *Toxicology Letters*, 151, 203-210.
- GONÇALVES, A. M. D., MENDES, S., DE SANCTIS, D., MARTINS, L. O. & BENTO, I. 2013. The crystal structure of *Pseudomonas putida* AzOR: the active site revisited. *FEBS J*, 280, 6643-6657.
- GONZALEZ, C. F., ACKERLEY, D. F., LYNCH, S. V. & MATIN, A. 2005. ChrR, a soluble quinone reductase of *Pseudomonas putida* that defends against H₂O₂. *J Biol Chem*, 280, 22590-5.
- GORMAN, J. & SHAPIRO, L. 2005. Crystal structures of the tryptophan repressor binding protein WrbA and complexes with flavin mononucleotide. *Protein Sci*, 14, 3004-12.
- GORREC, F. 2009. The MORPHEUS protein crystallization screen. *Journal of Applied Crystallography*, 42, 1035-1042.

- GOUDEAU, D. M., *et al.* 2013. The Salmonella Transcriptome in Lettuce and Cilantro Soft Rot Reveals a Niche Overlap with the Animal Host Intestine. *Applied and Environmental Microbiology*, 79, 250-262.
- GREEN, L. K., LA FLAMME, A. C. & ACKERLEY, D. F. 2014. *Pseudomonas aeruginosa* MdaB and WrbA are water-soluble two-electron quinone oxidoreductases with the potential to defend against oxidative stress. *J Microbiol*, 52, 771-7.
- GRODBERG, J. & DUNN, J. J. 1988. ompT encodes the Escherichia coli outer membrane protease that cleaves T7 RNA polymerase during purification. *Journal of Bacteriology*, 170, 1245-1253.
- HAAGEN NIELSEN, O. & BONDESEN, S. 1983. Kinetics of 5-aminosalicylic acid after jejunal instillation in man. *Br J Clin Pharmacol*, 16, 738-40.
- HALL-STOODLEY, L. & STOODLEY, P. 2009. Evolving concepts in biofilm infections. *Cell Microbiol*, 11, 1034-43.
- HALL, T. A. 1999. BioEdit: a user-friendly biological sequence alignment editor and analysis program for Windows 95/98/NT. *Nucleic Acids Symp Ser*, 41, 95-98.
- HANCOCK, R. E. 1998. Resistance mechanisms in *Pseudomonas aeruginosa* and other nonfermentative gram-negative bacteria. *Clin Infect Dis*, 27 Suppl 1, S93-9.
- HATCHETTE, T. F., GUPTA, R. & MARRIE, T. J. 2000. *Pseudomonas aeruginosa* Community-Acquired Pneumonia in Previously Healthy Adults: Case Report and Review of the Literature. *Clinical Infectious Diseases*, 31, 1349-1356.
- HAUSER, A. R. 2009. The type III secretion system of *Pseudomonas aeruginosa*: infection by injection. *Nat Rev Microbiol*, 7, 654-65.
- HAYASHI, M., OHZEKI, H., SHIMADA, H. & UNEMOTO, T. 1996. NADPH-specific quinone reductase is induced by 2-methylene-4-butyrolactone in *Escherichia coli*. *Biochim Biophys Acta*, 1273, 165-70.
- HAYES, J. D. & WOLF, C. R. 1990. Molecular mechanisms of drug resistance. *Biochemical Journal*, 272, 281-295.
- HEDOUX, A., *et al.* 2010. Influence of urea and guanidine hydrochloride on lysozyme stability and thermal denaturation; a correlation between activity, protein dynamics and conformational changes. *Physical Chemistry Chemical Physics*, 12, 13189-13196.
- HERVÁS, M., *et al.* 2012. ArsH from the cyanobacterium *Synechocystis* sp. PCC 6803 is an efficient NADPH-dependent quinone reductase. *Biochemistry*, 51, 1178-1187.
- HUSAIN, Q. 2006. Potential applications of the oxidoreductive enzymes in the decolorization and detoxification of textile and other synthetic dyes from polluted water: a review. *Crit Rev Biotechnol*, 26, 201-21.
- ISLAM, R. S., TISI, D., LEVY, M. S. & LYE, G. J. 2008. Scale-up of *Escherichia coli* growth and recombinant protein expression conditions from microwell to laboratory and pilot scale based on matched kLa. *Biotechnology and Bioengineering*, 99, 1128-1139.

- ITO, K., *et al.* 2006. Three-dimensional structure of AzoR from *Escherichia coli*. An oxidoreductase conserved in microorganisms. *J Biol Chem*, 281, 20567-76.
- ITO, K., *et al.* 2008. Expansion of substrate specificity and catalytic mechanism of azoreductase by X-ray crystallography and site-directed mutagenesis. *J Biol Chem*, 283, 13889-96.
- JACOBS, M. A., *et al.* 2003. Comprehensive transposon mutant library of *Pseudomonas aeruginosa*. *Proc Natl Acad Sci U S A*, 100, 14339-44.
- JADHAV, J. P., PARSHETTI, G. K., KALME, S. D. & GOVINDWAR, S. P. 2007. Decolourization of azo dye methyl red by *Saccharomyces cerevisiae* MTCC 463. *Chemosphere*, 68, 394-400.
- JUAN, C., MOYÁ, B., PÉREZ, J. L. & OLIVER, A. 2006. Stepwise Upregulation of the *Pseudomonas aeruginosa* Chromosomal Cephalosporinase Conferring High-Level β -Lactam Resistance Involves Three AmpD Homologues. *Antimicrobial Agents and Chemotherapy*, 50, 1780-1787.
- KABSCH, W. 2010. XDS. *Acta Crystallogr D*, 66, 125-132.
- KARP, P., *et al.* 2014. The EcoCyc Database. *EcoSal Plus*.
- KIPNIS, E., SAWA, T. & WIENER-KRONISH, J. 2006. Targeting mechanisms of *Pseudomonas aeruginosa* pathogenesis. *Med Mal Infect*, 36, 78-91.
- KISHKO, I., *et al.* 2013. 1.2 Å resolution crystal structure of *Escherichia coli* WrbA holoprotein. *Acta Crystallogr D Biol Crystallogr*, 69, 1748-57.
- KLEBER-JANKE, T. & BECKER, W.-M. 2000. Use of Modified BL21(DE3) *Escherichia coli* Cells for High-Level Expression of Recombinant Peanut Allergens Affected by Poor Codon Usage. *Protein Expression and Purification*, 19, 419-424.
- KLOCKGETHER, J., *et al.* 2013. Intracolon diversity of the *Pseudomonas aeruginosa* cystic fibrosis airway isolates TBCF10839 and TBCF121838: distinct signatures of transcriptome, proteome, metabolome, adherence and pathogenicity despite an almost identical genome sequence. *Environ Microbiol*, 15, 191-210.
- KOHANSKI, M. A., DWYER, D. J., HAYETE, B., LAWRENCE, C. A. & COLLINS, J. J. 2007. A Common Mechanism of Cellular Death Induced by Bactericidal Antibiotics. *Cell*, 130, 797-810.
- KOHLER, T., CURTY, L. K., BARJA, F., VAN DELDEN, C. & PECHERE, J. C. 2000. Swarming of *Pseudomonas aeruginosa* is dependent on cell-to-cell signaling and requires flagella and pili. *J Bacteriol*, 182, 5990-6.
- KOLB, R., BACH, N. C. & SIEBER, S. A. 2014. β -Sultams exhibit discrete binding preferences for diverse bacterial enzymes with nucleophilic residues. *Chem Coms*, 50, 427-429.
- KRAEMER, P. S., *et al.* 2009. Genome-wide screen in *Francisella novicida* for genes required for pulmonary and systemic infection in mice. *Infect Immun*, 77, 232-44.

- KRISSINEL, E. & HENRICK, K. 2004. Secondary-structure matching (SSM), a new tool for fast protein structure alignment in three dimensions. *Acta Crystallogr D Biol Crystallogr*, 60, 2256-68.
- KRISSINEL, E. & HENRICK, K. 2007. Inference of macromolecular assemblies from crystalline state. *J Mol Biol*, 372, 774-97.
- KUMAR, P. R., AHMED, M., BANU, N., BHOSLE, R., BONANNO, J., CHAMALA, S., CHOWDHURY, S., GIZZI, A., GLEN, S., HAMMONDS, J., HILLERICH, B., LOVE, J.D., SEIDEL, R., STEAD, M., TORO, R., WASHINGTON, E., ALMO, S.C., NEW YORK STRUCTURAL GENOMICS RESEARCH CONSORTIUM. 2012. *Crystal Structure of a putative quinone reductase from Klebsiella pneumoniae (Target PSI-013613)* [Online].
- LANDSTORFER, R., *et al.* 2014. Comparison of strand-specific transcriptomes of enterohemorrhagic *Escherichia coli* O157:H7 EDL933 (EHEC) under eleven different environmental conditions including radish sprouts and cattle feces. *BMC Genomics*, 15, 353.
- LEE, J.-Y., PARK, Y. K., CHUNG, E. S., NA, I. Y. & KO, K. S. 2016. Evolved resistance to colistin and its loss due to genetic reversion in *Pseudomonas aeruginosa*. *Scientific Reports*, 6, 25543.
- LIELEG, O., CALDARA, M., BAUMGÄRTEL, R. & RIBBECK, K. 2011. Mechanical robustness of *Pseudomonas aeruginosa* biofilms. *Soft matter*, 7, 3307-3314.
- LINARES, J., GUSTAFSSON, I., BAQUERO, F. & MARTINEZ, J. 2006. Antibiotics as intermicrobial signaling agents instead of weapons. *Proceedings of the National Academy of Sciences of the United States of America*, 103, 19484-9.
- LING, J. Q., *et al.* 2012. Protein aggregation caused by aminoglycoside action is prevented by a hydrogen peroxide scavenger. *Mol Cell*, 48, 713-722.
- LISTER, P. D., WOLTER, D. J. & HANSON, N. D. 2009. Antibacterial-resistant *Pseudomonas aeruginosa*: clinical impact and complex regulation of chromosomally encoded resistance mechanisms. *Clin Microbiol Rev*, 22, 582-610.
- LIU, G., ZHOU, J., FU, Q. S. & WANG, J. 2009. The *Escherichia coli* azoreductase AzoR is involved in resistance to thiol-specific stress caused by electrophilic quinones. *J Bacteriol*, 191.
- LIU, G., *et al.* 2007a. Azoreductase from *Rhodobacter sphaeroides* AS1.1737 is a flavodoxin that also functions as nitroreductase and flavin mononucleotide reductase. *Appl Microbiol Biotechnol*, 76, 1271-9.
- LIU, J., KRULWICH, T. A. & HICKS, D. B. 2008. Purification of two putative type II NADH dehydrogenases with different substrate specificities from alkaliphilic *Bacillus pseudofirmus* OF4. *Biochimica et biophysica acta*, 1777, 453-461.

- LIU, Z. J., *et al.* 2007b. Crystal structure of an aerobic FMN-dependent azoreductase (AzoA) from *Enterococcus faecalis*. *Arch Biochem Biophys*, 463, 68-77.
- LIVERMORE, D. M. 1995. beta-Lactamases in laboratory and clinical resistance. *Clinical Microbiology Reviews*, 8, 557-584.
- LIVERMORE, D. M. 2002. Multiple Mechanisms of Antimicrobial Resistance in *Pseudomonas aeruginosa*: Our Worst Nightmare? *Clinical Infectious Diseases*, 34, 634-640.
- LOSEN, M., FRÖLICH, B., POHL, M. & BÜCHS, J. 2004. Effect of Oxygen Limitation and Medium Composition on *Escherichia coli* Fermentation in Shake-Flask Cultures. *Biotechnology Progress*, 20, 1062-1068.
- LYCZAK, J. B., CANNON, C. L. & PIER, G. B. 2000. Establishment of *Pseudomonas aeruginosa* infection: lessons from a versatile opportunist¹*Address for correspondence: Channing Laboratory, 181 Longwood Avenue, Boston, MA 02115, USA. *Microbes and Infection*, 2, 1051-1060.
- MAHMOOD, S., KHALID, A., ARSHAD, M., MAHMOOD, T. & CROWLEY, D. E. 2016. Detoxification of azo dyes by bacterial oxidoreductase enzymes. *Critical Reviews in Biotechnology*, 36, 639-651.
- MAKINS, R. J. & COWAN, R. E. 2001. 5-amino-salicylate in the management of inflammatory bowel disease. *Colorectal Dis*, 3, 218-22.
- MANOIL, C. 2000. Tagging exported proteins using *Escherichia coli* alkaline phosphatase gene fusions. *Applications of Chimeric Genes and Hybrid Proteins, Pt A*, 326, 35-47.
- MAO, F., DAM, P., CHOU, J., OLMAN, V. & XU, Y. 2009. DOOR: a database for prokaryotic operons. *Nucleic Acids Res*, 37, D459-63.
- MARAN, U. & SLID, S. 2003. QSAR Modeling of Genotoxicity on Non-congeneric Sets of Organic Compounds. *Artificial Intelligence Review*, 20, 13-38.
- MAURIZI, M. R., TRISLER, P. & GOTTESMAN, S. 1985. Insertional mutagenesis of the lon gene in *Escherichia coli*: lon is dispensable. *Journal of Bacteriology*, 164, 1124-1135.
- MAYER, A. M. 2006. Polyphenol oxidases in plants and fungi: going places? A review. *Phytochemistry*, 67, 2318-31.
- MCCOY, A. J., *et al.* 2007. Phaser crystallographic software. *J Appl Crystallogr*, 40, 658-674.
- MCDUGALL, M., *et al.* 2017. Lethal dysregulation of energy metabolism during embryonic vitamin E deficiency. *Free Radical Biology and Medicine*, 104, 324-332.
- MCNICHOLAS, S., POTTERTON, E., WILSON, K. S. & NOBLE, M. E. M. 2011. Presenting your structures: the CCP4mg molecular-graphics software. *Acta Crystallogr D*, 67, 386-394.
- MCPHERSON, A. & GAVIRA, J. A. 2014. Introduction to protein crystallization. *Acta Crystallographica Section F-Structural Biology Communications*, 70, 2-20.
- MEEKS-WAGNER, D., WOOD, J. S., GARVIK, B. & HARTWELL, L. H. 1986. Isolation of two genes that affect mitotic chromosome transmission in *S. cerevisiae*. *Cell*, 44, 53-63.

- MENA, K. D. & GERBA, C. P. 2009. Risk Assessment of *Pseudomonas aeruginosa* in Water. In: WHITACRE, D. M. (ed.) *Reviews of Environmental Contamination and Toxicology Vol 201*. Boston, MA: Springer US.
- MINASOV, G., *et al.* 2011. 1.1 Angstrom Crystal Structure of Putative Modulator of Drug Activity (MdaB) from *Yersinia pestis* CO92.
- MINTON, N. P. 1984. Improved plasmid vectors for the isolation of translational lac gene fusions. *Gene*, 31, 269-273.
- MIYATA, S., CASEY, M., FRANK, D. W., AUSUBEL, F. M. & DRENKARD, E. 2003. Use of the *Galleria mellonella* caterpillar as a model host to study the role of the type III secretion system in *Pseudomonas aeruginosa* pathogenesis. *Infection and Immunity*, 71, 2404-2413.
- MORRISON JR, A. & WENZEL, R. 1984. Epidemiology of infections due to *Pseudomonas aeruginosa*. *Reviews of infectious diseases*, 6, S627.
- MOSKOWITZ, S. M., ERNST, R. K. & MILLER, S. I. 2004. PmrAB, a Two-Component Regulatory System of *Pseudomonas aeruginosa* That Modulates Resistance to Cationic Antimicrobial Peptides and Addition of Aminoarabinose to Lipid A. *Journal of Bacteriology*, 186, 575-579.
- MULLER, C., PLÉSIAT, P. & JEANNOT, K. 2011. A Two-Component Regulatory System Interconnects Resistance to Polymyxins, Aminoglycosides, Fluoroquinolones, and β -Lactams in *Pseudomonas aeruginosa*. *Antimicrobial Agents and Chemotherapy*, 55, 1211-1221.
- NAKANISHI, M., YATOME, C., ISHIDA, N. & KITADE, Y. 2001. Putative ACP phosphodiesterase gene (acpD) encodes an azoreductase. *J Biol Chem*, 276, 46394-9.
- NATHWANI, D., RAMAN, G., SULHAM, K., GAVAGHAN, M. & MENON, V. 2014. Clinical and economic consequences of hospital-acquired resistant and multidrug-resistant *Pseudomonas aeruginosa* infections: a systematic review and meta-analysis. *Antimicrobial Resistance and Infection Control*, 3, 32.
- NIESEN, F. H., BERGLUND, H. & VEDADI, M. 2007. The use of differential scanning fluorimetry to detect ligand interactions that promote protein stability. *Nat Protoc*, 2, 2212-21.
- NIKAIDO, H. & VAARA, M. 1985. Molecular basis of bacterial outer membrane permeability. *Microbiological Reviews*, 49, 1-32.
- NOVAGEN 2005. pET system manual 11th edition.
- OBRITSCH, M. D., FISH, D. N., MACLAREN, R. & JUNG, R. 2004. National Surveillance of Antimicrobial Resistance in *Pseudomonas aeruginosa* Isolates Obtained from Intensive Care Unit Patients from 1993 to 2002. *Antimicrobial Agents and Chemotherapy*, 48, 4606-4610.

- OGANESYAN, N., ANKOUDINOVA, I., KIM, S.-H. & KIM, R. 2007. Effect of osmotic stress and heat shock in recombinant protein overexpression and crystallization. *Protein Expression and Purification*, 52, 280-285.
- OGASAWARA, H., YAMAMOTO, K. & ISHIHAMA, A. 2011. Role of the biofilm master regulator CsgD in cross-regulation between biofilm formation and flagellar synthesis. *J Bacteriol*, 193, 2587-97.
- OKINAKA, Y., YANG, C. H., PERNA, N. T. & KEEN, N. T. 2002. Microarray profiling of *Erwinia chrysanthemi* 3937 genes that are regulated during plant infection. *Mol Plant Microbe Interact*, 15, 619-29.
- OLSEN, R. H., DEBUSSCHER, G. & MCCOMBIE, W. R. 1982. Development of broad-host-range vectors and gene banks: self-cloning of the *Pseudomonas aeruginosa* PAO chromosome. *Journal of Bacteriology*, 150, 60-69.
- OWCZARZY, R., *et al.* 2008. IDT SciTools: a suite for analysis and design of nucleic acid oligomers. *Nucleic Acids Research*, 36, W163-W169.
- PATRIDGE, E. V. & FERRY, J. G. 2006. WrbA from *Escherichia coli* and *Archaeoglobus fulgidus* is an NAD(P)H:quinone oxidoreductase. *J Bacteriol*, 188, 3498-506.
- PECHÈRE, J.-C. & KÖHLER, T. 1999. Patterns and modes of β -lactam resistance in *Pseudomonas aeruginosa*. *Clinical Microbiology and Infection*, 5, Supplement 1, S15-S18.
- PEPPERCORN, M. A. & GOLDMAN, P. 1972. The role of intestinal bacteria in the metabolism of salicylazosulfapyridine. *J Pharmacol Exp Ther*, 181, 555-62.
- PIDUGU, L. S. M., *et al.* 2016. A direct interaction between NQO1 and a chemotherapeutic dimeric naphthoquinone. *BMC Structural Biology*, 16, 1.
- PLOTNIKOVA, J. M., RAHME, L. G. & AUSUBEL, F. M. 2000. Pathogenesis of the human opportunistic pathogen *Pseudomonas aeruginosa* PA14 in Arabidopsis. *Plant Physiology*, 124, 1766-1774.
- POOLE, K. 2001. Multidrug efflux pumps and antimicrobial resistance in *Pseudomonas aeruginosa* and related organisms. *J Mol Microbiol Biotechnol*, 3, 255-64.
- POOLE, K., *et al.* 1996. Expression of the multidrug resistance operon mexA-mexB-oprM in *Pseudomonas aeruginosa*: mexR encodes a regulator of operon expression. *Antimicrobial Agents and Chemotherapy*, 40, 2021-2028.
- POSTNIKOVA, O. A., SHAO, J., MOCK, N. M., BAKER, C. J. & NEMCHINOV, L. G. 2015. Gene Expression Profiling in Viable but Nonculturable (VBNC) Cells of *Pseudomonas syringae* pv. *syringae*. *Frontiers in Microbiology*, 6.
- PRELICH, G. 2012. Gene Overexpression: Uses, Mechanisms, and Interpretation. *Genetics*, 190, 841-854.
- RAFII, F., FRANKLIN, W. & CERNIGLIA, C. E. 1990. Azoreductase activity of anaerobic bacteria isolated from human intestinal microflora. *Applied and Environmental Microbiology*, 56, 2146-2151.

- RAHME, L. G., *et al.* 1997. Use of model plant hosts to identify *Pseudomonas aeruginosa* virulence factors. *Proceedings of the National Academy of Sciences of the United States of America*, 94, 13245-13250.
- RAI, H. S., *et al.* 2005. Removal of Dyes from the Effluent of Textile and Dyestuff Manufacturing Industry: A Review of Emerging Techniques With Reference to Biological Treatment. *Critical Reviews in Environmental Science and Technology*, 35, 219-238.
- RAKHIMOVA, E., MUNDER, A., WIEHLMANN, L., BREDENBRUCH, F. & TUMMLER, B. 2008. Fitness of isogenic colony morphology variants of *Pseudomonas aeruginosa* in murine airway infection. *PLoS One*, 3, e1685.
- RAMÍREZ-ESTRADA, S., BORGATTA, B. & RELLO, J. 2016. *Pseudomonas aeruginosa* ventilator-associated pneumonia management. *Infection and Drug Resistance*, 9, 7-18.
- RARAN-KURUSSI, S. & WAUGH, D. S. 2012. The Ability to Enhance the Solubility of Its Fusion Partners Is an Intrinsic Property of Maltose-Binding Protein but Their Folding Is Either Spontaneous or Chaperone-Mediated. *Plos One*, 7.
- REDGRAVE, L. S., SUTTON, S. B., WEBBER, M. A. & PIDDOCK, L. J. V. 2014. Fluoroquinolone resistance: mechanisms, impact on bacteria, and role in evolutionary success. *Trends in Microbiology*, 22, 438-445.
- ROSANO, G. L. & CECCARELLI, E. A. 2009. Rare codon content affects the solubility of recombinant proteins in a codon bias-adjusted *Escherichia coli* strain. *Microbial Cell Factories*, 8, 41.
- ROSANO, G. L. & CECCARELLI, E. A. 2014. Recombinant protein expression in *Escherichia coli*: advances and challenges. *Frontiers in Microbiology*, 5, 172.
- ROSENTHAL, V. D., *et al.* 2012. International Nosocomial Infection Control Consortium (INICC) report, data summary of 36 countries, for 2004-2009. *Am J Infect Control*, 40, 396-407.
- ROSS, D. & SIEGEL, D. 2004. NAD(P)H:Quinone Oxidoreductase 1 (NQO1, DT-Diaphorase), Functions and Pharmacogenetics. *Methods in Enzymology*, 382, 115-144.
- RYAN, A. 2017. Azoreductases in drug metabolism. *British Journal of Pharmacology*, 174, 2161-2173.
- RYAN, A., KAPLAN, E., LAURIERI, N., LOWE, E. & SIM, E. 2011. Activation of nitrofurazone by azoreductases: multiple activities in one enzyme. *Sci Rep*, 1, DOI:10.1038/srep00063.
- RYAN, A., *et al.* 2014. Identification of NAD(P)H quinone oxidoreductase activity in azoreductases from *P. aeruginosa*: azoreductases and NAD(P)H quinone oxidoreductases belong to the same FMN-dependent superfamily of esnzymes. *PLoS ONE*, 9, e98551.
- RYAN, A., *et al.* 2010a. A Novel Mechanism for Azoreduction. *Journal of Molecular Biology*, 400, 24-37.
- RYAN, A., WANG, C. J., LAURIERI, N., WESTWOOD, I. & SIM, E. 2010b. Reaction mechanism of azoreductases suggests convergent evolution with quinone oxidoreductases. *Protein Cell*, 1, 780-90.

- SALMI, C., *et al.* 2008. Squalamine: An Appropriate Strategy against the Emergence of Multidrug Resistant Gram-Negative Bacteria? *PLoS ONE*, 3, e2765.
- SANDERS, C. C., *et al.* 1997. Penicillin-binding proteins and induction of AmpC beta-lactamase. *Antimicrobial Agents and Chemotherapy*, 41, 2013-2015.
- SANDERS, C. C. & SANDERS, W. E., JR. 1986. Type I beta-lactamases of gram-negative bacteria: interactions with beta-lactam antibiotics. *J Infect Dis*, 154, 792-800.
- SARATALE, R. G., SARATALE, G. D., KALYANI, D. C., CHANG, J. S. & GOVINDWAR, S. P. 2009. Enhanced decolorization and biodegradation of textile azo dye Scarlet R by using developed microbial consortium-GR. *Bioresource Technology*, 100, 2493-2500.
- SARVA, S. T., WALDO, R. H., BELLAND, R. J. & KLOSE, K. E. 2016. Comparative Transcriptional Analyses of *Francisella tularensis* and *Francisella novicida*. *PLoS One*, 11, e0158631.
- SCHNEIDER, K., HAFNER, C. & JÄGER, I. 2004. Mutagenicity of textile dye products. *Journal of Applied Toxicology*, 24, 83-91.
- SHARMA, R., *et al.* 2013. Design, synthesis and ex vivo evaluation of colon-specific azo based prodrugs of anticancer agents. *Bioorganic & Medicinal Chemistry Letters*, 23, 5332-5338.
- SIEVERT, D. M., *et al.* 2013. Antimicrobial-Resistant Pathogens Associated with Healthcare-Associated Infections: Summary of Data Reported to the National Healthcare Safety Network at the Centers for Disease Control and Prevention, 2009–2010. *Infection Control and Hospital Epidemiology*, 34, 1-14.
- SINGH, R. L., SINGH, P. K. & SINGH, R. P. 2015. Enzymatic decolorization and degradation of azo dyes – A review. *International Biodeterioration & Biodegradation*, 104, 21-31.
- SKELLY, J. V., *et al.* 1999. Crystal structure of human DT-diaphorase: a model for interaction with the cytotoxic prodrug 5-(aziridin-1-yl)-2,4-dinitrobenzamide (CB1954). *J Med Chem*, 42, 4325-30.
- SKURNIK, D., *et al.* 2013. A Comprehensive Analysis of *In Vitro* and *In Vivo* Genetic Fitness of *Pseudomonas aeruginosa* Using High-Throughput Sequencing of Transposon Libraries. *PLoS Pathog*, 9, e1003582.
- SLEKOVEC, C., *et al.* 2012. Tracking Down Antibiotic-Resistant *Pseudomonas aeruginosa* Isolates in a Wastewater Network. *Plos One*, 7.
- SOBALLE, B. & POOLE, R. K. 2000. Ubiquinone limits oxidative stress in *Escherichia coli*. *Microbiology*, 146 (Pt 4), 787-96.
- SOBEL, M. L., HOCQUET, D., CAO, L., PLESIAT, P. & POOLE, K. 2005. Mutations in PA3574 (nalD) Lead to Increased MexAB-OprM Expression and Multidrug Resistance in Laboratory and Clinical Isolates of *Pseudomonas aeruginosa*. *Antimicrobial Agents and Chemotherapy*, 49, 1782-1786.
- SONG, W., LEE, K. M., KANG, H. J., SHIN, D. H. & KIM, D. K. 2001. Microbiologic aspects of predominant bacteria isolated from the burn patients in Korea. *Burns*, 27, 136-139.

- SORENSEN, H. P. & MORTENSEN, K. K. 2005. Advanced genetic strategies for recombinant protein expression in *Escherichia coli*. *J Biotechnol*, 115, 113-28.
- SOUSA, A. M. & PEREIRA, M. O. 2014. *Pseudomonas aeruginosa* Diversification during Infection Development in Cystic Fibrosis Lungs—A Review. *Pathogens*, 3, 680-703.
- SPARLA, F., TEDESCHI, G., PUPILLO, P. & TROST, P. 1999. Cloning and heterologous expression of NAD(P)H:quinone reductase of *Arabidopsis thaliana*, a functional homologue of animal DT-diaphorase. *FEBS Lett*, 463, 382-6.
- SPOERING, A. L. & LEWIS, K. 2001. Biofilms and Planktonic Cells of *Pseudomonas aeruginosa* Have Similar Resistance to Killing by Antimicrobials. *Journal of Bacteriology*, 183, 6746-6751.
- STARKEY, M. & RAHME, L. G. 2009. Modeling *Pseudomonas aeruginosa* pathogenesis in plant hosts. *Nature Protocols*, 4, 117-124.
- STEPHENS, P. E., LEWIS, H. M., DARLISON, M. G. & GUEST, J. R. 1983. Nucleotide sequence of the lipoamide dehydrogenase gene of *Escherichia coli* K12. *Eur J Biochem*, 135, 519-27.
- STICKLAND, H. G., DAVENPORT, P. W., LILLEY, K. S., GRIFFIN, J. L. & WELCH, M. 2010. Mutation of *nfxB* Causes Global Changes in the Physiology and Metabolism of *Pseudomonas aeruginosa*. *Journal of Proteome Research*, 9, 2957-2967.
- STOVER, C. K., *et al.* 2000. Complete genome sequence of *Pseudomonas aeruginosa* PA01, an opportunistic pathogen. *Nature*, 406, 959-64.
- SUGIURA, W., YODA, T., MATSUBA, T., TANAKA, Y. & SUZUKI, Y. 2006. Expression and characterization of the genes encoding azoreductases from *Bacillus subtilis* and *Geobacillus stearothermophilus*. *Biosci Biotechnol Biochem*, 70, 1655-65.
- SWANSON, M. S., MALONE, E. A. & WINSTON, F. 1991. SPT5, an essential gene important for normal transcription in *Saccharomyces cerevisiae*, encodes an acidic nuclear protein with a carboxy-terminal repeat. *Mol Cell Biol*, 11, 4286.
- TAN, S. Y.-Y., *et al.* 2014. Comparative Systems Biology Analysis To Study the Mode of Action of the Isothiocyanate Compound Iberin on *Pseudomonas aeruginosa*. *Antimicrobial Agents and Chemotherapy*, 58, 6648-6659.
- TANIMOTO, K., TOMITA, H., FUJIMOTO, S., OKUZUMI, K. & IKE, Y. 2008. Fluoroquinolone Enhances the Mutation Frequency for Meropenem-Selected Carbapenem Resistance in *Pseudomonas aeruginosa*, but Use of the High-Potency Drug Doripenem Inhibits Mutant Formation. *Antimicrobial Agents and Chemotherapy*, 52, 3795-3800.
- THOMPSON, J. D., HIGGINS, D. G. & GIBSON, T. J. 1994. CLUSTAL W: improving the sensitivity of progressive multiple sequence alignment through sequence weighting, position-specific gap penalties and weight matrix choice. *Nucleic Acids Research*, 22, 4673-4680.

- TODAR, K. 2006. *Todar's online textbook of bacteriology*, University of Wisconsin-Madison Department of Bacteriology.
- TRIAS, J. & NIKAIDO, H. 1990. Outer membrane protein D2 catalyzes facilitated diffusion of carbapenems and penems through the outer membrane of *Pseudomonas aeruginosa*. *Antimicrob Agents Chemother*, 34, 52-7.
- TSUJI, S., *et al.* 2014. Community-acquired *Pseudomonas aeruginosa* pneumonia in previously healthy patients. *JMM Case Reports*, 1.
- TÜMMLER, B., *et al.* 1991. Nosocomial acquisition of *Pseudomonas aeruginosa* by cystic fibrosis patients. *Journal of Clinical Microbiology*, 29, 1265-1267.
- UNDEN, G., *et al.* 1995. O₂-sensing and O₂-dependent gene regulation in facultatively anaerobic bacteria. *Archives of microbiology*, Vol. 164, 81-90.
- VAKULENKO, S. B. & MOBASHERY, S. 2003. Versatility of Aminoglycosides and Prospects for Their Future. *Clinical Microbiology Reviews*, 16, 430-450.
- VALKO, M., MORRIS, H. & CRONIN, M. T. 2005. Metals, toxicity and oxidative stress. *Curr Med Chem*, 12, 1161-208.
- VAN DER LINDEN, I., *et al.* 2016. Microarray-Based Screening of Differentially Expressed Genes of *E. coli* O157:H7 Sakai during Preharvest Survival on Butterhead Lettuce. *Agriculture*, 6, 6.
- VAN DER ZEE, F. P. & VILLAVARDE, S. 2005. Combined anaerobic-aerobic treatment of azo dyes—A short review of bioreactor studies. *Water Research*, 39, 1425-1440.
- VANDER WAUVEN, C., PIÉRARD, A., KLEY-RAYMANN, M. & HAAS, D. 1984. *Pseudomonas aeruginosa* mutants affected in anaerobic growth on arginine: evidence for a four-gene cluster encoding the arginine deiminase pathway. *Journal of Bacteriology*, 160, 928-934.
- VETHANAYAGAM, J. G. & FLOWER, A. M. 2005. Decreased gene expression from T7 promoters may be due to impaired production of active T7 RNA polymerase. *Microbial Cell Factories*, 4, 3.
- VINCENT, J. L., *et al.* 2009. International study of the prevalence and outcomes of infection in intensive care units. *JAMA*, 302, 2323-9.
- VINCENT, J. L., *et al.* 2006. Sepsis in European intensive care units: results of the SOAP study. *Crit Care Med*, 34, 344-53.
- VOLAKLI, E., *et al.* 2010. Infections of respiratory or abdominal origin in ICU patients: what are the differences? *Critical Care*, 14, R32.
- WALSH, F. & AMYES, S. G. B. 2007. Carbapenem Resistance in Clinical Isolates of *Pseudomonas aeruginosa*. *Journal of Chemotherapy*, 19, 376-381.
- WANG, B., *et al.* 2016. Pleiotropic effects of temperature-regulated 2-OH-lauroyltransferase (PA0011) on *Pseudomonas aeruginosa* antibiotic resistance, virulence and type III secretion system. *Microbial Pathogenesis*, 91, 5-17.

- WANG, C. J., *et al.* 2007. Molecular cloning, characterisation and ligand-bound structure of an azoreductase from *Pseudomonas aeruginosa*. *J Mol Biol*, 373, 1213-28.
- WANG, C. J., *et al.* 2010. Role of Tyrosine 131 in the active site of paAzoR1, an azoreductase with specificity for the inflammatory bowel disease pro-drug balsalazide. *Acta Crystallogr F*, 66, 2-7.
- WANG, G. & MAIER, R. J. 2004. An NADPH quinone reductase of *Helicobacter pylori* plays an important role in oxidative stress resistance and host colonization. *Infect Immun*, 72, 1391-6.
- WANG, Z., LI, L., DONG, Y.-H. & SU, X.-D. 2014. Structural and biochemical characterization of MdaB from cariogenic *Streptococcus mutans* reveals an NADPH-specific quinone oxidoreductase. *Acta Crystallographica Section D*, 70.
- WEINSTEIN, R. A., GAYNES, R. & EDWARDS, J. R. 2005. Overview of Nosocomial Infections Caused by Gram-Negative Bacilli. *Clinical Infectious Diseases*, 41, 848-854.
- WEST, S. E. & IGLEWSKI, B. H. 1988. Codon usage in *Pseudomonas aeruginosa*. *Nucleic Acids Research*, 16, 9323-9335.
- WEST, S. E. H., SCHWEIZER, H. P., DALL, C., SAMPLE, A. K. & RUNYEN-JANECKY, L. J. 1994. Construction of improved Escherichia-Pseudomonas shuttle vectors derived from pUC18/19 and sequence of the region required for their replication in *Pseudomonas aeruginosa*. *Gene*, 148, 81-86.
- WHO 2016. *E. coli* Fact sheet.
- WHO 2017. List of bacteria for which new antibiotics are urgently needed. *World Health Organization*.
- WILLEY, J. M., SHERWOOD, L., WOOLVERTON, C. J., PRESCOTT, L. M. & WILLEY, J. M. 2011. *Prescott's microbiology*, New York, McGraw-Hill.
- WINSOR, G. L., *et al.* 2016. Enhanced annotations and features for comparing thousands of *Pseudomonas* genomes in the *Pseudomonas* genome database. *Nucleic Acids Res*, 44, D646-53.
- WINSOR, G. L., *et al.* 2011. *Pseudomonas* Genome Database: improved comparative analysis and population genomics capability for *Pseudomonas* genomes. *Nucleic Acids Res*, 39, D596-600.
- WINTER, G. 2010. xia2: an expert system for macromolecular crystallography data reduction. *J Appl Crystallogr*, 43, 186-190.
- WLODAWER, A., MINOR, W., DAUTER, Z. & JASKOLSKI, M. 2008. Protein crystallography for non-crystallographers, or how to get the best (but not more) from published macromolecular structures. *Febs Journal*, 275, 1-21.
- WORLITZSCH, D., *et al.* 2002. Effects of reduced mucus oxygen concentration in airway *Pseudomonas* infections of cystic fibrosis patients. *The Journal of Clinical Investigation*, 109, 317-325.

- WU, K., *et al.* 1997. Catalytic Properties of NAD(P)H:Quinone Oxidoreductase-2 (NQO2), a Dihyronicotinamide Riboside Dependent Oxidoreductase. *Arch Biochem Biophys*, 347, 221-228.
- XU, J. & JAISWAL, A. K. 2012. NAD(P)H:quinone oxidoreductase 1 (NQO1) competes with 20S proteasome for binding with C/EBPa leading to its stabilization and protection against radiation-induced myeloproliferative disease. *J Biol Chem*, 287, 41608-18.
- YANG, C. R., SHAPIRO, B. E., MJOLSNESS, E. D. & HATFIELD, G. W. 2005. An enzyme mechanism language for the mathematical modeling of metabolic pathways. *Bioinformatics*, 21, 774-80.
- YANG, W., NI, L. & SOMERVILLE, R. L. 1993. A stationary-phase protein of Escherichia coli that affects the mode of association between the trp repressor protein and operator-bearing DNA. *Proc Natl Acad Sci USA*, 90, 5796-5800.
- YANG, Y., *et al.* 2014. Clinical implications of high NQO1 expression in breast cancers. *Journal of Experimental & Clinical Cancer Research*, 33, 14.
- YANG, Z. & LU, C. D. 2007. Functional genomics enables identification of genes of the arginine transaminase pathway in *Pseudomonas aeruginosa*. *J Bacteriol*, 189, 3945-53.
- YE, J., YANG, H. C., ROSEN, B. P. & BHATTACHARJEE, H. 2007. Crystal structure of the flavoprotein ArsH from *Sinorhizobium meliloti*. *FEBS Lett*, 581, 3996-4000.
- YEUNG, A. T., *et al.* 2009. Swarming of *Pseudomonas aeruginosa* is controlled by a broad spectrum of transcriptional regulators, including MetR. *J Bacteriol*, 191, 5592-602.
- YILDIRIM, S., *et al.* 2005. Bacteriological profile and antibiotic resistance: comparison of findings in a burn intensive care unit, other intensive care units, and the hospital services unit of a single center. *J Burn Care Rehabil*, 26, 488-92.
- YOON, S. S., *et al.* 2002. *Pseudomonas aeruginosa* anaerobic respiration in biofilms: relationships to cystic fibrosis pathogenesis. *Dev Cell*, 3, 593-603.
- YOSHIHARA, E. & NAKAE, T. 1989. Identification of porins in the outer membrane of *Pseudomonas aeruginosa* that form small diffusion pores. *J Biol Chem*, 264, 6297-301.
- YOSHIMURA, F. & NIKAIDO, H. 1982. Permeability of *Pseudomonas aeruginosa* outer membrane to hydrophilic solutes. *Journal of Bacteriology*, 152, 636-642.
- YU, J., *et al.* 2014. Structures of AzrA and of AzrC complexed with substrate or inhibitor: insight into substrate specificity and catalytic mechanism. *Acta Crystallographica Section D*, 70, 553-564.
- ZANNONI, D. 1989. The Respiratory Chains of Pathogenic Pseudomonads. *Biochimica Et Biophysica Acta*, 975, 299-316.
- ZILBERBERG, M. D. & SHORR, A. F. 2013. Prevalence of multidrug-resistant *Pseudomonas aeruginosa* and carbapenem-resistant *Enterobacteriaceae* among specimens from hospitalized patients with pneumonia and bloodstream infections in the United States from 2000 to 2009. *J Hosp Med*, 8, 559-63.

